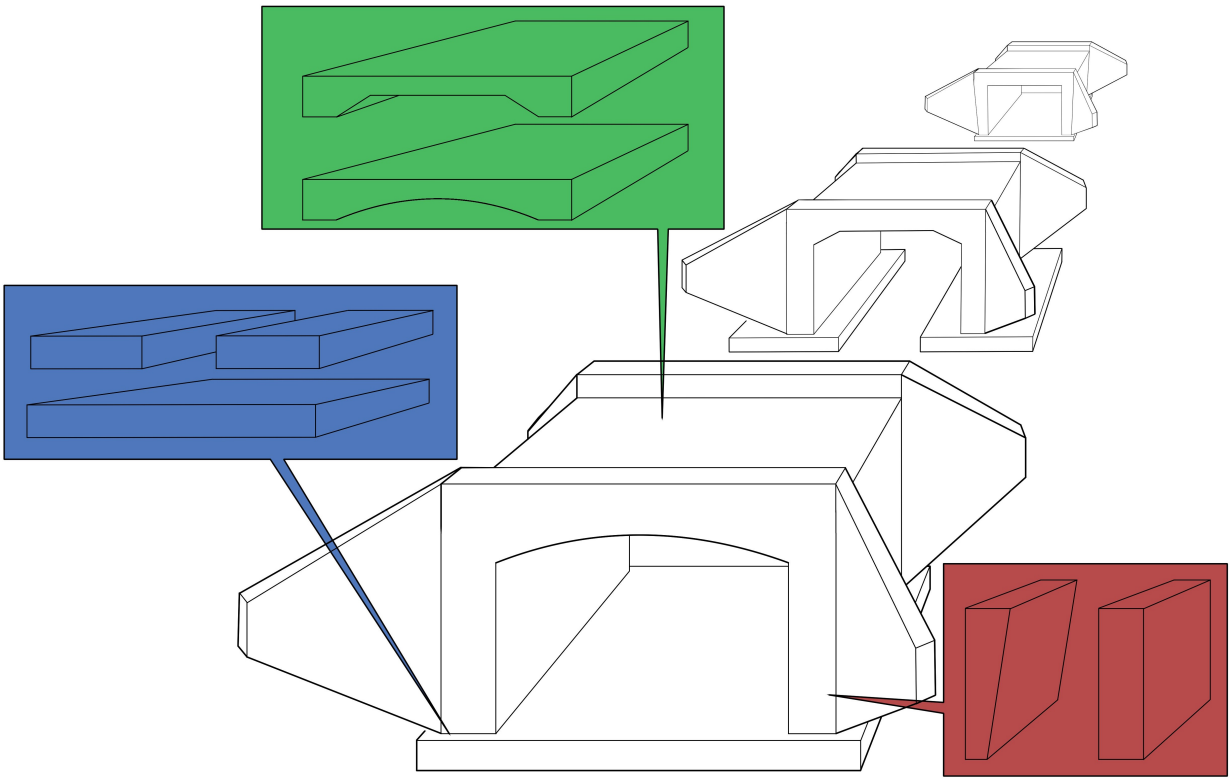

Grouping and optimization of several slab frame bridges

An analytic and parametric multi-criteria Set-Based Design of several slab frame bridges with a focus on grouping and optimization based on investment cost, environmental impact, and buildability

Master's thesis in Master Programme Structural Engineering and Building Technology

Hugo von Kraemer
Theodor Sjölund

DEPARTMENT OF ARCHITECTURE AND CIVIL ENGINEERING
CHALMERS UNIVERSITY OF TECHNOLOGY
Gothenburg, Sweden 2024
www.chalmers.se

Master's thesis 2024

Grouping and optimization of several slab frame bridges

An analytic and parametric multi-criteria Set-Based Design of several slab frame bridges with a focus on grouping and optimization based on investment cost, environmental impact, and buildability

Hugo von Kraemer
Theodor Sjölund

CHALMERS
UNIVERSITY OF TECHNOLOGY

Department of Architecture and Civil Engineering
Division of Structural Engineering
Chalmers University of Technology
Gothenburg, Sweden 2024

Grouping and optimization of several slab frame bridges
An analytic and parametric multi-criteria Set-Based Design of several slab frame bridges with a focus on grouping and optimization based on investment cost, environmental impact, and buildability
HUGO VON KRAEMER
THEODOR SJÖLUND

Supervisor: Thomas Appelgren, Ramboll
Supervisor: Johan Lagerkvist, Swedish Transport Administration/Chalmers University of Technology
Examiner: Rasmus Rempling, Department of Structural engineering

Master's Thesis 2024
Department of Architecture and Civil Engineering
Division of Structural Engineering
Chalmers University of Technology
SE-412 96 Gothenburg
Telephone +46 31 772 1000

Cover: Design of multiple slab frame bridges using geometrically different structural components.

Gothenburg, Sweden 2024

Grouping and optimizing of several slab frame bridges
An analytic and parametric multi-criteria Set-Based Design of several slab frame bridges with a focus on grouping and optimization based on investment cost, environmental impact, and buildability
Hugo von Kraemer
Theodor Sjölund
Department of Architecture and Civil Engineering
Chalmers University of Technology

Abstract

With today's increasing demand to reduce the carbon footprint of large infrastructure projects, a major focus on material optimization is commonly considered during design. On the other hand, long construction times and delays have created a need to increase productivity without compromising on other important factors such as CO_2-emission and investment cost. Previous research has shown that repetition of work steps and standardization of structural components reduces construction time. Using the same structural component for several bridges could be an alternative to reduce construction time.

This master's thesis presents research on grouping and optimization of slab frame bridges using Set-Based Design. Set-Based Design with multi-objective functions was implemented on a Finite Element Method model built in Sofistik, to analyze a large number of bridge alternatives. Different geometric shapes of structural components were combined and evaluated for three different span lengths: 12, 14, and 16 m. The evaluation of bridges was based on the multi-criteria object function Equivalent cost. A resulting library of bridge solutions could thereafter be formed, where it was possible to sort solutions according to object functions and group alternatives by structural components.

The result showed that it was possible to optimize a reference bridge and optimization of buildability gave the most noticeable impact on the reference objects. The result also showed that grouping of structural components over multiple spans was possible. A consequence of the grouping was that the bridges that were possible to group, had higher material usage compared to individually optimized bridges. Finally, it was concluded that Set-Based Design with a focus on grouping structural components can be advantageously adopted in future projects to reduce construction time, with the greatest possible impact on large projects.

Keywords: Set-Based Design, slab frame bridges, optimization, grouping, investment cost, environmental impact, buildability, repeatability, standardization, structural components, parametric design, concrete, Sofistik.

Acknowledgements

This master's thesis was conducted in collaboration with Ramboll, the Swedish Transport Administration and Chalmers University of Technology at the Department of Structural Engineering. During the working process of the master's thesis, we have received help and support from several individuals whom we would like to acknowledge.

We would like to thank our supervisor Thomas Appelgren at Ramboll for his shown interest and commitment to our work. From help with scripting in Sofistik to general questions regarding bridge design, you have always been available and supported us with your expertise. We would also like to thank our supervisor from The Swedish Transport Administration, Johan Lagerkvist, and our examiner and supervisor from Chalmers, Rasmus Rempling, for frequent consultations and support as well as your expertise regarding Set-Based Design throughout the whole course of this master thesis writing.

Hugo von Kraemer & Theodor Sjölund

Gothenburg, June 2024

List of Acronyms

Below is the list of acronyms that have been used throughout this thesis listed in alphabetical order:

AIA	American Institute of Architects
ALS	Accidental Limit State
CAE	Computer-Aided Engineering
FEM	Finite Element Method
FLS	Fatigue Limit State
IPD	Integrated Project Delivery
NBL	North Bothnia Line
NBLP	North Bothnia Line Project
PBD	Point-Based Design
SBPD	Set-Based Parametric Design
SBD	Set-Based Design
SCC	Self compacting concrete
SLS	Serviceability Limit State
STA	Swedish Transport Administration
ULS	Ultimate Limit State

Nomenclature

Below is the nomenclature of sets, parameters, and variables that have been used throughout this thesis:

Sets

$\mathbb{A}$	Design space $\mathbb{A}$
$\mathbb{B}$	Design space $\mathbb{B}$
$\mathbb{C}$	Design space $\mathbb{C}$
$\mathbb{D}$	Design space $\mathbb{D}$
$\mathbb{E}$	Design space $\mathbb{E}$

Parameters

K_0	Coefficient of earth pressure at rest
γ_{soil}	Unit weight of soil
α	Load classification factor
ϕ_2	Dynamic factor for railway
T_{min}	Minimum temperature
T_{max}	Maximum temperature
T_0	Casting temperature
δH	Horizontal support displacement
δV	Vertical support displacement

Variables

t_{slab}	Thickness of foundation slab
w_{slab}	Length of heel abutment
t_{FL}	Thickness straight frame legs
$t_{FL.ts}$	Thickness top of variables thick frame legs
$t_{FL.bs}$	Thickness bottom of variables thick frame legs
$t_{deck.FL}$	Thickness at outer ends of deck
$t_{deck.mid}$	Thickness at mid of deck
t_{haunch}	Thickness of haunch
$n_{layers.top}$	Number of reinforcement layers top side
$n_{layers.bot}$	Number of reinforcement layers bottom side
S_{top}	Center-to-center distance between reinforcement top side
S_{bot}	Center-to-center distance between reinforcement bottom side
S_{shear}	Center-to-center distance between shear reinforcement
ϕ	Reinforcement diameter

Contents

List of Figures

List of Tables

1

Introduction

In this Chapter, the background regarding the thesis subject is presented along with the aim, objectives, limitations, and methodology.

1.1 Background

Global action to combat climate change is a major challenge for humanity. Climate impact is a complex topic consisting of many parameters but is often measured by greenhouse-gas emissions ("Long-term climate change: Projections, commitments and irreversibility", 2013). Among all the greenhouse gases, carbon dioxide poses as one of the greatest threats to irreversible global environmental impact. Sweden is one of the countries at the forefront of combating climate change by using modern technological solutions to reduce carbon dioxide emissions (Ministry of the Environment & Government offices of Sweden, 2020). According to The Ministry of the Environment and Government offices of Sweden (2020), the main goal for the Swedish climate change actions is to produce net negative greenhouse-gas emissions as a country after 2045. To achieve this goal, large changes to mundane processes in key industries have to be implemented. One of these key industries is the construction and civil engineering sector, which contributes to 8% of the yearly Swedish territorial greenhouse-gas emissions (Ministry of the Environment & Government offices of Sweden, 2020).

The construction and civil engineering sector is globally one of the industries with the most negative impact on climate change (Zhou et al., 2020). Bridge construction is one of the most carbon-intensive sectors of the construction industry, mostly due to the heavy use of concrete and steel, which contributes to more than half of the greenhouse-gas emissions during the construction of infrastructure (Uppenberg et al., 2017). With a growing population and interest in expanding as well as upgrading the Swedish national transportation network, the demand for low-carbon dioxide bridge solutions is highly prioritized (Eliasson & Lundberg, 2024). While the demand for low-carbon emission design solutions is increasing in Sweden, the need for cheap and material-effective bridge designs is rising due to increases of costs.

Optimizing a structure's material efficiency during the design phase is often the most preferred way of reducing both the cost and the environmental impact of the project (Li et al., 2021). Reducing the amount of material to be used in future production, decreases the investment cost and the net carbon dioxide emissions. However, decreasing the amount of material used can have a negative impact on the structure's buildability.

The term buildability has many different definitions as the subject covers a wide range of aspects within the production of a structure (Simonsson, 2011). A simple interpretation of the expression would be to ease the building of a structure. It is of great importance to consider buildability during the design stage as it increases the safety of workers on site, creates a good workflow, and improves the economic use of labor (Simonsson, 2011). The problem with considering buildability while optimizing for material usage, is that the two aspects usually come into conflict with each other (Mogra et al., 2023). Optimizing for concrete material usage could result in more material usage for other materials compared to conventional structural design as it may increase the demand for other parameters such as extra form-work or temporary structures, which may negatively impact the overall economy (Simonsson, 2011).

One approach that has been used in recent years to address this conflict between material efficiency and buildability is Set-Based Design (SBD), which enables the opportunity to reduce material costs and environmental impact by up to 20% compared to traditional design methods such as Point-Based Design (PBD) (Lagerkvist et al., 2022). SBD challenges traditional bridge design techniques such as PBD by generating a large variety of structural alternatives by combining a varying range of input parameters, such as geometric and material properties (Mathern et al., 2018). The alternatives are gradually reduced using mathematical algorithms that check whether the structure meets certain design requirements (Parrish et al., 2007). For bridge design, these requirements are often Eurocode standards but can also be national regulations (Mathern et al., 2018). Design requirements of buildability and CO_2-emissions could be used to further optimize and filter the number of alternatives from SBD and contribute to a more effective and environmentally-friendly construction sector.

The traditional PBD approach of construction design involves choosing a small variety of early conceptual designs based on various conditions, designer experience, and previous reference projects (Girardet & Boton, 2021). The design phase proceeds in steps were the designs are individually mathematical evaluated, independently of changes in the basic conditions used during the conceptual design phase. Consequently, large changes during the design phase can force the process to be repeated, which creates a time-consuming process that leaves less opportunity for optimization.

Today's large construction projects require collaboration between many stakeholders, such as different areas of technical expertise and owners, to achieve a successful outcome (Lee et al., 2012). Involving multiple parties increases the risk of late changes during the design phase, which can be critical to the traditional PBD design procedure. The bridge construction sector is in particularly vulnerable regarding design condition-changes since projects often span over a longer time period (Girardet & Boton, 2021).

Every bridge made in Sweden today is designed as a unique structure (Bruneby et al., 2023). It is not unusual for a single project to involve the design of several bridges. These projects are particularly vulnerable to the time-consuming traditional iterative non-redundant PBD design methodology. To address this topic, the Swedish Transport Administration (STA) has implemented standardized bridges. Standardized bridges are pre-designed bridges with fixed geometries, materials, and cost, set to be used for locations with certain conditions. STA has created two concepts of railway slab frame bridges of this method, which should be tested on the large infrastructure railway project North Bothnia Line (NBL) which contains approximately 250 bridges, with the majority being slab frame bridges. The principle idea is to adapt the environment to the bridge to reduce the number of unique bridges. The goal of standardized bridges is to create a catalog of bridges that work for different conditions, making more efficient use of resources and increasing productivity.

To produce standardized bridges, individual components of bridges can be looked at and standardized. Large infrastructure projects where many bridges of the same type are projected to be built, could benefit from finding similarities between different components with minor variations in prerequisites. With the available modern day computing power, it is possible to use SBD at the early stage of bridge design to achieve a variety of different geometric bridge components and filter them into groups. These numerous different bridge components could form a network that shows different combinations of components that are compatible with each other, ultimately creating standard combinations that could achieve the most optimal solution based on various optimization parameters.

1.2 Aim

The aim of this master's thesis was to explore the feasibility of Set-Based Design for design decisions and optimization with respect to investment cost, environmental impact, and buildability. Moreover, the thesis explores the possibility of repeating the same structural component for different conditions and investigates the effects that grouping of structural components has on investment cost, environmental impact, and buildability.

1.3 Objectives

- Compare SBD and PBD to assess their strengths.
- Implementing Parametric Set-Based Design for a given site condition.
- Define buildability and quantify its parameters.
- Formulate a method to optimize slab frame bridges regarding investment cost, environmental impact, and buildability.
- Comparative analysis with the reference object to evaluate optimization.
- Develop a method to find groups of slab frame bridges with identical structural components and study the effect of grouping with regards to investment cost, environmental impact, and buildability.

1.4 Limitations

- Site conditions and load values for the SBD analysis were based on the reference object.
- Foundation design is limited to open and closed shallow foundations, i.e. piled foundation was not considered.
- Dynamic analysis was not considered.
- Only one set of conditions were evaluated, with a set of conditions referring to geotechnical conditions, in-plane curvature of the bridge, span lengths, levels for the highest and lowest parts of the bridge, and the number of railway tracks on the bridge.
- Only individual reinforcement bars and sheer stirrups were considered for the analysis, i.e. reinforcement cages and carpets were not considered.

1.5 Methodology

The first phase of the thesis involved a literature study that reviewed previous research on SBD. Furthermore, the implications of standardized bridges were investigated and reference objects were gathered. Finally, different optimization methods and different ways of using Computer-Aided Engineering (CAE) to analyze large sets of alternatives were evaluated.

The second phase involved formulating a method to reach the objectives of the thesis. The method choice culminated in a Finite Element Method (FEM) analysis where several geometric combinations were iterated through. The results of the FEM analysis were evaluated based on selected object functions in order to obtain optimized solutions. Furthermore, the possibility of finding groups, bridges with identical components, and the potential of grouping was evaluated according to the repeatability principle.

2

Theory

This Chapter contains information regarding different design processes, slab frame bridges, standardized bridges, optimization processes, and different methods of computer-aided engineering.

2.1 Design processes

There are various design approaches in the construction industry, each with its own methodology and application. The PBD process is commonly used as the main design process in structural engineering today (Parrish et al., 2007). PBD could be seen as a linear iteration design process where the structural engineer starts the process according to preferences and step-wise advances and iterates until a finalized solution is achieved (Parrish et al., 2007). Another design theory is SBD, where every possible solution is kept open until the last possible moment, enabling late decisions. Distinctions between SBD and PBD are presented in the following sections.

2.1.1 Point-Based Design

PBD calls for an iterative design process, as the first proposed solution may not compile with the given problem and is even more iterative if a late design change is given (Parrish et al., 2007). Depending on where the engineer starts the solution, the design process could be very time-consuming based on the iterative approach where one tries to satisfy most stakeholders by a trial-and-error process (Y.-E. Nahm & Ishikawa, 2006). The process of PBD is visualized in Figure 2.1.

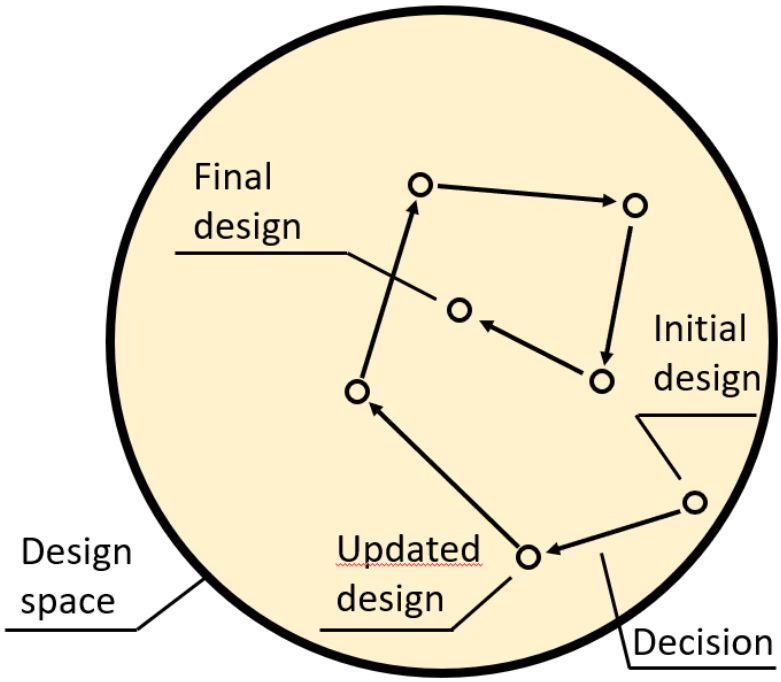

Figure 2.1: *Visualization of PBD, the design space, and the process.*

Figure 2.1 shows the design space where an initial design is chosen based on preferences. Further, a decision is taken that impacts the design such as an update is needed. This process continuous until a final design is chosen and no more updates are needed. PBD process is iterative and depending on how many decisions or late changes are made, the design could be further updated.

A major dilemma of the PBD method is that a feasible solution is quickly achieved as only one solution is needed, thus there is a major risk that more optimal solutions are lost (Y.-E. Nahm & Ishikawa, 2006). Consequently, there is a risk that the solution will never be found as the engineer could choose a faulty design space.

2.1.2 Set-Based Design

SBD has been used for several years in other industries and is mostly distinct as the main design process used by the car manufacturer Toyota (Ward et al., 1995). The design process of SBD is easiest observed as a set of all possible combinations in the design space which is funneled down through a number of "constraint gates", where non-viable solutions are sorted out, and at the end of the funnel all possible solutions are left. This design process allows for late design change with minimal efforts, as these late changes could be seen as a new funnel (Parrish et al., 2007).

The step process of SBD is generally defined as three steps, (1) Create the design space, (2) Identify constraints and combinations, (3) Commit to final solution (Parrish et al., 2007). The initial design space contains all possible solutions but it is usually beneficial to define constraints to reduce the number of start solutions. For structural projects, the design space constraints are predominately geometrical or upper and lower bound dimensions, e.g. geotechnical conditions or slab thickness. Constraints are divided into soft and hard, where hard constraints are usually defined as the current norms such as Eurocode. Soft constraints differ from hard as they are negligible and often built on stakeholders' preferences. When the funneling process is finalized one or more plausible concepts should exist, by weighing their advantages and disadvantages the engineer commits to a final solution (Parrish et al., 2007).

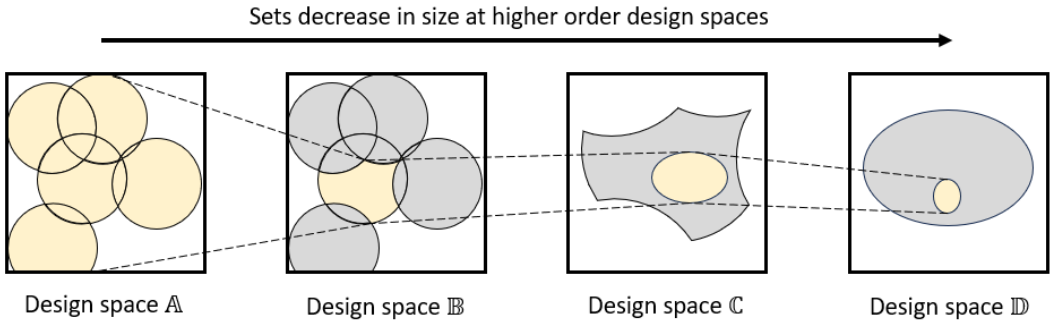

Figure 2.2: *Visualization of the SBD process including the different design spaces and "constraint gates".*

Figure 2.2 visualizes the process of SBD where an initial design space is chosen. A decision is taken and by applying a "constrain gate" the initial design space is funneled down into a higher-order design space and the number of available solutions is reduced. This process continuous until no more decision or late changes is needed. Theoretically, a small set of solutions still remains in the highest order design space, and the engineer could then weigh the advantages and disadvantages and commit to a final solution (Parrish et al., 2007).

The American Institute of Architects (AIA) has introduced Integrated Project Delivery (IPD), IPD's main task is to ease collaboration in the construction industry and increase productivity (AIA, 2007). Furthermore, IPD promotes concert between different stakeholders, especially in the design and construction phase and the methods described clearly correlates to the SBD way of thought. AIA (2007) divides a project into seven sub-processes: Conceptualization, Critera Design, Detailed Design, Implementation Documents, Agency Coord/Final Buyout, Construction, and Closeout. The difference between traditional and integrated design is easiest visualized with a "MacLeamy curve" in Figure 2.3.

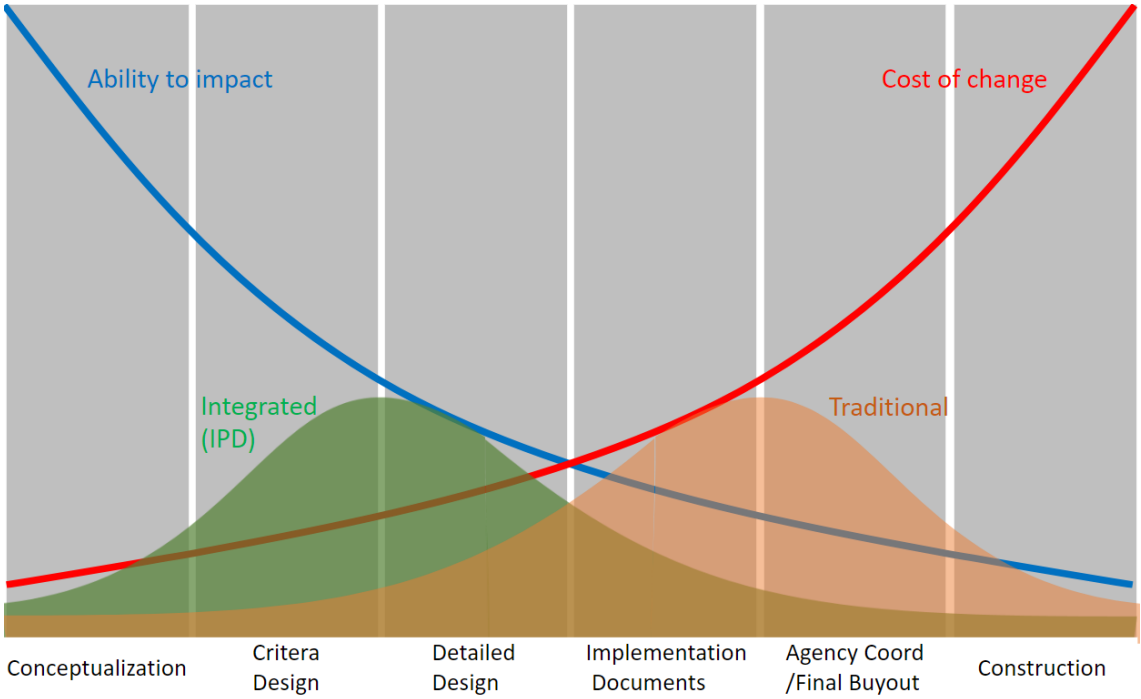

Figure 2.3: *Illustration of a "MacLeamy curve" for IPD according to AIA (2007).*

As visualized in Figure 2.3 integrated design emphasizes a higher workload earlier in the projects, thus the ability to impact is higher and the cost of change is lower compared to traditional design. Following this further it is important that all stakeholders are allowed into the project early so they themselves can impact the design space (AIA, 2007). AIA (2007) points out that IPD is only based on theory but that some benefits of implementing it could be: higher quality, shorter construction time, and more satisfied stakeholders. Further, applying the theory of integrated design on PBD and SBD is visualized in Figure 2.4

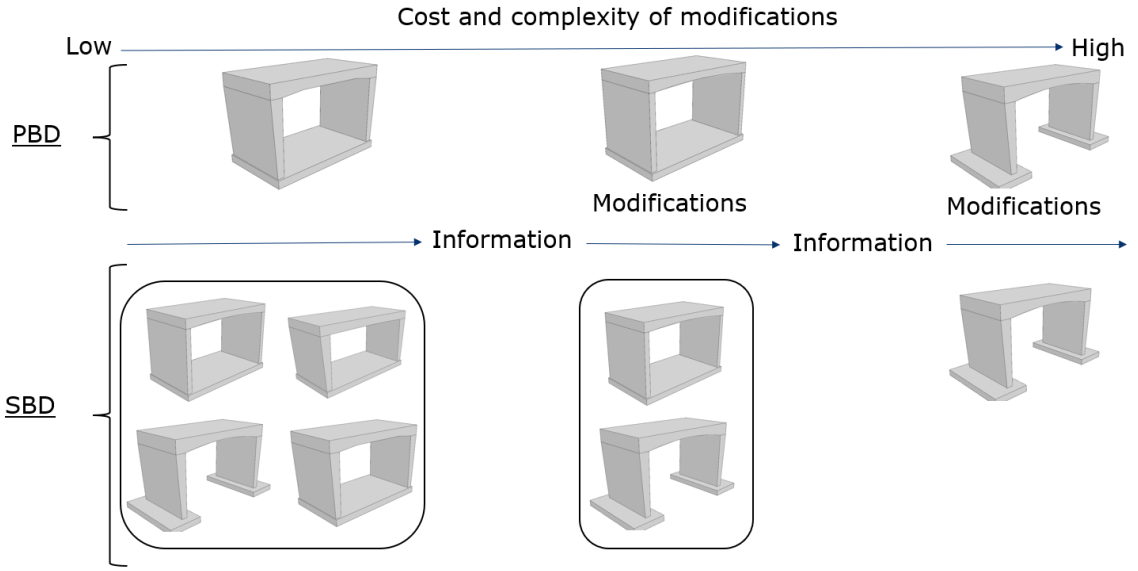

Figure 2.4: *Difference between PBD and SBD throughout the design processes.*

Figure 2.4 shows the implementation of using PBD or SBD in a general structural design process where the need for late changes is assumed. In the first step of the process an initial design is chosen for PBD and multiple designs are chosen for SBD. At the beginning of the design process the cost of designing multiple bridges results in a high initial cost for SBD. During the design process, some information is received which changes the conditions of the process, thus the initial design for both PBD and SBD needs revision. For PBD the revision results in an updated design, for SBD only a new "constraint gate" is necessary. As the design process has advanced, the cost of change increases according to the theory of IPD. For SBD, all design alternatives are already available, which means that it is only necessary to reduce the design space. At the end of the process, the high initial cost of the SBD should have been beneficial as the cost of updating the design several times would have been more expensive in the end.

SBD has evolved in combination with CAE into what is called Set-Based Parametric Design (SBPD) (Y. E. Nahm & Ishikawa, 2006). Briefly, SBPD could be explained as using the methodology of SBD in a parametric model, a more extensive explanation is concluded in Chapter 2.2.

2.2 Parametric design

Designing using parametric design is a common term, but there are no exact definitions of what parametric design actually means, even though the most common interpretation involves geometric constraints. According to Steinø and Veirum (2022), parametric design can be defined as a set of constraints that in turn define an object. In parameterized design, it is common to define three different types of constraints (Steinø & Veirum, 2022):

- **Dimensional constraints** are constraints built on keeping a set distance between two objects, e.g. keeping the concrete cover when modeling reinforcement.
- **Geometric constraints** focus on keeping a geometric relation between two objects, e.g. keeping a perpendicular angle between the intersection of two objects.
- **Non-geometrical constraints** are not geometry-related constraints but focus more on the engineering part of the problems, e.g. material data or manufacturing requirements, and are more relevant for SBPD.

The advantages of parameterized design are many, Steinø and Veirum (2022) reports that it simplifies the process of making late decisions as the model can be easily edited by rewriting constraints. Furthermore, it allows modeling to start already in the conceptual phase and not in the design phase. Additionally, Steinø and Veirum (2022) observes that parameterized design can be used to check whether simple requirements work in the conceptual phase, such as "Does this fit?" or "Can we move this?".

Set-Based Parametric Design SBPD is the combination of using parametric design in combination with SBD. As the SBPD is relatively new, there are no rules on how to use it and different authors and institutes have defined different methods to implement it. Y. E. Nahm and Ishikawa (2006) identifies two new models, the preference Set-Based Design model and the design information solid model to achieve SBPD. Rempling et al. (2019) investigates the use of "Critera design" in order to obtain an SBPD-model. In short, SBPD can be explained as using the three constraints shown above in combination with an objective function inside the active design space to generate a set of viable solutions.

2.3 Slab frame bridges

Approximately 75% of the existing bridges in Sweden have a shorter span length than 20 m (Uppenberg et al., 2017). Out of these bridges, 46% are slab frame bridges (Uppenberg et al., 2017), making slab frame bridges the most widely used bridge type in Sweden (Swedish Transport Administration, 2008).

The structural layout of a slab frame bridge consists of frame legs attached to one foundation slab or two separate foundation slabs (Swedish Transport Administration, 2008). A bridge deck connects to the frame legs and carries the vertical forces down to the foundation through primarily bending of the bridge deck. Contrary to a slab or beam bridge, the bridge deck of a slab frame bridge is interconnected with the frame legs, creating rigidly connected frame corners (Uppenberg et al., 2017). Lastly, wing walls are attached to the frame legs, with the prime purpose of retaining mass from the surrounding earth-filling material (Solat Yavari, 2017). Figure 2.5 shows an example of the structural layout of a single-span slab frame bridge.

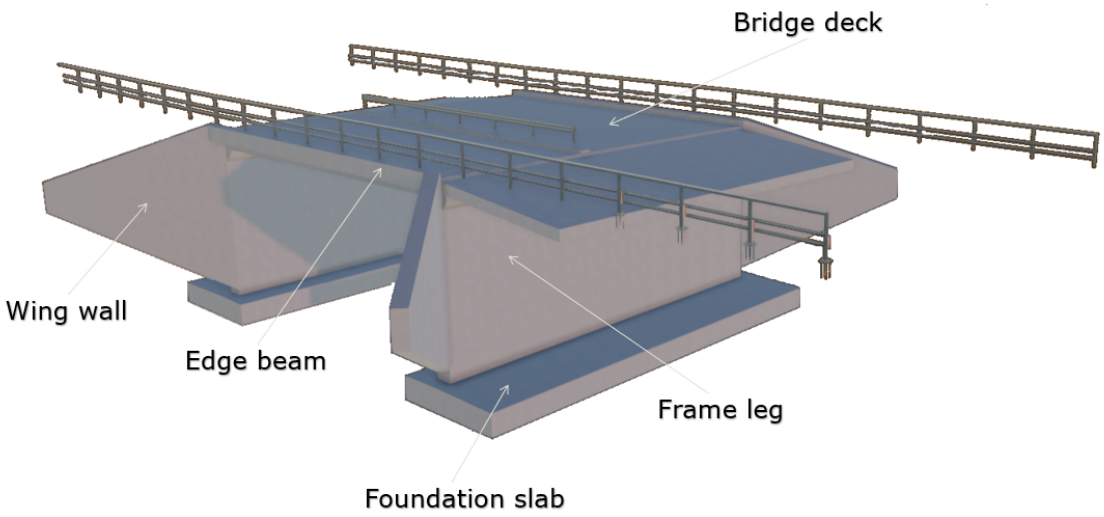

Figure 2.5: *Structural layout of single-span slab frame bridge.*

Slab frame bridges are made of reinforced concrete which are constructed either with or without pre-stressed reinforcement and are most of the time single-spanned (Swedish Transport Administration, 2008). Depending on the pre-stressing level, single-span lengths can reach up to approximately 35 m. However, designing slab frame bridges with spans over 20 m is not considered to be economically (Karlsson, 2022). The primary reason for choosing a slab frame bridge is the overall simple geometry and details, which enable good buildability. Other advantages of slab frame bridges are low construction height along with being adaptable to many different geotechnical conditions.

2.3.1 Structural components

A slab frame bridge consists of a superstructure and a foundation structure (Samuelsson & Wiberg, 1990, pp. 319–320). The foundation slab together with the frame legs and the wing walls form the so-called *foundation structure* while the bridge deck together with edge beams forms the *superstructure*. A slab frame bridge acts as a framework, which means that the different structural, geometrical, and material combinations that can be achieved between the superstructure and the foundation structure affect the structural behavior of the bridge. The following subsections describe the different structural components of a slab frame bridge more in-depth.

2.3.1.1 Foundation slab

The foundation of a slab frame bridge can consist of one or two slabs connected to the frame legs, i.e. closed or open foundation (Solat Yavari, 2017). The decisive factor for choosing an open or a closed foundation is the geotechnical conditions at the site of construction. Closed foundations are preferred in soft clays when piling is required and/or stability against horizontal loads is necessary (Karlsson, 2022). Other reasons for choosing a closed foundation can be if the bridge deck needs to be launched on-site, or if the combined size of the individual slabs for an open foundation exceeds the size of an equivalent closed slab. (Karlsson, 2022). Figure 2.6 shows the structural layout difference between a closed and an open single-span slab frame bridge.

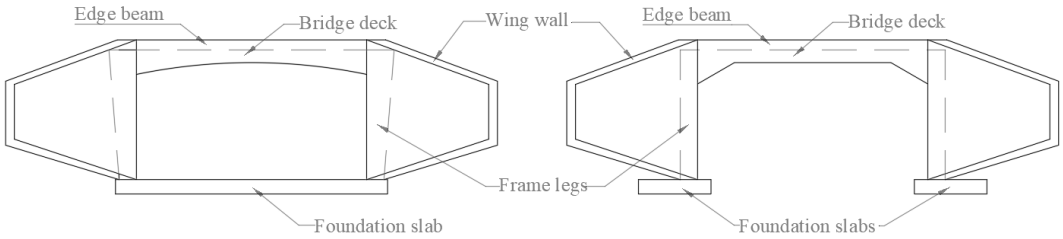

Figure 2.6: *Conceptual structural layout of closed and open foundations for slab frame bridges.*

2.3.1.2 Frame legs

Frame legs serve multiple functions in a slab frame bridge. The primary function of the frame legs is to carry down the vertical loads from the superstructure to the foundation and retain the earth pressure from the road/railway embankment (Solat Yavari, 2017). Frame legs are built either straight or inclined, meaning constant or linearly varying cross-section (Karlsson, 2022), see Figure 2.6. The height of the frame legs depends on the desired free height of the bridge, but also the geotechnical conditions and the chosen foundation method. A pile-supported foundation on soft clays requires a greater height of frame legs compared to a closed foundation on friction material. The height of frame legs for non-prestressed slab frame bridges

is typically around 16% of the bridge deck span. With a higher prestressing level, the frame legs can reach a height of 25% of the bridge deck span. Non-symmetrical height of the frame legs is not preferred since equilibrium between the horizontal earth pressure and the vertical loads is not achieved. Consequently, greater stresses arise in the shorter frame leg for non-symmetrical high frame legs (Karlsson, 2022).

The connection between the frame legs and the foundation slab is often considered to be pinned in design (Swedish Transport Administration, 2008). Because of this, slab frame bridges must theoretically be moment rigid at the connection between the superstructure and the foundation structure in order to take horizontal loads (Samuelsson & Wiberg, 1990, pp. 19–21), even though the active earth pressure decreases the lateral movement of the frame. This is achieved by fixating the deck and the frame legs with continuous reinforcement and casting the two structural components simultaneously, providing stiffness in the frame corners (Uppenberg et al., 2017).

2.3.1.3 Haunches

An economical way to achieve sufficient stiffness in the frame corner connection is to use haunches (Samuelsson & Wiberg, 1990, p. 27). Haunches are size increments in the frame corners between the superstructure and the foundation structure. A haunch can either be shaped into a parabolic or linearly increase in cross-section thickness (Swedish Transport Administration, 2008), see Figure 2.7. Haunches attract moments to the frame corners and reduce the moment in the most often critical reinforced mid-span of the bridge deck while also increasing the overall shear force capacity of the cross-section.

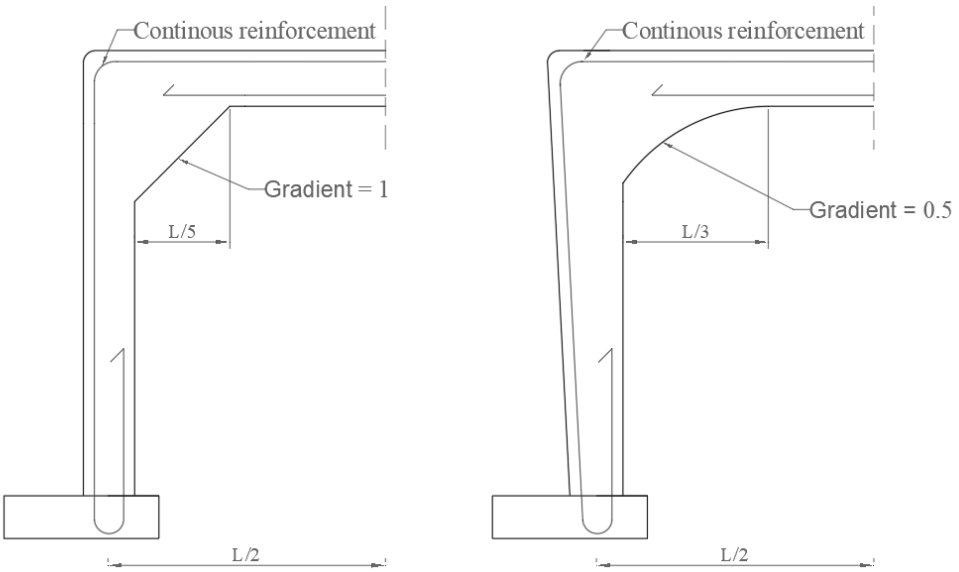

Figure 2.7: *Conceptual design comparison between linear and parabolic haunch for straight and linear increasing frame legs.*

Slab frame bridges are rarely constructed without haunches and all pre-stressed slab frame bridges are haunched for practical reasons (Karlsson, 2022). For slab frame bridges with spans over 10-12 m, haunches provide economic benefits. The typical length of a haunch is 20% of the span length but may vary depending on the type of haunch and capacity requirements. The gradient of the haunch is the slope of the depth change and is determined by designer choice. A large gradient, i.e. greater max cross-section height, can be used when decreased shear force and shear reinforcement in a cross-section is sought after (al-Emrani et al., 2011, B173-B190). Even if haunching is not deemed necessary, it is usually done for aesthetic reasons (Karlsson, 2022).

2.3.1.4 Bridge deck

The bridge deck consists of a slab, composed of reinforced concrete with homogeneous thickness or with cutouts, e.g. hollow core or ribbed beams, which are used to achieve longer spans. (Swedish Transport Administration, 2008), see Figure 2.8. Slab frame bridge decks are commonly constructed homogeneously due to the negative buildability aspects of the cutouts during construction. (Karlsson, 2022). Since slab frame bridge decks do not rely on beams that have greater depths than slabs, the bridge deck is often vastly reinforced to keep the structural height low. As previously mentioned, haunching redistributes the moment away from the mid-span, which makes haunching useful for reinforcement distribution design.

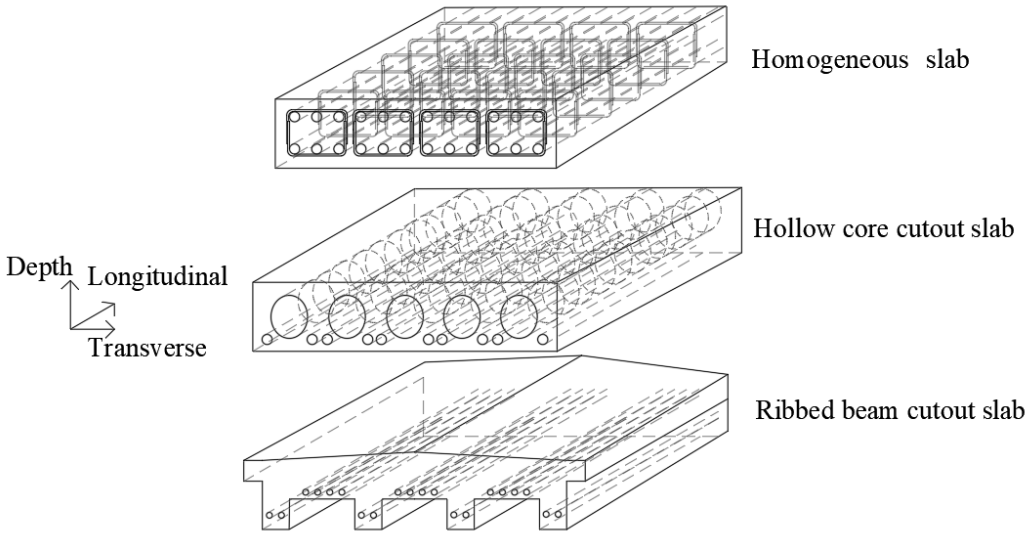

Figure 2.8: *Conceptual design of different bridge deck layouts.*

Since the bridge deck of a slab frame bridge is only supported by the frame legs on two opposite sides, the slab can be considered a one-way slab (Engström, 2014, p. 1). If only uniformly distributed loads were to occur on the bridge deck, all loads would theoretically be carried in the longitudinal direction of the deck, thus main reinforcement would only be required in the longitudinal direction. Since

design loads for road and railway bridges require point load analyses (*SS-EN 1991-2:2003*, n.d.), the slab must be designed to carry loads in the transverse direction as well, which means that reinforcement will be required in both in-plane directions of the slabs (Engström, 2014, pp. 2–20). Wider slabs result in larger transverse reinforcement amounts while a narrow slab operates more like a beam, consequently requiring less transverse reinforcement.

2.3.1.5 Edge beams

The function of an edge beam for a slab frame bridge can to a degree be compared to the function of a curbstone on a street road. Visually, the edge beam separates the roadway from the rest of the bridge deck but also serves important functional aspects such as providing fastening and space for railings, light posts, and drainage systems (Yaqoob, 2017). Different bridge types and traffic types affect the design of the edge beams and their function (Karlsson, 2022). For railway bridges, in addition to its usual function, the edge beam shall serve as derailment protection and support for ballast, rails, and sleepers. Due to the variety of functional requirements that edge beams shall fulfill, the structural geometry of edge beams can be designed in many different ways, see Figure 2.9. The sizing of edge beams is generally designed based on load-bearing, anchoring, and spacing requirements for the different functional attachments. The size increase of the cross section due to installations also adds stiffness to the superstructure which is favorable for the structural behavior of the bridge deck (Yaqoob, 2017).

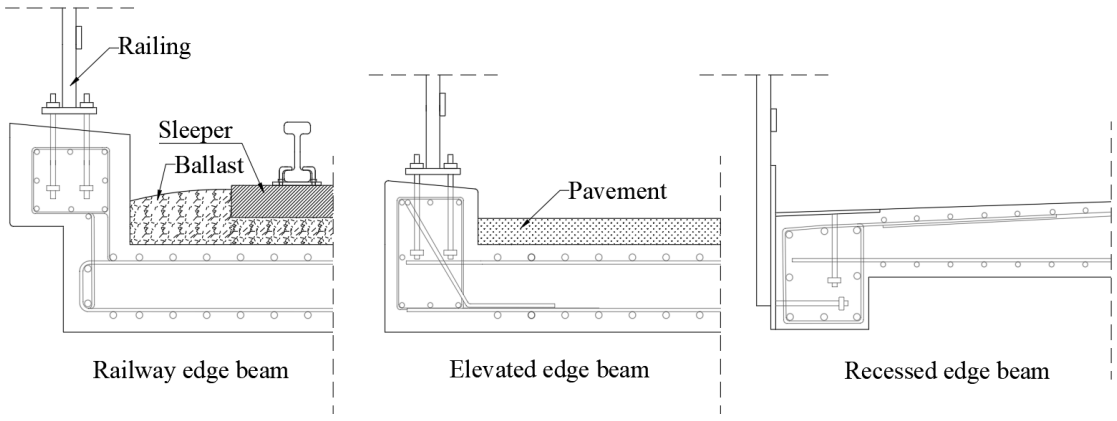

Figure 2.9: *Conceptual design of different edge beams.*

The position of the edge beams makes it the most replaced and repaired structural element on a slab frame bridge (Yaqoob, 2017). This is due to the increased exposure to degradation processes compared to other structural elements. Edge beams are exposed daily to a wider range of degradation factors such as road salt, water, and traffic impact hits that increase the risk of degradation damages such as reinforcement corrosion, frost damage, and mechanical friction degradation. Due to the need for repairs and replacements, the design of bridge decks must take into account scenarios where the edge beams are removed and the traffic load is still active. Consequently, edge beams are not considered as favorable stiffness-contributing

load-bearing elements in a global structural analysis (Pettersson & Sundquist, 2014). Even though the stiffness of the edge beams is neglected, the weight and geometry of the edge beams are considered in global structural analysis as well as local cross-section analysis of stresses (Pettersson & Sundquist, 2014).

2.3.1.6 Wing walls

Attached to the frame legs are wing walls which are designed for the main purpose of retaining the soil or back-fill material adjacent to the frame legs (Swedish Transport Administration, 2008). Wing walls are usually angled out of the longitudinal direction of the bridge but can also be placed perpendicular to the frame legs, parallel to the longitudinal direction of the bridge (Karlsson, 2022). The reason for choosing an angle on the wing walls is to reduce the length of the wing walls which reduces the amount of material for edge beams and fixings such as railings and lighting posts. On the other hand, angled wing walls result in decreased parallel tension in the frame legs which is favorable for crack control and the overall reinforcement design of the frame legs. Parallel wing walls are mainly used in case of increased soil pressures arising from movement in the embankment adjacent to the frame legs. The choice of geometry of the wing walls depends mainly on the geotechnical conditions and the height of the embankment. The thickness of the frame legs and connecting reinforcement should also be taken into consideration due to the two structural components being normally cast together.

By connecting the wing walls and frame legs with continuous reinforcement and casting them simultaneously, a monolithic connection is formed which impacts the stiffness and overall structural behavior of the slab frame bridge (Ekman & Sandin, 2018). The stiffness contribution from the wing walls attracts load, which leads to increased local stresses in the frame leg corners that increase the reinforcement amount in both the frame legs and the wing walls. Wing walls are traditionally not considered as stiffness-contributing structural elements during the global structural behavior of slab frame bridges. Instead, the structural element is designed separately for mainly horizontal geotechnical loads. With the rising interest in 3D FEM modeling for slab frame bridges, wing walls can be considered during global structural analysis which leads to different reinforcement layouts compared to traditional design. Although, increasing the computational time and the complexity of the reinforcement design.

2.3.2 Production

The vast majority of slab frame bridges in Sweden are produced by cast-in-situ concrete at the designated bridge site (Harryson, 2008). Internationally, it has become more common to prefabricate the reinforced concrete bridge components and assemble them on-site. Using prefabricated elements reduces the construction time and cost due to less labor being needed at the construction site during the casting of the bridge. The reason for the less shown interest in prefabrication of slab frame bridges in Sweden is due to traditional design approaches such as PBD. The increased logistical complexity in combination with decreasing flexibility in the late

stages during the design phase, are two unfavorable actions for PBD arising from prefabrication design. In addition, large infrastructure projects, such as North Bothnia Line (NBL), contain many bridges. However, the construction of bridges only makes up a fraction of the total investment cost of the whole project. Thus, less emphasis is put on decreasing the production time and cost of bridges by prefabrication. Furthermore, the ability to cope with late design changes is prioritized, resulting in prefabrication being deemed suboptimal to cast-in-situ methods.

The production of a typical open and a typical closed slab frame bridge in Sweden is done by cast-in-situ methods (Gapinski, 2023). The construction process begins with the excavation of the top soil layers and backfilling using aggregate. Temporary concrete form-work is then carried out for the slab or slabs if the foundation is designed to be closed or open. Longitudinal and transverse straight bottom reinforcement is then placed first before complementary anchorage and shear reinforcement is placed around the edges of the form-work and adjacent to the frame legs. Bent vertical reinforcement is then tied underneath the bottom transversal reinforcement to be used as the continuous reinforcement connecting to the frame legs after casting the bottom slab. Straight longitudinal and transversal top reinforcement is installed to complete the reinforcement of the foundation slab. Excavation, concrete form-work, and reinforcement for a closed and open foundation slab are visualized in Figure 2.10. Lastly, the foundation slab is cast and the form-work is demolished after an appropriate period of time before continuing with proceeding construction moments.

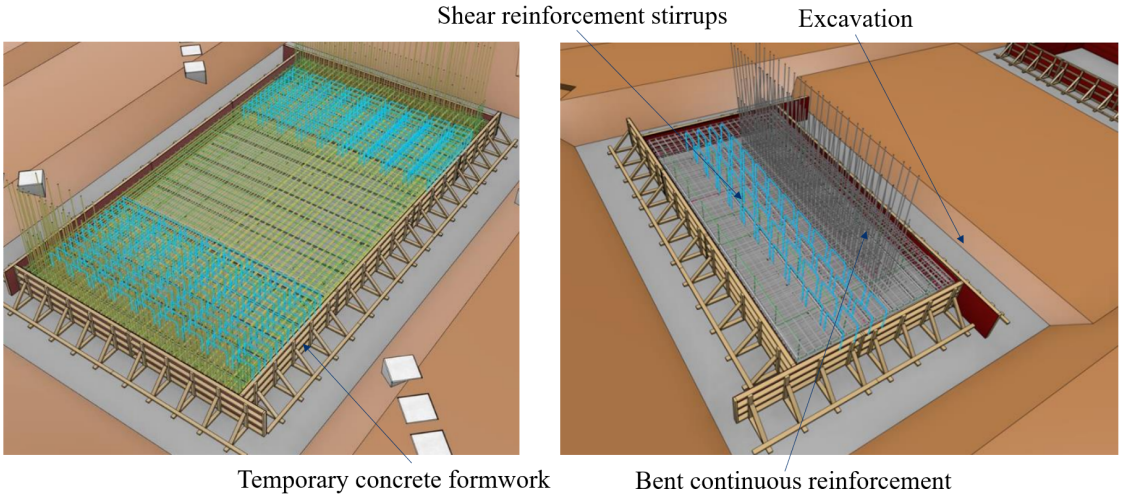

Figure 2.10: *Form-work and reinforcement installations for closed and open foundation slab (Gapinski, 2023).*

After the bottom slab/slabs have hardened and reached an acceptable level of strength, the temporary structures to the superstructure are installed (Gapinski, 2023). Tall moldings for frame legs and wing walls are mounted and braised against the bottom slab. Temporary support structures for the bridge deck and scaffolding for the workers are installed. Continuous reinforcement overlapping with the vertical reinforcement from the bottom slab and the main longitudinal bridge deck reinforcement are installed as well as transverse reinforcement for the frame legs.

Shear reinforcement consisting of stirrups is mounted at the bottom of the frame legs, wrapping around the main reinforcement of the frame legs. The wing walls are thereafter reinforced before the main longitudinal reinforcement for both the bridge deck slab and the edge beam are placed. Stirrups along with necessary installations such as electrical and lighting posts are installed in the separate edge beam form-work. Anchorage and shear reinforcement stirrups are placed around the edges of the bridge deck and close to the frame leg supports. Transverse reinforcement is then placed over the bridge deck before the whole superstructure and frame legs are cast simultaneously. Temporary form-work and scaffolding's along with reinforcement layout of the superstructure is visualized in Figure 2.11.

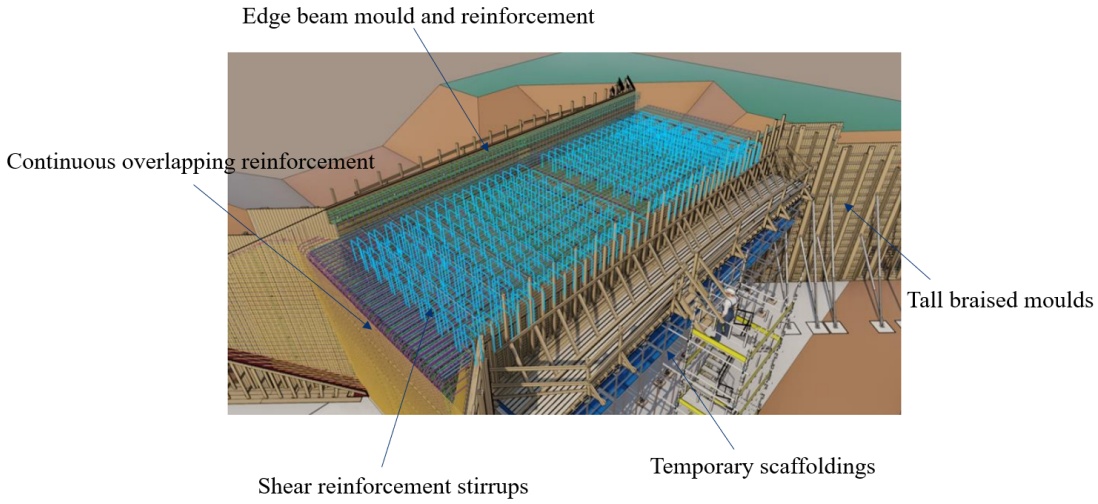

Figure 2.11: *Form-work and reinforcement installations of slab frame bridge superstructure (Gapinski, 2023).*

After the superstructure has been cast, the form-work is de-molded and the temporary scaffoldings are dismantled before the wing walls and frame legs can be back-filled (Gapinski, 2023). The last stage of production involves applying potential protection coatings such as graffiti and chloride protection and installing installations such as lighting posts and railings.

2.4 Buildability

The term buildability has been expressed and summarized in many different ways in previous research. Simonsson (2011) simply summarized the term as "the design for ease of construction". Considering buildability can often be related to decreasing construction time and cost, but may include other aspects such as improving safety and ergonomics for construction workers and improving the final result of the project (Simonsson, 2011). Given the importance of reducing the carbon footprint of modern infrastructure such as bridges, reducing construction time can be considered one of the more important aspects of buildability because of the reduced

carbon dioxide emissions due to reduced traffic and energy usage (Simonsson, 2011). Furthermore, designers that implement a buildability mindset during early design processes can increase the previously mentioned advantages up to 20 times compared to if buildability were not considered.

Good buildability is not only achieved by means of technical design choices but rather by obtaining a good buildability mindset throughout all parts of the project by including all of the stakeholders (Griffith & Sidwell, 1995). Buildability can be separated into two blocks, technical and non-technical buildability, which can be internally subdivided into specific buildability aspects presented in Figure 2.12. Designers such as structural engineers naturally tend to contribute to the technical buildability factors rather than the non-technical factors.

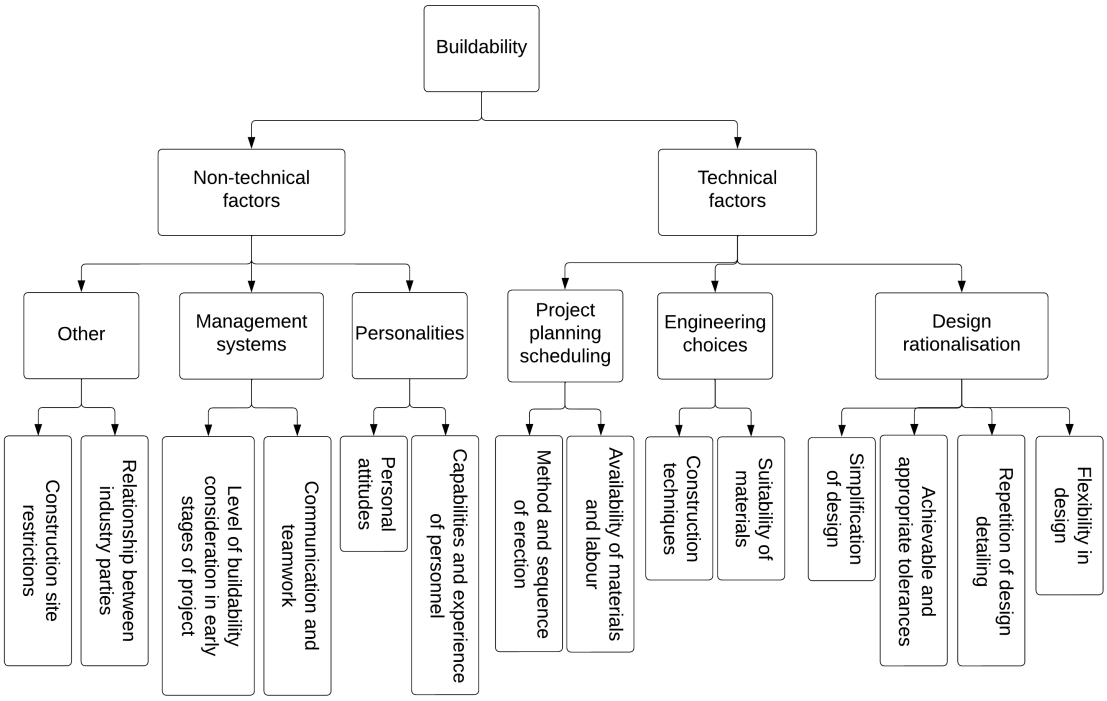

Figure 2.12: *Technical and non-technical buildability aspects (Griffith & Sidwell, 1995).*

The key contributor to well-implemented technical buildability in reinforced concrete structures is the number of reinforcement bars placed in a structure (Fernández-Mora & Yepes, 2020). Individual rebar installations that occur in cast-in-situ concrete bridges are time-inefficient. Research has shown that the use of prefabricated rebar-carpets and cages decreases the installation labor time up to 80% (Simonsson, 2011). Straight bridges should always be sought after due to the curvature of bridges affecting the reinforcement installation time negatively due to the increased rebar-fixation complexity created by the slightest curvature. Ekström et al. (2019) pointed out the specific importance of minimizing or completely skipping the use of shear reinforcement as well as considering the type and size of rebar. Shear reinforcement often consisting of stirrups, being highlighted in Figures 2.10 and 2.11,

complicates reinforcement installations when incorporated together with straight bars which decreases the technical buildability (Bergenram & Ulander, 2023). An increase in concrete thickness can be beneficial for the buildability of a structural element to avoid shear reinforcement. However, this also increases the volume of concrete, leading to a greater overall climate impact. Larger rebar diameters have been shown to increase buildability due to less installation time from needing to place fewer individual rebars for the same amount of steel area if smaller rebar diameters were used.

In addition to reinforcement installation, cast-in-situ concrete pouring has shown to be a challenging technical and non-technical buildability aspect because the usability of the material is time-dependent (Mahzuz et al., 2020). Efficient planning, communication, and technical aspects are required to achieve good buildability before, after, and especially during casting. The choice of concrete strength class has conflicting properties between buildability, cost, and environmental impact (Sonar, 2020). High-strength concrete is less workable during casting which leads to decreased buildability while also having a greater environmental impact from the increase in cement content. In contrast, higher concrete strength classes can have a positive effect as less material is needed due to its increased capacity which can be cost and environmentally beneficial. A possible alternative to increase the buildability of concrete without decreasing the capacity is the use of self-compacting concrete (SCC) (Siddique, 2019). The addition of chemical admixtures increases the workability of fresh concrete and decreases the demand for human labor, such as the frequent use of vibration required for traditional concrete. Simonsson (2011) estimated a potentially 65% decrease in casting time using SCC compared to traditional concrete. However, the increase in buildability often comes with an increased economic investment cost (Simonsson, 2011). The use of SCC also requires high demands on non-technical buildability factors such as personal attitudes and capabilities/experiences of SCC use (Siddique, 2019).

An influencing factor in the reinforcement layout and concrete usage is the geometry of a structural element. The search for materially optimized structures regarding concrete can lead to complex geometries resulting in longer reinforcement and concrete form-work installation time (Simonsson, 2011). Keeping structural elements for slab frame bridges straight with constant thicknesses while simultaneously avoiding slender structures reduces labor costs (Solat Yavari et al., 2016). Increased material usage can create simpler geometries benefiting buildability. An example of geometric modifications to increase the buildability of a reinforced concrete structure is shown in Figure 2.13.

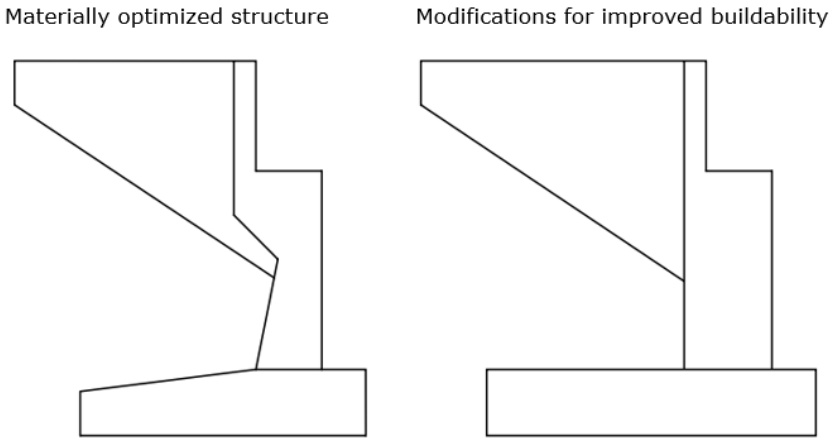

Figure 2.13: *Conceptual modification to improve buildability of reinforced concrete structure (Simonsson, 2011).*

2.4.1 Standardization and repeatability

Technical buildability for structural engineers concerns appropriate construction techniques and choice of material for the design of single bridges (Griffith & Sidwell, 1995). Using the concepts of design rationalization, seen in Figure 2.12, can lead to improved buildability, lowered construction time and costs for large infrastructure projects, e.g. North Bothnia Line Project (NBLP). Construction of structural components can be repeated at multiple construction sites, improving the buildability and decreasing the project's global construction time and cost through standardization of bridge components (Lagerkvist, 2023). The implementation of standardized bridges further explained in Chapter 2.5 is an attempt to insert a repetitive construction methodology by constructing the exact same bridge concept consecutively at different sites during the same project. By repeating the same construction processes, the productivity will increase based on the learning curve phenomenon (Simonsson, 2011).

According to Simonsson (2011), an increased number of identical structures within a project reduces construction time arising from the learning curve of the workers throughout the project. The reason is that experience is gained from previously constructed components, resulting in a successively faster building process. Additionally, concrete form-work and blueprints can be reused at the next construction site if standardized components are used. The relation of labor time and the number of repeated structural components referred to as the learning curve is presented in Figure 2.14. How steep and effective a learning curve is during construction is based on several other non-technical buildability factors such as previous experience and team-moral of the construction team (SaravanaPrabhu & Vidjeapriya, 2021).

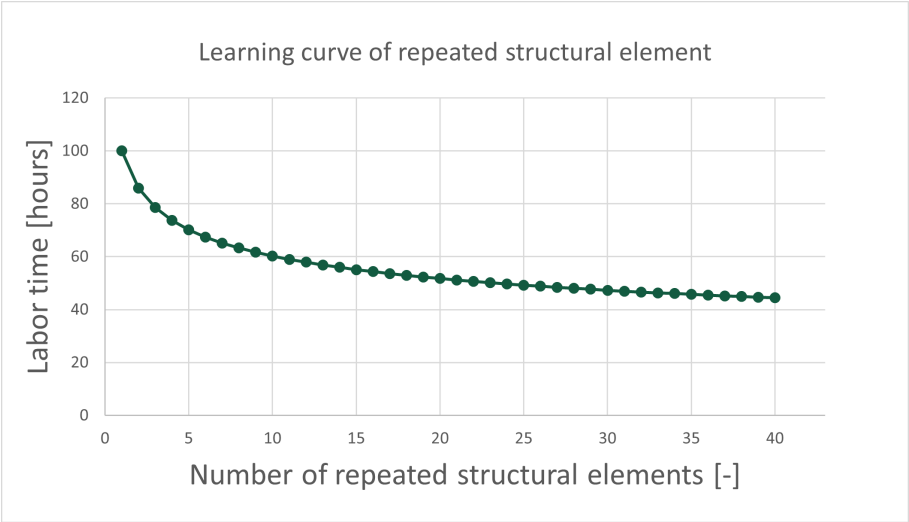

Figure 2.14: *Learning curve for reinforced concrete structural component (SaravanaPrabhu & Vidjeapriya, 2021).*

Figure 2.14 shows that the learning curve is decreasing according to a power law decay. At the start of the project, the productivity is seen increasing quickly as workers gain experience and find effective ways of construction (Simonsson, 2011). After the initial learning phase, the learning curve flattens out as the most optimal construction process has been achieved and construction routines are the reason for the continuation of reduced labor time.

Standardized structural elements in buildings have been tested for more than 20 years and shown to increase the buildability of the project due to the increase in repetitive work (Pheng & Abeyegoonasekera, 2001). Meanwhile, the productivity in the Swedish construction industry today has barely increased during the last 20 years, and standardizing individual structural components of slab frame bridges would increase the overall buildability of large infrastructure projects (Lagerkvist, 2023).

2.5 Standardized bridges

Starting in 2020 STA began planning to expand the current railway network in northern Sweden from Umeå to Luleå, this new railway is called North Bothnia Line (NBL) (Swedish Transport Administration, 2023). To increase efficiency, STA has come up with a report that aims to test the possibility of standardized bridges (Bruneby et al., 2023). STA estimates that a total of 250 bridges will be built along the NBLP, and most of the bridges are short and non-complex, making it a good trial project for standardizing bridges (Bruneby et al., 2023).

At the Swedish Bridge Builders Day in Gothenburg 2024, O. Bruneby and P. Veding (personal communication, January 29, 2024) described standard bridges as a complete bridge-product, containing pre-calculated structural component drawings, cost spreadsheets, and production descriptions that can theoretically be constructed

with minimal detail design. O. Bruneby and P. Veding (personal communication, January 29, 2024) further stated that the goal for the STA is to create a catalog of pre-package bridge solutions for different boundary conditions and design parameters such as span lengths and geotechnical conditions. Since practical infinite combinations of boundary conditions and design parameters exist, standardized bridges are designed on the principle of "adapt the site to the bridge" to achieve a realistic number of standardized bridges that are cost-effective with good buildability.

The STA predicts that the use of standardized bridges can decrease the detail design cost by 70% and the cost of construction by 20% (O. Bruneby & P. Veding, personal communication, January 29, 2024). At the current time, three examples of standardized bridges have been released by STA and all are slab frame bridges (Bruneby et al., 2023). These bridges are designed using traditional PBD for one set of conditions along the NBL. NBLP was considered to be such a massive project that investing time into using the same type of conditions for all sites would be beneficial for the overall project (O. Bruneby & P. Veding, personal communication, January 29, 2024).

2.5.1 Reference object

Intending to optimize through SBD, a reference object is preferable to use as a basis for comparison to determine whether an improvement or degradation of buildability, carbon emissions, or investment cost has been made.

At the current stage, three different types of standardized bridges have been designed and approved for implementation in the NBLP by STA. A 12 m and a 16 m railway bridge and a 16 m road bridge have been designed. The two railway bridges are single-track straight slab frame bridges. Sketches of the two railway bridges are presented in Figure 2.15 with their geometric dimensions tabulated in Table 2.1.

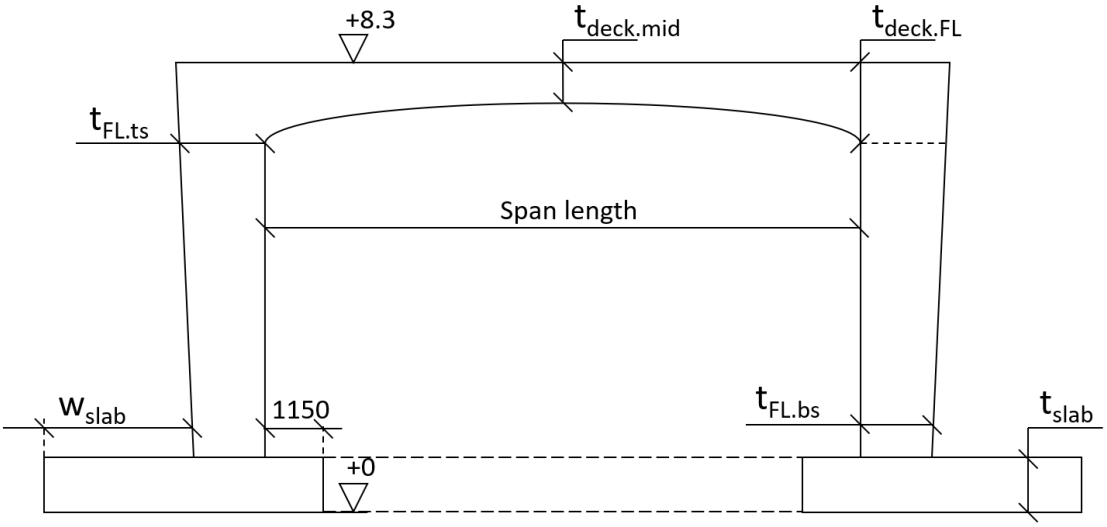

Figure 2.15: *Sketch of the reference objects.*

Variable	Unit	16 m bridge	12 m bridge
Foundation slab			
Configuration		Open	Closed
t_{slab}	[mm]	900	830
w_{slab}	[m]	2.75	-
Frame legs			
$t_{FL.ts}$	[mm]	1200	800
$t_{FL.bs}$	[mm]	700	800
Deck			
$t_{deck.FL}$	[mm]	1300	1200
$t_{deck.mid}$	[mm]	950	800

Table 2.1: *Geometric dimension of the reference bridges.*

Both reference bridges use a parabolic-shaped bridge deck. The 12 m reference bridge has straight frame legs, $t_{FL.ts}$ is equal to $t_{FL.bs}$, compared to the 16 m bridge which has linear variable frame legs, $t_{FL.ts}$ is different than $t_{FL.bs}$.

The reference bridges were designed with a FEM model in Brigade. Brigade is a commercially available FEM software (Technia, n.d.). The Brigade model was built with lower-order shell elements and reduced E-modulus in the transverse direction. Wing walls were modeled without stiffness, i.e. their E-modules were set to 0 GPa, which was done to be able to apply load to them.

The reference bridges are designed with a "worst-case" methodology, meaning that location-specific parameters such as temperature and wind speed are based on the worst possible case according to EC. In addition, a "possible" radius of 2500 m is used for the design even though the plan data states perfectly straight alignments curves. However, the geotechnical soil properties do not follow the "worst-case" design methodology instead they follow the standardized bridge mindset of using the same site conditions at multiple locations. The geotechnical soil properties for the reference bridge are compacted gravel.

2.6 Optimization

Optimization is a term that is commonly defined as the process of finding the most optimal solution from a set of data and constraints to a specific problem. The following sections explain the general definition, categories, stopping criteria, and parameters of the concept of optimization.

2.6.1 Definitions

To be able to conduct an optimization of a problem, a model is first established. The model should contain three main components, which are used to create the design space and the target function. The three main components are (NEOS, n.d.):

- **Objective** is generally defined as mathematical functions which the optimization is either trying to maximize or minimize, so-called *Objective function*, i.e. a way for the process to determine if each step is in the right direction or not. In short, a generic company is trying to maximize their profits and minimize their cost.
- **Variables** is seen as the input data for the specific problem that the optimization process is trying to solve. For a parametric process, these variables should remain unknown and it is up to the optimization process to find values that result in the best solution. For instance, a generic company would put the price and number of sold products as variables.
- **Constraints** is explained as the relations between the variables and the design space of the optimization process. A generic company could use the maximum number of crates their warehouse could store as a constraint.

A multi-objective optimization problem can be defined with the following Equation 2.1 according to Martí et al. (2016).

$$\left.\begin{array}{ll} \text{minimize} & F(x) = \langle f_1(x), ..., f_m(x) \rangle \,, \\ \text{subject to} & c_1(x), ..., c_C(x) \leq 0, \\ & d_1(x), ..., d_D(x) = 0, \\ & \text{with } x \in \mathbb{D}, \end{array}\right\} \tag{2.1}$$

Where:

$\mathbb{D}$	Design space.
$F(x)$	Objective function.
$c_1(x), ..., c_C(x)$	Constrain to variable x.
$d_1(x), ..., d_D(x)$	Constrain to variable x.

2.6.2 Categories of optimization

When considering optimization, the common practice is to define the category of optimization to be performed to choose the right procedure. Optimization processes are tuned, based on the category of the optimization model. The following section deals with the various optimization categories.

2.6.2.1 Continuous optimization vs. Discrete optimization

Discrete optimization treats optimization where variables only can take a fixed set of numbers, e.g. obtainable reinforcement diameters (NEOS, n.d.). Continuous optimization is optimization where variables can take any value (concerning the design space), e.g. thickness of a bridge deck. A continuous optimization problem is easier to solve, as there is more room to try different values.

2.6.2.2 Unconstrained optimization vs. Constrained optimization

An unconstrained problem, as the name implies, is where there are no constraints on the variables, or where variable constraints are incorporated into the objective function as a penalty term. (NEOS, n.d.). Constraint problems involve clearly defined constraints on the variables, the constraints can be simple equalities, inequalities, and even more intricate relations between variables.

2.6.2.3 Single-objective optimization vs. Multi-objective optimization

Single-objective problem utilizes only one objective function to solve the optimization problem (Solat Yavari, 2017). Multi-objective problems utilize two or more objective functions which makes the problem more complex to solve. Solat Yavari (2017) states that a common practice for multi-objective problems is to rewrite them into single-objective problems with penalty terms or utilizing weight functions.

2.6.3 Stopping criteria

An optimization process will run through all iterations if no errors occur, sometimes it is beneficial to implement a stopping criterion to terminate the process earlier. When discussing stopping criteria for optimization processes there are four common scenarios where terminate are favorable (Martí et al., 2016):

- An adequate solution is found.
- A non-optimal viable solution is found and improvement is unlikely.
- The process is not able to converge for any solution.
- Sufficient computation is already performed or it is unjustified to compute further.

Furthermore, Martí et al. (2016) emphasizes that the optimization processes are computer-heavy, thus much effort should go into making the stopping criteria as non-computer complex as possible. Moreover, a simple stopping criteria should only retrieve information from the current analysis horizon, i.e. information should only be stored and retrieved from and during the current iteration.

2.6.4 Optimization parameters

When handling large amounts of data, a way of ranking and sorting viable solutions is required, which can be implemented with a selection of parameters. Furthermore, the selected parameters can also be used in an optimization process to screen out non-viable solutions at an early stage. The following section will explain relevant optimization parameters, and how they are measured and used.

2.6.4.1 Buildability

Various approaches to quantifying buildability have been made in recent years in order to compare and optimize designs. Due to the complexity of buildability and the many non-technical and technical factors involved, no common standardized way exists to quantify the optimization evaluation criterion. The main focus of quantification has been on the technical factors which are most relevant for designers.

One approach to consider technical buildability factors such as reinforcement layout, concrete properties, and geometrical shapes of slab frame bridges is to consider additional labor costs or factors during investment cost evaluation. Bergenram and Ulander (2023) quantified the buildability impact of shear reinforcement installation by studying the time spent on stirrup installations and calculating an additional labor cost factor for structural elements constructed with or without shear reinforcement. Furthermore, the installation time of different rebar sizes was estimated for three common rebar diameters for slab frame bridges with accompanied labor cost factors. Labor cost factors and installation times of different reinforcement types and sizes provided by Bergenram and Ulander (2023) can be found in Appendix A.3.

Solat Yavari (2017) quantified geometric irregularities and size impact for reinforcement labor cost of reinforced concrete elements. Increased labor cost factors for reinforcement work for non-straight and slender members were considered as a result of narrower and more complex reinforcement installation. Moreover, an additional investment and labor-cost factor for subsequent anchorage and detail reinforcement installation was considered. In addition to reinforcement installation, varying labor costs for form-work installation of individual structural components for slab frame bridges were provided and are shown in Table A.3. Labor cost factors for varying thicknesses, additional anchorage, and detailing reinforcement can be found in Appendix A.3.

Solat Yavari (2017) further quantified the effect on buildability regarding concrete strength classes. Increased investment cost was used for higher strength grades shown in Table A.2 and an extra additional investment cost for negative workability aspects during casting for the highest considered strength class.

Contrary ways of quantifying buildability can be done by a comparative approach of assessing buildability. Fernández-Mora and Yepes (2020) created a simplified formula, shown in Equation 2.2, to calculate a unit-less buildability factor that was used to compare structural elements required "working crew time". The formula is based on the relationship between the amount and type of reinforcing steel in relation to the sectional area of the structural element. The steel-to-concrete ratio is then multiplied by a mean evaluation time or cost for the specific structural element. The calculated buildability factors for several alternatives of structural sections can be used as a comparison tool to design the most optimal cross-sections concerning technical buildability.

$$C = [((\sum_{i=1}^{n} n_n \cdot [(\frac{D_n}{2})^2 \cdot \pi]) \cdot \gamma_{steel})/(h \cdot w)] * x \tag{2.2}$$

Where:

C	Total buildability factor.
n_n	Number of bars in reinforcement layer.
D_n	Reinforcement diameter.
γ_{steel}	Unit weight of reinforcement steel.
h	Height of element section.
w	Width of element section.
x	Mean structural component value to evaluate buildability. E.g. Construction time $\frac{h}{m^2}$, investment cost $\frac{SEK}{m^3}$.

Efforts to assess buildability from a broader project perspective have been performed to emphasize design rationalization and repeatability. SaravanaPrabhu and Vidjeapriya (2021) used learning curve models to quantify the reduction of man hours for several built concrete walls and piles in a large infrastructure project. One of the learning curves used in the research was the most widely used learning curve today while also being the oldest used in the construction industry; the basic Wright model. The Wright model was originally used for aircraft manufacturing but can be implemented for any type of production as long as data on what the initial time or cost of a structural element has and the rate of construction improvement is given with Equation 2.3.

$$L = C \cdot x^{-n} \tag{2.3}$$

Where:

- L Labor time or cost.
- C Cost or time of the first constructed structural element.
- x Number of constructed structural elements.
- n Factor determining at what rate the improvements and routine of constructing a structural element occur [0-1].

For the case study used in the SaravanaPrabhu and Vidjeapriya (2021) research, a rate of construction improvement of $n = 0.22$ was used for the average construction time of concrete walls and $n = 0.18$ was used for average construction time of concrete piles.

Furthermore, Barakat et al. (2020) used a total buildability score to evaluate structural components for a large project of a commercial building. A large variety of buildability factors regarding repetition and standardization of structural components were set up to evaluate buildability. Utility values multiplied with internal weight factors for different buildability factors from Equation 2.4 were used to achieve a buildability index for each design concept. The concept with the highest buildability index was considered the most optimal structural solution regarding buildability.

$$C_t = \sum_{f=1}^{f} W_f \cdot U_f \tag{2.4}$$

Where:

- C_t Total buildability score.
- f Buildability factor. E.g. % of prefabricated components, % of standard dimensioned components used in the project, repeated slab and beam dimensions.
- W_f Relative Weight of each factor. I.e. Internally weighted importance of buildability factor ≤ 1.
- U_f Utility value of each factor. I.e. Assessed measurement of buildability achievement (0% very bad - 100% very good).

As an alternative to using the previously mentioned objective-based buildability optimization techniques, Rempling et al. (2019) used limitations in reinforcement design as optimization constraints to create solutions with increased technical buildability. The number of reinforcement layers for concrete beams was constrained to a maximum of two, disregarding generated alternatives with more reinforcement layers due to lack of buildability. These fixed variables allow especially designers and contractors to choose which design alternatives to consider with regard to buildability based on research, but more uniquely personal preferences. Implementing

buildability as a constraint decreases the number of optimization parameters, which can make the design processes easier because every generated alternative is considered effectively buildable. However, the increase in constrained variables can lead to less generated and acceptable alternatives during SBD which decreases the variety of available structural components and alternatives to choose from.

2.6.4.2 Investment cost

A common measurement tool in all industries is cost and it allows an outsider to get a picture of a project's size based on cost. In the construction industry, it is common to speak in terms of investment cost, which refers to the cost of producing a unit e.g. a bridge. A formula to recalculate the quantities of concrete and reinforcement and erection work as investment cost is given by Equation 2.5 (Solat Yavari et al., 2016). The formula uses collected data with units [SEK/(quantity)], see Appendix A.1, to calculate the investment cost for different reinforced concrete structures.

$$f_{inv}(x) = Cost_{concrete} + Cost_{formwork} + \alpha_{reinforcement} \cdot Cost_{reinforcement} \tag{2.5}$$

Where:

$\alpha_{reinforcement}$	Factor which considers the additional amount of reinforcement due to anchorage and details.

2.6.4.3 Environmental impact

In today's society, an increasing focus on the environment has emerged, especially in the construction industry. How environmental cost is measured and calculated differs between authors but usually revolves around CO_2-equivalents. Solat Yavari et al. (2017) has developed the following Equations 2.6 and 2.7 to calculate the environmental cost.

$$f_{env}(x) = EnvCost_{concrete} + \alpha_{reinforcement} \cdot EnvCost_{reinforcment} \tag{2.6}$$

$$EnvCost = \sum_{i=1}^{nr.of components} impact_i \cdot monetary_i \tag{2.7}$$

Where:

$EnvCost$	Total related environmental cost for the selected impact categories.
$impact_i$	According to the data characterizing the environmental impact modules, see Appendix A.2.
$monetary_i$	Environmental cost related to impact$_i$ according to the monetary weighting factors ecovalue or ecotax, see Appendix A.2.
$\alpha_{reinforcement}$	Factor which considers the additional amount of reinforcement due to anchorage and details.

2.6.4.4 Equivalent cost

To be able to compare solutions against each other, a quantifiable measurement is needed, this measurement is defined as equivalent cost. Equivalent cost is measured as the sum of the normalized cost for each sub-objective function. Sub-objective functions are defined as investment cost, environmental cost, and buildability cost. By observing the data in Appendix A it is possible to determine that each objective function will get result of different magnitudes. Thus, by normalizing each object function, it gives each object function an equal impact on the optimization.

2.7 Computer-aided engineering

The usage of computer programs for solving engineering problems is commonly referred to as Computer-Aided Engineering (CAE). The most common way to use CAE in structural engineering is the use of the finite element method (FEM).

The finite element method is a numerical approach that uses differential equations based on theories such as beam or plate theory to approximate a solution to a problem for a finite amount of unknowns, i.e a finite amount of elements (Ottosen & Petersson, 1992). Structural FE-modeling is based on converting physical geometries into a model and dividing the geometry into finite elements containing individual stiffness based on material and geometrical properties, which creates a stiffness relation between the elements. Depending on what element is chosen for the specific problem, a number of nodes that connect the element are formed which contain an element-specific amount of degrees of freedom which can be seen as the amount of directions or dimensions a node can be displaced. External loads or predefined displacements can thereafter be implemented on the corresponding nodes' degrees of freedom, which is related to the corresponding stiffness in the stiffness matrix, leading to a system of equations. The model needs to be equipped with boundary conditions, which can be seen as conditions for a structure to achieve equilibrium, to solve the mathematical problem. The resulting method is an efficient mathematical tool used in many of today's commercial software used in structural engineering.

Structural FEM can be analyzed and categorized in two different ways, linear or non-linear analysis (Pore et al., 2021). Linear analysis implies that the relation between applied external loads and deformations is linear and remains the same throughout the analysis, which implies constant stiffness and no need to update the stiffness matrix at any point during the analysis. A non-linear analysis is the opposite, where the relationship between deformations and external loads is not linear and has the potential to change at any point during the analysis, especially during large deformations, creating a need to update the stiffness matrix during the analysis.

These frequent updates of the stiffness matrix can lead to high computational times for large models but leave the potential to create a more realistic approximation of structural behavior. Linear analysis is usually considered to be valid enough in the field of structural engineering since deformations are usually low. In addition, linear analysis enables the use of superpositioning of loads which is favorable for scenarios with large amounts of varying load cases.

As previously mentioned, the choice of element type affects the number of degrees of freedom in the FE-model. Many elements exist in modern FEM and particularly for reinforced concrete design (Plos, 2000). Three of the commonly used element types used for the design of reinforced concrete structures are solid, shell, and beam elements. 3D solid elements are the most realistic elements to use for modeling of structures since all degrees of freedom and internal stiffness relations between nodes are considered in all of the directions in a 3D space (Ottosen & Petersson, 1992). However, their computational times are high due to the number of required nodes needed to achieve 3D stiffness relations. Plate elements or so-called shell elements can decrease the number of nodes of a model through simplifications and approximations of the problem. Shell elements utilize certain deformation assumptions and an assigned thickness to reduce the 3D problem to a 2D problem. This reduces the number of nodes in the model while retaining the 3D degrees of freedom, reducing the computation time and enabling 3D-load applications, displacement, and rotations. Even though shell elements are effective for modeling of 3D loads, they are mainly used for structures subjected to primarily bending from out-of-plane loads such as slabs, since they cannot describe out-of-plane shear behavior (Plos, 2000).

A 2D FE-problem can further be simplified by the use of truss or beam elements, reducing the computation time even further (Ottosen & Petersson, 1992). Truss and beam elements consist of two in-plane nodes having only a one-dimensional stiffness correlation between the nodes. Truss elements are used when compression or tension in the axial direction of the element is dominant and beam elements are used when bending is the dominant structural behavior. Another reason for using truss or beam elements is to simplify large structural systems in a global analysis of structures, perhaps to get a better grasp of the overall structural behavior and forces rather than detail design (Plos, 2000). One consequence of the simplifications needed to implement truss or beam elements is that out-of-plane load effects such as load distribution and shrinkage can not be considered since no degrees of freedom exist out of the plane (Ottosen & Petersson, 1992).

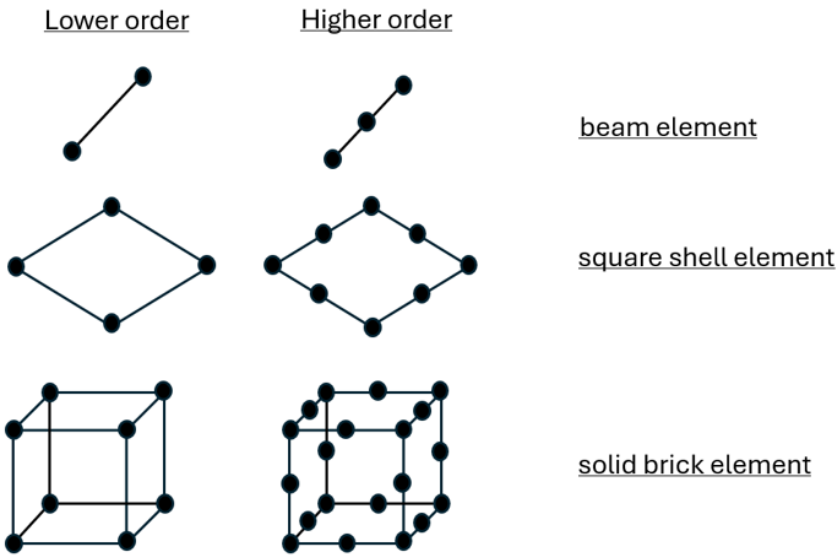

Figure 2.16: *Typical beam, shell and 3D brick elements with lower and higher order configurations.*

Figure 2.16 shows that the previously mentioned typical element types can be considered either as higher or lower-order elements (Netz et al., 2013). Lower-order elements contain only the vital nodes needed to rectify the stiffness relations for the particular element. Higher order elements use subdivisions of a lower order element to create intermediate nodes seen in Figure 2.16 to improve more complex FEM problems, often non-linear analysis. Even though higher order elements can improve and avoid certain problems in complex FEM, Netz et al. (2013) states that the improvement is considered inferior to the save in computational time when using lower order elements.

By implementing FEM it is possible to calculate more accurate capacities by enabling the use of different effects. Plos et al. (2012) has identified several positive effects of using FEM or more specifically 3D finite analysis. One possible improvement explained is the increased calculation accuracy by considering 3D effects from point loads and torsion. Plates and wall mechanically connected, e.g. bridge deck and frame legs, are both necessary in the model even if the results of the bridge deck are only of interest. Plos et al. (2012) further reports that mechanical connection need to have sufficient fine mesh at connecting points, moreover it should be noted that a fine mesh at connection or supports could lead to singularities.

Generally, FEM programs were only programmed to give out sectional forces but with development, more potential has emerged (Weber, 2022). Industry-specific FEM programs, such as Sofistik and Brigade, can now calculate required reinforcement based on section forces and reinforcement placement (Sofistik, 2024). The required reinforcement is a measurement of how much reinforcement is necessary to cope with the applied loads, see Figure 2.17. In detailed design, one usually talks about actual reinforcement, which usually corresponds to the final blueprint, see Figure 2.17 for actual reinforcement. The working process for a structural engineer

starts with the reinforcement requirements and section forces to create a blueprint with actual reinforcement. In this process it is possible to reduce the actually placed reinforcement and consequently the material usage as seen in the difference between Figure 2.17a and 2.17b.

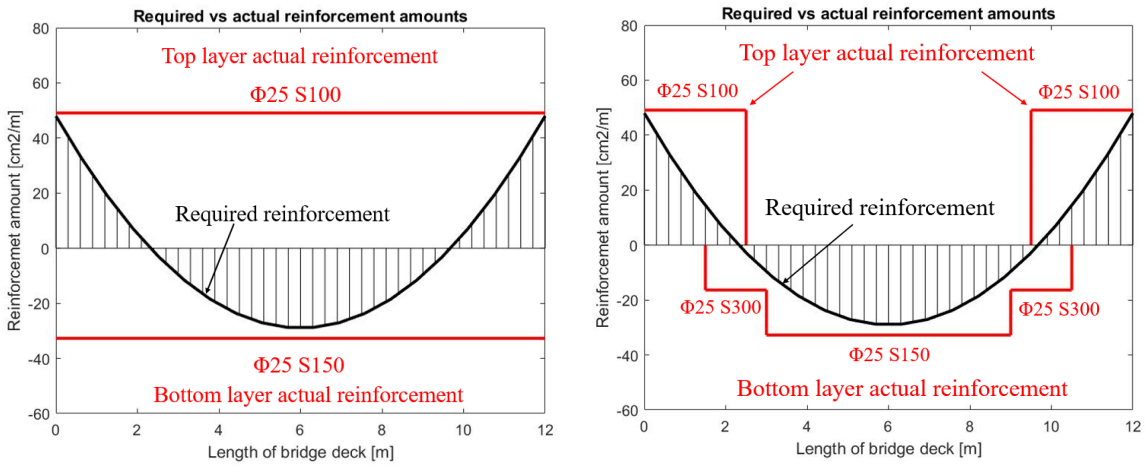

(a) *Simplified solution* **(b)** *Material effective solution*

Figure 2.17: *Required reinforcement for bridge deck loaded with evenly distributed load designed for two different approaches of actual reinforcement design.*

3

Methods

Different methodologies and approaches to parametric design, CAE, and the overall optimization procedure were considered to achieve the aim of this thesis.

The advantages and disadvantages of CAE for the analysis and design of slab frame bridges were studied with regards to reliability, credibility, and computational time. The use of commercial FEM-programs such as Sofistik or Brigade has great potential to implement load effects, design and evaluate 3D geometries. However, it leaves gaps of unawareness and knowledge in the process, leading to a large amount of trust, knowledge, and verification of the software being needed to be used. This gap of unawareness and knowledge during the method is further explained in Section 3.3. Different commercial FEM software can also be limited by the amount of computer hardware, resulting in less effective usage of potential computing power. The contrary method using programming languages such as Python or Grasshopper to analyze and design using self-implemented calculations, was considered as an alternative to commercial CAE programs, to have oversight of every stage in the work process.

Different modeling approaches with respect to boundary conditions and the inclusion of structural components were tested. Modeling only the frame legs and bridge deck similar to the reference objects by using rotational springs as the connection to the foundation slab/slabs was tested, and compared to modeling all the structural components' full geometry and using springs under the foundation slab to achieve equivalent rotations. The inclusion of edge beams and wing walls in the structural model could be performed in several different ways. The stiffness, self-weight, loaded area, and overall design of the model were affected depending on how the two components were modeled.

The large amount of data that is used and processed during SBD requires reflection on variables being computed as free or constrained during the parametric design phase of the work process. More free variables allow more combinations of bridges to be evaluated, which can provide more conclusive results even if it requires longer calculation times as a result. Constraining certain variables could impact different goals of the thesis in various ways. Evaluating different reinforcement diameters as free variables would lead to more diverse and decisive results regarding buildability but may require other free variables such as span lengths to be constrained due to computational time. Hence, interchanging which variables are free for the analysis could give rise to different results, which may defeat the purpose of the thesis.

Optimization can be divided into several categories. To achieve the aim of the thesis, it was necessary to select an ideal optimization method. Continuous versus Discrete optimization controls the number of variables in each geometric variation. Continuous optimization would result in a higher probability of finding the most optimized solution but would increase the number of variables, thus increasing the computational time. Discrete optimization with a refinement of the variables should result in a lower computing time while retaining a relatively high probability of reaching the optimal solution. During the discussion of unconstrained versus constrained optimization, a combination of both was deemed necessary. An unconstrained optimization would result in a larger design space but a higher computational, time as more variables are varying independently of each other. Constraint optimization decreases the number of combinations with the same set of variables, thus reducing the computational time. Single versus multi-objective optimization determines how many objective functions the analysis treats. A combination of multiple single-objective functions could be treated as a multi-objective function if the results are combined.

3.1 Chosen method

Ultimately the chosen method for the Set-Based optimization was a multi-objective optimization model evaluating data from a 3D calculation model in Sofistik, a FEM analysis and design software. A chosen number of geometric variation options and their respective amount of internal free variables created a set of slab frame bridge combinations that were analyzed and designed using Sofistik. Relevant data for all analyzed bridges concerning buildability, investment cost, and environmental impact was exported and evaluated using the objective functions in Excel.

The results from the objective functions were normalized individually and the probability density was calculated for each objective function. By plotting the probability density against the normalized cost, it was possible to determine if refinement of the internal free variables was needed to create a new more optimized set of bridges. If a refinement of the internal free variables was needed, the set-based optimization process was repeated until an acceptable solution set was achieved. The final resulting data could also be inserted into a data visualization tool called Design Explorer to improve readability and visualize the grouping of different bridge alternatives.

A "similarity-seeking" script was created in Python and used on all the evaluated bridges, to identify bridge alternatives with one or more identical structural components. Seven possible cases were identified and the largest group for each case was compared against the most optimized bridge alternative. Furthermore, a large infrastructure project was simulated to be able to compare building individual optimized bridges to using bridges with identical structural components.

3.2 Work process

To perform a large-scale analysis, a work process is often fabricated to structure the work. To be able to visualize the chosen work process, a flowchart was created, as seen in Figure 3.1. The chosen work process contained three separate stages to easily divide the individual task into subtasks. The three stages were **Selection of bridge alternatives**, **Structural calculation model** and **Evaluation of bridge alternatives**. The chosen SBD work process contains five different design spaces: $\mathbb{A}$, $\mathbb{B}$, $\mathbb{C}$, $\mathbb{D}$ & $\mathbb{E}$. The following sections 3.1.1 - 3.1.3 explain each stage and the design spaces more in-depth.

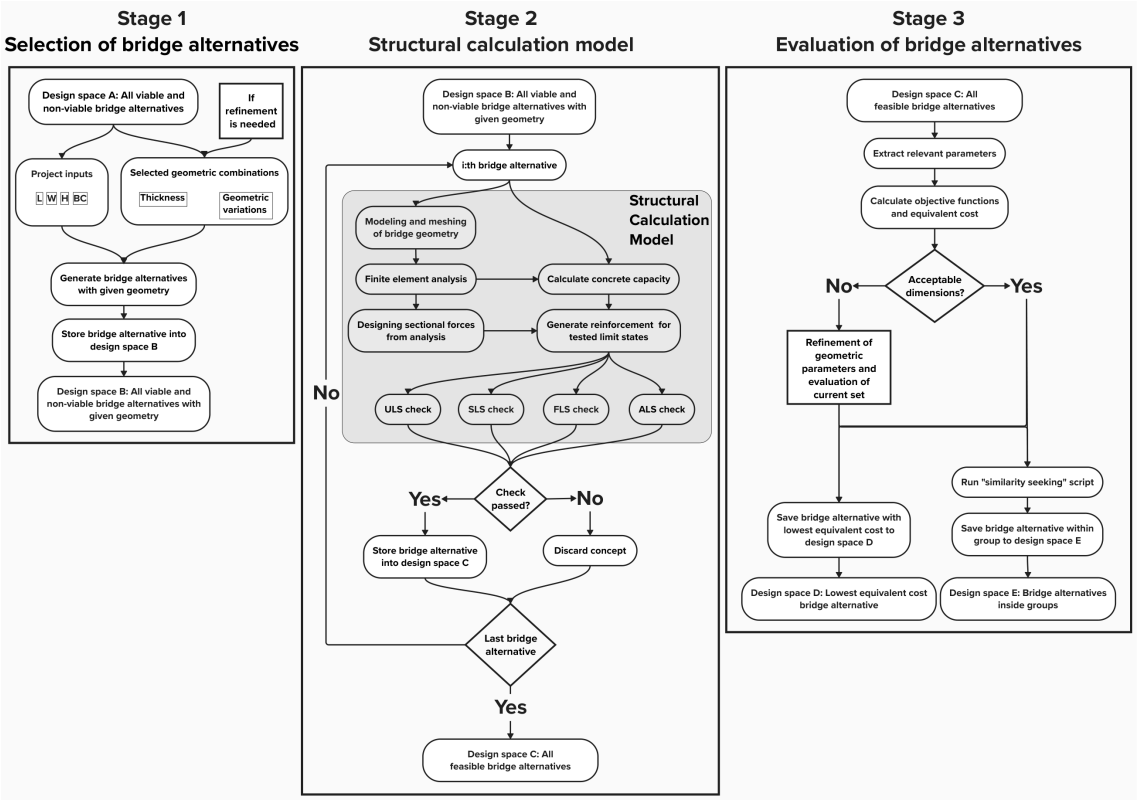

Figure 3.1: *Work process of SBD method.*

3.2.1 Stage 1 - Selection of bridge alternatives

To be able to perform SBD and optimization of a problem, a first choice of which variables should be free and which are fixed by problem-specific parameters was formed. In Figure 3.1, the process begins in the design space $\mathbb{A}$, encompassing all feasible and unfeasible bridge alternatives. To enhance problem specificity and reduce computational time, a preliminary filtering process was conducted, choosing reasonable geometric parameters based on engineering judgment, and narrowing the focus to design space $\mathbb{B}$. The variables that were allowed to be free or constrained by project-specific demands are further explained in the following subsections.

3.2.1.1 Free variables

The main free variables, which were iterated over, were determined as the geometrical properties of the bridge and the span length of the bridge. It was decided that each structural component and its variations will a have number of different combinations. To be able to group the structural components, an overlap of geometric variations of at least two step sizes was determined for the different span lengths. The different combinations and geometric variations are further described in Table 3.1.

	Geometric	**Span length**	12	14	16
Components	**variation**	**Options**	**Combinations**	**Combinations**	**Combinations**
Foundations slab	Open	$t_{slab}[mm]$	700 : 100 : 900	800 : 100 : 1000	900 : 100 : 1100
		$w_{slab}[m]$	2.15 : 0.2 : 2.55	2.35 , 0.2 , 2.75	2.55 , 0.2 , 2.95
	Closed	$t_{slab}[mm]$	700 : 100 : 900	800 : 100 : 1000	900 : 100 : 1100
Frame legs	Straight	$t_{FL}[mm]$	600 : 50 : 1150	800 : 50 : 1350	1000 : 50 : 1550
	Linear increasing	$t_{FLts}[mm]$	1100 : 100 : 1400	1200 : 100 : 1500	1300 : 100 : 1600
		$t_{FLbs}[mm]$	600 : 100 : 900	700 : 100 : 1000	800 : 100 : 1100
Bridge deck	Straight	$t_{deck}[mm]$	900 : 100 : 1200	1000 : 100 : 1300	1100 : 100 : 1400
	Parabolic	$t_{deckmid}[mm]$	700 : 100 : 1000	800 : 100 : 1100	900 : 100 : 1200
		$t_{deckFL}[mm]$	1050 : 150 : 1500	1200 : 150 : 1600	1350 : 150 : 1650
Haunches*	20% length	$t_{haunch}[mm]$	0 , 300 : 100 : 500	0 , 300 : 100 : 500	0 , 300 : 100 : 500

Table 3.1: *Structural components, their geometric variation, and iterated combination values. Geometric dimensions are read (Start value: Step size: End Value). *Different haunches were only applied when a straight bridge deck was used.*

As seen in Table 3.1 two different geometric variations were used for the frame legs. The straight variation is a constant thickness along the height as seen in the left picture of Figure 2.7, the linear increasing utilizes a starting value at the bottom and an end value at the top, as seen in the right picture of Figure 2.7. For the bridge deck, two different geometric variations were considered: a constant thickness along the length, denoted straight, and a varying thickness along the span length, denoted parabolic, see Figure 2.6. Only homogeneous cross-sections were considered, as cutouts impact the buildability of the superstructure negatively, as previously mentioned in Section 2.3.1.4. For the straight variation of the bridge deck, haunches were considered. These haunches had a variable height but a fixed length of 20 % of the span length. For the foundation slab, two geometric variations were considered, open and closed foundation slab, see Figure 2.6. Variations of abutment lengths were dependent on the thickness of the foundation slab for the open bridge type and fixed for the closed bridge type.

3.2.1.2 Constrained variables

The geometrical properties of the site were considered hard constraints, including free height and free width. The level at the topside of the bridge deck was locked to +8.3 m and the level at the bottomside of the foundation was locked to +0.0 m, in accordance with Figure 2.15. In addition, the toe of the foundation slab was locked to 1150 mm, according to Figure 2.15. The geotechnical properties were also

considered constrained as the geotechnical properties of the reference object were used. The soil properties used were compacted gravel with the following properties: $K_0 = 0.29$ and $\gamma_{soil} = 20$ kN/m^3. The decision to fix the previously mentioned variables as constraints connects to standardized bridges where one should adapt the site to the bridge and not the other way around.

Further constraint variables were reinforcement diameters and concrete strength class. These variables were chosen as constraints after discussion with the supervisors. Reinforcement diameters were constrained to $\phi 25$ in the main direction, $\phi 16$ in the transverse direction, and $\phi 16$ for the shear reinforcement of every component. The concrete strength class utilized in the Swedish industry of bridge construction is almost solely C35/45 and only a few bridges are made with lower or higher strength class according to the supervisors. Therefore, C35/45 was chosen as the concrete strength class for all bridge alternatives.

3.2.2 Stage 2 - Structural calculation model

The first step of Stage 2 was to analyze and design a single slab frame bridge using Sofistik before implementing SBD and optimization parameters, thus a simpler script was used which allowed for a more comprehensive verification. To simplify the later verification process and comparison with the thesis's reference objects, two separate Sofistik models were created to replicate the two reference bridges with the chosen FEM setup. Implementation of the required loads was studied and followed up by a comparison of load implementation used in the design of the reference projects to justify the comparison. Further work included load combining, meshing, and selecting elements and boundary conditions. Further, a linear elastic analysis was performed for both models to create sectional forces that were later used for design.

The design of the bridges was performed with Sofistik's built-in design-function BEMESS, which checks all the required concrete capacity requirements and possible reinforcement needs according to Swedish and European standards for all required limit states (Sofistik, 2024). Lastly, appropriate outputs from the model were chosen for further post-processing optimization.

3.2.2.1 FEM setup

The FEM model was designed with each structural component represented as its own 2D area. Separating structural components into their own areas simplified the possibility of evaluating components individually.

Considering the increasing 3D design complexity and computational time of implementing wing walls in the FEM geometry, a decision of not considering wing walls during the design phase for both geometric models was made. However, the wing walls, self-weight, and increased earth pressure area were considered during the structural analysis. The stiffness of the wing walls was set to infinitely small to keep the wing walls from contributing to the structural behavior. The decision could further be justified due to the fact that the wing walls for the reference bridges were treated in a separate model and designed in a traditional manner.

Geometric modeling of the edge beams was neglected, considering the favorable effects of edge beams and the possible scenario of repair or removal of the edge beams, as previously discussed in Chapter 2.3.1.5. The self-weight of the edge beams was considered and modeled as a load, explained in more detail in subsequent chapters.

Shell elements were chosen as the best-suited element type for the slab frame bridge structure due to the dominant out-of-plane bending behavior, the need for 3D load applications, and the relatively low computational time compared to other element types. All the structural components in both geometric models were equipped with first-order shell elements and with an assigned thickness. Sofistisk's automatic MESH function was used to mesh the surfaces by determining the largest acceptable side length of a quadrilateral shell element. Verification of the chosen element size was later done through a convergence study on the largest chosen span to ensure convergence for all analyzed bridges.

Linear springs were used to represent the horizontal stiffness from the backfill on the frame legs. Linear springs connecting the bottom nodes of the foundation slab to a fixed ground acted as vertical boundary conditions. Lateral and longitudinal spring stiffness was also modeled to replicate geotechnical conditions between the foundation slab and the ground. The meshed geometry and used boundary conditions for the open and closed slab frame bridge models can be seen in Figures 3.2 and 3.3.

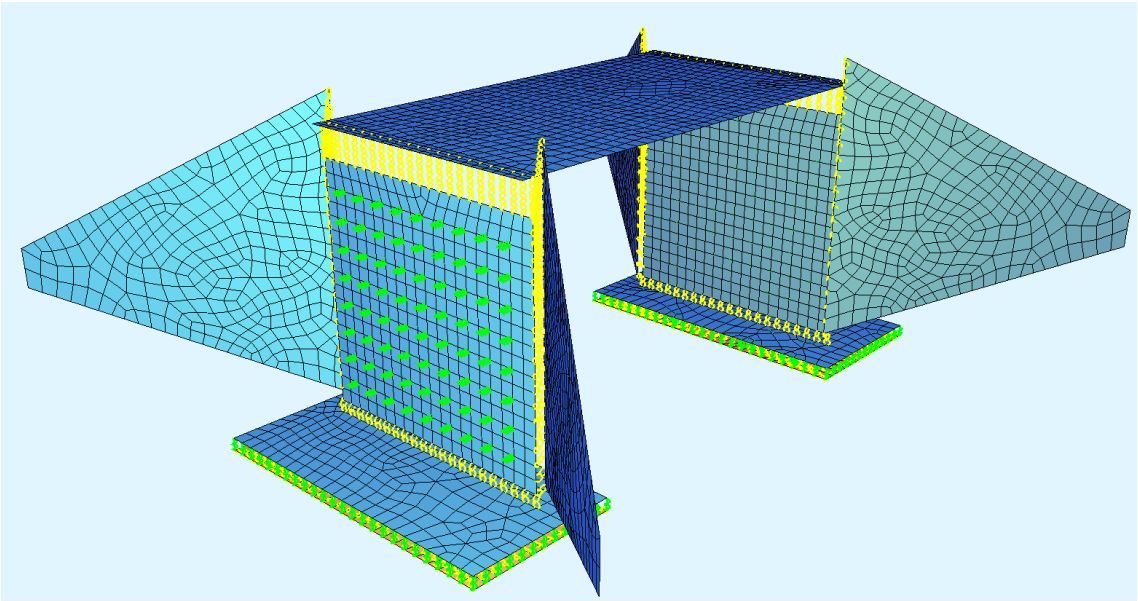

Figure 3.2: *FEM geometry, mesh and boundary conditions for open foundation model.*

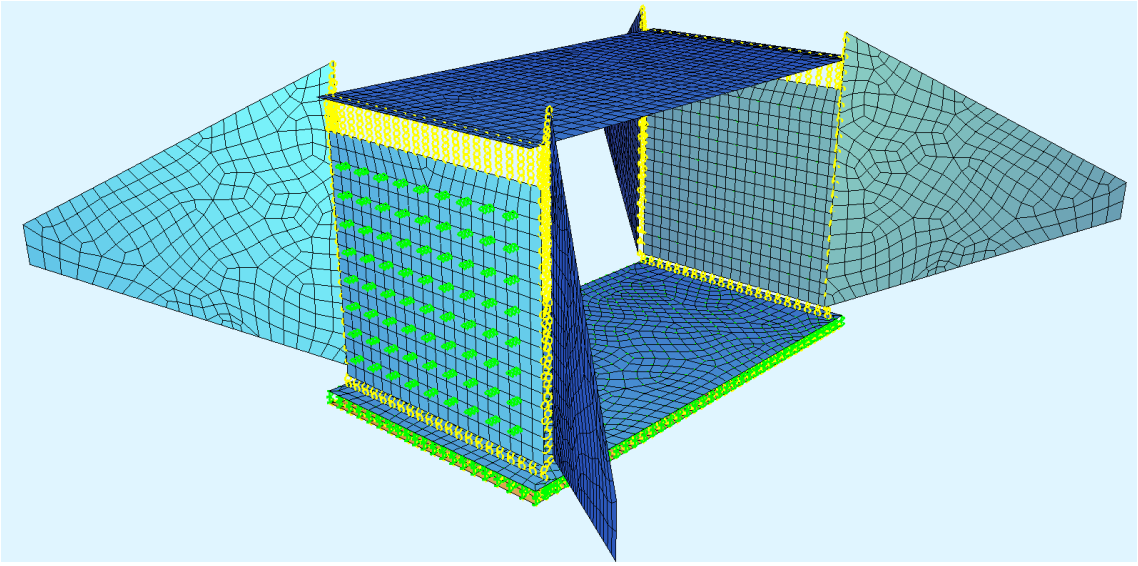

Figure 3.3: *FEM geometry, mesh and boundary conditions for closed foundation model.*

An open foundation structural model consists of ten different structural groups: bridge deck, right frame leg, left frame leg, two foundation slabs, ground, and the four wing walls. A closed foundation structural model consists of nine different structural groups: bridge deck, right frame leg, left frame leg, one foundation slab, ground, and the four wing walls. As these groups interact, they need to be kinetically coupled to transfer forces. The coupling in between the groups is seen in Figures 3.2 and 3.3 as yellow chains. The coupling was modeled as fixed, meaning the same internal forces and stiffness are used for the nodes connected.

3.2.2.2 Loads and Load combinations

Loads utilized in the model are copied from the reference object and verified against SS-EN 1991-X and norms, this was done to be able to have the same prerequisites while following the governing rules and norms. The loads used and applied on the structure are as follows and shown in Figure 3.4 and 3.5.

- Dead-weight
- Ballast, surfacing
- LM71, "Rail-change car"
- Nosing force
- Windload, both on structure and train cart
- Road traffic, on closed foundation slab
- Centrifugal force
- Derailment load

- Surcharge load
- Earth pressure
- Shrinkage
- Temperature variations
- Support movement

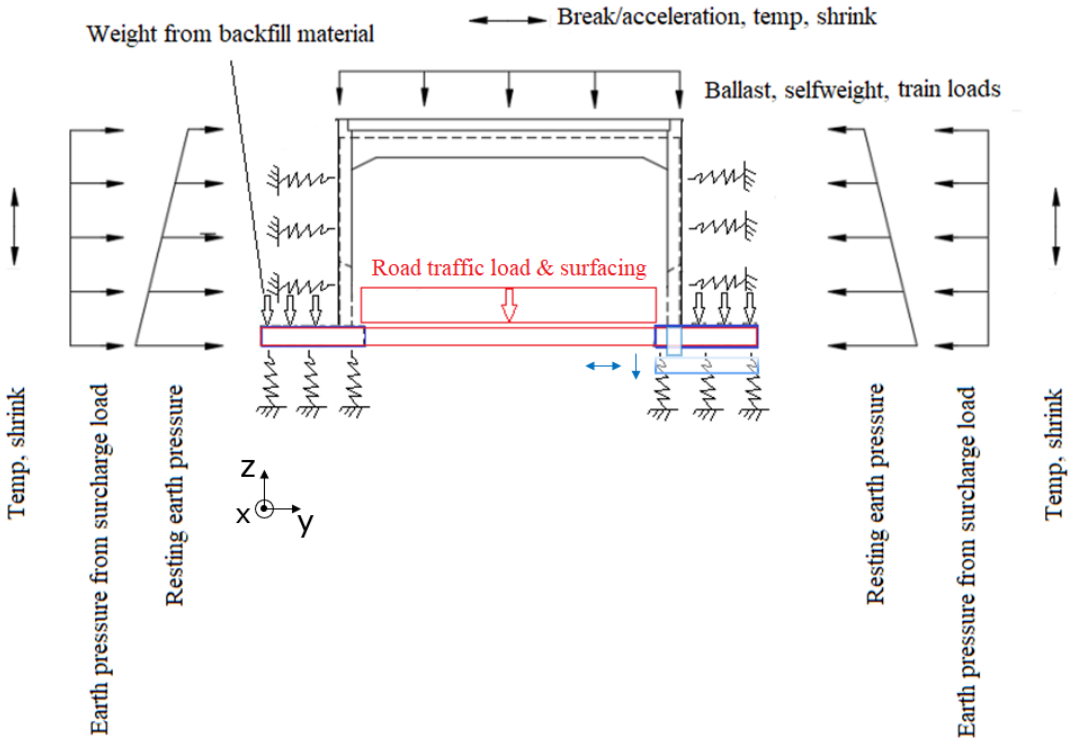

Figure 3.4: *Longitudinal view of the load implementation on the structural model. Red loads were only applied for closed foundations. Blue arrows, symbolizing support movement, were only applied for open foundations.*

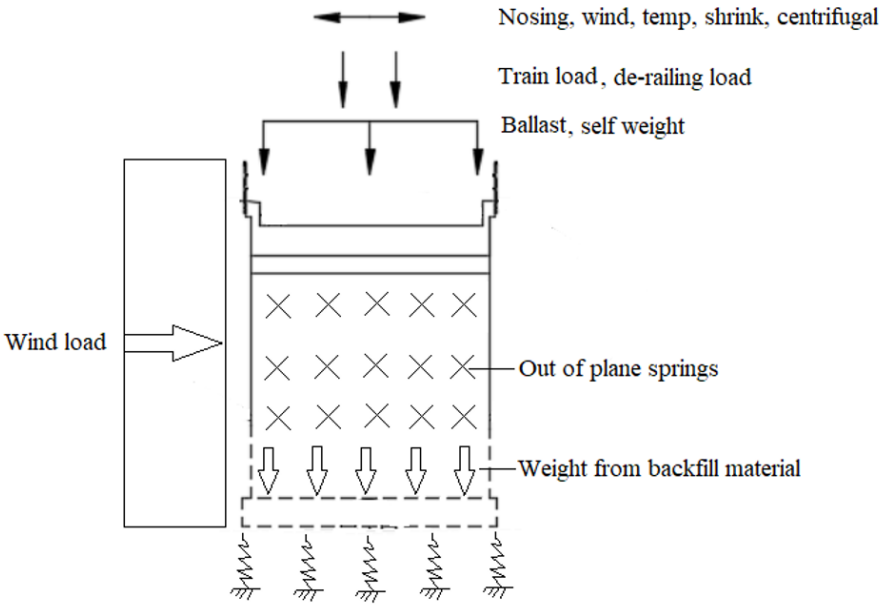

Figure 3.5: *Transversal view of load implementation on the structural model.*

As seen in Figure 3.4 different loads are used for open and closed foundation slabs, this is symbolized by the different colored loads in the Figure. Closed foundation alternatives were modeled with a surfacing load, LM1 and LM2 applied on the foundation slab. Load value inside of LM1 and LM2 was based on *SS-EN 1991-2:2003* (n.d.). The surfacing load was set to 69 kN/m^2 to replicate the reference bridge. Open foundation bridge alternatives had an additional support movement, symbolized by the blue arrows in Figure 3.4. Support movement was determined using Sofistik, by first applying a test load which resulted in a single-axis movement of the bridge. Secondly, the deformation value was extracted and compared to the intended support movement. Finally, the applied load was scaled with a factor such that the intended movement was achieved. The intended support movement was chosen to δH of 10 mm and a δV of 30 mm in accordance with the reference objects.

Self-weight of structural components was embedded in their structural areas. Self-weight from edge beams was modeled as distributed load at the edge of the bridge deck, visualized in Figure 3.6a. The ballast was modeled as two different sized evenly distributed loads, due to the thickening of the ballast under the railway tracks. The two thicknesses were set to 420 mm and 820 mm under the railway track. Shrinkage was calculated to 24 $^0/_{00}$ and applied on the every structural component (*SS-EN 1992-1-1:2005*, n.d.). Furthermore, creep was applied by reducing the load effect of temperature and the modulus of elasticity for long-term loads. The creep coefficient was calculated to 2.0 according to *SS-EN 1992-1-1:2005* (n.d.).

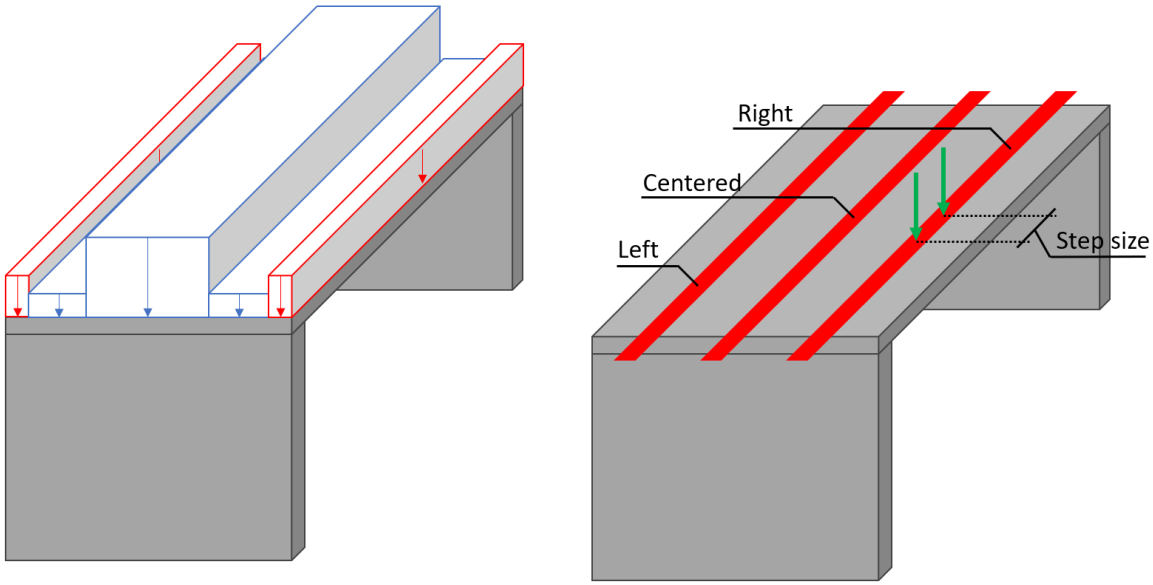

(a) *Sketch of how the self-weight from edge beams (red) and ballast (blue) was applied on the bridge*

(b) *Sketch of the three possible train locations and the definition of step sizes*

Figure 3.6: *Sketches for relevant loads applications and definitions for the modeling of loads.*

LM71 and rail change cart was applied in accordance with SS-EN 1991-2 and TRVINFRA-00227. The moving loads were simplified to 10 different positions along the railroad. The 10 different positions are calculated by dividing the length of the bridge deck into 10 steps, Figure 3.6b shows the measure of one step length. Furthermore, *TRVINFRA-00227* (2023) states that other possible track locations should be tested, resulting in moving loads could be placed on three possible track locations: Left, Center, and Right, Figure 3.6b shows the three different possible track locations.

Furthermore, LM71 contains nosing force, centrifugal force, and breaking- and acceleration force (*SS-EN 1991-2:2003*, n.d.). The nosing force was applied as a point load in the center of the load model, acting in the transverse direction. Centrifugal force was generated as a result of the speed of the train and the radius of the rails defined in Sofistik. The speed of the train was set to 250 km/h and the radius was 2500 m. Braking- and acceleration force were also generated automatically by Sofistik when assigning the load model to a lane. The load itself is generated as a uniform distributed load in the y-direction. SS-EN 1991-2 allow vertical loads which are applied on top of ballast and sleepers to be distributed with a 1:4 ratio from the top of the rail to the top of the bridge deck, in the transversal direction of the bridge (*SS-EN 1991-2:2003*, n.d., Section 6.3.6.3). Moreover, the α factor and the dynamic addition factor, ϕ_2, were multiplied with the LM71 loads in accordance with *SS-EN 1991-2:2003* (n.d.). TSFS states that the α factor should be set to 1.33 for generally railway bridges (*TSFS 2018:57*, n.d., Section 11, § 11). The dynamic addition factor was automatically calculated by Sofistik and should vary between

1.5 to 1.7.

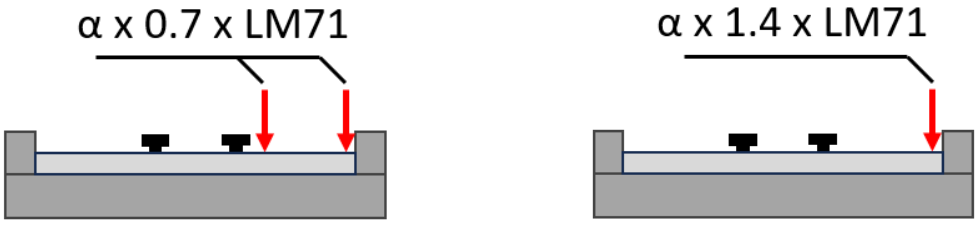

(a) *Design situations 1 for derailment load*

(b) *Design situations 2 for derailment load*

Figure 3.7: *Sketches of the two different design situations for derailment load described by (*SS-EN 1991-2:2003*, n.d.).*

SS-EN 1991-2:2003 (n.d.) describes two different design situations for derailment, Figure 3.7 shows the two situations. The reference objects only use design situation 2, which was used in the analysis as well. Design situation 2 describes a train that has overturned due to derailment, in other words only one of the train wheels is in contact with the bridge. Similar to LM71, the derailment load was modeled stepwise as vertical loads, the point load was distributed on a 0.45x0.45 m^2 area and the line load was distributed on a 0.45 m width (*SS-EN 1991-2:2003*, n.d.).

The temperature changes were modeled according to the reference object, which utilizes a worst-case principle and uses the highest positive and lowest negative temperatures in Sweden. This resulted in a T_{min} equal to -48°C, a T_{max} equal to 40°C and a T_0 equal to 10°C. Temperature was applied as four load cases: two as uniformed expansions and contraction on all structural components and two as uniformed expansion and contraction only on the bridge deck according to *SS-EN 1991-1-5:2003* (n.d., Section 6.1.5).

Wind load was modeled as site-specific according to the reference object and uses the highest wind speed for northern Sweden. The wind speed was set to 26 m/s, which is the highest possible speed for Sweden, which was done to comply with the "worst-case" methodology used in the design of the reference bridges. The terrain type was set to II and the reference height of the bridge to 8.3 m. In addition, the form factor equation according to *SS-EN 1991-1-4:2005* (n.d.) was utilized. The total wind load intensity was calculated to 1.79 kN/m^2. The wind load itself was applied as four different load cases: one where the wind was applied uniformly distributed on only the bridge and the three others where the wind was applied uniformly distributed on the bridge and the train for the three possible track locations.

Vertical soil pressure on the heel of the bottom slab/slabs was modeled as distributed load, counteracting rotation in the bottom slab, especially for the model with the open foundation. Horizontal earth pressure and residual earth pressure were modeled as distributed loads in the y-direction of both frame legs and on the wing walls. The soil properties used for vertical and horizontal earth pressure were based on the reference objects which were $K_0 = 0.29$ and $\gamma_{soil} = 20$ kN/m^3, representing compacted gravel. Surcharge load was calculated according to *SS-EN 1991-2:2003* (n.d.) and amounted to 8.45 kN/m^2.

To represent the restraining effect of the increased earth pressure arising from loads displacing the bridge longitudinal towards the backfill, spring beds were used on the frame legs. The choice of using a spring bed instead of applying a load is based on *TRVINFRA-00227* (2023, Section 7.2.1.1.2.1.2), where the displacement towards the backfill in combination with the increased pressure can be recalculated into an equivalent spring stiffness. This method allows a smaller number of load cases to be modeled, as no extra load cases were required to represent the increased soil pressure resulting from the displacement. Load effects that affected the springs automatically were: expansion caused by temperature change, horizontal earth pressure, surcharge load, breaking- and acceleration load.

Load combinations were created in Sofistik with the MAXIMA function. The MAXIMA function utilizes the superposition principle to determine the maximum and minimum sectional forces in each node. By utilizing the built-in sub-functions of MAXIMA and adding the correct particular factors, load combination was performed according to SS-EN 1990 and Swedish norms.

3.2.2.3 Design procedure

The design of reinforcement was performed with the built-in function BEMESS in Sofistik. BEMESS utilizes the internal forces and stresses generated by analysis and superpositioning to design the geometry against Ultimate, Serviceability, Fatigue, and Accidental Limit state (ULS, SLS, FLS, ALS) checks according to relevant Eurocode and Swedish norms (Sofistik, 2024).

The built-in function BEMESS provides three different procedures for concrete design: the Baumann method, Layer design, and Sandwich model. Sandwich model and Baumann are similar in procedure but can only be utilized for straight concrete geometry and orthogonal reinforcement. Using layer design, it is possible to evaluate skewed concrete geometries. Furthermore, according to Sofistik (2024) using layer design, it is possible to achieve a more accurate design compared to the Baumann method. Thus, the scripts that were used utilized layer design to design the reinforcement. Layer design is an iterative process that calculates three strains ($\epsilon_x,\ \epsilon_y,\ \epsilon_{xy}$) and three curvatures ($\kappa_x,\ \kappa_y,\ \kappa_{xy}$) to obtain equilibrium between the outer and inner forces.

BEMESS was also utilized to design the shear reinforcement for the concrete geometry in ULS (Sofistik, 2024). According to BEMESS, shear reinforcement is needed if one of Equation 3.1 or 3.2 is not fulfilled.

$$V_{Rd.c} \geq V_{Ed} \tag{3.1}$$

$$V_{Rd,max} \geq V_{Ed} \tag{3.2}$$

Where:

$V_{Rd.c}$	Design shear resistance of concrete section and longitudinal reinforcement without shear reinforcement.
$V_{Rd.max}$	Design shear resistance of concrete section and longitudinal reinforcement with shear reinforcement.
V_{Ed}	Design value of the shear force.

$V_{Rd,c}$ is calculated from the available concrete section, and additional capacity is added from longitudinal reinforcement. If Equation 3.1 is not fulfilled, shear reinforcement is added until the shear force capacity, $V_{Rd,max}$, is higher than the dimensional shear force, V_{Ed}. BEMESS Sofistik (2024) also performs a check of the ratio between concrete and reinforcement, shear reinforcement and longitudinal reinforcement.

ALS was evaluated using BEMESS´s sub-function ULTI. The same designing theory as for ULS is applied when using ULTI, except accidental partial coefficients and accidental material safety factors are used (Sofistik, 2024). Additionally, ULTI provides design based on alternative load paths to ensure structural stability and more ductile collapse mechanisms. Only permanent and derailment loads were considered during the ALS design.

Furthermore, it was possible to utilize BEMESS to perform relevant SLS checks for the design with sufficient capacity according to ULS and ALS verifications. If the SLS verifications were not fulfilled, the functions provided re-designed reinforcement layout with sufficient capacity according to the SLS verification's (Sofistik, 2024). These SLS verifications include a minimum thickness of the compression zone, maximum allowed deflection, crack width control, and minimum reinforcement design. Crack width limitations, concrete cover, and reinforcement diameters used in the design are shown in Figure 3.2.

	Crack width limit [mm]	Concrete cover [mm]	ϕ longitudinal [mm]	ϕ transversal/shear [mm]
Bridge deck				
Upper side	0.3	40	25	16
Lower side	0.15	55	25	16
Frame legs				
Earth side	0.4	40	25	16
Air side	0.15	55	25	16
Foundation slab				
Upper side	0.2	40	25	16
Lower side	0.4	50	25	16

Table 3.2: *Crack width limitations, concrete cover, and reinforcement diameters for each structural component.*

Lastly, the design of fatigue in the reinforcement and concrete was checked for cyclic loading by LM71 equivalent to 25.06 million tons of loading per year, considering a service life of 120 years. Using BEMESS with user-specified safety factors, partial coefficients, and critical stress amplitudes, fatigue checks for both the reinforcement and concrete could be performed (Sofistik, 2024). If the calculated stress amplitude exceeded the critical stress amplitude for either concrete or reinforcement, the relevant reinforcement area was increased to satisfy the fatigue requirements. Since Sofistik does not design an actual reinforcement amount and a type of rebar, adjustment was needed for rebars requiring any type of radius due to stress concentrations. Section/areas that shall contain stirrups or bent continuous reinforcement in the final design, had their critical stress amplitude reduced. The critical stress amplitude was reduced for the top main reinforcement layer in the bridge deck, considering the bent continuous rebar in the frame corners. The critical stress amplitude was reduced for all shear reinforcement stirrups in all structural components. The critical stress amplitude was reduced using partial factors based on the diameters and radiuses of stirrups or bent reinforcement. The reduction of critical stress amplitude and the calculations for the fatigue design for the reinforcement can be found in Appendix C.

3.2.2.4 Iteration of bridge alternatives

After creating a script that evaluated one design concept, an up-scaling was executed to be able to iterate several design alternatives. It was decided that the script should be split into several scripts following Figure 3.8. The decision to split the script was based on limitations in Sofistik and reducing computing time. The iterating procedure was implemented with the built-in function TEMPLATE which can be seen as a global logical loop. The TEMPLATE function iterates using both for and while loops, making it a powerful tool when intricate combinations need to be considered. The iteration procedure included every available geometric combination of components from Table 3.1.

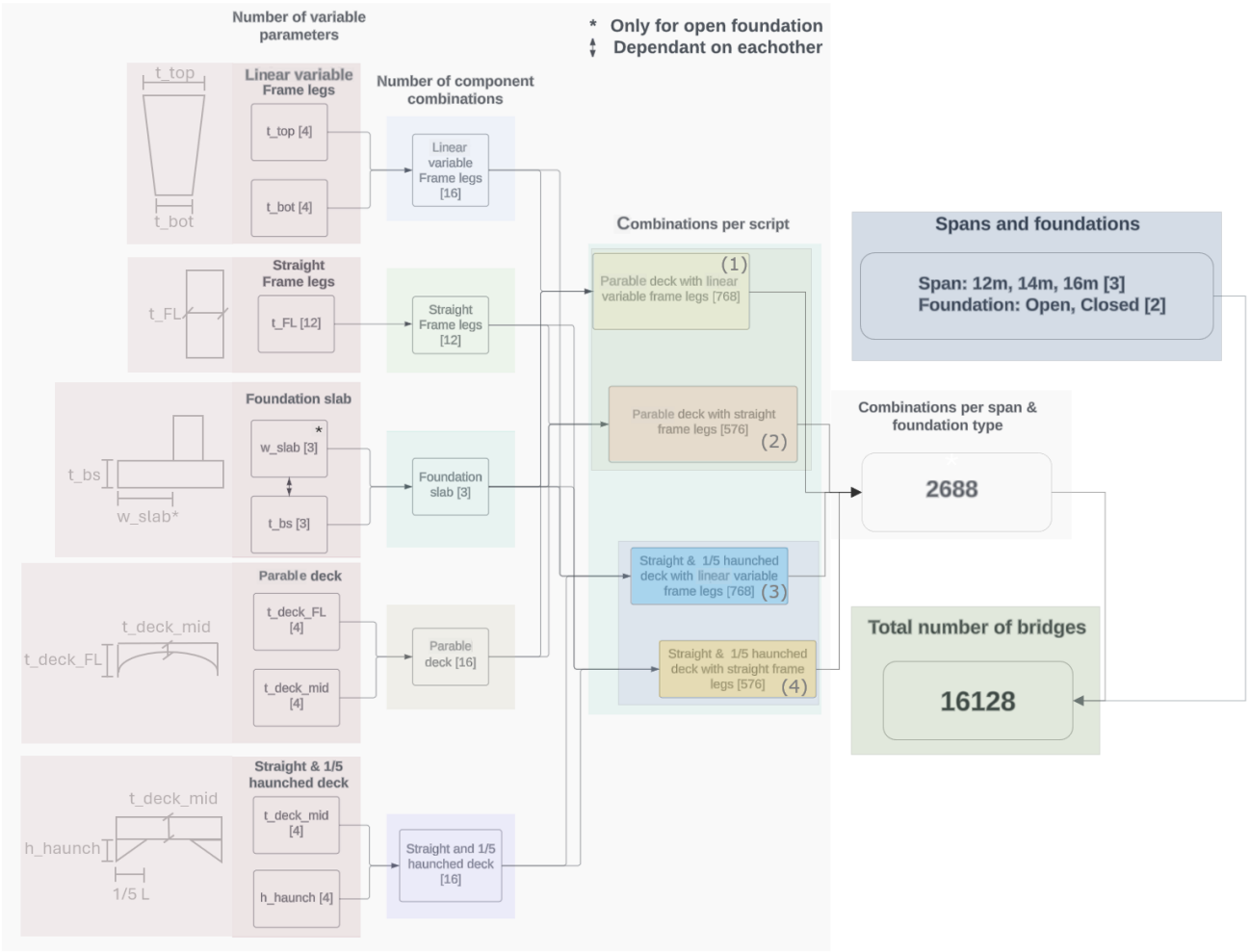

Figure 3.8: *Combination iteration set up.*

Figure 3.8 shows that the analysis starts as two different scripts, one for each foundation slab configuration. Secondly, the scripts were split further into three individual scripts for each span length, a total of six scripts. Thirdly, each script was split into four individual scripts, a total of 24 scripts, four scripts for each foundation slab configuration and length. The given name, the geometry, and the number of iterations per geometry are seen in Figure 3.8 under "Combination per script". A total of 16 128 bridge alternatives were tested for the initial chosen dimensions.

3.2.3 Stage 3 - Evaluation of bridge alternatives

To be able to evaluate the designed bridges, multiplied properties needed to be extracted from the script and used further to calculate the objective functions. Data to be used further were: concrete geometry including quantity and shape, reinforcement quantity and layout, if shear reinforcement was needed, and the quantity. The extracted properties were separated into data of individual components and combined into a total value.

3.2.3.1 Objective function

Investment cost was evaluated as a function of the amount of concrete and reinforcement used and the sizes of concrete geometry as seen in Equation 2.5. The amounts used were calculated into [SEK/quantity] values using Tables A.1, A.2, A.3, and A.7.

Environmental cost was calculated as a function of the amount of concrete and reinforcement used, as viewed in Equation 2.6 and 2.7. Firstly, an environmental cost per concrete and reinforcement was calculated using Equation 2.7, in combination with values from Table A.4 and A.5. Secondly, the calculated value for concrete and reinforced was added together to a total environmental cost for the i:th bridge alternative as seen in Equation 2.6.

Buildability cost was evaluated based on two parameters, the amount of stirrups and the geometric shape of structural components. Stirrups were evaluated using Table A.6, such that if stirrups were used, the price for the reinforcement used as stirrups was multiplied by a factor. The geometric shape of structural components was evaluated using Table A.7, such that if the structural components had a variable thickness, the cost of constructing their form-work and reinforcement was multiplied by a factor, based on how much of the structural component had variable thickness.

3.2.3.2 Equivalent cost

To be able to evaluate and optimize one bridge alternative, an optimization model was formed. The model was rewritten from the general multi-optimization equation presented in Equation 2.1. Equation 3.3 was used to evaluate and optimize the bridge alternative.

$$\left.\begin{array}{ll} \text{minimize} & F_{eqv}(x) = \langle f_{inv}(x), f_{env}(x), f_{build}(x) \rangle \,, \\ & \text{with } x \in \mathbb{C}, \end{array}\right\} \tag{3.3}$$

Where:

$\mathbb{C}$	Design space which contains all feasible bridge alternatives.
$F_{eqv}(x)$	Calculated equivalent cost.
$f_{inv}(x)$	Objective function which controls investment cost.
$f_{env}(x)$	Objective function which controls environmental cost.
$f_{build}(x)$	Objective function which controls buildability cost.
x	One bridge alternative.

As seen in Equation 3.3, the main objective is to minimize the equivalent cost which can be seen as a sum of the three normalized objective functions: **Investment cost**, **Environmental cost** and **Buildability cost**. Feasible bridge alternatives are alternatives that have passed the four testes limit states.

3.2.3.3 Parametric optimization

After applying the object functions to all bridge concepts in design space $\mathbb{C}$, it was possible to evaluate whether the precise geometric variables had been initially selected. This procedure was done by calculating the probability density and the previously mentioned normative objective function costs for each concept and plotting them against each other. Two possible shapes of these curves are shown in Figure 3.9.

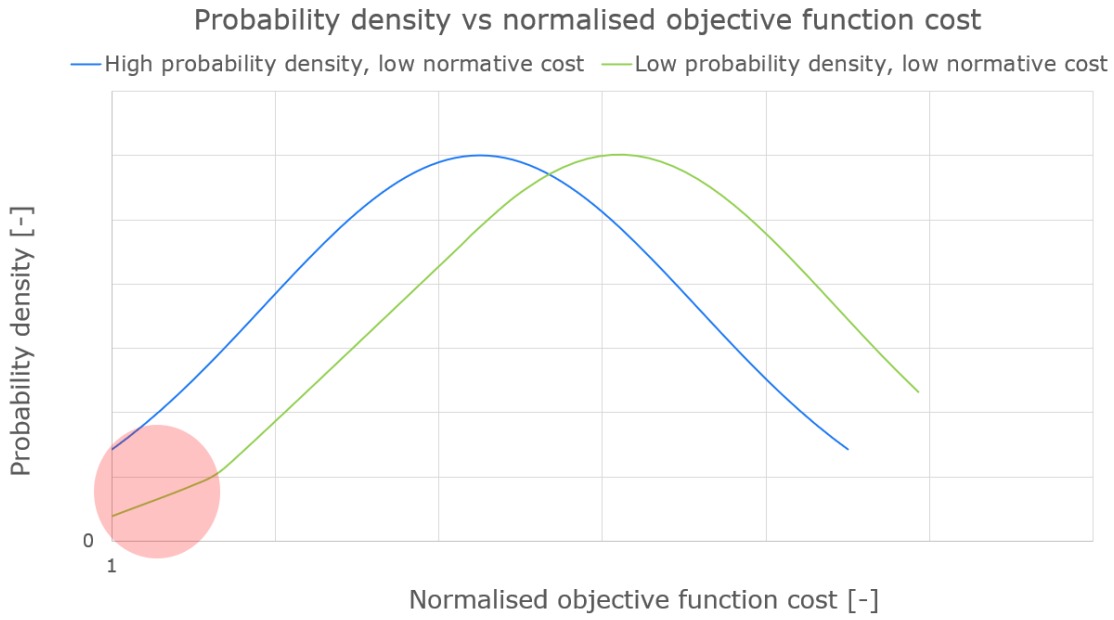

Figure 3.9: *Probability density vs. normalized objective function cost plot showing if refinement of geometric parameters is needed.*

The curves in Figure 3.9 indicated how optimized each bridge alternative was for each individual objective function while describing what probability there was to find other bridge alternatives with similar optimized costs. If the curves showed a subset with high probability density and low normative cost, shown in the left bottom corner for the blue curve in Figure 3.9, it meant that there are alternatives with smaller dimensions and lower costs left to evaluate, thus a second analysis with refined geometrical variables was needed. On the contrary, if the curves showed a subset with low probability density and a low normative cost, shown in the left bottom corner for the green curve in Figure 3.9, the chosen dimension was deemed acceptable.

If a refinement was deemed necessary, a linear regression analysis on the used geometrical variables was done to evaluate which geometric variable influences the objective function the most, thus making the refining process easier. If the tested set of results was not considered optimized, the optimization process was repeated, hence multiple sets of bridges can be achieved.

3.2.3.4 Grouping

Using FEM-design software such as Sofistik which designs the required amount of reinforcement for each node to a specific value, makes the probability of finding numerically-identical components virtually impossible. Thus, numerical comparison of required reinforcement needed to be converted to more practical and comparable data in order to group structural components with different foundation types, spans, and accompanying structural components.

Actual top and bottom longitudinal and shear reinforcement were determined to be the most significant and decisive factors for the grouping of structural components. Required longitudinal and shear reinforcement amounts for elements inside a meter-wide section, seen in Figure 3.10, were exported for each bridge iteration to be further processed into actual reinforcement amounts.

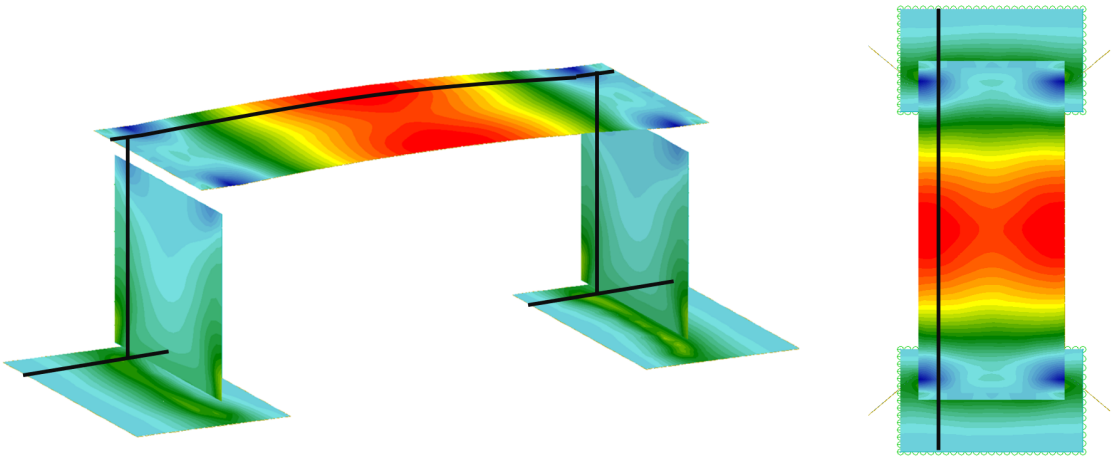

Figure 3.10: *Cut for longitudinal actual reinforcement conversion.*

As seen in Figure 3.10, a section was placed in the yz-plane offset towards the edge. The position of the section was chosen as the location with the highest absolute stress while simultaneously avoiding peak values caused by 3D effects regarding load distribution. The section provided required reinforcement amounts over a meter-wide strip similar to Figure 2.17.

Based on the maximum required reinforcement from the section, a maximum actual reinforcement amount could be set as depicted in Figure 2.17a for each structural component. The maximum required reinforcement for upper and lower longitudinal reinforcement was divided by the rebar cross-sectional area to achieve transversal reinforcement spacing seen in Figure 3.11. The spacing was rounded down to the closest multiplication of 25 mm to achieve practical and applicable reinforcement spacing. A minimum spacing was set to 75 mm for the bottom side and 125 mm for the top side reinforcement after discussion with the supervisor regarding build-ability during casting, e.g. to be able to thread the concrete hose through the top reinforcement. To further improve the grouping of components, an additional decisive parameter concerning the number of top and bottom longitudinal reinforcement

layers was added. If the required reinforcement needed a closer spacing than the set limit, an additional layer of reinforcement was added. If a third layer of reinforcement was necessary to fulfill the required reinforcement, the bridge alternative was discarded entirely from the Set-Based evaluations with respect to the previously mentioned buildability constraint.

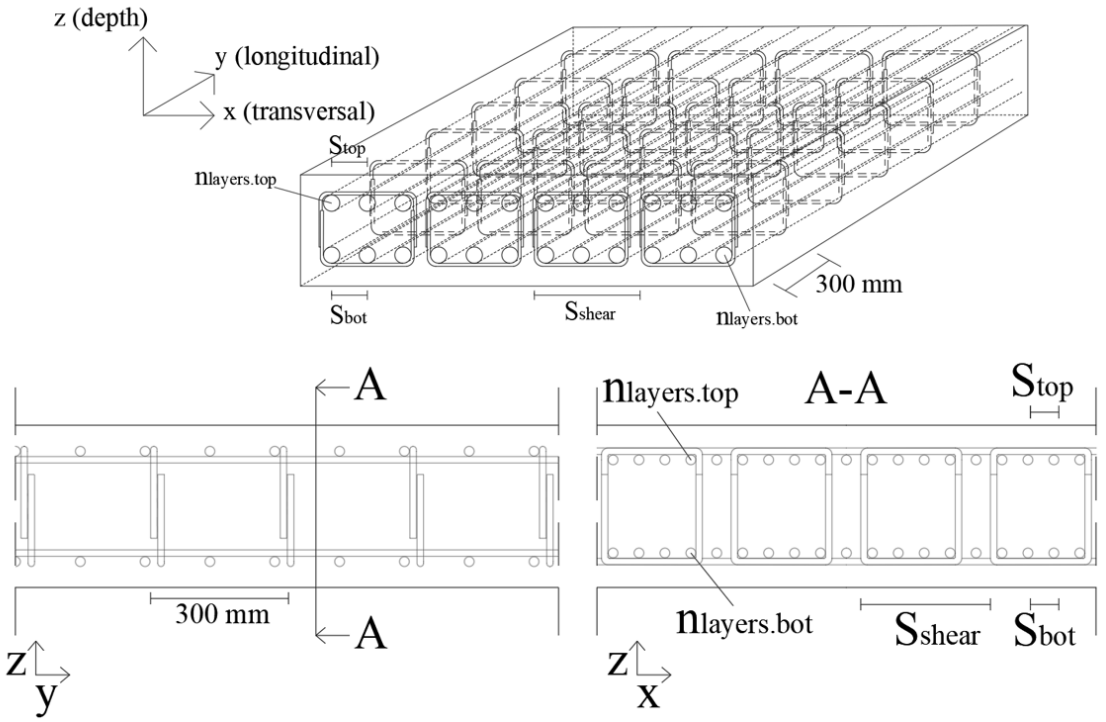

Figure 3.11: *Description of reinforcement spacing and number of reinforcement layers.*

Spacing for shear reinforcement stirrups was handled differently, due to multiple possible combinations of transversal and longitudinal spacing. One standing and one resting bent C-type rebar formed a closed stirrups as seen in Figure 3.11 with a fixed longitudinal spacing of 300 mm, the same as the reference objects. Based on the maximum required shear reinforcement from the section, the total actual number of stirrups for the entire width of the relevant structural component was calculated and converted to a transversal spacing of stirrups using the stirrups' cross-sectional area. The transversal spacing was rounded down to the closest multiplication of 100 mm to achieve practical and applicable reinforcement spacing.

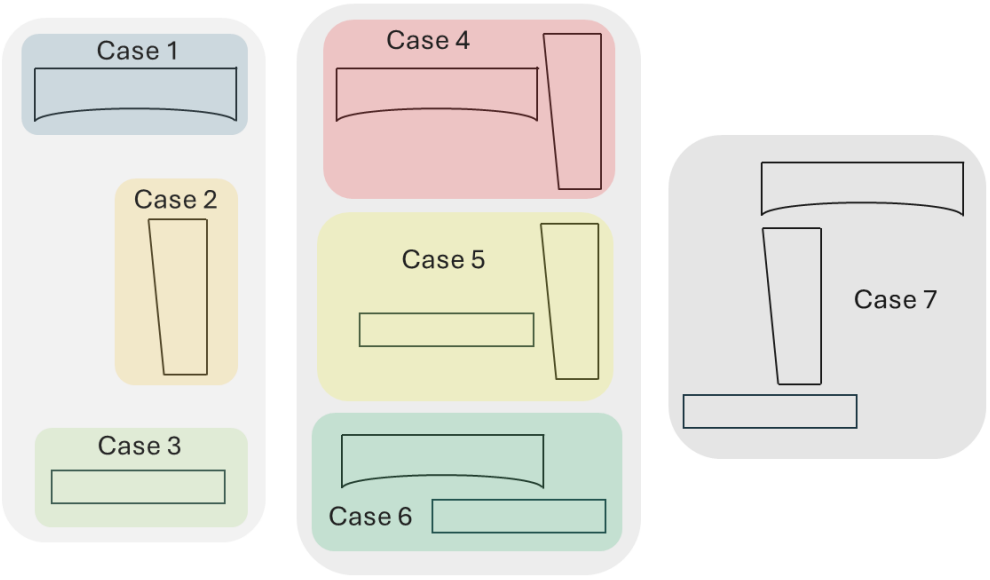

Figure 3.12: *The seven developed grouping cases containing bridges with identical structural components.*

Figure 3.12 shows the seven possible cases capable of sharing structural components for different spans and foundation types. Cases 1-3 consist of bridges that share one single structural component. Cases 4-6 consist of bridges that share two structural components. Case 7 shows possible bridges with the same structural components for different spans and/or foundation types. Cases 1-3 are referred to as single-component cases and cases 4-7 are referred to as multi-component cases throughout this thesis.

Grouping of structural components was performed according to an established rule set. Table 3.3 describes the rule set of which geometric variables and actual reinforcements had to be equal in order to belong to the same group. The rule set was applied in a Python script which scans the bridge alternatives for the seven grouping cases and adds them to different groups. Moreover, after grouping the bridge alternatives, it was possible to evaluate the cases internally to find a group with the most number of shared structural components per case, ultimately showing the most versatile groups. Each group could thereafter be highlighted in the probability density vs. normalized equivalent cost plot for comparison and evaluation.

	Grouping determining variables		
Components	**Concrete geometry**	**Longitudinal reinforcement**	**Shear reinforcement**
Foundation slab	t_{slab}, w_{slab}	$n_{layers.top}, S_{top}, n_{layers.bot}, S_{bot}$	S_{shear}
Frame legs	$t_{FL}, t_{FL.ts}, t_{FL.bs}$	$n_{layers.top}, S_{top}, n_{layers.bot}, S_{bot}$	S_{shear}
Bridge deck	$t_{deck}, t_{deck.mid}, t_{deck.fl}, t_{haunch}$	$n_{layers.top}, S_{top}, n_{layers.bot}, S_{bot}$	S_{shear}

Table 3.3: *Variables determining if structural components for different bridge iterations are identical.*

Furthermore, within the grouping, it was important to distinguish which groups were produced. The established set of rules allowed two different types of groups to be produced. Figure 3.13 shows a Venn diagram where the two different groups can be distinguished

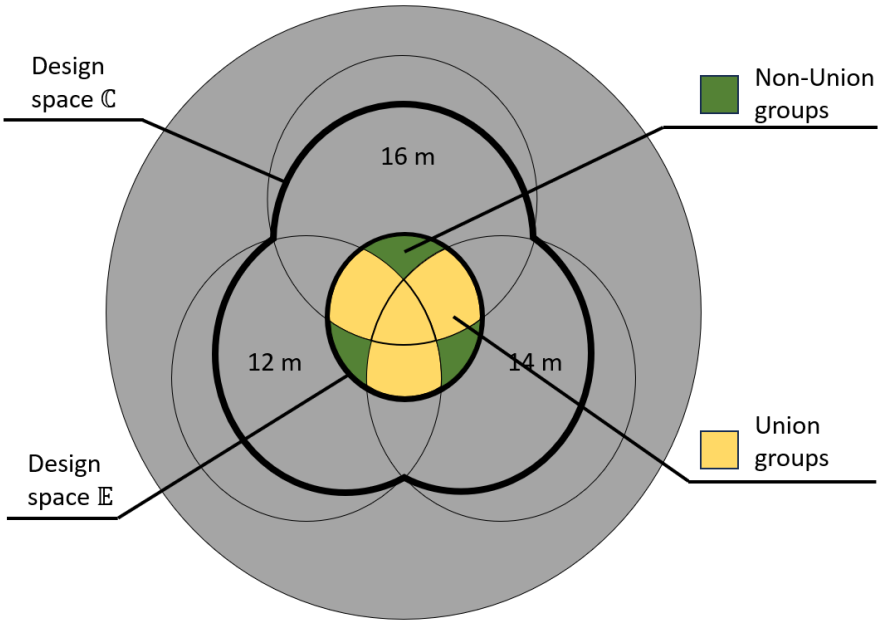

Figure 3.13: *Venn diagram showing the different groups which can be identified.*

Figure 3.13 shows the two groups that were possible to find. Union groups (UG) (yellow) which intersects between two different spans and non-union groups (dark green) a subgroup inside a single analyzed span. With the chosen conditions of only considering straight bridges and fixed geotechnical conditions, UGs were considered more interesting for the aim of this thesis concerning repeatability and to simulate a theoretical real project.

3.2.3.5 Data visualization tool

To visualize the result from the analyses, a data visualization tool was utilized, creating a library of designed slab frame bridges containing chosen design parameters. This tool allows the user to distinguish between each iteration and sort the different parameters utilizing sliders, creating the possibility for designers to select a bridge design based on e.g. client demands or personal preferences such as carbon emissions or maximum reinforcement spacings. The tool also presents an alternative way to visualize repeatability with regards to the grouping of components, by enabling the possibility to self-select groups instead of considering the group with the most number of shared structural components, as mentioned in the previous section. Figure 3.14 shows the data visualization tool highlighting a single slab frame bridge inside the library and Table 3.4 clarifies the names and units of the different parameters within the visualization tool.

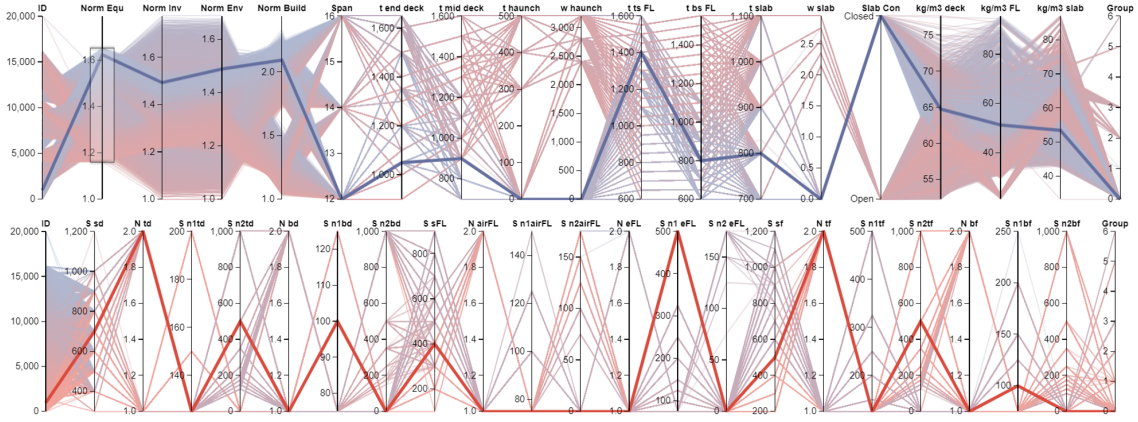

Figure 3.14: *Visualization tool highlighting a random bridge alternative.*

Name of parameter	Description	Name of parameter	Description
Geometric and optimization parameters		**Reinforcement and grouping parameters**	
ID [-]	Number/name of a designed slab frame bridge.	Group [-]	Refers to bridges that is a part of the largest UG for a selected grouping case/cases. See Figure 3.12.
Norm Equ/Inv/Env/build [-]	Normalized objective function value for equivalent/investment/environmental/ buildability-cost.	S [mm]	Transversal c-c reinforcement spacing. See Figure 3.11.
Span [m]	Distance between the two in/air-sides of the frame legs.	N [-]	Number of reinforcement layers. See Figure 3.11.
t end/mid deck [mm] t/w haunch [mm]	Bridge deck thickness at end/frame legs or in the middle of span. Thickness or width of possible haunch in the bridge deck. See Figure 3.8.	n1/2	Refers to what number of reinforcement layer.
t ts/bs FL [mm]	Thickness at top or bottom side of frame legs. See Figure 3.8.	s	Shear reinforcement. See Figure 3.11.
t/w slab [mm]/[m]	Thickness of foundation slab. Protrusion of open foundation slab. See Figure 3.8.	t/b	Refers to top or bottom placement of longitudinal reinforcement in the bridge deck or foundation slab. Top side being the layer with largest z-coordinate according to Figure 3.11.
Slab con [Open/Closed]	Foundation slab configuration. i.e open or closed foundation. See Figure 2.6.	air/e	Reference to air or earth side placement of reinforcement in the frame legs. Earth side is the outer side of the frame legs closest to the back fill while air side referee to the inside.
kg/m3 deck/FL/slab [$\frac{kg}{m^3}$]	Unit describing the average reinforcement weight per unit volume of concrete for each structural component.	d/FL/f	Structural component reinforcement is placed in. bridge deck / frame legs / foundation slab

Table 3.4: *Description of parameter names and units inside the visualization tool.*

The variables in the visualization tool were separated into two categories of parameters for easier visualization; Geometric and optimization parameters and Reinforcement and grouping parameters, as shown at the top of Table 3.4. An additional parameter showing the average weight of reinforcement per unit volume of concrete for each structural component can be seen in the top right corner of Figure 3.14. This parameter was not necessary to achieve the aim of this thesis but rather introduced a more practical optimization parameter. This optimization parameter is possibly more relatable to bridge designers used to traditional design philosophies such as PBD, compared to using normalized optimization costs.

An example of using the sliders to sort and set parameter boundaries can be observed in the "Norm Equ" category at the top left of Figure 3.14. This particular slider interval creates a group of bridges with all alternatives having normalized equivalent costs within the slider boundaries. The possibility to visualize the UG with the most number of shared structural components was still possible with the "Group" category, shown in the top right corner in Figure 3.14. Setting the slider interval to 0 in the "Group" column shows alternatives that were not included in any one of

the separately calculated UGs while setting the slider interval at another number showed the corresponding UG for that numbered grouping case. The two reference bridges were separated from the other alternatives by naming them with a higher ID-number for easier comparison, as seen by the outlying lines at the top of the ID-column in Figure 3.14.

3.2.3.6 Potential of grouping

In order to assess the potential of grouping, an evaluation method had to be developed. The chosen methodology was based on the NBLP where approximately 250 bridges will be built, where the total cost of using individually optimized bridges was compared to using grouped bridges. The theoretical potential improvement of grouped bridges came from the re-usage of form-work and the learning curve theory which is based on the fact that repetition of the same work-step shortens the construction time for further repetitions of the same work-step. The learning curve theory was applied through Equation 2.3 with a factor of n = 0.22, which was intended for concrete walls but it was considered possible to equate the construction of reinforced concrete walls to the construction of individual structural components for a slab frame bridge. To carry out the comparison, some assumptions were made:

- Every bridge was considered unique with the exception of the case-specific structural components.
- Material cost for form-work was only counted once for the case-specific structural components.
- Learning curve theory was applied for labor cost on the case-specific structural components.
- Total number of bridges used was set to 252.
- The same working crew was assumed to carry out the construction for all 252 bridges.
- An initial even distribution of bridges per span was chosen because no information regarding how many 12, 14 or 16m bridges the NBLP includes.
- If the total cost of optimized bridges was lower than grouped bridges for the initial bridges per span, the ratio between bridges per span was altered to favor grouped bridges.

3.3 Verification

To achieve the goal of this master's thesis, a combination of commercial software was used. The use of different computer programs with many input variables created a high priority to verify each step of the work process in order not to give rise to the *snowball effect* (Mc Avoy, 2004). Faulty variable choices at the beginning of the process or computational errors could occur in the process which is then used as input to subsequent steps. Equations found in civil engineering tend to be of higher order, thus making the error between calculation steps grow exponentially. This phenomenon resembles a snowball rolling down a snowy hill which increases in size the further distance it travels.

Verifying commercial FEM software such as Sofistik was pivotal concerning the snowball effect since the program analyzes and calculates the input data to be used as the basis for the optimization process. Sofistik performs both analysis and design of structures by user inputs which leaves a large gap of information in between input and output of the model. This can be referred to as the *black box problem* which is not uncommon in modern complex numerical analysis where the user has little to no influence on what operations are performed between two processing steps and must rely on human verification (Petch et al., 2022). The black box problem was addressed and countered by studying and reviewing the standards and computational methodologies used in the Sofistik software and subsequently comparing the structural behavior and design of the model with analytical hand calculations, based on the same principles used in the commercial software. To further verify the design function of the numerical model, an approximated replica of one reference object-bridge was designed in Sofistik and the results could thereafter be compared with the real designed reference object. This could be done due to the fact that the reference object was also designed based on commercial FEM software.

In addition, the use of Sofistik's built-in programming language TEDDY was used to improve the user control of the numerical model. Iterative functions such as implementing the SBD methodology were performed by scripting in TEDDY and could consequently be verified by the visualization of the underlying mathematics for each step in the process. Scripting enabled the possibility of switching on and off different parameters to verify their impact on individual steps in the iterative process and enabling the possibility to make adjustments if needed.

3.3.1 Structural behavior

To properly verify the structural behavior of the FEM model, a simplified slab frame structural layout needed to be set up in order to be comparable with analytical hand calculations based on elementary cases. The foundation slab and its associated stiffness were removed. Instead, fixed boundary conditions were implemented for the bottom of the frame legs to replicate a fixed frame. The frame legs and the bridge deck were modeled with the same thickness and transversal depth to replicate a 2D frame system with equal stiffness to simplify the analytical calculations. In order to use superpositioning of elementary load cases, linear analysis assuming uncracked

gross concrete section was used during calculations. The frame corner moments connecting the bridge deck to the frame legs and the fixation moments between the frame legs and bottom slab were chosen as the comparative parameters between the analytical and numerical model, creating four sections where comparisons were performed. The choice of sections was due to the limited set of elementary cases used.

The implementation of the large variety of different load types and combinations required for a railway bridge described in Section 3.2.2.2 needed to be verified to justify that the existing load application and combination functions in Sofistik were implemented correctly. Theoretically, all load types and combinations should be checked and compared with analytical hand calculations to avoid inherent black box issues and rectify verifications. Due to the SBD scope of this thesis and the limitations of analytical elementary cases, the verification of the numerical models' structural behavior and load combination was deemed to be justified using one load case containing the following loads:

- Self-weight of the bridge
- Dead-weight of ballast
- LM71 load model including vertical gravitational and horizontal acceleration loads
- Permanent horizontal earth pressure

Since the used Sofistik's reinforcement design-function BEMESS operates based on the largest sectional forces (Sofistik, 2024), appropriate load combination based on unfavorable and favorable load effects according to (*SS-EN 1990:2002*, n.d.) (6.10b) needed to be correctly implemented in order to continue with verification of the numerical design functions. The four resulting analytical sectional moments were compared with sectional results from the Sofistik model. The overall structural behavior of both the analytical and numerical slab frame models was also compared for the individual load combination. Based on chosen acceptable margins between the numerical and analytical sectional moments and the overall structural behavior comparison, the structural behavior and load application of the numerical model could be deemed successful, and proceeding verifications could be initiated.

The structural response from the wind load acting on the train needed to be verified due to torsional and non-symmetrical loading on the bridge. In addition, wind loads are location-dependent and highly affected by designers' estimated choices (*SS-EN 1991-1-4:2005*, n.d.). The impact from non-symmetrical and torsional loading on the structure was deemed to be incomparable with sectional moments from 2D frame elementary cases. Consequently, the wind load acting on the train was verified in a separate Sofistik model, using the same geometry as previously and LM71. By comparing the resulting load distribution from simplified analytical calculations and the reaction forces from the wind load in the Sofistik model, the wind load application in Sofistik could be verified.

The load combination was verified with the TRAC function which prints out the utilized load and the combination factors caused by the worst superpositioning of load applications. This allowed for verification against the analytically set up load case.

3.3.2 Convergence study

Due to the nature of the SBD, a large amount of data and iterations inside the FEM software were predicted to be used in the numerical analyzes. To keep the computational time as low as possible and still achieve accurate solutions, the Sofistik FEM model needed to be equipped with the appropriate amount of elements to reach convergence (Ottosen & Petersson, 1992). Convergence in a FEM model is achieved when decreasing element size does not impact the internal element output results, such as stresses and sectional forces.

To check the internal element output of the model, a simple load case in Sofistik with only self-weight could be implemented on the same slab frame geometry used in Subsection 3.3.1 to test different element and mesh sizes. The average midpoint von Mises stress for all elements in the slab frame geometry was plotted against the total number of shell elements for a specific mesh size. Based on the plotted von Mises stresses, a minimum global element size could be determined to be used to create an appropriate mesh size for the proceeding numerical analyses. Frame corner sectional moments calculated in Subsection 3.3.1, could also be used to determine if convergence had been reached since the chosen mesh resulted in acceptable margins between the analytical and numerical results.

A computational time-analysis for the final model containing the largest amount of elements (16m closed foundation with parabolic deck and variable frame legs), was performed for relevant mesh sizes from the convergence study. This was done to look at a possible mesh size increase in order to reduce computational time for the analyses while still justifying the convergence of the model.

3.3.3 Design

The design function BEMESS uses internal forces to perform load-bearing capacity checks of the input geometry and materials, as well as designing reinforcement amounts if necessary (Sofistik, 2024). The design is by default based on the most unfavorable sectional forces regarding all required limit states or designed for user-selected limit states. To achieve a realistic design situation where any one of the limit states at any section could be governing for design, a complete structural model of the closed slab frame bridge was set up and evaluated. This model was considered as an approximated FEM replica of the designed closed slab frame reference bridge in Chapter 2.5.1.

Similar geometric properties, boundary conditions, and loading conditions were approximately set up to replicate the structural behavior of the reference project. Applicable and appropriate design codes were verified against the ones used for the design of the reference bridge. A full structural and design analysis was executed

and two separate critical sections of the bridge deck were evaluated. The first section was placed in the midspan of the bridge deck, where the positive bending moment is the dimension sectional force, resulting in a critical main reinforcement design. The second section was placed close to the connection to the left frame leg, to evaluate the more critical shear force-related design.

Since limit state design involves many checks and requirements, specific design checks deemed to be most critical for the aim of this thesis had to be chosen. The designing factors shown below were chosen as the critical design functions from BEMESS to verify, due to the high impact on the material usage and buildability results from the performed design functions.

ULS	Main longitudinal reinforcement, shear reinforcement, and shear capacity of concrete without reinforcement.
SLS	Crack width limitation and minimum reinforcement
FLS	Main longitudinal reinforcement and shear reinforcement stirrups

Analytical designing calculations using applicable and appropriate design codes were performed using the same sectional forces taken from the numerical analysis. The designed reinforcement amounts and associated checks were compared with the numerical results from the Sofistik model. Based on acceptable margins between the numerical and analytical results, the design functions of the Sofistik model could be approved and the numerical model could proceed to be used in Set-Based iterations.

To further approve the designing function of BEMESS and justify potential Set-Based optimized improvements of the reference bridges, the total required reinforcement amount for all structural parts of the model could be extracted and compared with the required reinforcement amounts of the real reference bridges. A large difference in results could be an indicator of a difference in the modeling and could also lead to false optimized results later on for other tested geometries. If noticeable smaller reinforcement amounts were designed and approved for the approximately same geometries as the reference objects, the optimization would not be because of SBD, but rather a potentially different FEM model.

4

Results

This chapter contains verification of the structural calculation model and results achieved from the SBD analysis. Furthermore, grouping of bridges and the effects of the grouped bridges are also presented.

4.1 Verification of structural calculation model

This section presents the results from the convergence and analysis-time study. Further, the verification of structural behavior and the design procedure are also presented.

4.1.1 Convergence study

The results from the convergence and analysis-time study are shown in Figure 4.1 and 4.2.

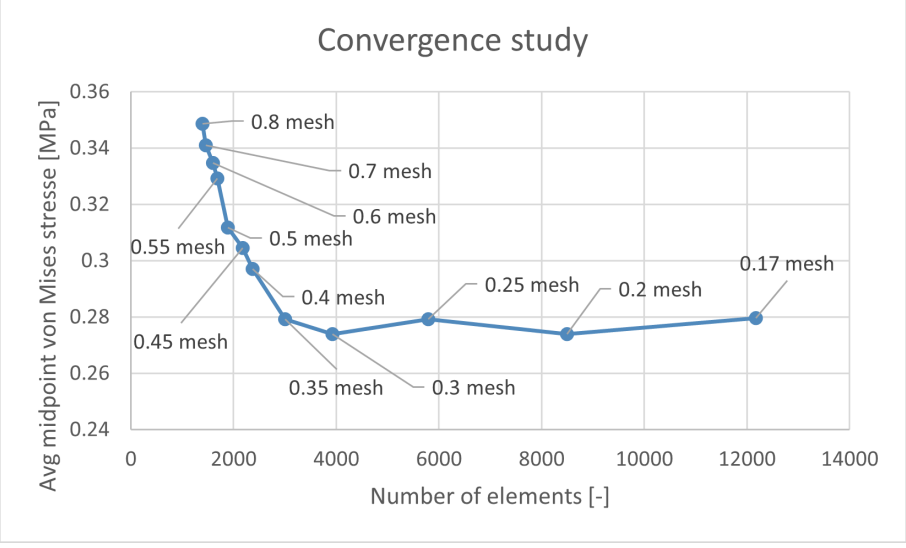

Figure 4.1: *Convergence study of FE-model.*

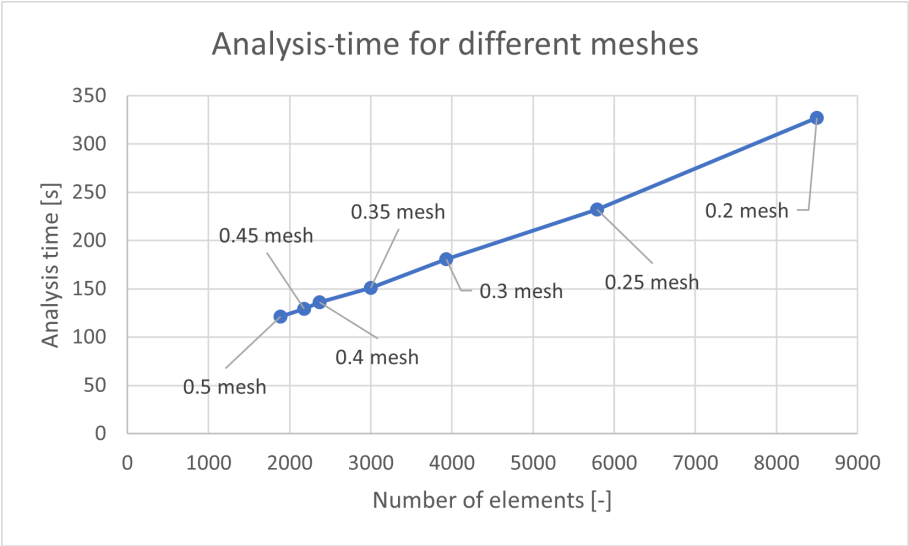

Figure 4.2: *Analysis-time study for relevant meshes.*

Considering the convergence study in Figure 4.1, a mesh using 0.35 m^2 sized elements was deemed the largest possible mesh size to establish convergence of the structural model. Based on Figures 4.1 and 4.2 the time reduction achieved from increasing to a 0.4 m^2 mesh was not considered significant enough to risk the convergence of the model and therefore a 0.35 m^2 mesh was chosen as the final mesh size to be used in the proceeding numerical analysis.

4.1.2 Structural behavior

The results from the structural behavior verification can be seen in Table 4.1 and used calculations can be found in Appendix B.

	Analytical $[\frac{kNm}{m}]$	**Numerical** $[\frac{kNm}{m}]$	**Difference** [%]
Slab-leg joint A	-294.60	-301.70	2.35
Frame corner B	-968.33	-958.38	1.04
Frame corner C	-1082.28	-1065.60	1.56
Slab-leg joint D	429.47	425.36	0.97

Table 4.1: *Bending moment results from structural verification of Sofistik model.*

Based on the average difference of 1.48% from Table 4.1 between the numerical and analytical results, the structural behavior of modeled bridges could be approved.

4.1.3 Design

The results from the design verification can be seen in Table 4.2 and the used calculations can be found in Appendix C.

	Numerical					
	ULS	**SLS**	**FLS**	**Required**	**Required analytical**	**Difference** [%]
$A_{s.main.bot}$ $[\frac{cm^2}{m}]$	44.78	68.72	68.72	68.72	70.35	2.32
A_{sw} $[\frac{cm^2}{m^2}]$	10.99	-	10.99	10.99	10.95	0.35
$A_{s.min.BD}$ $[\frac{cm^2}{m}]$	-	-	-	16.97	16.965	0.03
$A_{s.min.FL}$ $[\frac{cm^2}{m}]$	-	-	-	7.6	7.6	0.0
$A_{s.min.BS}$ $[\frac{cm^2}{m}]$	-	-	-	7.2	7.2	0.0

Table 4.2: *Reinforcement results from design verification of Sofistik model.*

With a maximum difference of 2.32% observed in Table 4.2 between the numerical and analytical results along with confirmation that the required reinforcement will be the maximum value from the tested limit state designs, the design function used in Sofistik could be approved.

The reinforcement results from implementing the reference bridge geometries in Sofistik showed differences compared to the results from the reference bridges designed in Brigade. Due to the difference, the reinforcement design comparison of the Brigade reference bridges against the tested bridge alternative from Sofistik was deemed inequity. Instead, the geometry from the reference objects was used to create Sofistik models of the reference bridges. This gave a more valid comparison between the reference bridges and the tested bridge alternatives compared to using the data from the Brigade runs of the reference bridges. Results from the reinforcement comparison between Sofistik and Brigade models can be found in Appendix D.

4.2 Evaluation of bridge alternatives

The first set of analyzed bridge geometries presented in Table 3.1 was evaluated using their respective four objective functions together with probability density to determine if refinement of geometric parameters was needed.

Nr of analyzed bridges (design space $\mathbb{B}$)	**Nr of acceptable bridges (design space $\mathbb{C}$)**	**Total analysis time per span [days]**	**Average analysis time [min/bridge]**
16 128	16 085	3.4	6.2

Table 4.3: *Evaluated bridge alternatives and relevant computational times.*

Table 4.3 showed the total number of tested bridges in design space $\mathbb{B}$ and the total number of bridges that passed the requirements between design space $\mathbb{B}$ and $\mathbb{C}$. The

requirements between $\mathbb{B}$ and $\mathbb{C}$ were if the alternative met the design requirements for the four limit states and if two or fewer layers of reinforcement were needed. Table 4.3 also showed the average run time for each alternative and the total run time for one script. It was possible to run eight scripts simultaneously, thus giving a total run time of 10.2 days for all configurations.

The resulting number of acceptable bridges from Table 4.3 was evaluated for further possible parameter refinement. The resulting objective costs and corresponding probability densities were plotted individually for each tested span and foundation configuration, as shown in Figures 4.3 - 4.6. The decision to plot foundation configurations separately for each span was made in order to produce a fair comparison of geometric parameters.

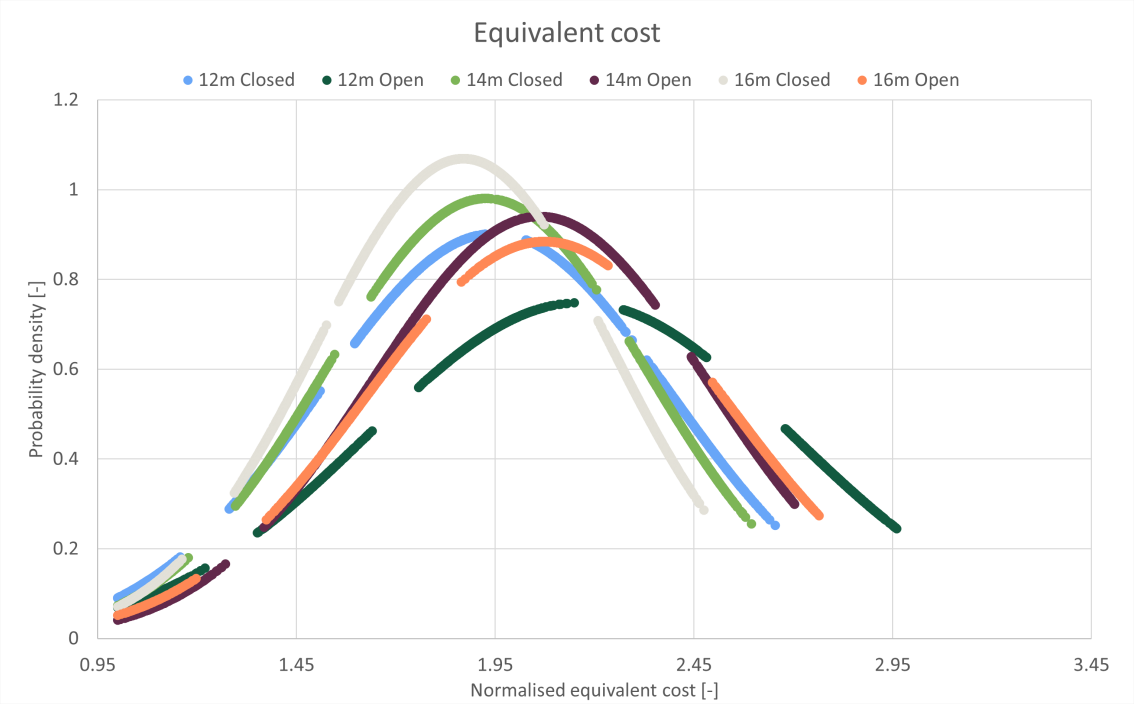

Figure 4.3: *Probability density vs. Normalized equivalent cost per span and foundation configuration.*

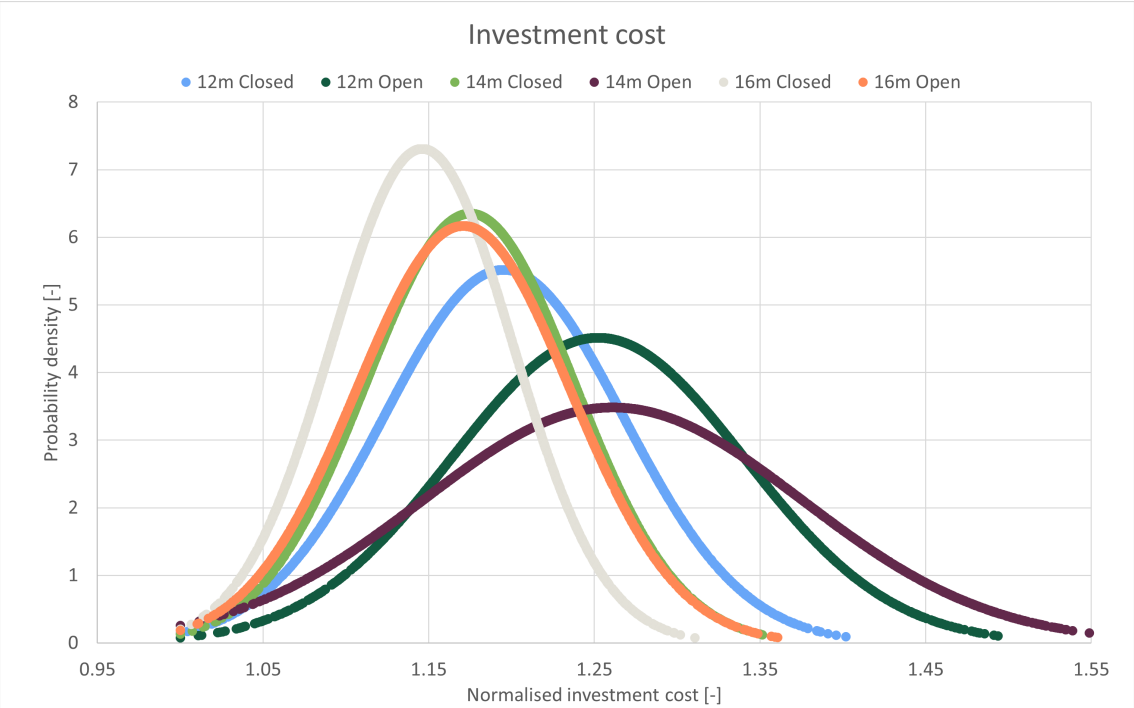

Figure 4.4: *Probability density vs. Normalized investment cost per span and foundation configuration.*

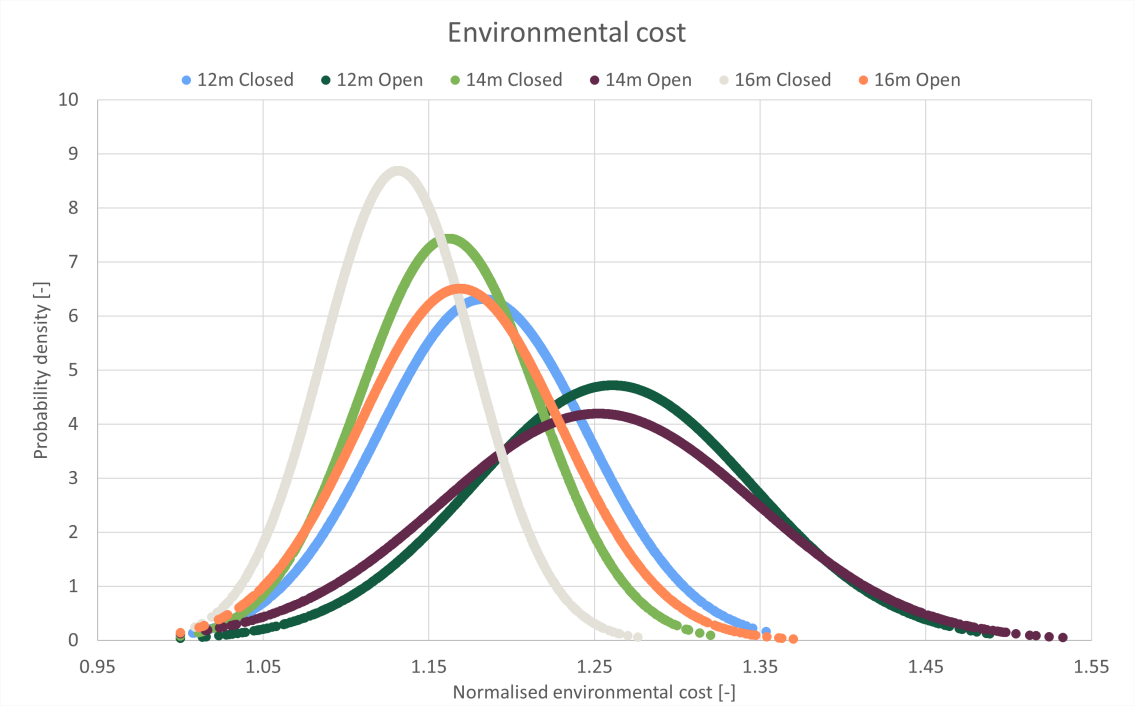

Figure 4.5: *Probability density vs. Normalized environmental cost per span and foundation configuration.*

Figure 4.6: *Probability density vs. Normalized buildability cost per span and foundation configuration.*

To verify if the initial set of geometrical variables was correct, an inspection of the bottom-left side of the plots in Figures 4.3 - 4.6 was performed. The resulting plots showed that the evaluated bridges reached a low probability density and low normative cost which concluded that the chosen dimensions from Table 3.1 were deemed acceptable according to Section 3.2.3.3 and no refinement of geometric parameters was needed.

4.2.1 Set-Based Optimization

One of the objectives of this thesis was to investigate if the use of SBD could produce more optimized bridge designs compared to the two reference objects with respect to investment cost, environmental impact, and buildability. By utilizing the object functions, it was possible to identify if more optimized alternatives existed. In order to fairly compare bridge alternatives with the reference objects, the decision to separate the alternatives by span lengths was made as shorter bridges had an unfair advantage due to naturally requiring less material volume. Figure 4.7 shows the probability density vs. normalized equivalent cost per span for all bridge alternatives separated by span length, the figure also includes the reference bridges.

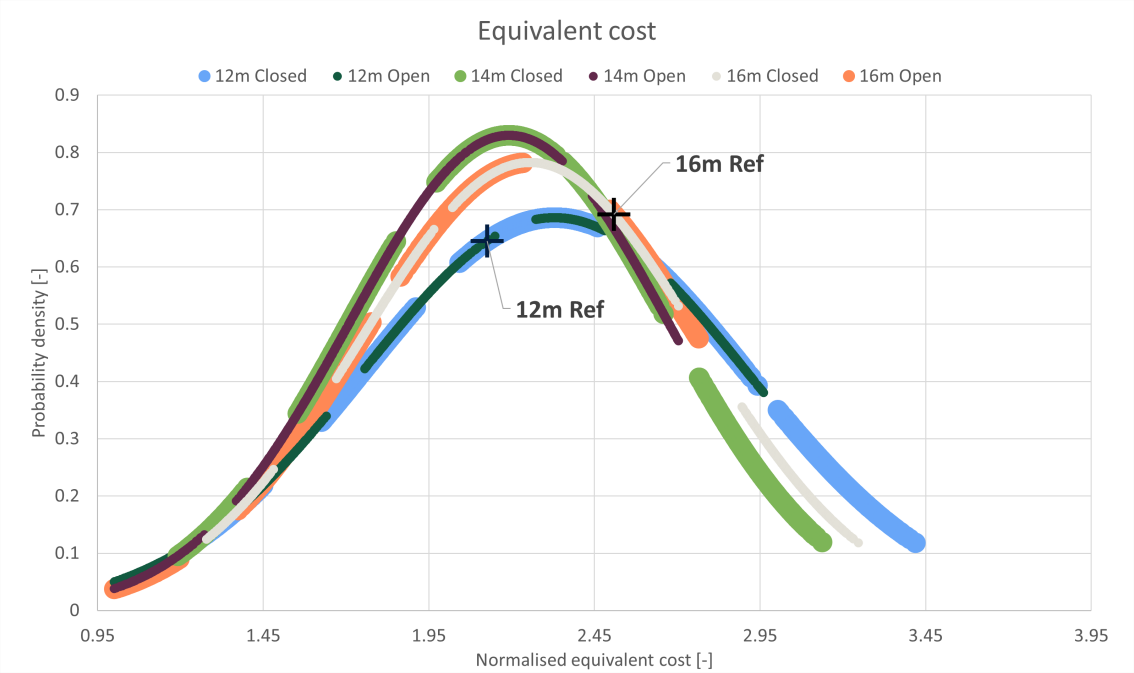

Figure 4.7: *Probability density vs. Normalized equivalent cost per span and reference bridge.*

Observation of Figure 4.7 indicates that peaks of the probability density curves for each span length are close to each other, suggesting that the most probable equivalent cost values for these spans are similar. Furthermore, Figure 4.7 showed that the *Open* foundation configurations had alternatives with lower equivalent cost compared to the most optimized *Closed* foundation configurations for all spans. However, there existed *Open* foundation configurations with higher equivalent cost than *Closed* foundation configurations for all spans. Figure 4.7 reveals that there exist bridge alternatives with lower equivalent costs compared to the reference bridges for both slab configurations, proving that more optimal slab frame bridge designs exist. Tables 4.4 and 4.5 highlights the difference between the bridge alternative with the lowest equivalent cost compared to the reference bridges.

	12m Reference bridge	**12m Optimized bridge**	**Decrease [%]**
Equivalent cost [SEK]	2 185 149	1 621 115	34.79
Investment cost [SEK]	1 658 745	1 248 517	32.86
Environmental cost [SEK]	457 409	353 817	29.28
Buildability cost [SEK]	68 995	18 780	267.38

Table 4.4: *12 m reference bridge compared to optimized 12 m bridge.*

Table 4.4 further demonstrates the difference between the reference bridge and the most optimized alternative for the 12 m span, with ID 4035. Moreover, the Table illustrated that the largest improvement of the reference bridge was buildability cost. The geometry of the optimized 12 m bridge alternative is shown in Figure 4.8 plotted on top of the 12 m reference bridge geometry.

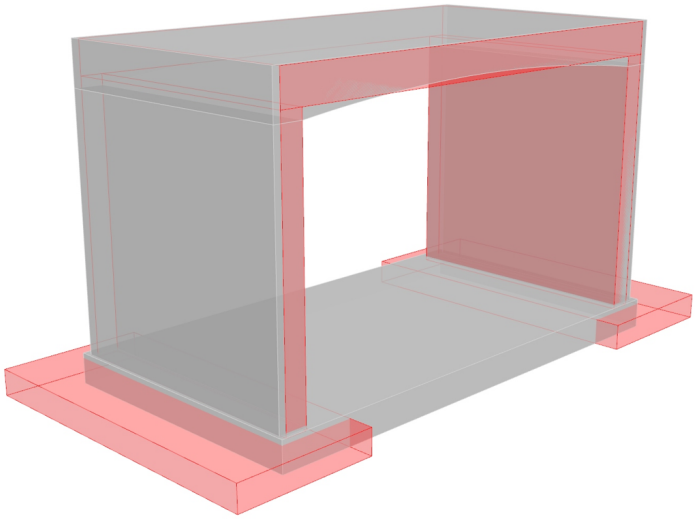

Variable	Unit	Opti	Ref
Foundation slab			
t_{slab}	$[mm]$	700	830
w_{slab}	$[m]$	2.15	0
Ø25 $S_{max.top.slab}$*	$[mm]$	125	125,500
Ø25 $S_{max.bot.slab}$	$[mm]$	200	75
Ø16 $S_{max.shear}$	$[mm]$	800	300
Frame legs			
t_{FL}	$[mm]$	650	800
Ø25 $S_{max.top.FL}$	$[mm]$	75	100
Ø 25 $S_{max.bot.FL}$	$[mm]$	250	325
Ø16 $S_{max.shear}$	$[mm]$	400	300
Deck			
$t_{deck.FL}$	$[mm]$	900	1200
$t_{deck.mid}$	$[mm]$	900	800
Ø25 $S_{max.top.deck}$ *	$[mm]$	125,250	125
Ø25 $S_{max.bot.deck}$	$[mm]$	75	75
Ø16 $S_{max.shear}$	$[mm]$	300	500

* *First, second layer reinforcement*

Figure 4.8: *Optimized 12m bridge (red) compared to 12m reference bridge (gray).*

Figure 4.8 verified that Table 4.4 was correct, with regard to all objective functions. Studying Figure 4.8, it can be observed that the optimized bridge was both smaller and straighter than the reference bridge, which is consistent with the used object functions. The optimized bridge showed higher maximum required reinforcement amounts in the bridge deck and frame legs, however noticeably lower shear reinforcement amounts in the foundation slab.

	16m Reference bridge	**16m Optimized bridge**	**Decrease [%]**
Equivalent cost [SEK]	2 521 500	2 413 170	4.49
Investment cost [SEK]	1 872 893	1 861 297	0.62
Environmental cost [SEK]	513 556	526 902	-2.53*
Buildability cost [SEK]	135 051	24 971	440.83

Table 4.5: *16 m reference bridge compared to optimized 16 m bridge. *Minus sign (-) indicates that the reference bridge had a lower cost than the optimized alternative.*

Studying Table 4.5, it can be observed that the biggest improvement of the 16 m reference object was made in buildability cost. The 16 m optimized bridge has the analysis ID 9408. Furthermore, the study of Table 4.5 demonstrated that the concrete and reinforcement quantities used for the 16 m reference object are optimized

with regard to investment and environmental cost for the tested set of bridge alternatives. However, there was potential for improvement in buildability. Moreover, comparing the results from Table 4.5 and Figure 4.7, it can be observed that using the normalized cost for the three sub-object functions yielded a significant disparity compared to using the actually cost in SEK, as using the normalized equivalent cost resulted in a difference of 150.89 %. The geometry of the optimized 16 m bridge alternative is shown in Figure 4.9, plotted on top of the 16 m reference bridge geometry.

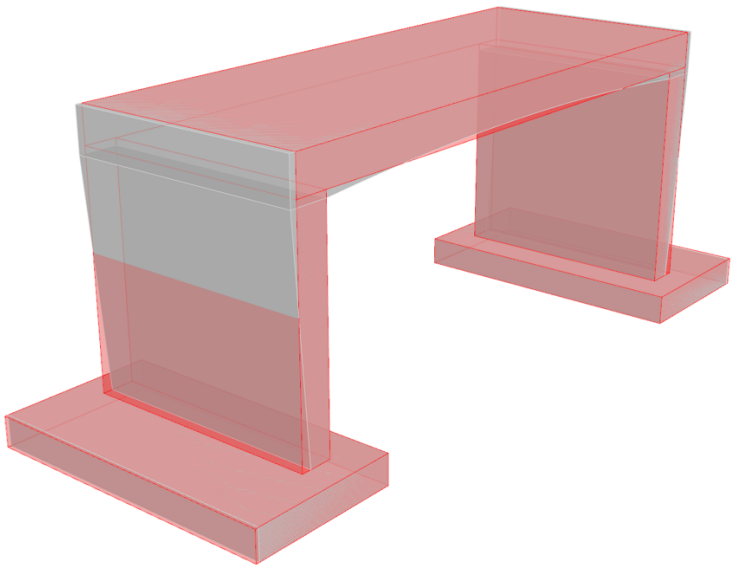

Variable	Unit	Opti	Ref
Foundation slab			
t_{slab}	$[mm]$	900	900
w_{slab}	$[m]$	2.5	2.75
Ø25 $S_{max.top.slab}$	$[mm]$	200	200
Ø25 $S_{max.bot.slab}$	$[mm]$	150	125
Ø16 $S_{max.shear}$	$[mm]$	800	700
Frame legs			
$t_{FL.top}$	$[mm]$	1000	1200
$t_{FL.bot}$	$[mm]$	1000	700
Ø25 $S_{max.top.FL}$	$[mm]$	75	75
Ø 25 $S_{max.bot.FL}$	$[mm]$	250	200
Ø16 $S_{max.shear}$	$[mm]$	500	500
Deck			
$t_{deck.FL}$	$[mm]$	1100	1300
$t_{deck.mid}$	$[mm]$	1100	950
Ø25 $S_{max.top.deck}$ *	$[mm]$	125,150	125,200
Ø25 $S_{max.bot.deck}$	$[mm]$	75	75
Ø16 $S_{max.shear}$	$[mm]$	500	600

$*$ *First, second layer reinforcement*

Figure 4.9: *Optimized 16m bridge (red) compared to 16m reference bridge (gray).*

Observation of Figure 4.9 showed that the needed volume of concrete for the reference bridge and the optimized bridge are similar but distributed differently, which could be seen in Table 4.5. The biggest difference between the two bridges is their geometric shape, whereas the optimized bridge utilized only straight structural components. The optimized bridge showed higher maximum required reinforcement amounts in the bridge deck but lower required reinforcement in the frame legs.

Furthermore, it was possible to plot individual objective functions and compare whether the optimized bridge based on equivalent cost was still the most optimized within individual objective functions and further compare them to the reference bridges in these plots. Figure 4.10 shows the probability density vs. normalized investment cost. Figure 4.11 shows the probability density vs. normalized environmental cost. Figure 4.12 shows the probability density vs. normalized buildability cost.

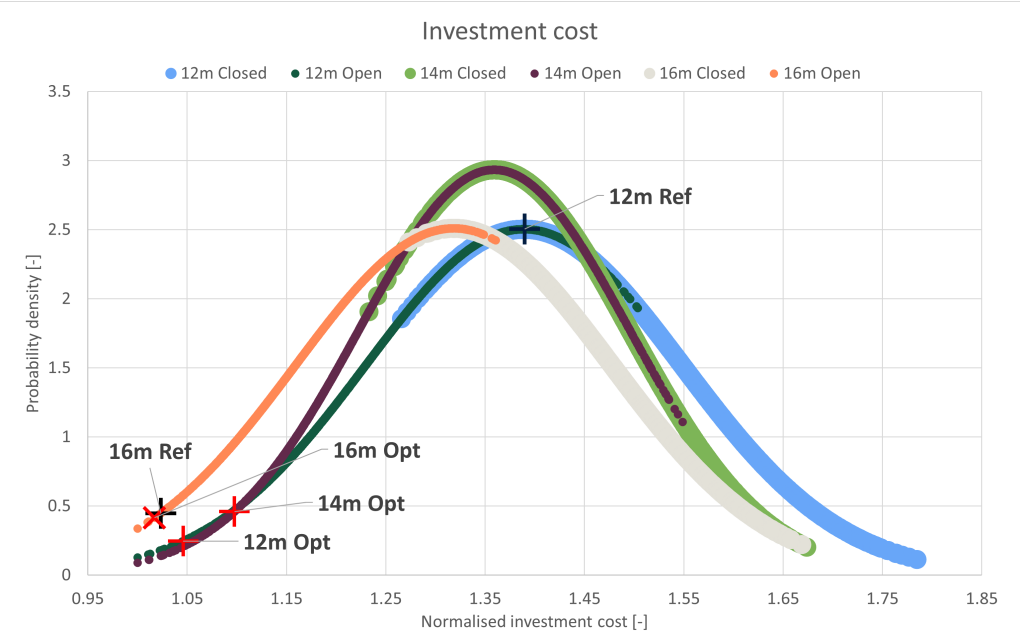

Figure 4.10: *Probability density vs. Normalized investment cost per span and reference bridge. Most optimized bridges are based on equivalent cost marked with red crosses.*

Figure 4.10 identified that optimizing based on equivalent cost did not result in alternatives automatically having the lowest investment cost.

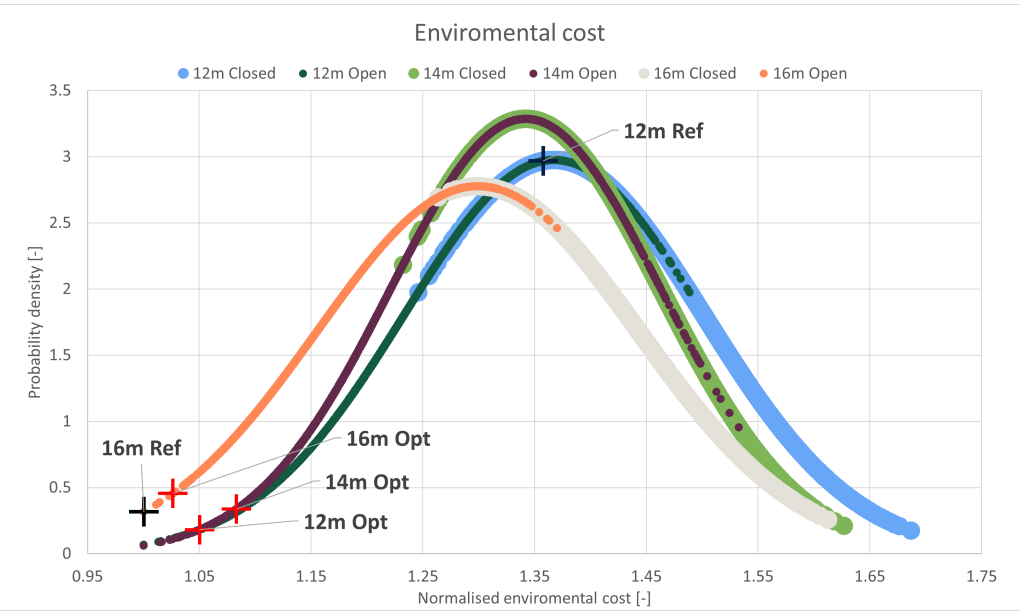

Figure 4.11: *Probability density vs. Normalized environmental cost per span and reference bridge. Most optimized bridges are based on equivalent cost marked with red crosses.*

Figure 4.11 further added to the identification that optimizing based on equivalent cost did not result in alternatives automatically having the lowest cost for other objective function costs.

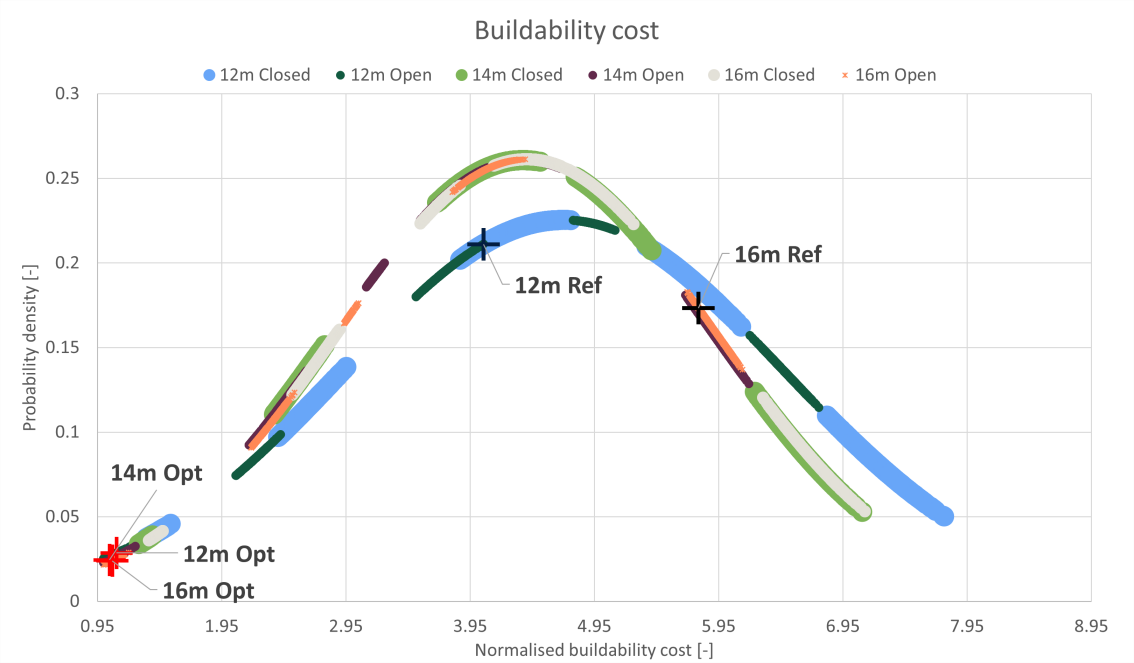

Figure 4.12: *Probability density vs. Normalized buildability cost per span and reference bridge. Most optimized bridges are based on equivalent cost marked with red crosses.*

Figure 4.12 confirms what was shown in Tables 4.4 and 4.5 that the reference bridges had a high buildability cost compared to other bridge alternatives. Figures 4.10 - 4.12 shows that the range of normalized buildability cost is larger than the range of normalized investment and environmental cost, which resulted in that buildability cost has the largest impact on equivalent cost for all three sub-objective functions. Further investigation of the buildability objective functions is shown in Figure 4.13.

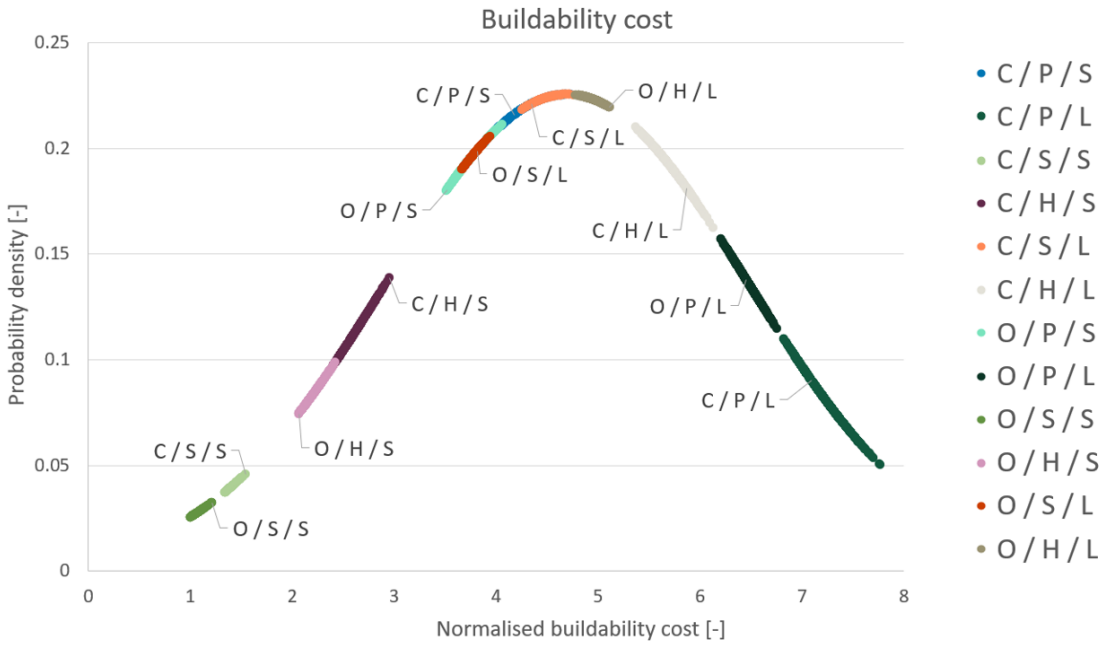

Foundation configuration	/	Deck	/	Frame legs
O = open	/	S = straight	/	S = straight
C = closed	/	H = haunched	/	L = linear variable
	/	P = parabolic	/	

Figure 4.13: *Probability density vs. Normalized buildability cost for 12 m span highlighting different geometric configurations of structural components.*

Figure 4.13 presents the buildability results for the 12 different geometric configurations of structural components that were tested. Analyzing the resulting curve from left to right, straight deck in combination with straight frame legs had the lowest buildability cost, followed by the haunched deck with straight frame legs. In the probability density peak, a cluster of three geometric configurations is found. This cluster is valid for this plot as it is based on all the 12 m bridge options, where the bridge decks are 12 m long and the frame legs have a height of 6.15 m, giving them equal impact on buildability. The highest buildability cost is achieved from a parabolic deck and linear variable frame legs. Studying Figure 4.13, it can also be observed that *Closed* foundation configuration always has higher buildability cost compared to *Open* configuration for 12 m bridge alternatives. This observation of differences in foundation configuration ought to be true for 14 m and 16 m spans as well since *Closed* foundation has a larger volume which should be reinforced with shear reinforcement, which increases the buildability cost.

4.2.2 Grouping

The second aim of the thesis was to investigate if grouping of bridge alternatives with shared structural components was possible. Grouping of bridges was performed by identifying the seven different grouping cases from Figure 3.12. Grouped alternatives could subsequently be compared with individual optimized bridges using the objective functions to see the potential advantages or drawbacks of more repeatable solutions. Observation of Table 4.6 showed that identification of groups was possible for six cases, but not possible for case 7. Case 7 searched for identical bridge decks, frame legs, and foundation slabs.

Case	**Number of groups**	**Alternatives in largest group**
1	1550	64
2	1470	89
3	632	262
4	2142	3
5	3150	25
6	2455	8
7	-	-

Table 4.6: *Number of found groups per case and the largest group found per case.*

Table 4.6 demonstrated that the grouping script was successful for 6/7 cases. No group was found for case 7. As mentioned in Section 3.2.3.4, there were two different types of groups that could be identified, UG and non-UG, and the result from the grouping in Table 4.6 identified both these types. However, groups that are unions of two or more bridge alternatives with different spans were more interesting, as explained in Section 3.2.3.4. Studying figures 4.14, 4.16, 4.18, 4.20 and 4.22, it can be observed the five largest groups for cases 1, 2, 3, 5 and 6 which had alternatives in two or more different span lengths. Case 4 considering identical frame legs and bridge deck had no group that was a union of several span lengths, therefore it was disregarded.

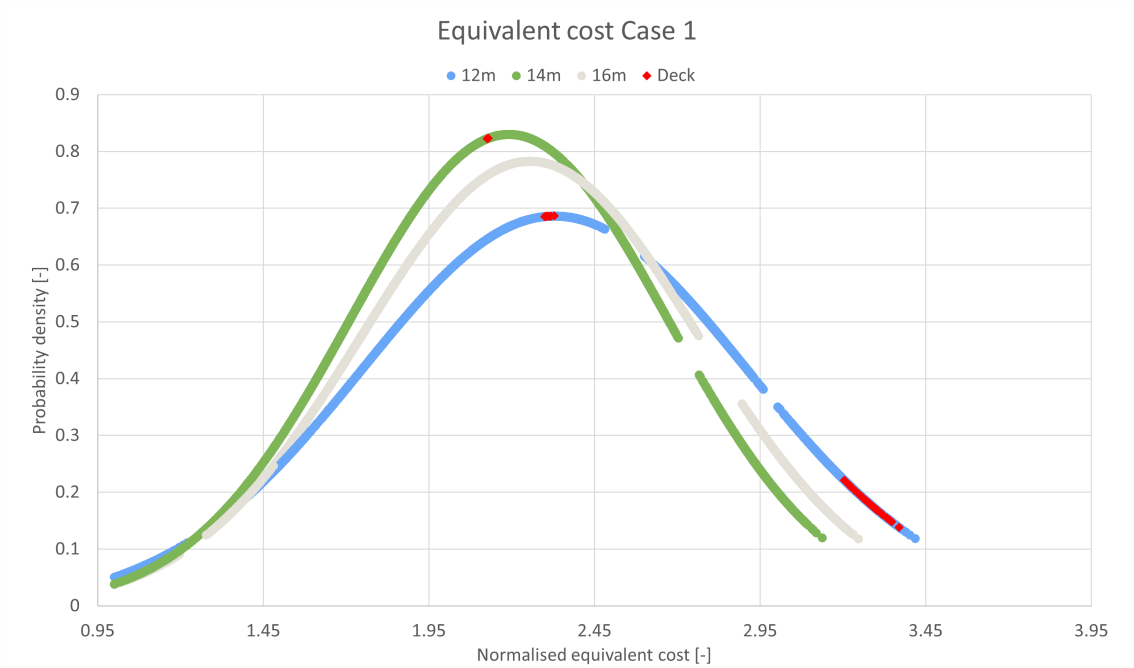

Figure 4.14: *Largest UG for case 1 (identical bridge decks) plotted on probability density vs. normalized equivalent cost curve.*

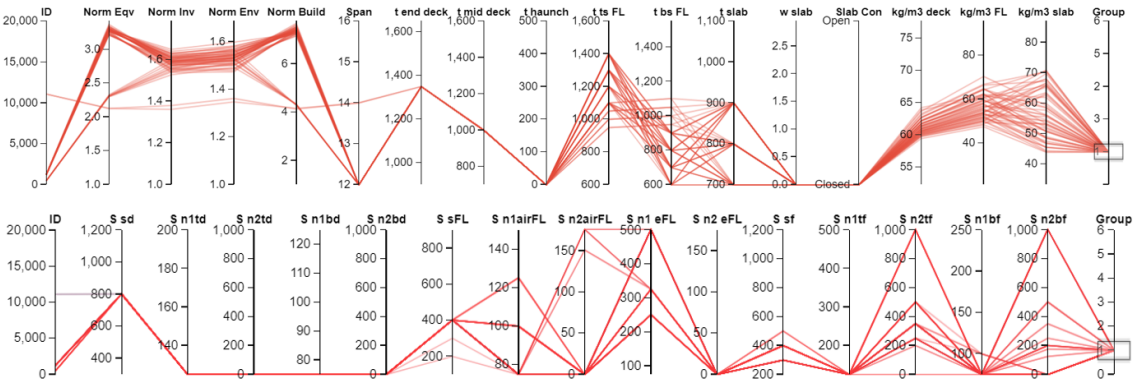

Figure 4.15: *Properties of bridge alternatives in UG case 1 (identical bridge decks.)*

A resulting total of 53 bridges using the same bridge deck geometries and reinforcement were registered inside the largest UG for case 1. Figure 4.15 shows that all alternatives included a closed foundation configuration complimented by a parabolic bridge deck with thickness in the upper bound of the tested geometries for the 12 m spans. The deck contains one maximized bottom and top reinforcement layer. Foundations slabs varied in thicknesses and frame leg configuration also varied although mostly linearly variable. Figure 4.14 further shows that the group contained two entries with 14 m span and 51 entries with 12 m span. The grouped bridges for the 12 m span can be seen to be situated compactly together in two separate

clusters in the probability density plot which states that the alternatives inside the clusters are similarly optimized.

	12m Optimized bridge	**12m Grouped bridge**	**Increase [%]**
Bridge ID	4035	528	
Equivalent cost [SEK]	1 621 115	2 398 979	47.98
Investment cost [SEK]	1 248 517	1 822 472	45.97
Environmental cost [SEK]	353 817	502 689	42.08
Buildability cost [SEK]	18 780	73 818	293.07

Table 4.7: *Optimized 12m bridge vs. most Optimized 12m bridge within UG case 1 (identical bridge decks).*

	14m Optimized bridge	**14m Grouped bridge**	**Increase [%]**
Bridge ID	14 784	11 085	
Equivalent cost [SEK]	2 159 749	2 740 793	26.9
Investment cost [SEK]	1 677 820	2 081 778	24.08
Environmental cost [SEK]	460 133	572 520	24.42
Buildability cost [SEK]	21 796	86 494	296.83

Table 4.8: *Optimized 14m bridge vs. most Optimized 14m bridge within UG case 1 (identical bridge decks).*

Comparing the most optimized alternative inside UG 1, considering identical bridge decks, with the overall most optimized bridge for each span seen in Tables 4.7 and 4.8 proved that the grouped bridges were noticeably less optimized, especially regarding buildability. The difference between investment and environmental costs was similar for each span.

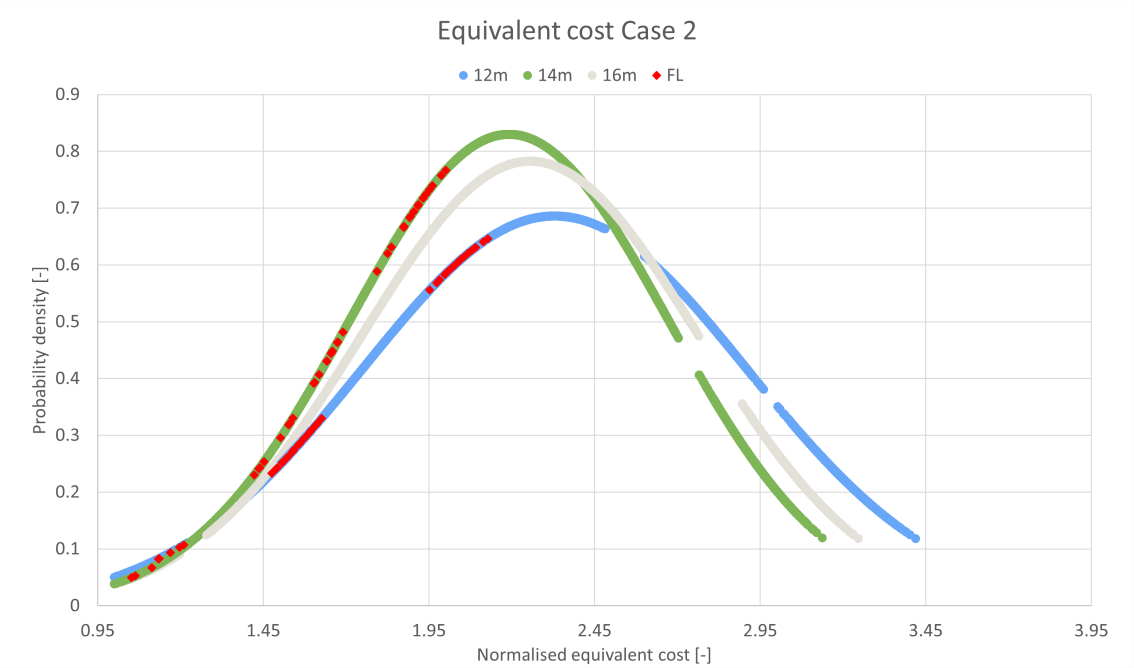

Figure 4.16: *Largest UG for case 2 (identical frame legs) plotted on probability density vs. normalized equivalent cost curve.*

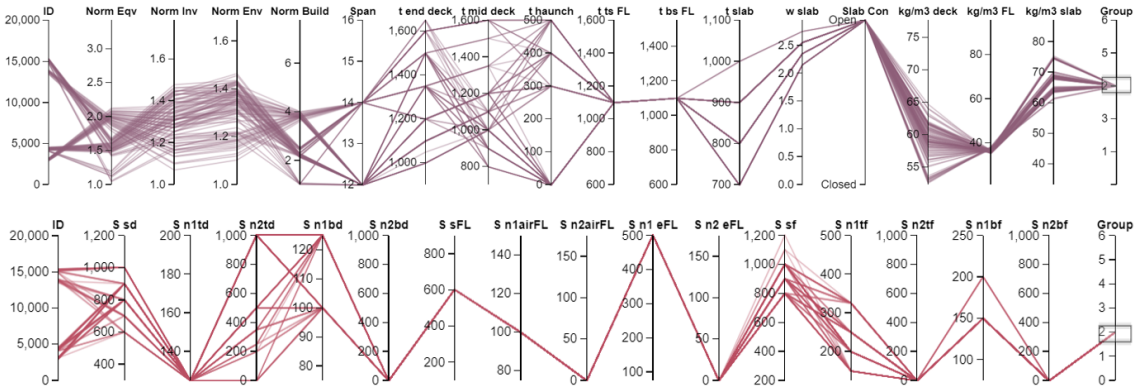

Figure 4.17: *Properties of bridge alternatives in UG case 2 (identical frame legs).*

A resulting total of 89 bridges using the same frame leg geometries and reinforcements were registered inside the largest UG for case 2. Figure 4.17 shows that all alternatives included an open foundation configuration complemented by straight frame legs using the upper bound thicknesses for the tested 12 m spans, with one layer reinforcement for both the air and earth side. Four foundation slab configurations can be observed and a variety of different sizes for all types of bridge decks are included within the group. Figure 4.16 further shows a more even distribution between spans regarding viable alternatives and more optimized solutions compared to UG 1. UG 2 contained 38 entries with 14 m span and 51 entries with 12 m span.

	12m Optimized bridge	12m Grouped bridge	Increase [%]
Bridge ID	4035	4100	
Equivalent cost [SEK]	1 621 115	1 968 816	21.45
Investment cost [SEK]	1 248 517	1 496 139	19.83
Environmental cost [SEK]	353 817	455 267	28.67
Buildability cost [SEK]	18 780	17 410	-7.29*

Table 4.9: *Optimized 12m bridge vs. most Optimized 12m bridge within UG 2 (identical frame legs). *Minus sign (-) indicates that the grouped bridge alternative had a lower cost than the optimized alternative.*

	14m Optimized bridge	14m Grouped bridge	Increase [%]
Bridge ID	14 784	14 802	
Equivalent cost [SEK]	2 159 749	2 311 423	7.02
Investment cost [SEK]	1 677 820	1 784 523	6.36
Environmental cost [SEK]	460 133	505 277	9.81
Buildability cost [SEK]	21 796	21 622	-0.8*

Table 4.10: *Optimized 14m bridge vs. most Optimized 14m bridge within UG 2 (identical frame legs). *Minus sign (-) indicates that the grouped bridge alternative had a lower cost than the optimized alternative.*

Comparing the most optimized alternative inside UG 2 with the overall most optimized bridge for each span seen in Tables 4.9 and 4.10 showed an overall lower increase for each optimization category, especially considering buildability, compared to UG 1. In addition, both optimized grouped bridges proved to be better regarding buildability than the overall most optimized bridges. The increase in investment and environmental cost was not as coherent as for UG 1, showing a larger difference in environmental cost.

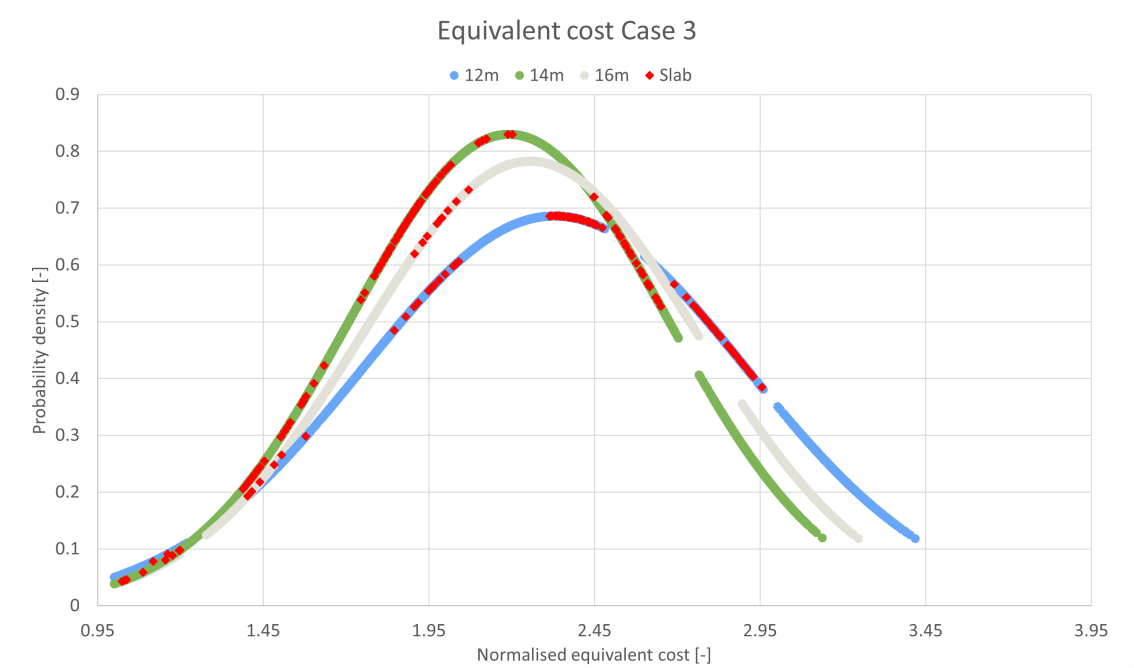

Figure 4.18: *Largest UG for case 3 (identical foundation slabs) plotted on probability density vs. normalized equivalent cost curve.*

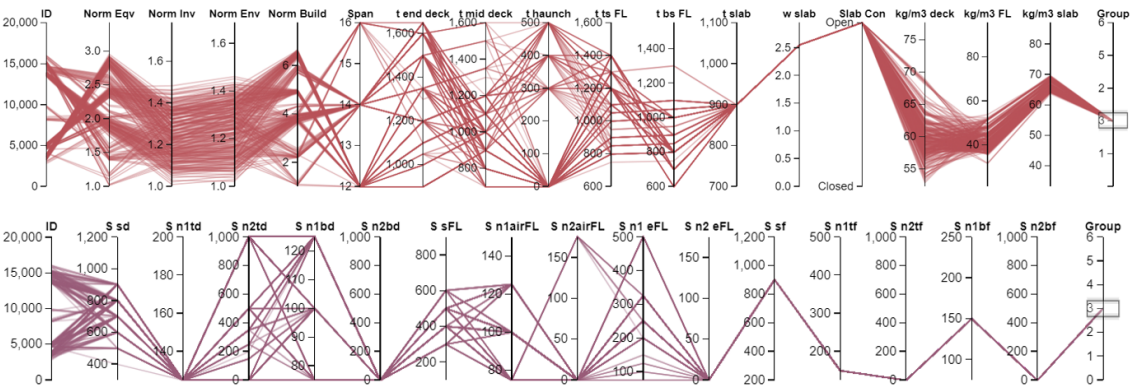

Figure 4.19: *Properties of bridge alternatives in UG case 3 (identical foundation slabs).*

Figure 4.18 showed the largest UG for case 3, which resulted in the largest and most span-compatible grouping with a total of 261 bridges with 129 entries of 12 m, 118 entries of 14 m, and 14 entries of 16 m span. As evidenced in Figure 4.19, all bridges had identical open foundation configurations requiring one layer of S100 reinforcement in the top layer and one reinforcement layer of S150 in the bottom layer. The used foundation slab had a thickness of 900 mm and heel abutment length of 2.55 m, which are the largest tested slab geometry for the 12 m bridges and the smallest tested slab geometry for the 16 m bridges. Both straight and linearly varying frame legs is represented within the group with varying reinforcement amounts along with

a variety of shapes and sizes for different bridge decks. All bridge decks had at least one layer of maximized reinforcement on the top side of the bridge deck.

	12m Optimized bridge	**12m Grouped bridge**	**Increase [%]**
Bridge ID	4035	4121	
Equivalent cost [SEK]	1 621 115	1 921 990	18.56
Investment cost [SEK]	1 248 517	1 473 853	18.05
Environmental cost [SEK]	353 817	430 029	21.54
Buildability cost [SEK]	18 780	18 108	-3.58*

Table 4.11: *Optimized 12m bridge vs. most Optimized 12m bridge within UG 3 (identical foundation slabs). *Minus sign (-) indicates that the grouped bridge alternative had a lower cost than the optimized alternative.*

	14m Optimized bridge	**14m Grouped bridge**	**Increase [%]**
Bridge ID	14 784	14 785	
Equivalent cost [SEK]	2 159 749	2 190 943	1.44
Investment cost [SEK]	1 677 820	1 695 482	1.05
Environmental cost [SEK]	460 133	472 985	2.79
Buildability cost [SEK]	21 796	22 476	3.12

Table 4.12: *Optimized 14m bridge vs. most Optimized 14m bridge within UG 3 (identical foundation slabs).*

	16m Optimized bridge	**16m Grouped bridge**	**Increase [%]**
Bridge ID	9408	9843	
Equivalent cost [SEK]	2 413 170	2 586 817	7.2
Investment cost [SEK]	1 861 297	1 988 426	6.83
Environmental cost [SEK]	526 902	546 675	3.75
Buildability cost [SEK]	24 971	51 716	107.10

Table 4.13: *Optimized 16m bridge vs. most Optimized 16m bridge within UG 3 (identical foundation slabs).*

Comparisons of the most optimized alternative inside UG 3 with the overall most optimized bridge for each span are shown in Tables 4.11, 4.12 and 4.13. Similar to the two previous UGs, the results for the 12 m span bridges showed the largest overall increase of cost, 14 m span lengths required the lowest average increase while 16 m span bridges had an intermediate increase in objective costs.

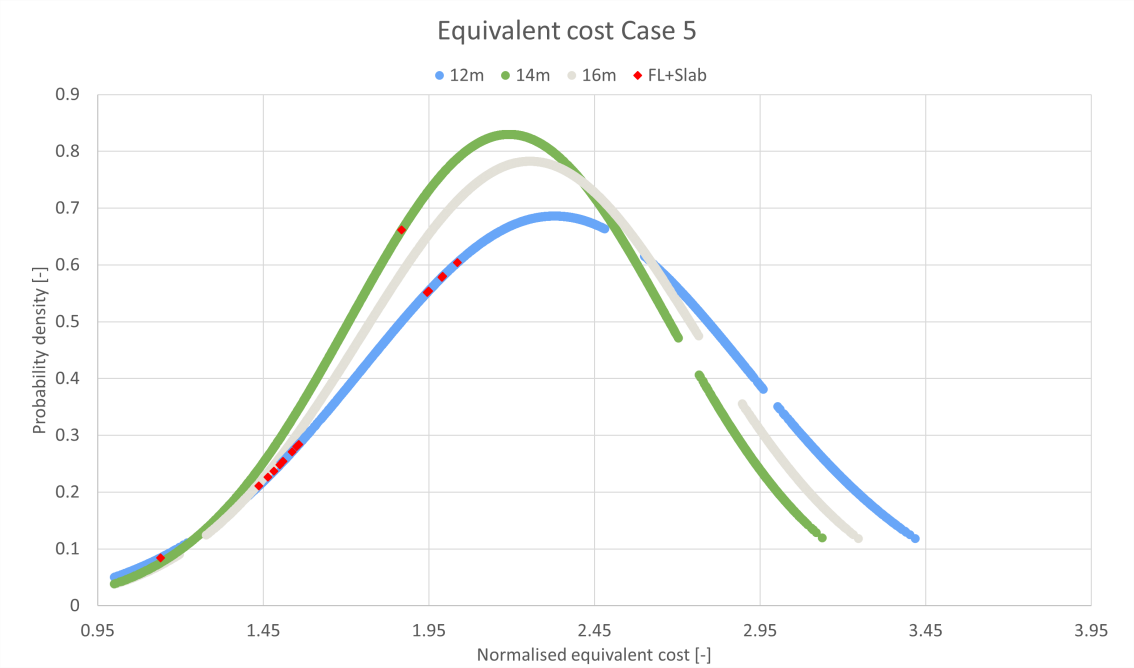

Figure 4.20: *Largest UG for case 5 (identical foundation slabs and frame legs) plotted on probability density vs. normalized equivalent cost curve.*

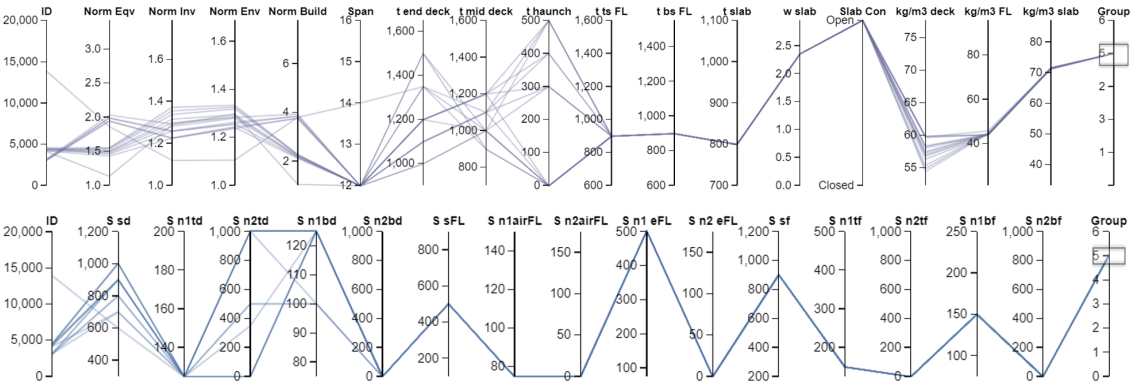

Figure 4.21: *Properties of bridge alternatives in UG case 5 (identical foundation slabs and frame legs).*

Figure 4.20 showed the largest UG for case 5 considering bridges with shared frame legs and foundation slabs. The group consisted of 15 bridges where one had a span length of 14 m and the remainder had 12 m span lengths. Figure 4.21 shows that all bridges use an open foundation configuration with straight frame legs. A variation of straight, haunched, and parabolic bridge decks exists to achieve possible bridge concepts for 12 m spans. However, for the 14 m span, only a specific parabolic deck geometry was compatible with the grouped frame legs and foundation slab for this UG. Figure 4.21 further showed that longitudinal reinforcement configurations for the different deck options did not vary as much as for previous groups.

	12m Optimized bridge	12m Grouped bridge	Increase [%]
Bridge ID	4035	4159	
Equivalent cost [SEK]	1 621 115	1 995 718	23.11
Investment cost [SEK]	1 248 517	1 540 318	23.37
Environmental cost [SEK]	353 817	437 378	23.62
Buildability cost [SEK]	18 780	18 022	-4.04*

Table 4.14: *Optimized 12m bridge vs. most Optimized 12m bridge within UG 5 (identical foundation slabs and frame legs). *Minus sign (-) indicates that the grouped bridge alternative had a lower cost than the optimized alternative.*

	14m Optimized bridge	14m Grouped bridge	Increase [%]
Bridge ID	14 784	13 878	
Equivalent cost [SEK]	2 159 749	2 262 898	4.78
Investment cost [SEK]	1 677 820	1 713 361	2.12
Environmental cost [SEK]	460 133	470 392	2.23
Buildability cost [SEK]	21 796	79 145	263.12

Table 4.15: *Optimized 14m bridge vs. most Optimized 14m bridge within UG 5 (identical foundation slab and frame legs).*

Comparing the most optimized alternative inside UG 5 with the overall most optimized bridge for each span seen in Tables 4.14 and 4.15 showed clear discrepancies in results between the two spans. The 12 m span showed a larger increase in investment and environmental costs but a decrease in buildability. Similar to the most optimized 14 m span bridge in UG 1, the increase in investment and environmental cost, resembled in Table 4.15, is correlated with a high buildability cost. Both 14 m optimized grouped bridge alternatives from UG 1 and 5 use a parabolic deck.

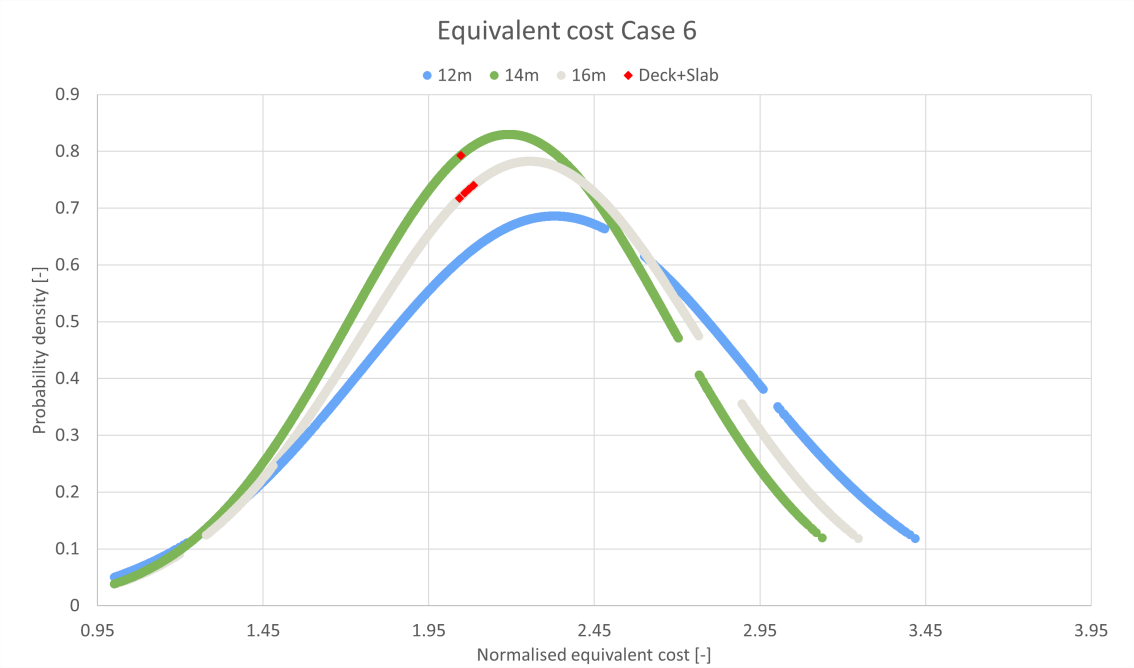

Figure 4.22: *Largest UG for case 6 (identical foundation slabs and bridge deck) plotted on probability density vs. normalized equivalent cost curve.*

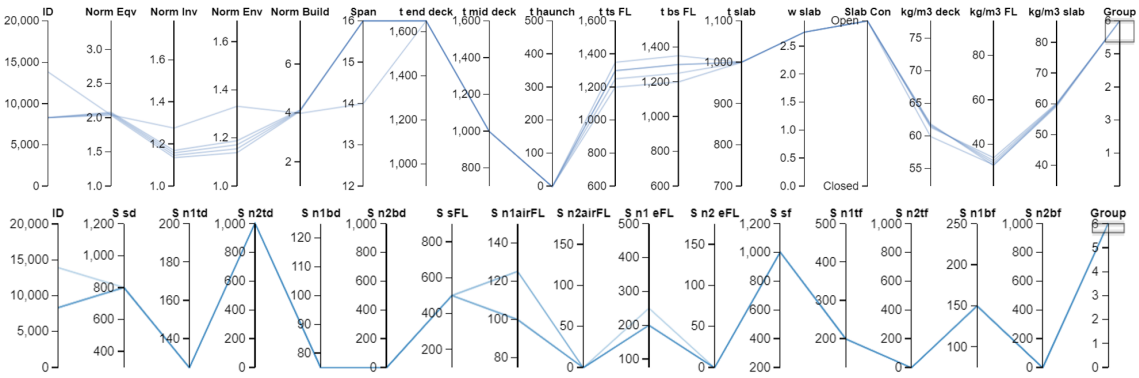

Figure 4.23: *Properties of bridge alternatives in UG case 6 (identical foundation slabs and bridge deck).*

Figure 4.22 showed the largest UG for case 6 considering bridges with identical foundation slabs and bridge decks. One bridge with a 14 m span and four alternatives with 16 m span formed the smallest UG. Similar to UG 1, the grouped bridges are clustered regarding probability density and equivalent cost, indicating that the alternatives are similar in design. This can further be proven in Figure 4.23 where the only difference between the alternatives is four different straight frame leg thicknesses with 2 alternative actual reinforcement layouts. All bridges inside UG 6 were designed with an open foundation configuration using a parabolic deck with the maximum tested deck thickness at the ends together with a foundation slab modeled with the maximum tested abutment.

	14m Optimized bridge	14m Grouped bridge	Increase [%]
Bridge ID	14 784	13 868	
Equivalent cost [SEK]	2 159 749	2 602 389	20.49
Investment cost [SEK]	1 677 820	1 953 030	16.4
Environmental cost [SEK]	460 133	566 180	23.05
Buildability cost [SEK]	21 796	83 179	281.63

Table 4.16: *Optimized 14m bridge vs. most Optimized 14m bridge within UG 6 (identical foundation slabs and bridge deck).*

	16m Optimized bridge	16m Grouped bridge	Increase [%]
Bridge ID	9408	8329	
Equivalent cost [SEK]	2 413 170	2 762 810	14.49
Investment cost [SEK]	1 861 297	2 081 746	11.84
Environmental cost [SEK]	526 902	585 815	11.18
Buildability cost [SEK]	24 971	95 248	281.43

Table 4.17: *Optimized 16m bridge vs. most Optimized 16m bridge within UG 6 (identical foundation slabs and bridge deck).*

Comparing the most optimized alternative inside UG 6 with the overall most optimized bridge for each span seen in Tables 4.16 and 4.17 showed that buildability had the largest increase compared to the other objective functions. The 14 m span showed scattered resulting differences while the 16 m spans displayed a similar relation between investment and environmental cost as UG 1. As previous results show, the bridge with the longer span also had a lower difference in optimization compared to bridges with a shorter span.

4.2.3 Effects of grouping

The hypothesis of grouping is that the benefits of reusing form-work and repeating the construction of the same components multiple times will out-weight the higher equivalent cost of more optimized alternatives. To test this hypothesis, a comparison of grouped bridges needs to be made against the most optimized ones. Tables 4.18 - 4.22 shows the results of implementing repeatability to the grouped bridges in Chapter 4.2.2 into a fictitious multi-bridge infrastructure project to see if improvements of total cost are possible.

		Equivalent cost. Even dist.			Equivalent cost. Optimized dist.	
Span [m]	Nr of bridges even dist.	Optimized [MSEK]	Grouped [MSEK]	Nr of bridges Optimized dist.	Optimized [MSEK]	Grouped [MSEK]
12	126	204.3	259.3	1	1.6	2.4
14	126	272.1	295.5	251	542.1	582.1
Total	252	476.4	554.8	252	543.7	584.5

Table 4.18: *Effects of grouping for UG case 1 (identical bridge decks).*

Table 4.18 shows that no improvement of total cost could be performed for a case of evenly distributed bridge spans. The Table further shows that the less optimized and shorter bridge within the UG made up the majority of difference to the total project cost. Even when considering a favorable case using a distribution of one 12 m bridge, the total cost of the project was still not improved, indicating that the grouping of bridge decks was unfavorably compared to constructing unique optimized bridges for the tested scenario and conditions.

		Equivalent cost. Even dist.	
Span [m]	**Nr of bridges even dist.**	**Optimized [MSEK]**	**Grouped [MSEK]**
12	126	204.3	211.6
14	126	272.1	250.5
Total	252	476.4	462.1

Table 4.19: *Effects of grouping for UG case 2 (identical frame legs).*

Table 4.19 shows that an improvement of 14.3 MSEK in total cost could be performed for a case of an even distribution of bridge spans, indicating that grouping of identical frame legs can be beneficial. The largest decreasing cost comes from the 14 m span bridges, which have the lowest increase in total costs for both spans.

		Equivalent cost. Even dist.			Equivalent cost. Optimized dist.	
Span [m]	Nr of bridges even dist.	Optimized [MSEK]	Grouped [MSEK]	Nr of bridges Optimized dist.	Optimized [MSEK]	Grouped [MSEK]
12	84	136.2	150.5	60	97.3	108.2
14	84	181.4	171.0	132	285.1	267.4
16	84	202.7	201.0	60	144.8	144.5
Total	252	520.3	522.5	252	527.1	520.1

Table 4.20: *Effects of grouping for UG case 3 (identical open foundation slabs).*

Table 4.20 shows that no improvement of total cost could be performed for a case of an even distribution of bridge spans. The reason for this is due to the 12 m bridges not achieving a sufficient cost reduction. However, a redistribution towards a favorable span distribution made it possible to reduce the total cost by 7 MSEK, indicating that the largest UG using identical open foundation slabs could be beneficial for a specific distribution of bridge spans. The specific span distribution used to achieve a reduction in total cost reduced the amount of grouped 12 m bridges from 33% to 23.8%.

		Equivalent cost. Even dist.	
Span [m]	**Nr of bridges even dist.**	**Optimized [MSEK]**	**Grouped [MSEK]**
12	126	204.3	195.9
14	126	272.1	218.3
Total	252	476.4	414.1

Table 4.21: *Effects of grouping for UG case 5 (identical frame legs and open foundation slabs).*

		Equivalent cost. Even dist.	
Span [m]	**Nr of bridges even dist.**	**Optimized [MSEK]**	**Grouped [MSEK]**
14	126	272.1	249.0
16	126	304.1	260.9
Total	252	576.2	509.9

Table 4.22: *Effects of grouping for UG case 6 (identical and open foundation slabs and bridge decks).*

Tables 4.21 and 4.22 show the comparison for both the two multi-component UGs resulting in a reduced total cost for an even distribution of spans. A 62.3 MSEK reduction in total cost can be seen for the grouping case of identical frame legs and open foundation slabs, and a 66.3 MSEK reduction for the grouping case of identical open foundation slabs and bridge decks. With the demonstrated cost reductions, it can be concluded that multi-component UGs (cases 5 and 6) have a higher potential for cost reduction than single-component UGs (cases 1-3) for the tested scenario and conditions. Considering the UGs with identical bridge decks and open foundation slabs, the reduction in total cost was more than for the UGs with identical frame legs and open foundation slabs. This is likely due to bridge decks generally representing the majority of materials and labor time compared to other structural components, which leads it to have the greatest positive effects of repeatability. Tables 4.21 and 4.22 further show that the longer spanned bridges have the largest decrease in total cost for cases 5 and 6. A redistribution favoring the longer-spanned bridges could potentially lead to additional total cost reductions.

5

Discussion

This chapter presents a discussion regarding the chosen method, the achieved results, sources of errors, and further development of the researched topic.

5.1 Method

The two decisive factors for the choice of method proved to be computational time and geometric modeling. Being able to correctly model and iterate between different geometric shapes of structural components was considered the most important aspect of achieving the optimization and grouping goal of this thesis. The use of Sofistik is an effective tool to model different geometric structural components and iterate between them while performing a fully realistic detail design for every limit state. Using a large amount of different variables to create the optimization model further improved the goals of the thesis although largely limited by computational time. Various alternative ways to reduce the computational time such as using a computer cluster were discussed but in the end, Sofistik is dependent on individual cores clock rate and only allows five instances to be run simultaneously. Thus, using a computer cluster with more cores but a slower clock rate does not increase the speed of analysis. The choice to split the FE-model into 24 individual scripts, as shown in Figure 3.8, allowed five simultaneous runs with a lower number of iterations compared to one large run with more iterations, resulting in reduced computational time.

Due to the high computational time, minimization of the amount of free buildability-relevant variables such as different reinforcement diameters and concrete classes was chosen in order to prioritize a larger amount of geometric combinations. This method increases the probability of finding and grouping of structural components. After discussions with the supervisor, using different reinforcement diameters and concrete classes other than 25 mm, 16 mm, and C35/45 was not deemed relevant for the tested spans, loads, and industry norms in Sweden. An alternative way of testing the impact of different types of concrete, such as green concrete, without impacting the computational time was considered by using a different set of data in the environmental cost objective function.

Reinforcement cages and carpets were not considered as an option in the analysis as the previously discussed benefits of reduced construction time would not make any difference between the alternatives. It should be theoretically possible to prefabricate every possible configuration of reinforcement carpets or cages, thus the decrease would have been applied to every alternative.

The initial idea with the reference bridges was to take the designed required reinforcement from Brigade and use them as calibration of the Sofistik model. The required reinforcement results from the analysis of the Sofistik model showed for the majority of structural components the same reinforcement design trends seen in Appendix D. However, the peak reinforcement value proved to be less for the Sofistik model compared to the Brigade model. Similar shear forces although different moment distributions in the superstructure proved that the right loads had been implemented but the structural behavior of the two models was different. The difference in achieved results is probably due to different modeling in the two FEM models. The Brigade model was built with rotational springs instead of modeling a foundation slab geometry connected to a spring bed using vertical and horizontal springs, approximating the site's ground stiffness. As modeling of all relevant structural components is important for the aim of the thesis, a foundation slab on a spring bed was used instead of rotational springs. This gave rise to different structural behavior between the two different FEM models, i.e. the rotation occurred in different parts of the foundation structure, resulting in different force distributions in the structures. Another difference between the models is how increased earth pressure from longitudinal deformations is modeled. The reference bridges model the increased soil pressure with a load and the Sofistik model converts them to an equivalent spring bed. The results of the two methods should be identical, but modeling with springs reduces the number of load cases tested, which reduces the calculation time. The difference in the two ways of modeling was ignored to reduce calculation time

The choice of using a 3D FEM model instead of a 2D FEM or Python script with elementary cases was based on various factors. 3D FEM modeling allows for realistic load applications and distributions, compared to 2D FEM where simplification of loads generally occurs. In addition, 3D FEM has the ability to capture out-of-plane effects which is closer to a realistic behavior. However, 3D FEM is generally more complicated to model and also requires longer calculation time than 2D FEM due to more degrees of freedom. If the thesis aimed to focus solely on testing a large number of geometries and finding many groups, perhaps 2D FEM would be an advantage. However, a higher level of detail in modeling was chosen to replicate a real structural engineer's work process and to evaluate if SBD in 3D FEM is a useful tool in professional life. Modeling in Python with elementary cases would further improve computational time but would make it very difficult to model geometries that varied in thickness as the elementary cases require a stiffness for the whole component. A component that varies in thickness along the length will have different stiffness at different sections, which cannot be replicated in elementary cases. However, Python modeling would eliminate the risk of singularities and unrealistic 3D load distributions, which occurred due to the choice of a 3D FEM model.

The method of grouping structural components was based on their geometric dimensions, number of reinforcement layers, and minimum reinforcement spacing for the bottom and top sides. The minimum spacing was determined from the observed peak required reinforcements as seen in Figure 2.17a. This approach is unrealistic compared to what is done in practice, but it is possible to construct a bridge like this. The limitation of basing the grouping on this measure is that two alternatives with the same observed peak value may have different required reinforcement curves, which would lead to different final blueprints in practice. Moreover, the idea of implementing a script that designed according to Figure 2.17b was discussed during the research but this was not implemented due to two reasons: Firstly, the process to adapt the actual reinforcement to the required reinforcement is an iterative process which would increase the computational time. Secondly, implementing a way for the script to know when the actual reinforcement is adapted "good enough" to the required reinforcement is challenging.

In addition, when a structural engineer converts required reinforcement to actual reinforcement, the amount of reinforcement in the structure increases. This increase can be seen in Figure 2.17 where the red lines (actual) are further from the y-axis than the black lines (required). This difference between the lines and with the chosen method where optimizations are based on required reinforcement may lead to a shift in the results of the optimization process if all bridges are evaluated using the actual reinforcement.

Furthermore, identical bridge decks or closed foundation slabs for different spans theoretically do not exist because longer spans require longer components. The idea behind the grouping of these components is that the same thickness and actual reinforcement amounts for different spans give similar blueprints, except for being longitudinally extended or retracted.

When running the "similarity-seeking" script it was possible to find two different groups. One group where alternatives matched in case and span, UG, and the other when they only matched in case but had different span, non-UG. Both these groups are interesting but depending on the conditions when considering the design of several bridges in a project, one group may be of more interest. For the conditions used in this thesis, where only straight bridges with identical geotechnical conditions were considered, the group with different spans was more interesting. The philosophy of the standard bridges is based on adapting the site to the bridge, resulting in the given conditions. Instead, if the conditions required both straight and curved bridges or varying geotechnical conditions with the same span length, the non-UGs would be more interesting. However, these conditions are less in line with the standard bridge philosophy.

To evaluate the potential of grouping, several assumptions were needed. The assumption to consider every bridge as unique, except for the case-specific structural component was made, thereby abandoning the standard bridge mindset of adapting the site to the bridge. Abandoning the standard bridge mindset was done to explore the potential of grouping in a traditional project where the bridge is adapted to the site. If the standard bridge mindset were to be used, the most optimized

bridges would have the lowest total cost because they have the lowest equivalent cost and all components are identical, i.e. learning curve theory could be applied for all structural components. Another assumption made is the even distribution of bridges per span as the initial condition. An even distribution was made because the highest probability of resulting in such a distribution would be achieved with enough sampling. A disadvantage of this distribution is that the initial distribution may be favorable for the grouped bridges, in other words, there are distributions of spans not tested that could be unfavorable for the grouped bridges. Moreover, altering the distribution in favor of grouped bridges was made to show that it was possible to reduce the total costs with grouping. A further unrealistic assumption is that the same construction crew would build all 252 bridges. As previously mentioned, the learning curve flattens out after a low amount of repetitions and the difference after the flattening is low. Thus, the evaluation of grouping would show the same result, that grouping works, but the difference between unique and grouped would decrease if several construction crews were implemented.

5.2 Results

Observing the four result sets in Figure 4.7 and 4.10 - 4.12, it is possible to see indications of the potential of SBD. The used reference bridges were designed as PBD with a high utilization ratio, i.e. they are considered as an optimized solution. However, observing the four results, only the 16 m reference object could be considered optimized with regard to investment cost and environmental impact. To truly achieve a bridge that is optimized, it is important to specify which optimization parameters are sought after and to investigate solutions that may be considered unconventional. To find unconventional solutions that achieve a higher optimization degree, SBD is a potential tool, as the four results show that several more optimized alternative solutions exist.

The results showed that open foundation slabs had a lower equivalent cost than closed ones. It is important to point out that this relationship is unlikely to hold for all geotechnical conditions. A closed foundation configuration is generally more structurally robust compared to open ones. Furthermore, the closed foundation has a generally larger surface contact area resulting in a more even spread of forces into the ground compared to an open one, which benefits closed foundations in weaker geotechnical conditions, such as soft clay. However, the larger surface contact area for a closed foundation also means more material usage compared to an open foundation.

Bearing the aforesaid in mind, it would be interesting to vary the geotechnical conditions and check whether there would be a shift between which configuration has the lower equivalent cost. It is possible to speculate that geotechnical conditions, such as soft clay and shorter spans favor closed foundation slabs and vice versa, that longer spans and geotechnical conditions, such as bedrock favor open configurations, but for the other cases, further analysis is needed to establish conclusions.

Table 4.5 and Figure 4.9 showed that the relation between investment cost and environmental cost is not linear. The 16 m reference bridge has a lower volume of concrete and reinforcement but a larger area than the most optimized 16 m bridge. This results in a higher investment cost as the cost of the concrete form-work is included, however lower environmental cost due to less amount of concrete and reinforcement.

Ease of construction, referred to as buildability, is a difficult parameter to measure. Tables 4.4 and 4.5 suggest that buildability had a major impact on optimization. In this thesis, buildability is measured by the amount of shear reinforcement and whether the structural members are uniformly thick or not. This has some limitations, which gives uniform thick structural components a major advantage over others. The data used for buildability evaluations suggests that a parabolic deck takes more time to construct compared to a straight deck. However, the achieved results show that the parabolic deck has a 250% higher buildability cost compared to a straight deck, shown in Figure 4.13. This raises questions about whether the optimization results are realistic as differences between bridges with similar material volumes can result in extreme differences in buildability costs, as shown in the Table 4.5 and Figure 4.9. It would be interesting to further research the actual construction time difference between different geometrical configurations.

One limitation of implementing minimum reinforcement is that bridges with large cross-section need a higher amount of required reinforcement compared to small cross-section bridges. However, it is important to note that small cross-section bridges need a higher amount of actual longitudinal reinforcement than larger cross-sections, i.e. small cross-section needs more reinforcement for load carrying, which can be seen in Figure 4.8. On the other hand, the implementation of minimum reinforcement is realistic and gives a result that is closer to a complete detailed design. Implementation of minimum reinforcement may explain why the smaller tested bridge alternative ends up in the lower percentile for equivalent cost, as only the required amount is used in the objective functions. Actual reinforcement was solely used for grouping, but can also be used to preliminary determine the design of a final chosen bridge.

Furthermore, one could argue that constructing multiple layers of reinforcement takes more time than one layer. Thus, it would have been interesting to add some form of penalty term inside the buildability evaluation for bridge alternatives that require more than one layer of reinforcement, instead of removing alternatives that require three or more layers. The decision to not consider a penalty term was established based on the scope of the thesis, where only already researched data regarding buildability would be used.

With the introduction of green concrete, the construction industry has seen concrete with lower CO_2 emissions compared to ordinary Portland cement concrete. For the environmental cost objective function, the used data is based on ordinary Portland cement concrete. Implementation of green concrete would change the relation between concrete and reinforcement in the environmental objective function such that the amount of concrete would have a lower influence on the result i.e. the amount of

reinforcement would have a greater impact on the result. However, the previously discussed observations regarding minimum reinforcement proved that the amount of required reinforcement was related to the size of the cross-section. Thus, this implementation of green concrete did not make any difference in environmental cost and equivalent cost. Consequently, the same bridge alternatives remained the most optimized bridges after the implementation of green concrete.

As previously shown in Table 4.6, no groups were found for case 7 (identical foundation slabs, frame legs, and bridge decks). This was expected, as the probability of finding such a group is 0.019 % for the chosen dimensions. Case 7 is searching for alternatives with exactly the same geometry and actual reinforcement for all structural components. For the chosen dimension it only existed one bridge for each span with equal geometry. Furthermore, no group which was a union of several span lengths was found in case 4 (identical frame legs and bridge decks), even though Table 4.6 showed that 2142 groups were found in case 4. The sorting of UGs and non-UGs was done manually, therefore the previous statement that there exists no UGs for case 4 may not be entirely true as only about 500 groups were sorted through. The largest group in case 4 contained three bridge alternatives which makes the probability of finding UGs rather small. It is important to point out that how many groups and how large these groups are, is to a large extent influenced by how large the range and steps inside the range were chosen for the geometric dimensions. Thus, if a larger range or more intricate steps were chosen, the probability of finding groups should increase.

The results from the comparison between the overall optimized and most optimized bridge within a certain UG show variations in results depending on what cases and spans are considered. UG 1 (identical bridge decks) was the only UG that contained bridges with a closed foundation. This is probably due to open foundation slabs being designed with the same amount of actual bottom reinforcement independent of span or abutment length since it was based on minimum reinforcement shown in Appendix D.3. Consequently, the amount of variables needed for a foundation slab to match with another designed foundation slab is reduced, resulting in open foundation slabs being very versatile with regards to grouping. This could further be observed by the UG for case 3 (identical foundation slabs) being the largest UG, including bridges with all three tested spans.

Looking at the three UGs containing one identical structural component (single-component UG for cases 1-3), it could be noted that UG 3 had the lowest increase in optimization costs compared to the other single-component UGs. As the group contains identical structural components that are compatible with all three tested spans, it is reasonable to assume that it has the highest possible positive effect of repeatability. However, the results shown in Tables 4.18 - 4.22 showed that the group had the fourth lowest reduction in total cost during the evaluation of grouping effects, and redistribution of spans was required. This is probably due to the fact that the largest possible tested geometry was required on the foundation slabs of the 12 m grouped bridge, which was the reason that a reduction of the total cost was achieved only by reducing the number of 12 m bridges.

Although UG 3 (identical foundation slabs) has the lowest difference in optimization costs, the multi-component UGs for cases 5 and 6 are better in terms of repeatability as they share two structural components, as shown in Tables 4.18 - 4.22. Even though the UG for case 6 (identical foundation slabs and bridge decks) showed the largest total cost reduction caused by grouping, the UG for case 5 is particularly interesting in terms of repeatability because it contains the same foundation structure and only requires a unique bridge deck. Constructing multiple bridges and reusing the form-work for the entire foundation structure should provide an advantage in terms of buildability compared to other cases. This assumption is based on that the identical foundation structures in case 5 only need two unique reinforcement joints, between the frame legs and the bridge deck, whereas other tested cases need four. UG 6 containing shared bridge decks may also not be quite as effective due to previously discussed issues with grouping and reusing blueprints for bridge decks with multiple spans.

An interesting observation can be seen for bridges in UGs with shared bridge decks (UG 1 and 6). All alternatives performed generally poorly with regard to all optimization costs, especially regarding buildability, compared to the most overall optimized bridges. This is likely due to the fact that a large parabolic bridge deck represents the majority of the total material usage for the entire bridge and is the worst bridge deck type in terms of buildability, seen in Figure 4.13. In the UG for case 6, a parabolic deck with the largest tested end-thickness was required to be compatible with multiple spans. This trend was also seen for UGs 1 and 2 where the shared components inside of the group were in the upper bound of the tested geometric variations. This observation was consistent with the hypothesis that larger structural components are needed in order to be compatible with multiple spans. This observation further emphasizes the previously discussed trend that larger spans showed less increase in optimization costs compared to the most optimized bridge. A larger component increases the percentage of material usage for a shorter bridge compared to a longer bridge and thus becomes less optimized in terms of objective function costs.

Although the effects of grouping showed the great potential to reduce the total equivalent costs for constructing multiple bridges in a large infrastructure project, it is most likely a fraction of the reduced societal costs resulting from reduced construction time. The possibility of finalizing the load-bearing construction earlier should greatly move up the access timeline for other professions which would bring forward the timeline entire infrastructure project. The results of bringing forward the timeline would potentially lead to reduced societal costs such as environmental impact due to reducing the time that an alternative longer route needs to be used. Furthermore, social sustainability would also benefit from short construction times as more transportation options would be available sooner.

5.3 Sources of error

The initial thought of the analysis was to implement a stopping criteria for bridge alternatives that did not pass the four tested limit states. The stop criterion was supposed to function so that if Sofistik could not design a bridge alternative, the output of that run would have been deleted. However, this proved difficult as eight singularities appeared at the same spots for all bridge alternatives with lower bound dimensions. Furthermore, the limitation in Sofistik only allowed "continuation on all errors" or "full stop if error". These eight spots were the four corners of each frame leg which made them easy to observe in the output. The solution to the problem was to put a maximum allowed total reinforcement area of 80 cm^2, which still was high compared to the regular output. The choice of selecting a high maximum allowed reinforcement compared to putting a low maximum allowed reinforcement or deleting that element was based on not giving small bridge alternatives any advantages because singularities occurred in their runs.

3D effects are a common problem when running three-dimensional FEM models and referee to an unrealistic stress concentration toward edges of structural areas and connection between parts. The models built in Sofistik had some problems with this effect, most noticeable in the edges of the bridge deck. It is possible to observe the effect in Figure 3.10 where four dark blue areas at the bridge deck and in the bottom corner of the frame legs occur, which indicated unrealistic high peak values at these spots. No exact solution was found for the problem; instead, some workarounds were taken to avoid the problem. One of the workarounds is the above-mentioned maximum allowed reinforcement, and another workaround was to move the section cut towards the middle, as seen in Figure 3.10. A more detailed analysis of why the 3D effect arose could lead to more realistic behavior. One possible solution that was found out afterward the analysis was to make a mesh refinement around the free edges and the connection. However, this would lead to a longer calculation time and if the problem arises from singularities, mesh refinement would worsen the problem.

A limitation of the analysis is the relation between abutment length and slab thickness. The relation was locked such as an increase of 200 mm abutment meant a 100 mm increase in slab thickness. There exists a small possibility that this relation holds true but the main reason for the lock was to decrease the number of combinations and thus reduce computing time. If abutment length and slab thickness are allowed to vary independently of each other the number of tested alternatives would increase by a factor of 3 which would increase the total run time by a factor of 3 as well, giving a total run time of 30.6 days. On the other hand, locking the relation could have limited the result. Abutment length proved to mostly affect where the rotation behavior of the foundation structure happens and slab thickness is mostly beneficial against shear forces. Therefore, if one of these behaviors was dimensioning, a smaller dimension on the locked variable could have been chosen to create a more optimized result. Furthermore, the chosen locked relation of 200/100 is probably too low, and a relation of 400/100 or even higher would have produced more distributed results.

An interesting observation was made when comparing the reference bridges to the most optimized bridge. In Figure 4.10 the 16 m reference bridge had a low normalized investment cost compared to other 16 m bridge alternatives. Furthermore, in Figure 4.11 the 16 m reference bridge had the absolute lowest normalized environmental cost. These two observations raised concerns about the right initial geometries that were in fact chosen for the 16 m bridge alternatives. A thorough examination of Table 3.1 and 2.1 shows that the 16 m reference bridge was not centered for the chosen dimension, as the method described. This error was probably caused by splitting the script into 24 different scripts, which caused problems as a detected error needed to be edited on 23 other scripts as well. This suggests that it probably exists more optimized 16 m bridges even though Figure 4.3 indicated that correct initial dimensions were chosen according to Section 3.2.3.3. However, one could argue that this mistake increased the probability of finding groups because the geometric dimension would not overlap across the spans if these intervals were not selected.

A limitation of the structural analysis is that dynamic checks were not considered in the analysis. It is possible to reflect afterward whether a dynamic analysis would have affected the number of bridges in design space $\mathbb{C}$. The general view is that large and heavy cross-sections can withstand dynamic loads, but smaller and lighter cross-sections increase the risk of dynamic problems. The selected geometrical dimensions used for design space $\mathbb{B}$ were assumed large enough to withstand dynamic effects based on the opinions of the supervisors. If dynamic analysis had been implemented in Sofistik the approximate computational time increase would be 2 minutes per bridge alternative, which would have resulted in a total increase of 22 days.

5.4 Future developments

With the rising knowledge and popularity of machine learning and artificial intelligence, there is great potential to increase the efficiency of SBD. Implementing an algorithm that can learn and adapt the tested geometric variables for structural components based on where one bridge-iteration results objective function curve would reduce the number of geometries that need to be tested to achieve optimized results. The method used in this thesis is based on the designer selecting a large number of "realistic" geometric variables, i.e. skipping the design space $\mathbb{A}$ due to computational time, and evaluates the selected geometric variables in design space $\mathbb{B}$ to possibly find alternatives that still are considered optimized in design space $\mathbb{A}$. Instead, a small set of random geometric variables could be used in design space $\mathbb{A}$, and implemented machine learning or artificial intelligence could find which variables to decrease or increase in the coming iterations based on what objective functions cost the tested bridge achieved. This would result in fewer tested alternatives beca-

use the algorithm can determine the next alternative's dimensions based on the previous alternative's object function results. Thus, alternatives with high objective function costs are avoided, consequently reducing the critical computational time. However, as shown in the results, alternatives with high object function costs that are avoided may be alternatives that are repeatable across spans, suggesting that such an implementation may harm the grouping of bridges but lead to faster and better optimization of bridges within the same span.

A main field of development within this thesis would be grouping, by both increasing the design space $\mathbb{B}$ and also by testing different site conditions. An increase in the design space $\mathbb{B}$ would increase the computation time, but it is certainly possible to optimize the code further. Even greater reductions in computational time would be possible if Sofistik were further developed to allow multiprocessor operation or a change in used software. Testing of different conditions such as a variety of geotechnical conditions, allowing different in-plane curvatures of bridges or even increasing the number of train tracks on the bridge could lead to more data regarding if grouping is possible for all imaginable conditions.

A further development of the thesis would be to implement grouping of slab frame bridges on a large infrastructure project containing multiple bridges with a varying distribution of spans and conditions. An implementation of grouping for a real project would give the research more data for both evaluating buildability and the potential of grouping. Further, It would also be interesting to measure buildability from a broader perspective by investigating how much societal cost is saved by being able to open up for traffic earlier due to decreased construction time from repeatability.

Lastly, further developing the library of components could be done by generating reinforcement blueprints for each structural component, giving bridge designers a complete catalog of slab frame bridges that can be used without modification. This is highly unlikely due to the previously discussed issues regarding required and actual reinforcement since blueprints can be carried out in different ways with regard to reinforcement layouts. A possibility could be to produce several blueprints for each structural component with various actual reinforcement layouts, i.e. being more optimized toward material usage or buildability. Thus, enabling a stakeholder to choose which solution to prioritize.

6

Conclusion

The aim of this master's thesis was to optimize slab frame bridges and investigate if grouping of bridges by structural components was possible using SBD. The results show that it is possible to optimize a single slab frame bridge through Set-Based Design in terms of investment, environmental, and buildability costs, with buildability being the main area of improvement by using straight bridge decks and frame legs. For the given conditions used in this thesis, open foundation configurations proved to generate the most optimized bridges for all tested spans. In general, more optimized bridges showed overall less required reinforcement although a higher maximum actual reinforcement.

Grouping of bridges was shown to be possible for 6/7 cases of structural component-sharing combinations. Thousands of groups were found, where the largest multiple-span UGs are the most interesting for the set conditions used in this thesis, and were further studied. For the further studied UGs, open foundation configurations are represented in the vast majority of resulting UGs, indicating that open foundations are more groupable than closed foundation configurations for the studied UGs.

Choosing a more versatile and repeatable bridge from any of the UGs, showed increased investment and environmental costs as a consequence of increased material usage compared to the most optimized individual bridge for each span. The bridge decks emerge as the main contributor to material ineffectiveness for bridge alternatives inside the UGs. Specifically, parabolic decks markedly reduce the buildability of bridge alternatives, as variable thick components are harder to construct compared to straight components based on the used data. The UG containing only identical open foundation slabs was the largest UG with the lowest material increase compared to the most optimized bridges for each tested span, making open foundation slabs the most versatile structural component to group, as they are the only UG compatible with all three tested spans.

UGs containing bridges with two identical structural components are the best UGs for repeatability benefits under the conditions tested. Although, UGs with multiple components have a higher material usage and markedly worse buildability than individually optimized bridges, the possibility to standardize multiple components outweighs these downsides for large infrastructure projects. Grouping by identical foundation slabs and bridge decks had the largest reduction in total cost with 66.3 MSEK for grouping of 252 bridges, although grouping of foundation slabs and frame legs (the foundation structure) may have greater potential for much larger societal profits through decreased overall construction time.

In addition, it is important to take into account that the results of this master's thesis are given for the conditions used and may not apply to other tested conditions. For a broader conclusion, a larger design space $\mathbb{B}$ would be needed but computational time is compromised.

Finally, the most important learning from this thesis is the thought processes of SBD and its implementation in today's construction industry. Claiming that a bridge is optimized in today's construction industry often refers to the amount of material used, but in reality, many different stakeholders affect the whole construction process. Implementing SBD in the design of slab frame bridges makes it easier to incorporate multiple views and interests to create an optimized solution that satisfies all stakeholders.

References

AIA. (2007). *Integrated Project Delivery: A Guide* (tech. rep.). American Institute of Architects. Chicago. https://info.aia.org/siteobjects/files/ipd_guide_2007.pdf

al-Emrani, M., Engström, B., Johansson, M., & Johansson, P. (2011). *Bärande konstruktioner Del 1* (Vol. 1). Chalmers University of Technology.

Barakat, S., Abdel Rasheed, I., & El-Mikawi, M. A. (2020). Measuring the Constructability of a Project using BIM as Data Collecting Tool. *Al-Azhar University Civil Engineering Research Magazine (CERM)*, *42*(2). https://www.azharcermjournal.com/CERMF2004/P20-04-19.pdf

Bergenram, F., & Ulander, S. (2023, June). *Set-Based Multi-Criteria Optimization of Slab Frame Bridges - A study on the implementation of a set-based multi criteria optimization algorithm on slab frame bridges, considering investment cost, environmental impact and buildability* [Master's thesis, Chalmers University of Technology].

Bruneby, O., Vedin, P., Ljungdahl, C., & Uneklint, P. (2023). *Standardbroar : Vad är det, och vad innebär det för oss och för mig?* (Tech. rep.). Swedish Transport Administration. Borlänge. https://trafikverket.diva-portal.org/smash/get/diva2:1795942/FULLTEXT01.pdf

Ekman, A., & Sandin, C. (2018, June). *Linear and non-linear FE-analysis of cracking behavior of wing walls in integral bridges* [Master's thesis, Lunds Tekniska Högskola].

Ekström, D., Rempling, R., & Claseson Jonsson, C. (2019). *Predicting project performance using pre-construction performance indicators - a case study evaluation* (tech. rep.). 20th Congress of IABSE. New York City 2019. https://research.chalmers.se/publication/515781/file/515781_Fulltext.pdf

Eliasson, J., & Lundberg, M. (2024). *Inriktningsunderlag inför infrastrukturplaneringen för perioden 20262037* (tech. rep.). Swedish Transport Administration. Borlänge, Trafikverket. https://trafikverket.diva-portal.org/smash/record.jsf?pid=diva2%3A1827847&dswid=5566

Engström, B. (2014). *Design and analysis of slabs and flat slabs* (2014th ed.). Chalmers University of Technology.

Fernández-Mora, V., & Yepes, V. (2020). Constructability criterion for structural optimization in BIM and Hybrid Digital Twins. *EAAE – ARCC INTERNATIONAL CONFERENCE*. https://victoryepes.blogs.upv.es/files/2021/02/Constructability-criterion-for-structural-optimization-in-BIM-and-Hybrid-Digital-Twins.pdf

Gapinski, T. (2023, November). *Standardbro med fasta mått JVG-12m-01* (tech. rep.). Swedish Transport Administration.

Girardet, A., & Boton, C. (2021). A parametric BIM approach to foster bridge project design and analysis. *Automation in Construction*, *126*. https://doi.org/10.1016/j.autcon.2021.103679

Griffith, A., & Sidwell, T. (1995). *Constructability in Building and Engineering Projects*. https://doi.org/10.1007/978-1-349-13137-2

Harryson, P. (2008). *Industrial Bridge Engineering - Structural developments for more efficient bridge construction* [Doctoral dissertation, Chalmers University of Technology].

Karlsson, M. (2022). *Broprojekteringshandbok Utgåva 1* (tech. rep.). Brosamverkan.

Lagerkvist, J., Berrocal, C., & Rempling, R. (2022, September). Climate-smarter design of soil-steel composite bridges using set-based design. In *Current perspectives and new directions in mechanics, modelling and design of structural systems* (pp. 2001–2006). CRC Press. https://doi.org/10.1201/9781003348443-328

Lagerkvist, J. (2023). *Improving productivity in design and construction of bridges* [Doctoral dissertation, Chalmers University of Technology]. https://research.chalmers.se/publication/535306/file/535306_Fulltext.pdf

Lee, S. I., Bae, J. S., & Cho, Y. S. (2012). Efficiency analysis of Set-based Design with structural building information modeling (S-BIM) on high-rise building structures. *Automation in Construction*, *23*. https://doi.org/10.1016/j.autcon.2011.12.008

Li, M., Wong, B. C., Liu, Y., Chan, C. M., Gan, V. J., & Cheng, J. C. (2021). DfMA-oriented design optimization for steel reinforcement using BIM and hybrid metaheuristic algorithms. *Journal of Building Engineering*, *44*. https://doi.org/10.1016/j.jobe.2021.103310

Long-term climate change: Projections, commitments and irreversibility. (2013). In *Climate change 2013 the physical science basis: Working group i contribution*

to the fifth assessment report of the intergovernmental panel on climate change (Vol. 9781107057999). https://doi.org/10.1017/CBO9781107415324.024

Mahzuz, H. M., Bhuiyan, M. M. H., & Oshin, N. J. (2020). Influence of delayed casting on compressive strength of concrete: an experimental study. *SN Applied Sciences*, *2*(3). https://doi.org/10.1007/s42452-020-2135-3

Martí, L., García, J., Berlanga, A., & Molina, J. M. (2016). A stopping criterion for multi-objective optimization evolutionary algorithms. *Information Sciences*, *367-368*, 700–718. https://doi.org/https://doi.org/10.1016/j.ins.2016.07.025

Mathern, A., Rempling, R., Ramos, D. T., & Fernández, S. L. (2018). Applying a set-based parametric design method to structural design of bridges. *IABSE Symposium, Nantes 2018: Tomorrow's Megastructures*. https://doi.org/10.2749/nantes.2018.s5-215

Mc Avoy, T. J. (2004). Using optimization to detect snowball effects. *IFAC Proceedings Volumes (IFAC-PapersOnline)*, *37*(9). https://doi.org/10.1016/s1474-6670(17)31929-8

Ministry of the Environment & Government offices of Sweden. (2020). Sweden's long-term strategy for reducing greenhouse gas emissions. *United Nations Framework Convention on Climate Change*. https://unfccc.int/sites/default/files/resource/LTS1_Sweden.pdf

Mogra, M., Asaf, O., Sprecher, A., & Amir, O. (2023). Design optimization of 3D printed concrete elements considering buildability. *Engineering Structures*, *294*. https://doi.org/10.1016/j.engstruct.2023.116735

Nahm, Y. E., & Ishikawa, H. (2006). A new 3D-CAD system for set-based parametric design. *International Journal of Advanced Manufacturing Technology*, *29*(1-2), 137–150. https://doi.org/10.1007/s00170-004-2213-5

Nahm, Y.-E., & Ishikawa, H. (2006). Novel space-based design methodology for preliminary engineering design. *International Journal of Advanced Manufacturing Technology*, *28*(11-12), 1056–1070. https://doi.org/10.1007/s00170-004-2463-2

NEOS. (n.d.). NEOS (Network-Enabled Optimization System). https://neos-guide.org/guide/

Netz, T., Düster, A., & Hartmann, S. (2013). High-order finite elements compared to low-order mixed element formulations. *ZAMM Zeitschrift fur Angewandte Mathematik und Mechanik*, *93*(2-3). https://doi.org/10.1002/zamm.201200040

Ottosen, N., & Petersson, H. (1992). *Introduction to the finite element method* (Vol. 1). Pearson Education Limited.

Parrish, K., Wong, J.-M., Tommelein, I., & Stojadinovic, B. (2007). Exploration of set-based design for reinforced concrete structures. *Lean Construction: A New Paradigm for Managing Capital Projects - 15th IGLC Conference*, 213–222.

Petch, J., Di, S., & Nelson, W. (2022). Opening the Black Box: The Promise and Limitations of Explainable Machine Learning in Cardiology. https://doi.org/10.1016/j.cjca.2021.09.004

Pettersson, L., & Sundquist, H. (2014, October). *Optimala kantbalkssystem Resultat av genomfört FUD-projekt* (tech. rep.). Royal Institute of technology. Stockholm.

Pheng, L. S., & Abeyegoonasekera, B. (2001). Integrating buildability in ISO 9000 quality management systems: Case study of a condominium project. *Building and Environment*, *36*(3). https://doi.org/10.1016/S0360-1323(00)00004-4

Plos, M. (2000, April). *Finite element analyses of reinforced concrete structures*. Chalmers University of Technology.

Plos, M., Pacoste, C., Johansson, M., Plos, M., & Johansson, M. (2012). *Recommendations for finite element analysis for the design of reinforced concrete slabs* (tech. rep.). https://publications.lib.chalmers.se/records/fulltext/176734/local_176734.pdf

Pore, T., Thorat, S. G., & Nema, A. A. (2021). Review of contact modelling in nonlinear finite element analysis. *Materials Today: Proceedings*, *47*. https://doi.org/10.1016/j.matpr.2021.04.504

Rempling, R., Mathern, A., Tarazona Ramos, D., & Luis Fernández, S. (2019). Automatic structural design by a set-based parametric design method. *Automation in Construction*, *108*. https://doi.org/10.1016/j.autcon.2019.102936

Samuelsson, A., & Wiberg, N.-E. (1990). *Byggnadsmekanik Bärverk* (10th ed.). Studentlitteratur.

SaravanaPrabhu, G., & Vidjeapriya, R. (2021). Comparative Analysis of Learning Curve Models on Construction Productivity of Diaphragm Wall and Pile. *IOP Conference Series: Materials Science and Engineering*, *1197*(1). https://doi.org/10.1088/1757-899x/1197/1/012004

Siddique, R. (2019). *Self-compacting concrete: Materials, properties and applications*. Woodhead publishing Series. https://doi.org/10.1016/c2018-0-01683-7

Simonsson, P. (2011, April). *Buildability of Concrete Structures Processes, Methods and Material* [Doctoral dissertation, Luleå University of Technology].

Sofistik. (2024). BEMESS Design of Plates and Shells. [user manual].

Solat Yavari, M. (2017). *Slab Frame Bridges Structural Optimization Considering Investment Cost and Environmental Impacts* [Doctoral dissertation, KTH Royal Institute of Technology]. https://www.diva-portal.org/smash/get/diva2:1079393/FULLTEXT01.pdf

Solat Yavari, M., Du, G., Pacoste, C., & Karoumi, R. (2017). Environmental Impact Optimization of Reinforced Concrete Slab Frame Bridges. *Journal of Civil Engineering and Architecture*, *11*(4). https://doi.org/10.17265/1934-7359/2017.04.001

Solat Yavari, M., Pacoste, C., & Karoumi, R. (2016). Structural Optimization of Concrete Slab Frame Bridges Considering Investment Cost. *Journal of Civil Engineering and Architecture*, *10*(9). https://doi.org/10.17265/1934-7359/2016.09.002

Sonar, I. (2020). Variation of Strength and Workability of Concrete with Type of Cement and Water Reducer. https://www.researchgate.net/publication/340454882_Variation_of_Strength_and_Workability_of_Concrete_with_Type_of_Cement_and_Water_Reducer

SS-EN 1990:2002 (tech. rep.). (n.d.). European Committee for Standardization.

SS-EN 1991-1-4:2005 (tech. rep.). (n.d.). European Committee for Standardization.

SS-EN 1991-1-5:2003 (tech. rep.). (n.d.). European Committee for Standardization.

SS-EN 1991-2:2003 (tech. rep.). (n.d.). European Committee for Standardization.

SS-EN 1992-1-1:2005 (tech. rep.). (n.d.). European Committee for Standardization.

Steinø, N., & Veirum, N. E. (2022). A Parametric Approach to Urban Design. *Proceedings of the 23th International Conference on Education and Research in Computer Aided Architectural Design in Europe (eCAADe)*. https://doi.org/10.52842/conf.ecaade.2005.679

Swedish Transport Administration. (2008, June). *Kodförteckning och beskrivning av Brotyper* (tech. rep.). Trafikverket. Borlänge.

Swedish Transport Administration. (2023, December). Presentation of Norrbotniabanan. https://www.trafikverket.se/vara-projekt/projekt-som-stracker-sig-over-flera-lan/norrbotniabanan/

Technia. (n.d.). Brigade Standard. https://www.technia.se/software/brigade/brigade-standard/

TRVINFRA-00227 (tech. rep.). (2023, July). Swedish Transport Administration.

TSFS 2018:57 (tech. rep.). (n.d.). the Swedish Transport Agency.

Uppenberg, S., Ekström, D., Liljenroth, U., & Al-Ayish, N. (2017, May). *Klimatoptimerat byggande av betongbroar Råd och vägledning* (tech. rep.). SBUF-PROJEKT 13207. https://vpp.sbuf.se/Public/Documents/ProjectDocuments/5091a3fe-9f6c-4f98-b1e2-c2416df0aa42/FinalReport/SBUF%2013207%20Slutrapport%20Klimatoptimerat%20byggande%20av%20betongbroar.pdf

Ward, A., Liker, J., Cristiano, J., & Sobek, D. (1995). The second toyota paradox: How delaying decisions can make better cars faster. *Sloan Management Review*, *36*(3), 43–61.

Weber, M. (2022, September). Finite Element Method in Structural Engineering. https://concrete.ethz.ch/blog/finite-element-method-in-structural-engineering/

Yaqoob, S. (2017). *Bridge Edge beam Non-linear analysis of reinforced concrete overhang slab by finite element method* [Master's thesis, Royal Institute of technology].

Zhou, Z. W., Alcalá, J., & Yepes, V. (2020). Bridge carbon emissions and driving factors based on a life-cycle assessment case study: Cable-stayed bridge over hun he river in liaoning, china. *International Journal of Environmental Research and Public Health*, *17*(16). https://doi.org/10.3390/ijerph17165953

A

Data for objective functions

Data to be used for the evaluation of investment, environmental, and buildability costs is listed below.

A.1 Investment cost

Description	Value	Unit
Concrete material C32/40	1700	SEK/m^3
Concrete material C35/45	1800	SEK/m^3
Concrete material C50/60	2000	SEK/m^3
Reinforcement material	9	SEK/kg

Table A.1: *Material cost for concrete and reinforcement according to Solat Yavari et al. (2016).*

Description of work	Value	Unit
Concrete, wing walls	1000	SEK/m^3
Concrete, frame legs	750	SEK/m^3
Concrete, bridge deck	800	SEK/m^3
Extra work, concrete C50/60	200	SEK/m^3
Reinforcement, wing walls	17.5	SEK/kg
Reinforcement, frame legs	15	SEK/kg
Reinforcement, bridge deck	17.5	SEK/kg

Table A.2: *Work cost for concrete and reinforcement according to Solat Yavari et al. (2016).*

Description of form-work	Value	Unit
Concrete, wing walls, constant thickness	1250	SEK/m^2
Concrete, wing walls, variable thickness	1850	SEK/m^2
Concrete, frame legs, constant thickness	1000	SEK/m^2
Concrete, frame legs, variable thickness	1300	SEK/m^2
Concrete, bridge deck, constant thickness	1250	SEK/m^2
Concrete, bridge deck, variable thickness	1500	SEK/m^2

Table A.3: *Form-work cost for concrete according to Solat Yavari et al. (2016).*

Category of impact	Unit	Concrete, C32/40 [m^3]	Concrete, C35/40 [m^3]	Concrete, C50/60 [m^3]	Reinforcement [ton]
Global warming potential (GWP)	kg · CO_2 · eq	344.505	352.694	383.748	2387.489
Human toxicity potential (HTP)	kg · 1.4 · DB · eq	20.381	20.835	21.968	417.752
Photochemical oxidantformation potential (POFP)	kg · NMVOC	0.969	0.989	1.051	10.060
Terrestrial acidification potential (TAP)	kg · SO_2 · eq	0.918	0.934	0.998	9.428
Marine eutrophication potential (MEP)	kg · N · eq	0.052	0.036	0.038	0.243
Marine ecotoxicity potential (METP)	kg · 1.4 · DB · eq	0.237	0.240	0.249	2.956

Table A.4: *Environmental impact sorted by category according to Solat Yavari et al. (2017).*

A.2 Environmental impact

Category of Environmental impact	Acronym	Unit	Ecovalue [SEK]	Ecotax [SEK]
Global warming	GWP	kg · CO_2 · eq	2.85	0.63
Human toxicity	HTP	kg · 1.4 · DB · eq	2.81	1.5
Photochemical oxidant formation	POFP	kg · NMVOC	16	156
Terrestrial acidification	TAP	kg · SO_2 · eq	30	15
Marine eutrophication	MEP	kg · N · eq	90	12
Marine ecotoxicity	METP	kg · 1.4 · DB · eq	12	0.3

Table A.5: *Environmental impact and monetary value sorted by category according to Solat Yavari et al. (2017).*

A.3 Buildability costs

Reinforcement diameter [mm]	**Labor hours [h/ton]**	**Labor cost factor [-]**
ϕ16	20	1.25
ϕ20	18.22	1.14
ϕ25	16	1.0
Shear reinforcement	**Labor hours [h/ton]**	**Labor cost factor [-]**
If not added	0	1.0
If added	25	1.56

Table A.6: *Reinforcement labor hours and additional labor cost factors according to Bergenram and Ulander (2023).*

Description of factor	Labor cost factor [-]
Straight thickness	1.0
Variable thickness	1.15
Thickness <40 cm	1.2
40 cm $\leq$ Thickness <60 cm	1.1
60 cm $\leq$ Thickness	1.0
Anchorage and detailing reinforcement $\alpha_{reinforcement}$	1.4

Table A.7: *Labor cost factors considering the thickness of the concrete section and additional reinforcement Solat Yavari et al. (2016).*

B

Structural verification FE-model

(1)

Verification of Sofistik structural model

Verification of the FE Sofistik structural model were done by comparing the numerical Sofistik model with analytical hand calculations performed with linear superposition of elementary cases for a fixed 2D frame. Elementary cases based on Table A25:34b s85 and Table A25:35 s60-62 in (Handboken bygg Byggtabeller, 1983) were used for the analytical hand calculations. A fixed slab frame without wing walls and bottom slab was set up in Sofistik and evaluated for a load combination of dead weight, train load LM71 vertical and horisontal-acceleration load and permanent earth pressure. Frame corner moments were compared from the Sofistik FEM model with analytical calculations. A chosen acceptable percentage of difference in results between the frame corner moments were chosen as the main verification factor for the structural behaviour of the numerical model.

Since Sofistiks built in reinforcement design-function BEMESS designs based on the largest sectional forces, independant of the sign convention, favourable and unfavourable effects of the different loads had to be considered in order to replicate the dimensioning sectional moments used for design and also verify that the dimensioning load combination function worked as assumed. The chosen load combination comparisson was ULS 6.10b from SS EN 1990 (6.10b) load combination for train load group 12 according to SS EN 1991-2 Table 6.1.1 dimensioning load combination koefficients from TSFS 2018:57 .

Wind load on the train were verfied in a separate Sofistik model by comparing the load distribution from analytical handcalculations based on SS EN 1991-1-4 with Sofistiks built in wind load on train function. Characteristic values without any load combination was used.

Assumptions in analytical global structural analysis:

- Uncracked cross-sections, using gross concrete section
- Equal stiffness of frame legs and bridge deck (I1=I2)
- Infinite stiffness of between frame leg and bottom slag = Fixed boundary condition to foundation slab
- Linear elastic analysis, superposition can be used
- Simplified acceleration load with horizontal point load in analytical calculations

(2)

Table of contents

(3)

1. Partial factors and material properties

1.1 Partial factors

$\gamma_{\varphi} := 1.3$	Saftey factor for friction angle	TSFS 2018:57 38 kap 6§
$\psi_{bal} := 1.3$	Upper bound ballast depth	SS-EN 1991-1-1 5.2.3 (2)

1.2 Material properties

$\gamma_{ccr} := 25\ \frac{kN}{m^3}$	Self weight for reinforced concrete	SS-EN 1991-1-1 Table A.1
$\gamma_{bal} := 20\ \frac{kN}{m^3}$	Self weight for ballast	SS-EN 1991-1-1 Table A.6
$\gamma_{soil} := 20\ \frac{kN}{m^3}$	Self weight backfill, gravel	TK GEO 13, 5.2.2.2 Table 5.2-1
$\phi := 45 \cdot deg$	Friction angle of backfill, gravel	TK GEO 13, 2.3.1 Table 5.2-3
$\phi' := \operatorname{atan}\left(\frac{\tan(\phi)}{\gamma_{\varphi}}\right) = 37.569\ deg$	Design friction angle	TK GEO 13, 13.1.2.1.2
$K_0 := 1 - \sin(\phi') = 0.39$	Design residual earth pressure coeff	TK GEO 13, 5.2.2.2.1.2

(4)

2. Geometry

$I_1 := 1$ Moment of inertia for frame legs, normalised

$I_2 := 1$ Moment of inertia for bridge deck, normalised

$L := 12.5\ m$ Span lenght

$h := 7.6\ m$ Frame leg height

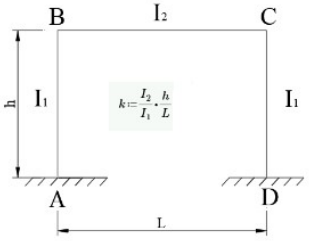

$k := \frac{I_2}{I_1} \cdot \frac{h}{L} = 0.608$ Stiffness/height relation

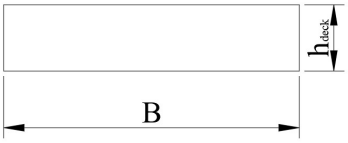

$h_{deck} := 0.5\ m$ Height of bridge deck and thickness of frame legs

$B := 5.6\ m$ Width of bridge deck and frame legs

$h_{nom.ballast} := 600\ mm$ Nominal ballast depth TSFS 2018:57 6 kap 2§

(5)

3. Distributed loads

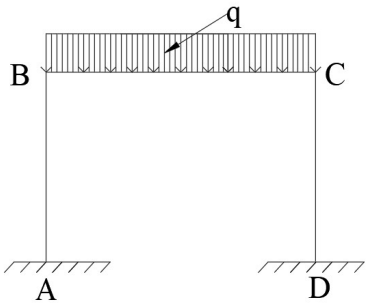

3.1 Permanent loads on concrete deck

$g_{k.1.1} := \gamma_{ccr} \cdot B \cdot h_{deck} = 70 \ \frac{kN}{m}$ Characteristic load concrete

$g_{k.1.2} := \gamma_{bal} \cdot B \cdot h_{nom.ballast} \cdot \psi_{bal} = 87.36 \ \frac{kN}{m}$ Upper characteristic load ballast SS-EN 1991-1-1 5.2.3 (2)

$q_{d.1.1} := \left(g_{k.1.1} + g_{k.1.2}\right) = 157.36 \ \frac{kN}{m}$ Characteristic dead weight

$M_{A.1.1} := \frac{q_{d.1.1} \cdot L^2}{12 \cdot (k+2)} = 785.644 \ kN \cdot m$ Fixation moment A Handboken Byggtabeller Table A25:34b

$M_{B.1.1} := -\frac{q_{d.1.1} \cdot L^2}{6 \cdot (k+2)} = -1571.287 \ kN \cdot m$ Frame corner moment B Handboken Byggtabeller Table A25:34b

$M_{C.1.1} := M_{B.1.1} = -1571.287 \ kN \cdot m$ Frame corner moment C Handboken Byggtabeller Table A25:34b

$M_{D.1.1} := M_{A.1.1} = 785.644 \ kN \cdot m$ Fixation moment D Handboken Byggtabeller Table A25:34b

(6)

3.2 LM71 train distributed load

LM71 load model were placed centric symmetricaly on the bridge deck according to SS EN 1991-2 6.3.2

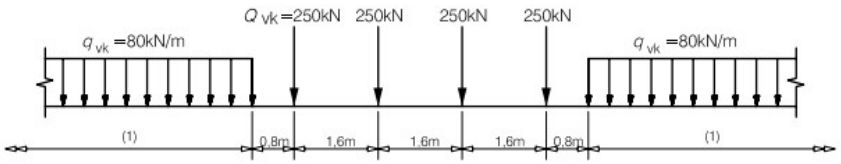

$\alpha := 1.33$	Load factor	TSFS 2018:57 11 kap 11 §
$L_m := \frac{1}{3} \cdot (2 \cdot h + L) = 9.233\ m$		SS-EN 1991-2 Table 6.2 - 5.3
$k_\phi := 1.3$		SS-EN 1991-2 Table 6.2 - 5.3
$L_\phi := \frac{k_\phi \cdot L_m}{m} = 12.003$	Defining dynamic length	SS-EN 1991-2 Table 6.2 - 5.3
$\phi_2 := \frac{1.44}{\sqrt{L_\phi} - 0.2} + 0.82 = 1.261$	Dynamic factor	TSFS 2018:57 11 kap 13 §
$q_{LM71} := 80\ \frac{kN}{m}$	Characteristic distributed load	SS-EN 1991-2 6.3.2 (2)P
$q_{d.1.2} := q_{LM71} \cdot \phi_2 \cdot \alpha = 134.181\ \frac{kN}{m}$	Characteristic design distributed load	SS-EN 1991-2 6.4.5.2 (1)P TSFS 2018:57 11 kap 11 §

(7)

$b_{1.2} := 6.4\ m$ SS-EN 1991-2 6.3.2 (2)P

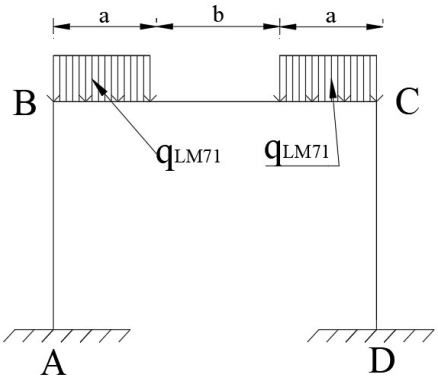

$$a_{1.2} := \frac{(L - b_{1.2})}{2} = 3.05\ m$$

Separating the bridge deck and assuming partially (50%) fixed connections to the frame corner. Then separating the frame leg from the bridge deck and applying the calculated frame corner moment to calculate the fixation moment. Elementary cases from Table A 24:35 s60-62 in Handboken Byggtabeller were used.

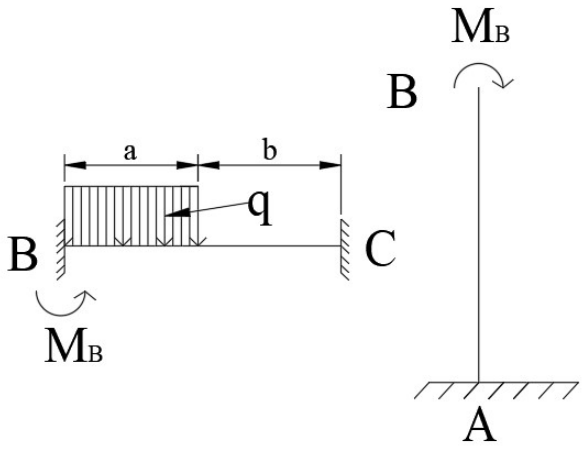

(8)

$$M_B := -\frac{q_{d.1.2} \cdot {a_{1.2}}^2}{16} \cdot \left(3 \cdot \frac{{a_{1.2}}^2}{L^2} - 8 \cdot \frac{a_{1.2}}{L} + 6\right) = -329.733 \ \boldsymbol{kN \cdot m}$$

Fixation moment B from elemntary case 33

$$M_C := -\frac{q_{d.1.2} \cdot {a_{1.2}}^3}{16 \cdot L} \cdot \left(4 - 3 \cdot \frac{a_{1.2}}{L}\right) = -62.207 \ \boldsymbol{kN \cdot m}$$

Fixation moment C from elementary load case 33

$$M_{B.1.2} := M_B + M_C = -391.94 \ \boldsymbol{kN \cdot m}$$

Frame corner moment B, super positioning of two distributed LM71 loads

$$M_{C.1.2} := M_{B.1.2} = -391.94 \ \boldsymbol{kN \cdot m}$$

Frame corner moment C, symmetri

$$M_{A.1.2} := -\frac{M_{B.1.2}}{2} = 195.97 \ \boldsymbol{kN \cdot m}$$

Fixation moment A from elementary load case 42

$$M_{D.1.2} := -\frac{M_{C.1.2}}{2} = 195.97 \ \boldsymbol{kN \cdot m}$$

Fixation moment D from elementary load case 42

(9)

4. Vertical LM71 train point loads

$a_{2.1} := a_{1.2} + 0.8\ m = 3.85\ m$ 1st point load from left

$b_{2.1} := L - a_{2.1} = 8.65\ m$

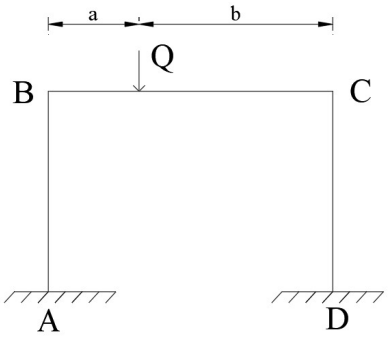

$a_{2.2} := a_{2.1} + 1.6\ m = 5.45\ m$ 2nd point load from left

$b_{2.2} := L - a_{2.2} = 7.05\ m$

$a_{2.3} := a_{2.2} + 1.6\ m = 7.05\ m$ 3rd point load from left

$b_{2.3} := L - a_{2.3} = 5.45\ m$

$a_{2.4} := a_{2.3} + 1.6\ m = 8.65\ m$ 4th point load from left

$b_{2.4} := L - a_{2.4} = 3.85\ m$

$Q_{LM71} := 250\ kN$	Characteristicloads	SS-EN 1991-2 6.3.2 (2)P
$Q_{d.2} := Q_{LM71} \cdot \phi_2 \cdot \alpha = 419.315\ kN$	Characteristic design point load	SS-EN 1991-2 6.4.5.2 (1)P TSFS 2018:57 11 kap 11 §

(10)

$$\alpha_{2.1} := \frac{a_{2.1}}{L} = 0.308$$

$$M_{A.2.1} := \frac{Q_{d.2} \cdot a_{2.1} \cdot b_{2.1}}{2 \cdot L} \cdot \frac{5 \cdot k - 1 + 2 \cdot \alpha_{2.1} \cdot (k+2)}{(k+2) \cdot (6 \cdot k + 1)} = 168.029 \ \boldsymbol{kN \cdot m}$$ Fixation moment A for point load 1
Handboken Byggtabeller Table A25:34b

$$M_{B.2.1} := -\frac{Q_{d.2} \cdot a_{2.1} \cdot b_{2.1}}{2 \cdot L} \cdot \frac{13 \cdot k + 4 - 2 \cdot \alpha_{2.1} \cdot (k+2)}{(k+2) \cdot (6 \cdot k + 1)} = -474.498 \ \boldsymbol{kN \cdot m}$$ Frame corner moment B point load 1
Handboken Byggtabeller Table A25:34b

$$M_{C.2.1} := -\frac{Q_{d.2} \cdot a_{2.1} \cdot b_{2.1}}{2 \cdot L} \cdot \frac{11 \cdot k + 2 \cdot \alpha_{2.1} \cdot (k+2)}{(k+2) \cdot (6 \cdot k + 1)} = -382.204 \ \boldsymbol{kN \cdot m}$$ Frame corner moment C point load 1
Handboken Byggtabeller Table A25:34b

$$M_{D.2.1} := \frac{Q_{d.2} \cdot a_{2.1} \cdot b_{2.1}}{2 \cdot L} \cdot \frac{7 \cdot k + 3 - 2 \cdot \alpha_{2.1} \cdot (k+2)}{(k+2) \cdot (6 \cdot k + 1)} = 260.322 \ \boldsymbol{kN \cdot m}$$ Fixation moment D for point load 1
Handboken Byggtabeller Table A25:34b

$$\alpha_{2.2} := \frac{a_{2.2}}{L} = 0.436$$

$$M_{A.2.2} := \frac{Q_{d.2} \cdot a_{2.2} \cdot b_{2.2}}{2 \cdot L} \cdot \frac{5 \cdot k - 1 + 2 \cdot \alpha_{2.2} \cdot (k+2)}{(k+2) \cdot (6 \cdot k + 1)} = 229.356 \ \boldsymbol{kN \cdot m}$$ Fixation moment A for point load 2
Handboken Byggtabeller Table A25:34b

$$M_{B.2.2} := -\frac{Q_{d.2} \cdot a_{2.2} \cdot b_{2.2}}{2 \cdot L} \cdot \frac{13 \cdot k + 4 - 2 \cdot \alpha_{2.2} \cdot (k+2)}{(k+2) \cdot (6 \cdot k + 1)} = -511.954 \ \boldsymbol{kN \cdot m}$$ Frame corner moment B point load 2
Handboken Byggtabeller Table A25:34b

$$M_{C.2.2} := -\frac{Q_{d.2} \cdot a_{2.2} \cdot b_{2.2}}{2 \cdot L} \cdot \frac{11 \cdot k + 2 \cdot \alpha_{2.2} \cdot (k+2)}{(k+2) \cdot (6 \cdot k + 1)} = -476.459 \ \boldsymbol{kN \cdot m}$$ Frame corner moment C point load 2
Handboken Byggtabeller Table A25:34b

$$M_{D.2.2} := \frac{Q_{d.2} \cdot a_{2.2} \cdot b_{2.2}}{2 \cdot L} \cdot \frac{7 \cdot k + 3 - 2 \cdot \alpha_{2.2} \cdot (k+2)}{(k+2) \cdot (6 \cdot k + 1)} = 264.85 \ \boldsymbol{kN \cdot m}$$ Fixation moment D for point load 2
Handboken Byggtabeller Table A25:34b

(11)

$$\alpha_{2.3} := \frac{a_{2.3}}{L} = 0.564$$

$$M_{A.2.3} := \frac{Q_{d.2} \cdot a_{2.3} \cdot b_{2.3}}{2 \cdot L} \cdot \frac{5 \cdot k - 1 + 2 \cdot \alpha_{2.3} \cdot (k+2)}{(k+2) \cdot (6 \cdot k + 1)} = 264.85\ \boldsymbol{kN \cdot m}$$ Fixation moment A for point load 3 Handboken Byggtabeller Table A25:34b

$$M_{B.2.3} := -\frac{Q_{d.2} \cdot a_{2.3} \cdot b_{2.3}}{2 \cdot L} \cdot \frac{13 \cdot k + 4 - 2 \cdot \alpha_{2.3} \cdot (k+2)}{(k+2) \cdot (6 \cdot k + 1)} = -476.459\ \boldsymbol{kN \cdot m}$$ Frame corner moment B point load 3 Handboken Byggtabeller Table A25:34b

$$M_{C.2.3} := -\frac{Q_{d.2} \cdot a_{2.3} \cdot b_{2.3}}{2 \cdot L} \cdot \frac{11 \cdot k + 2 \cdot \alpha_{2.3} \cdot (k+2)}{(k+2) \cdot (6 \cdot k + 1)} = -511.954\ \boldsymbol{kN \cdot m}$$ Frame corner moment C point load 3 Handboken Byggtabeller Table A25:34b

$$M_{D.2.3} := \frac{Q_{d.2} \cdot a_{2.3} \cdot b_{2.3}}{2 \cdot L} \cdot \frac{7 \cdot k + 3 - 2 \cdot \alpha_{2.3} \cdot (k+2)}{(k+2) \cdot (6 \cdot k + 1)} = 229.356\ \boldsymbol{kN \cdot m}$$ Fixation moment D for point load 3 Handboken Byggtabeller Table A25:34b

$$\alpha_{2.4} := \frac{a_{2.4}}{L} = 0.692$$

$$M_{A.2.4} := \frac{Q_{d.2} \cdot a_{2.4} \cdot b_{2.4}}{2 \cdot L} \cdot \frac{5 \cdot k - 1 + 2 \cdot \alpha_{2.4} \cdot (k+2)}{(k+2) \cdot (6 \cdot k + 1)} = 260.322\ \boldsymbol{kN \cdot m}$$ Fixation moment A for point load 4 Handboken Byggtabeller Table A25:34b

$$M_{B.2.4} := -\frac{Q_{d.2} \cdot a_{2.4} \cdot b_{2.4}}{2 \cdot L} \cdot \frac{13 \cdot k + 4 - 2 \cdot \alpha_{2.4} \cdot (k+2)}{(k+2) \cdot (6 \cdot k + 1)} = -382.204\ \boldsymbol{kN \cdot m}$$ Frame corner moment B point load 4 Handboken Byggtabeller Table A25:34b

$$M_{C.2.4} := -\frac{Q_{d.2} \cdot a_{2.4} \cdot b_{2.4}}{2 \cdot L} \cdot \frac{11 \cdot k + 2 \cdot \alpha_{2.4} \cdot (k+2)}{(k+2) \cdot (6 \cdot k + 1)} = -474.498\ \boldsymbol{kN \cdot m}$$ Frame corner moment C point load 4 Handboken Byggtabeller Table A25:34b

$$M_{D.2.4} := \frac{Q_{d.2} \cdot a_{2.4} \cdot b_{2.4}}{2 \cdot L} \cdot \frac{7 \cdot k + 3 - 2 \cdot \alpha_{2.4} \cdot (k+2)}{(k+2) \cdot (6 \cdot k + 1)} = 168.029\ \boldsymbol{kN \cdot m}$$ Fixation moment D for point load 4 Handboken Byggtabeller Table A25:34b

(12)

$M_{A.2} := M_{A.2.1} + M_{A.2.2} + M_{A.2.3} + M_{A.2.4} = 922.557\ kN \cdot m$ Total point load fixation moment A

$M_{B.2} := M_{B.2.1} + M_{B.2.2} + M_{B.2.3} + M_{B.2.4} = -1.845 \cdot 10^3\ kN \cdot m$ Total point load frame corner moment B

$M_{C.2} := M_{C.2.1} + M_{C.2.2} + M_{C.2.3} + M_{C.2.4} = -1.845 \cdot 10^3\ kN \cdot m$ Total point load frame corner moment C

$M_{D.2} := M_{D.2.1} + M_{D.2.2} + M_{D.2.3} + M_{D.2.4} = 922.557\ kN \cdot m$ Total point load fixation moment D

(13)

5. Horizontal acceleration load

Simplification of acceleration load from SS-EN 1991-2 6.5.3 (6.20) by inserting a equivalent point load on the frame corner instaid of distributed axial load on bridge deck. Considering distributed axial load only effects the local cross sectional normal force and not the global structural behavour

$$Q_{lbk} := min\left(33\ \frac{kN}{m} \cdot \left(L + h_{deck}\right), 1000\ kN\right) = 429\ kN$$

Characteristic acceleration load SS-EN 1991-2 6.5.3 (6.20)

$$Q_{d.3} := Q_{lbk} \cdot \alpha = 570.57\ kN$$

Characteristic design acceleration load SS-EN 1991-2 6.4.5.2 (1)P
TSFS 2018:57 11 kap 11 §

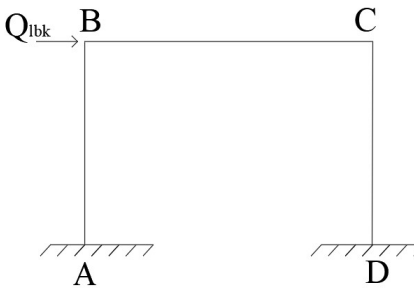

$$M_{A.3} := -\frac{Q_{d.3} \cdot h}{2} \cdot \frac{3 \cdot k + 1}{6 \cdot k + 1} = -1317.319\ kN \cdot m$$

Fixation moment A
Handboken Byggtabeller Table A25:34b

$$M_{B.3} := \frac{Q_{d.3} \cdot h}{2} \cdot \frac{3 \cdot k}{6 \cdot k + 1} = 850.847\ kN \cdot m$$

Frame corner moment B
Handboken Byggtabeller Table A25:34b

$$M_{C.3} := -M_{B.3} = -850.847\ kN \cdot m$$

Frame corner moment C
Handboken Byggtabeller Table A25:34b

$$M_{D.3} := -M_{A.3} = 1317.319\ kN \cdot m$$

Fixation moment D
Handboken Byggtabeller Table A25:34b

(14)

6. Permanent resting earth pressure load

$$q_{d.A} := \left(\gamma_{soil} \cdot h \cdot K_0\right) = 59.324 \ \frac{1}{m} \cdot \frac{kN}{m}$$

Characteristic permanent earth pressure

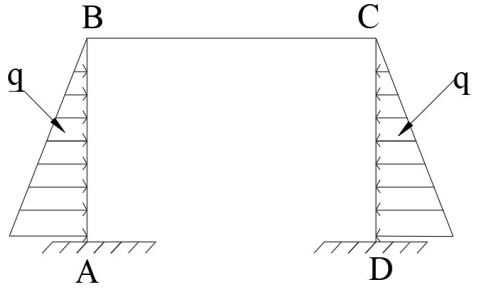

$$M_{A.A} := -\frac{q_{d.A} \cdot h^2}{60} \cdot \frac{3 \cdot k + 8}{k + 2} = -215.123 \ \frac{1}{m} \cdot kN \cdot m$$

Fixation moment A
Handboken Byggtabeller Table A25:34b

$$M_{B.A} := -\frac{q_{d.A} \cdot h^2}{30} \cdot \frac{k}{k + 2} = -26.628 \ \frac{1}{m} \cdot kN \cdot m$$

Frame corner moment B
Handboken Byggtabeller Table A25:34b

$$M_{C.A} := M_{B.A} = -26.628 \ \frac{1}{m} \cdot kN \cdot m$$

Frame corner moment C
Handboken Byggtabeller Table A25:34b

$$M_{D.A} := M_{A.A} = -215.123 \ \frac{1}{m} \cdot kN \cdot m$$

Fixation moment D
Handboken Byggtabeller Table A25:34b

(15)

7. Load combination

To compare the analytical handcalculations with the pre-implimented load combination-functions MAXIMA and COMB in the Sofistik model, load combinations of sectional moments based on unfavourable and favourable loads for this particular load cases needed to be performed for the analytical calcuations according TSFS 2018:57 Table 4.4 and SS EN 1990 (6.10b).

$\gamma_d := 1.0$	Saftey class 3 partial coefficient	TSFS 2018:57 2 kap 8§
$\xi := 0.89$	Reduction for unfavourable permanent loads	TSFS 2018:57 2 kap 8§
$\gamma_{G.unf} := 1.35$	Unfavourable permanent loads	TSFS 2018:57 2 Table 4.4
$\gamma_{G.fav} := 1.0$	Favourable permanent loads	TSFS 2018:57 2 Table 4.4
$\gamma_{Q.unf} := 1.5$	Unfavourable LM71 variable loads	TSFS 2018:57 Table 4.4
$\gamma_{Q.fav} := 0$	Favourable LM71 variable loads	TSFS 2018:57 2 Table 4.4
$\psi_{0.acc} := 0.5$	Acceleration secondary load gr 12	SS EN 1991-2 Table 6.11

(16)

Vertical load favourable for negativ fixation moment at A

$$M_{E.A} := \frac{\gamma_d \cdot \gamma_{G.fav} \cdot M_{A.1.1} + \gamma_d \cdot \gamma_{Q.fav} \cdot \left(M_{A.1.2} + M_{A.2}\right) + \gamma_d \cdot \gamma_{Q.unf} \cdot \psi_{0.acc} \cdot M_{A.3}}{B} = -294.604 \ \frac{1}{m} \cdot kN \cdot m$$
$$+ \gamma_d \cdot \xi \cdot \gamma_{G.unf} \cdot M_{A.4}$$

Acceleration favourable for negative frame corner moment B

$$M_{E.B} := \frac{\gamma_d \cdot \xi \cdot \gamma_{G.unf} \cdot M_{B.1.1} + \gamma_d \cdot \gamma_{Q.unf} \cdot \left(M_{B.1.2} + M_{B.2}\right) + \gamma_d \cdot \gamma_{Q.fav} \cdot \psi_{0.acc} \cdot M_{B.3}}{B} = -968.329 \ \frac{1}{m} \cdot kN \cdot m$$
$$+ \gamma_d \cdot \xi \cdot \gamma_{G.unf} \cdot M_{B.4}$$

All loads unfavourable for negative frame corner moment C

$$M_{E.C} := \frac{\gamma_d \cdot \xi \cdot \gamma_{G.unf} \cdot M_{C.1.1} + \gamma_d \cdot \gamma_{Q.unf} \cdot \left(M_{C.1.2} + M_{C.2}\right) + \gamma_d \cdot \gamma_{Q.unf} \cdot \psi_{0.acc} \cdot M_{C.3}}{B} = -1082.282 \ \frac{1}{m} \cdot kN \cdot m$$
$$+ \gamma_d \cdot \xi \cdot \gamma_{G.unf} \cdot M_{C.4}$$

Permanent earth pressure favourable for positive fixation moment D

$$M_{E.D} := \frac{\gamma_d \cdot \xi \cdot \gamma_{G.unf} \cdot M_{D.1.1} + \gamma_d \cdot \gamma_{Q.unf} \cdot \left(M_{D.1.2} + M_{D.2}\right) + \gamma_d \cdot \gamma_{Q.unf} \cdot \psi_{0.acc} \cdot M_{D.3}}{B} = 429.472 \ \frac{1}{m} \cdot kN \cdot m$$
$$+ \gamma_{G.fav} \cdot M_{D.4}$$

(17)

8. Verification

8.1 Sectional moment output from Sofistik model

Sectional moments for every node along the joint of the top frame corners and the fixation joints at the bottom slab-frame leg connection were extracted from the Sofistik model. An average moment was calculated and compared with the 2D analytical calculations.

Left fixation corner A

	NODE	LC	LC-title	mxx [kNm/m]	nx [kN/m]	ASOQ [cm2/m]	ASUQ [cm2/m]	X [m]	ZMIN [m]	Y [m]	Z [m]
1										-6.25	2.5
1	1072	60202	MIN-MXX QUAD TEST	-275.31	-279.06	12.22	2.77	2.800	0.397	-6.250	2.500
2	1073	60202	MIN-MXX QUAD TEST	-280.72	-275.29	12.77	2.44	-2.800	0.383	-6.250	2.500
3	1232	60202	MIN-MXX QUAD TEST	-287.50	-226.60	12.52	5.37	2.400	0.403	-6.250	2.500
4	1233	60202	MIN-MXX QUAD TEST	-308.06	-220.31	13.83	6.70	2.000	0.399	-6.250	2.500
5	1234	60202	MIN-MXX QUAD TEST	-309.23	-217.04	13.95	7.09	1.600	0.400	-6.250	2.500
6	1235	60202	MIN-MXX QUAD TEST	-307.77	-215.81	13.89	6.39	1.200	0.405	-6.250	2.500
7	1236	60202	MIN-MXX QUAD TEST	-309.41	-215.21	13.98	6.18	0.800	0.405	-6.250	2.500
8	1237	60202	MIN-MXX QUAD TEST	-314.43	-214.72	14.30	6.03	0.400	0.405	-6.250	2.500
9	1238	60202	MIN-MXX QUAD TEST	-308.34	-214.40	13.94	5.88	0.000	0.405	-6.250	2.500
10	1239	60202	MIN-MXX QUAD TEST	-306.49	-212.93	13.84	6.02	-0.400	0.405	-6.250	2.500
11	1240	60202	MIN-MXX QUAD TEST	-316.82	-210.65	14.47	6.18	-0.800	0.405	-6.250	2.500
12	1241	60202	MIN-MXX QUAD TEST	-286.24	-209.28	12.75	6.14	-1.200	0.405	-6.250	2.500
13	1242	60202	MIN-MXX QUAD TEST	-318.22	-209.59	14.77	7.32	-1.600	0.399	-6.250	2.500
14	1243	60202	MIN-MXX QUAD TEST	-307.11	-216.76	13.83	6.65	-2.000	0.398	-6.250	2.500
15	1244	60202	MIN-MXX QUAD TEST	-289.72	-225.32	12.70	5.07	-2.400	0.405	-6.250	2.500
min	1072	60202	-	-318.22	-279.06	12.22	2.44	-2.800	0.383	-6.250	2.500
max	1244	60202	-	-275.31	-209.28	14.77	7.32	2.800	0.405	-6.250	2.500

$M_{FEM.A} := -301.7 \ \frac{1}{m} \cdot kN \cdot m$ Average designing moment

(18)

Left frame corner B

	NODE	LC	LC-title	mxx [kNm/m]	ny [kN/m]	ASOQ [cm2/m]	ASUQ [cm2/m]	X [m]	ZMIN [m]	Y [m]	Z [m]
										-6.25	9.85
1	1074	60202	MIN-MXX QUAD TEST	-851.08	-186.36	64.61	0.00	2.800	0.351	-6.250	9.850
2	1075	60202	MIN-MXX QUAD TEST	-850.69	-229.87	62.78	0.00	-2.800	0.349	-6.250	9.850
3	1076	60202	MIN-MXX QUAD TEST	-981.89	-198.93	54.47	0.00	1.400	0.366	-6.250	9.850
4	1077	60202	MIN-MXX QUAD TEST	-1005.66	-155.62	56.12	0.00	0.000	0.364	-6.250	9.850
5	1078	60202	MIN-MXX QUAD TEST	-1002.73	-204.63	55.73	0.00	-1.400	0.364	-6.250	9.850
6	1283	60202	MIN-MXX QUAD TEST	-811.41	-253.86	47.42	0.00	2.590	0.369	-6.250	9.850
7	1284	60202	MIN-MXX QUAD TEST	-880.85	-167.82	48.24	0.00	2.380	0.371	-6.250	9.850
8	1285	60202	MIN-MXX QUAD TEST	-938.50	-265.10	51.24	0.00	2.100	0.369	-6.250	9.850
9	1286	60202	MIN-MXX QUAD TEST	-958.10	-232.55	52.61	0.00	1.820	0.367	-6.250	9.850
10	1287	60202	MIN-MXX QUAD TEST	-970.14	-211.90	53.58	0.00	1.610	0.366	-6.250	9.850
11	1288	60202	MIN-MXX QUAD TEST	-992.24	-199.29	55.14	0.00	1.190	0.365	-6.250	9.850
12	1289	60202	MIN-MXX QUAD TEST	-990.01	-194.79	54.72	0.00	0.980	0.364	-6.250	9.850
13	1290	60202	MIN-MXX QUAD TEST	-1005.31	-214.97	55.57	0.00	0.700	0.362	-6.250	9.850
14	1291	60202	MIN-MXX QUAD TEST	-982.09	-159.48	54.07	0.00	0.420	0.364	-6.250	9.850
15	1292	60202	MIN-MXX QUAD TEST	-1012.89	-159.69	56.64	0.00	0.210	0.364	-6.250	9.850
16	1293	60202	MIN-MXX QUAD TEST	-1002.31	-164.06	55.79	0.00	-0.210	0.364	-6.250	9.850
17	1294	60202	MIN-MXX QUAD TEST	-1003.98	-187.40	55.48	0.00	-0.420	0.363	-6.250	9.850
18	1295	60202	MIN-MXX QUAD TEST	-1014.46	-224.71	55.74	0.00	-0.700	0.362	-6.250	9.850
19	1296	60202	MIN-MXX QUAD TEST	-1002.71	-206.53	55.32	0.00	-0.980	0.363	-6.250	9.850
min	1074	60202	-	-1014.46	-265.10	46.52	0.00	-2.800	0.349	-6.250	9.850
max	1302	60202	-	-811.41	-155.62	64.61	0.00	2.800	0.374	-6.250	9.850

$$M_{FEM.B} := -958.38 \ \frac{1}{m} \cdot kN \cdot m$$ Average designing moment

Right frame corner C

Filter rule: #1

	NODE	LC	LC-title	mxx [kNm/m]	ny [kN/m]	ASOQ [cm2/m]	ASUQ [cm2/m]	X [m]	ZMIN [m]	Y [m]	Z [m]
										6.25	9.85
1	1067	60202	MIN-MXX QUAD TEST	-924.50	-221.90	70.80	0.00	2.800	0.342	6.250	9.850
2	1068	60202	MIN-MXX QUAD TEST	-950.99	-251.04	72.01	0.00	-2.800	0.344	6.250	9.850
3	1069	60202	MIN-MXX QUAD TEST	-1093.26	-213.24	63.90	0.00	1.400	0.357	6.250	9.850
4	1070	60202	MIN-MXX QUAD TEST	-1118.08	-155.72	66.28	0.00	0.000	0.354	6.250	9.850
5	1071	60202	MIN-MXX QUAD TEST	-1114.97	-210.32	64.37	0.00	-1.400	0.356	6.250	9.850
6	1212	60202	MIN-MXX QUAD TEST	-910.79	-238.10	51.12	0.00	2.590	0.371	6.250	9.850
7	1213	60202	MIN-MXX QUAD TEST	-994.50	-247.16	55.94	0.00	2.380	0.366	6.250	9.850
8	1214	60202	MIN-MXX QUAD TEST	-1038.15	-284.88	58.56	0.00	2.100	0.362	6.250	9.850
9	1215	60202	MIN-MXX QUAD TEST	-1068.61	-253.34	61.02	0.00	1.820	0.359	6.250	9.850
10	1216	60202	MIN-MXX QUAD TEST	-1081.91	-229.73	61.86	0.00	1.610	0.359	6.250	9.850
11	1217	60202	MIN-MXX QUAD TEST	-1103.36	-214.13	64.23	0.00	1.190	0.356	6.250	9.850
12	1218	60202	MIN-MXX QUAD TEST	-1101.75	-207.69	64.53	0.00	0.980	0.355	6.250	9.850
13	1219	60202	MIN-MXX QUAD TEST	-1107.85	-204.76	63.40	0.00	0.700	0.355	6.250	9.850
14	1220	60202	MIN-MXX QUAD TEST	-1115.34	-181.39	62.93	0.00	0.420	0.357	6.250	9.850
15	1221	60202	MIN-MXX QUAD TEST	-1117.55	-159.26	66.81	0.00	0.210	0.354	6.250	9.850
16	1222	60202	MIN-MXX QUAD TEST	-1123.46	-168.93	67.16	0.00	-0.202	0.352	6.250	9.850
17	1223	60202	MIN-MXX QUAD TEST	-1115.98	-189.06	64.38	0.00	-0.404	0.355	6.250	9.850
18	1224	60202	MIN-MXX QUAD TEST	-1114.56	-219.17	64.29	0.00	-0.688	0.353	6.250	9.850
19	1225	60202	MIN-MXX QUAD TEST	-1115.57	-215.61	64.56	0.00	-0.972	0.354	6.250	9.850
min	1067	60202	-	-1123.46	-284.88	51.12	0.00	-2.800	0.342	6.250	9.850
max	1231	60202	-	-910.79	-155.72	72.01	0.00	2.800	0.371	6.250	9.850

$$M_{FEM.C} := -1065.6 \ \frac{1}{m} \cdot kN \cdot m$$ Average designing moment

(19)

Right fixation corner D

	NODE	LC	LC-title	mxx [kNm/m]	nx [kN/m]	ASOQ [cm2/m]	ASUQ [cm2/m]	X [m]	ZMIN [m]	Y [m]	Z [m]
										6.25	2.5
1	1065	60201	MAX-MXX QUAD TEST	372.86	-829.52	3.38	11.87	2.800	0.391	6.250	2.500
2	1066	60201	MAX-MXX QUAD TEST	382.51	-905.19	3.02	11.98	-2.800	0.386	6.250	2.500
3	1161	60201	MAX-MXX QUAD TEST	399.30	-670.58	3.99	14.02	2.400	0.400	6.250	2.500
4	1162	60201	MAX-MXX QUAD TEST	434.47	-646.22	3.85	16.56	2.000	0.398	6.250	2.500
5	1163	60201	MAX-MXX QUAD TEST	443.71	-622.96	4.48	17.52	1.600	0.396	6.250	2.500
6	1164	60201	MAX-MXX QUAD TEST	431.62	-613.69	3.39	16.84	1.200	0.396	6.250	2.500
7	1165	60201	MAX-MXX QUAD TEST	439.93	-615.35	4.40	17.19	0.800	0.399	6.250	2.500
8	1166	60201	MAX-MXX QUAD TEST	435.52	-641.77	3.93	16.55	0.400	0.399	6.250	2.500
9	1167	60201	MAX-MXX QUAD TEST	436.27	-655.10	3.98	16.38	0.000	0.399	6.250	2.500
10	1168	60201	MAX-MXX QUAD TEST	437.90	-661.03	3.93	16.40	-0.400	0.399	6.250	2.500
11	1169	60201	MAX-MXX QUAD TEST	439.78	-667.75	3.87	16.70	-0.800	0.396	6.250	2.500
12	1170	60201	MAX-MXX QUAD TEST	442.12	-674.35	3.86	17.20	-1.200	0.394	6.250	2.500
13	1171	60201	MAX-MXX QUAD TEST	443.86	-683.69	4.05	17.37	-1.600	0.390	6.250	2.500
14	1172	60201	MAX-MXX QUAD TEST	441.57	-700.58	4.28	16.70	-2.000	0.394	6.250	2.500
15	1173	60201	MAX-MXX QUAD TEST	398.91	-727.03	4.13	13.32	-2.400	0.401	6.250	2.500
min	1065	60201	-	372.86	-905.19	3.02	11.87	-2.800	0.386	6.250	2.500
max	1173	60201	-	443.86	-613.69	4.48	17.52	2.800	0.401	6.250	2.500

$M_{FEM.D} := 425.36 \ \frac{1}{m} \cdot kN \cdot m$ Average designing moment

(20)

8.2 Sectional moment comparison

$$P_A := 1 - \frac{M_{E.A}}{M_{FEM.A}} = 2.352\%$$

$$P_B := 1 - \frac{M_{E.B}}{M_{FEM.B}} = -1.038\%$$

$$P_C := 1 - \frac{M_{E.C}}{M_{FEM.C}} = -1.566\%$$

$$P_D := 1 - \frac{M_{E.D}}{M_{FEM.D}} = -0.967\%$$

Avergage procentual difference

$$\frac{|P_A| + |P_B| + |P_C| + |P_D|}{4} = 1.481\%$$

(21)

8.3 Wind load application

$v_b := 26\ \frac{m}{s}$	Reference wind speed at Norrbotniabanan	TSFS 2018:57 Figure 7.1
$q_p := 0.86\ \frac{kN}{m^2}$	Characteristik wind speed pressure	TSFS 2018:57 Table 7.2 Terrain type II, h = 8m
$h_{train} := 4\ m$	Height of train	
$b_{train} := 1.435\ m$	Distance between rails	
$d_{tot} := h_{deck} + h_{train} = 4.5\ m$	Height substructure	SS-EN 1991-1-4 Figure 8.3
$c_{fx.o} := min\left(\begin{array}{l}\text{if } \frac{B}{d_{tot}} \geq 5 \\ \quad 1 \\ \text{else} \\ \quad 1 + 0.3 \cdot \left(5 - \frac{B}{d_{tot}}\right)\end{array}\right) = 2.127$		SS-EN 1991-1-4 Figure 8.3 for wind on traffic + bridge
$c_{fx} := c_{fx.o}$		SS-EN 1991-1-4 (8.1)
$q_{w.d} := q_p \cdot c_{fx} = 1.829\ \frac{kN}{m^2}$	Characteristik wind load on train	SS-EN 1991-1-4 (4.8)

(22)

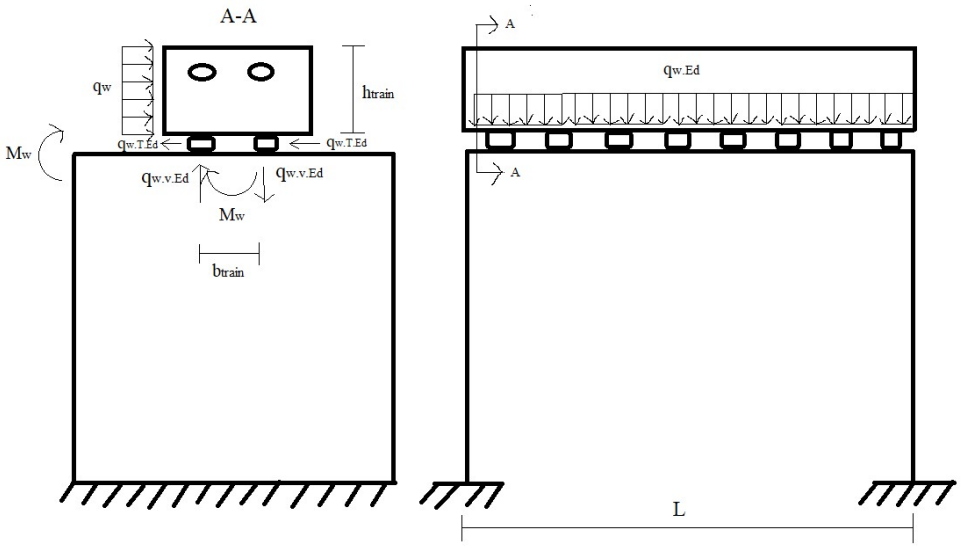

$$q_{w.v.Ed} := \frac{q_{w.d} \cdot h_{train}^{\ 2}}{2 \cdot b_{train}} = 10.2 \ \frac{kN}{m}$$

Distributed vertical load
From equilibrium equation Mw = Mw

$$q_{w.T.Ed} := \frac{q_{w.d} \cdot h_{train}}{2} = 3.66 \ \frac{kN}{m}$$

Transversal loading on two rails

(23)

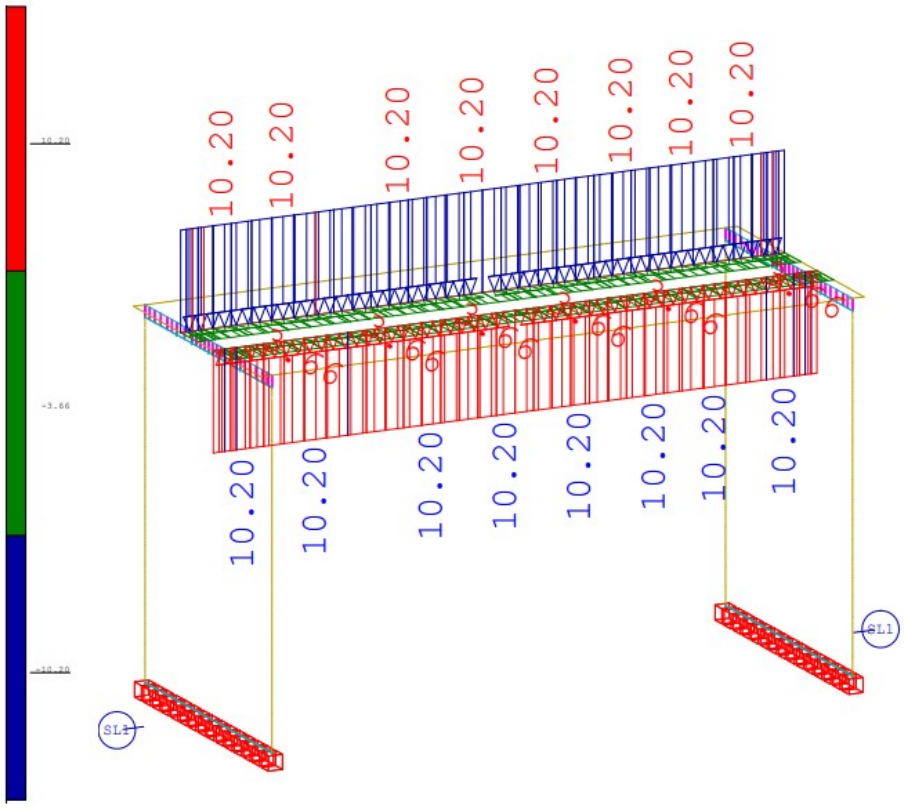
10.20
10.20
10.20
10.20
10.20
10.20
10.20
10.20
10.20
10.20
10.20
10.20
10.20
10.20
SL1
SL1

C

Design function verification of FE-model

(1)

Verification of Sofistik design function

To verify Sofistiks built in ULS, SLS and FLS design function BEMESS, a complete slab frame model later used for the set-based itterations was set up and fully analysed and design. The resulting reinforcement amount for two sections of the bridge deck (mid-span and close to support/frame leg) was studied and compared with analytical handcalculations. Due to the many design parameters used in BEMESS, the most critical parts of detail design in concrete structures with regards to the aim of the thesis were chosen to be studied. ULS reinforcement design and shear failure check without reinforcement, SLS crack controll and fatigue checks of reinforcement were deemed the most critical parts to verify. Additionally, minimum reinforcement for all structural components were verified.

ULS reinforcement design, crack controll in SLS and fatigue checks of the main bottom longitudinal reinforcement was verified in the mid-span section shown in the Figure below. ULS shear design and fatigue checks of the shear reinforcement was verified at the support/frame leg section shown in the Figure below. Minimum reinforcement was calculated and verified for all structural components.

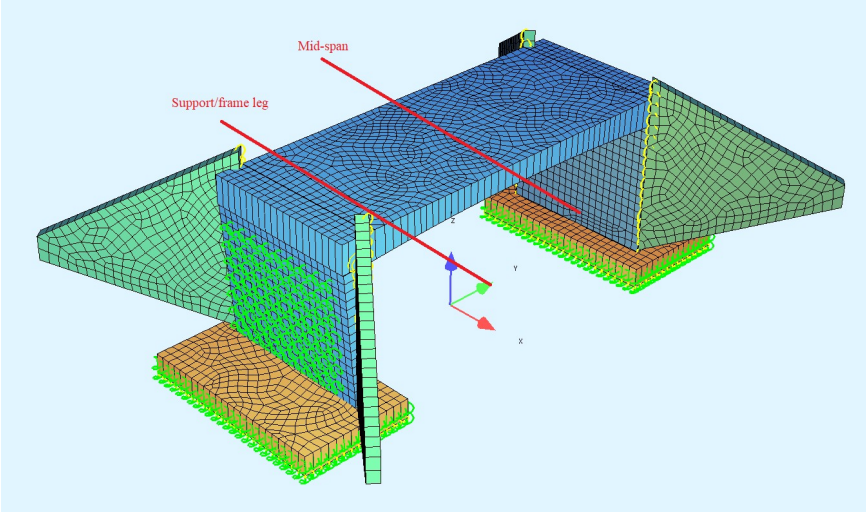

Dimensioning sectional forces were extracted from the model and analytical handcalculations based on relevant and active Swedish bridge design codes and standards were performed. Results from the analytical calculations were compared with the numerical results from the design function in the model. An chosen acceptable percentage of difference in results were chosen as the main verification factor for the design function in the numerical model.

(2)

Table of contents

(4)

1. Dimensioning sectional forces from FEM model

1.1 Dimensioning sectional forces ULS

	LC	LC-title	QUAD	mxx [kNm/m]	nx [kN/m]
☑ 1			10001		
1	30101	MAX-MXX QUAD ULS 6.10b Main brid	10001	1674.49	-212.69

$M_{Ed.ULS} := 1674.49 \ \frac{kN \cdot m}{m}$

$N_{Ed.ULS} := -212.69 \ \frac{kN}{m}$

Mid-span section dimensioning moment and normal force

	LC	LC-title	QUAD	vx [kN/m]	nx [kN/m]
☑ 1			10361		
1	30107	MAX-VX QUAD ULS 6.10b Main bridg	10361	929.39	-794.64

$V_{Ed.ULS} := 929.36 \ \frac{kN}{m}$

$N_{Ed.ULS.shear} := -794.64 \ \frac{kN}{m}$

Support-span section dimensioning shear and normal force

(5)

1.2 Dimensioning sectional forces SLS

Sectional forces from SLS quasi permanent load combinations were used for crack controll verification

	QUAD	LC	LC-title	mxx [kNm/m]	nx [kN/m]
1	10001				
1	10001	30901	MAX-MXX QUAD SLS-Q	778.21	-147.91

$M_{Ed.quasi} := 778.21 \ \frac{kN \cdot m}{m}$

Mid-span section dimensioning moment and normal force

$N_{Ed.quasi} := -147.91 \ \frac{kN}{m}$

1.3 Dimensioning sectional forces FLS

Maximum and minimum mid-span section dimensioning moment and normal force

	LC	LC-title	QUAD	mxx [kNm/m]	nx [kN/m]
1			10001		
1	40001	MAX-MXX QUAD FAT	10001	891.20	-320.06
2	40002	MIN-MXX QUAD FAT	10001	487.93	-209.46
min	40001	-	10001	487.93	-320.06
max	40002	-	10001	891.20	-209.46

$M_{Ed.Fat.max} := 891.2 \ \frac{kN \cdot m}{m}$ $N_{Ed.fat.max} := -320.06 \ \frac{kN}{m}$

$M_{Ed.Fat.min} := 487.93 \ \frac{kN \cdot m}{m}$ $N_{Ed.fat.min} := -209.46 \ \frac{kN}{m}$

(6)

Maximum and minimum support-span section dimensioning shear force

	LC	LC-title	QUAD	vx [kN/m]
1			10361	
1	40007	MAX-VX QUAD FAT	10361	520.96
2	40008	MIN-VX QUAD FAT	10361	294.72
min	40007	-	10361	294.72
max	40008	-	10361	520.96

$V_{Ed.Fat.max} := 520.96 \ \frac{kN}{m}$ $V_{Ed.Fat.min} := 294.72 \ \frac{kN}{m}$

(7)

2. Partial factors and material properties

2.1 Partial factors

$\gamma_s := 1.15$	SS-EN 1992-1-1:2005 2.4.2.4 Table 2.1N
$a_{cc} := 1.0$	SS-EN 1992-1-1:2005 3.1.6 eq (3.15)
$\gamma_c := 1.5$	SS-EN 1992-1-1:2005 2.4.2.4 Table 2.1N
$\gamma_{F.fat} := 1.0$	SS-EN 1992-1-1:2005 2.4.2.3
$\gamma_{s.fat} := 1.15$	SS-EN 1992-1-1:2005 2.4.2.4
$\gamma_{c.fat} := 1.5$	SS-EN 1992-1-1:2005 2.4.2.4

2.2 Material properties

C30/37 Concrete ， K500B-T Reinforcement

$f_{yk} := 500\ MPa$	SS-EN 1992-1-1:2005 3.2.2 (3)P
$f_{ck} := 30\ MPa$	SS-EN 1992-1-1:2005 3.1.3 Table (3.1)
$f_{ctm} := 2.9\ MPa$	SS-EN 1992-1-1:2005 3.1.3 Table (3.1)
$f_{ctk.0.05} := f_{ctm} \cdot 0.7 = 2.03\ MPa$	SS-EN 1992-1-1:2005 3.1.3 Table (3.1)
$f_{cd} := a_{cc} \cdot \frac{f_{ck}}{\gamma_c} = 20\ MPa$	SS-EN 1992-1-1:2005 3.1.6 eq (3.15)

(8)

$f_{yd} := \frac{f_{yk}}{\gamma_s} = 434.8\ \boldsymbol{MPa}$	SS-EN 1992-1-1:2005 3.2.7 Figure 3.8
$E_s := 200\ \boldsymbol{GPa}$	SS-EN 1992-1-1:2005 3.2.7 (4)
$E_{cm} := 33\ \boldsymbol{GPa}$	SS-EN 1992-1-1:2005 Table 3.1
$\varphi := 2$	Final creep coefficient used in model
$\varepsilon_{cs} := 0.24 \cdot 10^{-3}$	Final shrinkage used in model
$E_{c.eff} := \frac{E_{cm}}{1+\varphi} = 11\ \boldsymbol{GPa}$	SS-EN 1992-1-1:2005 7.4.3 eq (7.20)
$\alpha_{ef} := \frac{E_s}{E_{c.eff}} = 18.182$	SS-EN 1992-1-1:2005 7.4.3
$f_{ywd} := 300\ \boldsymbol{MPa}$	Chosen reduced yield limit for stirups due to large shear crack risk

(9)

3. Geometry

$\phi := 25\ mm$	Main longitudinal reinforcement diameter
$c := 87\ mm$	Cover thickness to main longitudinal reinforcement
$d' := c + \frac{\phi}{2} = 99.5\ mm$	Edge distance to top and bottom main reinforcement
$\phi_{stirup} := 16\ mm$	Stirup shear reinforcement diameter
$D := 125\ mm$	Stirup bending radius for ϕ_{shear}=16 mm
$b_{BD.FL} := 7.2\ m$	Width of bridge deck and frame legs
$b_{FS} := 9\ m$	Width foundation slab

3.1 Mid-span section

$h_{deck} := 950\ mm$	Height of cross section
$d := h_{deck} - d' = 850.5\ mm$	Cross sections effective height

3.2 Support section

$t_{deck} := 1231\ mm$	Height of cross section
$z_1 := t_{deck} - d' = 1.132\ m$	Cross sections effective height

(10)

4. ULS design

4.1 Mid-span bottom longitudinal main reinforcement

Design of the main longitudnial main reinforcement were simplified assuming no need for compression reinforcement based on equations from
(al-Emrani 2011, Bärande konstruktioner del 1, section B5.6.5)

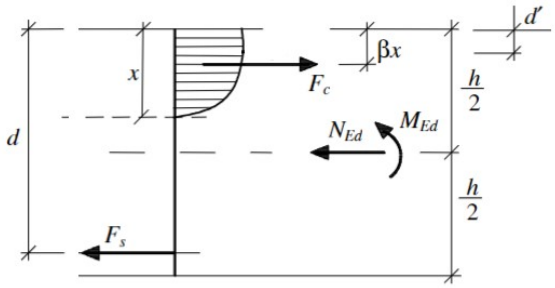

$\alpha := 0.81$ Table B5.1

$\beta := 0.416$ Table B5.1

$x_0 := 100\ mm$ Value to start itteration process

$$x_A := \mathbf{root}\left(M_{Ed.ULS} - N_{Ed.ULS}\cdot\left(d - \frac{h_{deck}}{2}\right) - \alpha\cdot f_{cd}\cdot x_0\cdot\left(d - \beta\cdot x_0\right), x_0\right) = 136.434\ mm$$

Height of compressive zone (B5-36)

$$A_{s.ULS} := \frac{\alpha\cdot f_{cd}\cdot x_A + N_{Ed.ULS}}{f_{yd}} = 45.943\ \frac{cm^2}{m}$$ Required reinforcement area (B5-36)

(11)

4.2 Support section concrete check and shear reinforcement design

Concrete shear force checks and shear reinforcement design according to SS-EN 1992-1-1:2005 6.2.1-6.2.3 and TSFS 2018:57 6.2.3(2)

Positioning of main contributing load in dimensioning shear force load case

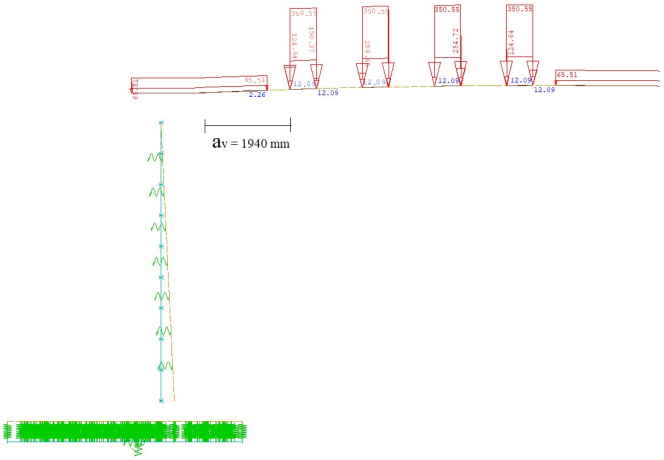

$A_{sl} := 40.76 \cdot \frac{cm^2}{m}$ — Designed ULS tension reinforcement in support section

$a_v := 1940\ mm$ — Distance from applied load and chosen section
SS-EN 1992-1-1:2005 6.2.2 Figure 6.4

$$\beta := \begin{cases} \frac{a_v}{2 \cdot z_1} & \text{if } 0.5 \cdot z_1 \le a_v \le 2 \cdot z_1 \\ 0.25 & \text{else if } a_v \le 0.5 \cdot z_1 \\ 1 & \text{else} \end{cases} = 0.857$$

Reduction of shear force
SS-EN 1992-1-1:2005 6.2.2 (6)

$V_{Ed.ULS.RED} := V_{Ed.ULS} \cdot \beta = 796.712\ \frac{kN}{m}$ — Reduktion of shear force
SS-EN 1992-1-1:2005 6.2.2 (6)

(12)

$v := 0.6 \cdot \left(1 - \frac{f_{ck}}{250\ \mathit{MPa}}\right) = 0.528$ SS-EN 1992-1-1:2005 6.2.2 eq (6.6N)

$V_{Rd} := 0.5 \cdot z_1 \cdot v \cdot f_{cd} = \left(5.974 \cdot 10^3\right)\ \frac{\mathit{kN}}{\mathit{m}}$ SS-EN 1992-1-1:2005 6.2.2 eq (6.5)

if $V_{Ed.ULS} \leq V_{Rd}$ = "Comp strut check ok!"
  "Comp strut check ok!"
else
  "Comp strut check NOT ok!"

Utalization ratio

$\frac{V_{Ed.ULS}}{V_{Rd}} = 15.6\%$

$k_1 := 0.15$ SS-EN 1992-1-1:2005 6.2.2

$\sigma_{cp} := min\left(\frac{\left|N_{Ed.ULS.shear}\right|}{t_{deck}}, 0.2 \cdot f_{cd}\right) = 0.646\ \mathit{MPa}$ SS-EN 1992-1-1:2005 6.2.2

$\rho_I := min\left(\frac{A_{sl}}{z_1}, 0.02\right) = 0.36\%$ SS-EN 1992-1-1:2005 6.2.2

$k := min\left(1 + \sqrt{\frac{200\ \mathit{mm}}{z_1}}, 2\right) = 1.42$ SS-EN 1992-1-1:2005 6.2.2

$C_{Rd.c} := \frac{0.18}{\gamma_c} = 0.12$ SS-EN 1992-1-1:2005 6.2.2

$V_{min} := 0.035 \cdot k^{\frac{3}{2}} \cdot \left(\frac{f_{ck}}{\mathit{MPa}}\right)^{\frac{1}{2}} \cdot \mathit{MPa} = 0.325\ \mathit{MPa}$ SS-EN 1992-1-1:2005 6.2.2 eq (6.3N)

(13)

$$V_{Rd.c} := \max\left(\left[C_{Rd.c}\cdot k\cdot\left(100\ \rho_l\cdot\frac{f_{ck}}{MPa}\right)^{\frac{1}{3}}\cdot MPa + k_1\cdot\sigma_{cp}\right]\cdot z_1, \left(V_{min}+k_1\cdot\sigma_{cp}\right)\cdot z_1\right) = 535.965\ \frac{kN}{m}$$

SS-EN 1992-1-1:2005 6.2.2 (eq 6.2.a & 6.2.b)

if $V_{Ed.ULS.RED} \le V_{Rd.c}$ = "NOT ok! Add reinforcement!"
  "Shear crack check ok!"
else
  "NOT ok! Add reinforcement!"

Utalization ratio

$$\frac{V_{Ed.ULS.RED}}{V_{Rd.c}} = 148.65\%$$

$\theta := \operatorname{acot}(2.5) = 0.381$ TSFS 2018:57 6.2.3(2)

$\alpha_{cw} := 1$ SS-EN 1992-2:2005 6.11.aN

$v_1 := 0.6$ SS-EN 1992-1-1:2005 6.2.3 eq (6.10.aN)

$$V_{Rd.max} := \alpha_{cw}\cdot z_1\cdot v_1\cdot\frac{f_{cd}}{\cot(\theta)+\tan(\theta)} = 4682.069\ \frac{kN}{m}$$ SS-EN 1992-1-1:2005 6.2.3 eq (6.9)

if $V_{Ed.ULS} \le V_{Rd.max}$ = "Comp strut check ok!"
  "Comp strut check ok!"
else
  "NOT ok! Add reinforcement!"

Utalization ratio

$$\frac{V_{Ed.ULS}}{V_{Rd.max}} = 19.849\%$$

$$A_{sw.ULS} := \frac{V_{Ed.ULS}}{z_1\cdot f_{ywd}\cdot\cot(\theta)} = 10.951\ \frac{cm^2}{m^2}$$

Required amount of reinforcement
SS-EN 1992-1-1:2005 6.2.3 eq (6.8)

(14)

5. SLS crack limit design

Design of the main longitudinal reinforcement in the mid-span section due to crack width limitations were performed based on (SS-EN 1992-1-1:2005 7.3.4 and TSFS 2018:57 7.3.4(3) kap11) standards. Steels stresses were calculated using equations from (al-Emrani 2011, Bärande konstruktioner del 2) sections B7.3.3 & B.7.5.1

$w_{max} := 0.15\ mm$ — Maximum allowed crack width bottom side bridge deck TSFS 2018:57 12 kap Table 12.2 (XS3, XD3, L100)

$A'_{s.ULS} := 7.98\ \frac{cm^2}{m}$ — Calculated compression reinforcement from Sofistik ULS design

$F_{cs} := E_s \cdot \varepsilon_{cs} \cdot A_{s.ULS} = 220.528\ \frac{kN}{m}$ — (al-Emrani 2011, Bärande konstruktioner del 2) (B7-61)

$F'_{cs} := E_s \cdot \varepsilon_{cs} \cdot A'_{s.ULS} = 38.304\ \frac{kN}{m}$ — (al-Emrani 2011, Bärande konstruktioner del 2) (B7-61)

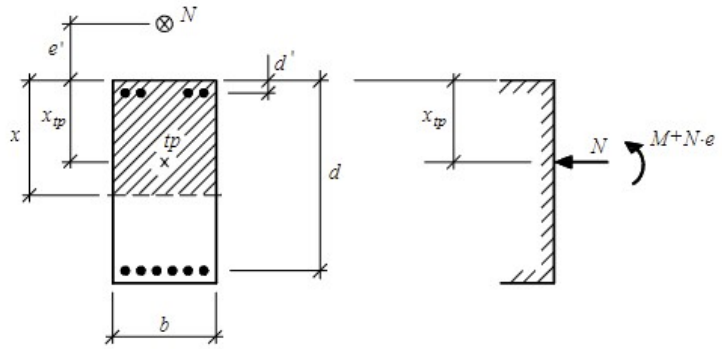

$x := 100\ mm$ — Initial guess to start itteration

$A_{II.ef}(x) := x + (\alpha_{ef} - 1) \cdot A'_{s.ULS} + \alpha_{ef} \cdot A_{s.ULS}$ — B7.3.3 (al-Emrani 2011, Bärande konstruktioner del 2)

(15)

$$x_{tp.eff}(x) := \frac{\frac{x^2}{2} + (\alpha_{ef} - 1) \cdot A'_{s.ULS} \cdot d' + \alpha_{ef} \cdot A_{s.ULS} \cdot d}{A_{II.ef}(x)}$$

(al-Emrani 2011, Bärande konstruktioner del 2) B7.3.3

$$I_{II.ef}(x) := \frac{x^3}{12} + x \cdot \left(\frac{x}{2} - x_{tp.eff}(x)\right)^2 + (\alpha_{ef} - 1) \cdot A'_{s.ULS} \cdot (x_{tp.eff}(x) - d')^2 + \alpha_{ef} \cdot A_{s.ULS} \cdot (d - x_{tp.eff}(x))^2$$

(al-Emrani 2011, Bärande konstruktioner del 2) B7.3.3

$$e_{ef}(x) := \frac{h_{deck}}{2} - x_{tp.eff}(x)$$

(al-Emrani 2011, Bärande konstruktioner del 2) B7.3.3

$$e_{s.ef}(x) := d - x_{tp.eff}(x)$$

(al-Emrani 2011, Bärande konstruktioner del 2) B7.3.3

$$e'_{s.ef}(x) := d' - x_{tp.eff}(x)$$

(al-Emrani 2011, Bärande konstruktioner del 2) B7.3.3

$$z(x) := x - x_{tp.eff}(x)$$

(al-Emrani 2011, Bärande konstruktioner del 2) B7.3.3

$$\sigma_c(x) := \frac{N_{Ed.quasi} + F_{cs} + F'_{cs}}{A_{II.ef}(x)} + \frac{N_{Ed.quasi} \cdot e_{ef}(x) + F_{cs} \cdot e_{s.ef}(x) + F'_{cs} \cdot e'_{s.ef}(x) + M_{Ed.quasi}}{I_{II.ef}(x)} \cdot z(x)$$

(al-Emrani 2011, Bärande konstruktioner del 2) B7-73a

(16)

$x := \mathbf{root}\left(\sigma_c(x), x\right) = 284.005\ mm$

Finding for what x the concrete stress = 0
B7.3.3 (al-Emrani 2011, Bärande konstruktioner del 2)

$z_s := d - x_{tp.eff}(x) = 554.791\ mm$

Distance from neutral axis to tension reinforcement
B7.3.3 (al-Emrani 2011, Bärande konstruktioner del 2)

$$\sigma_c(x) := \frac{N_{Ed.quasi} + F_{cs} + F'_{cs}}{A_{II.ef}(x)} + \frac{N_{Ed.quasi} \cdot e_{ef}(x) + F_{cs} \cdot e_{s.ef}(x) + F'_{cs} \cdot e'_{s.ef}(x) + M_{Ed.quasi}}{I_{II.ef}(x)} \cdot z_s$$

Concrete stress at reinforcement level
B7-73a (al-Emrani 2011, Bärande konstruktioner del 2)

$$\sigma_{s.SLS} := \frac{-F_{cs}}{A_{s.ULS}} + \alpha_{ef} \cdot \sigma_c(x) = 208.044\ MPa$$

Tension reinforcement stress
B7-75 (al-Emrani 2011, Bärande konstruktioner del 2)

$k_1 := 0.8$

SS-EN 1992-1-1:2005 7.3.4

$k_2 := 0.5$

SS-EN 1992-1-1:2005 7.3.4

$$k_3 := 7 \cdot \frac{\phi}{c} = 2.011$$

TSFS 2018:57 7.3.4(3) 11

$k_4 := 0.425$

SS-EN 1992-1-1:2005 7.3.4

$k_t := 0.4$

SS-EN 1992-1-1:2005 7.3.4

$$A_{c.eff} := min\left(2.5 \cdot \left(h_{deck} - d\right), \frac{h_{deck} - x}{3}, \frac{h_{deck}}{2}\right) = 221.998\ mm$$

SS-EN 1992-1-1:2005 7.3.2 (3)

(17)

$\rho_{\rho.eff} := \frac{A_{s.ULS}}{A_{c.eff}} = 2.07\%$ SS-EN 1992-1-1:2005 7.3.4

$S_{r.max} := k_3 \cdot c + k_1 \cdot k_2 \cdot k_4 \cdot \frac{\phi}{\rho_{\rho.eff}} = 380.36\ mm$ SS-EN 1992-1-1:2005 7.3.4 eq (7.11)

$\varepsilon_{sm} := \max\left(\frac{\sigma_{s.SLS} - k_t \cdot \frac{f_{ctm}}{\rho_{\rho.eff}} \left(1 + \alpha_{ef} \cdot \rho_{\rho.eff}\right)}{E_s}, 0.6 \cdot \frac{\sigma_{s.SLS}}{E_s}\right) = 0.065\%$ SS-EN 1992-1-1:2005 7.3.4 eq (7.9)

$w_k := S_{r.max} \cdot \varepsilon_{sm} = 0.25\ mm$ SS-EN 1992-1-1:2005 7.3.4 eq (7.8)

if $w_{max} \geq w_k$	= “Crack width NOT ok!, increase reinforcement”
‖ “Crack width ok!”	
else	
‖ “Crack width NOT ok!, increase reinforcement”	

$A_{s.SLS} := 70.35\ \frac{cm^2}{m}$ Increased reinforcement amount

$F_{cs} := E_s \cdot \varepsilon_{cs} \cdot A_{s.SLS} = 337.68\ \frac{kN}{m}$ Uppdated shrinkage on reinforcement eq (B7-61)

(18)

Recalculating the steel stress with updated reinforcement area As.SLS with same equations as previously

$\sigma_{s.SLS} := \frac{-F_{cs}}{A_{s.SLS}} + \alpha_{ef} \cdot \sigma_c(x) = 138.441\ MPa$ — New tension reinforcement stress (B7-75)

$A_{c.eff} := min\left(2.5 \cdot (h_{deck} - d), \frac{h_{deck} - x}{3}, \frac{h_{deck}}{2}\right) = 208.616\ mm$ — SS-EN 1992-1-1:2005 7.3.2 (3)

$\rho_{\rho.eff} := \frac{A_{s.SLS}}{A_{c.eff}} = 3.372\%$ — SS-EN 1992-1-1:2005 7.3.4

$S_{r.max} := k_3 \cdot c + k_1 \cdot k_2 \cdot k_4 \cdot \frac{\phi}{\rho_{\rho.eff}} = 301.029\ mm$ — SS-EN 1992-1-1:2005 7.3.4 eq (7.11)

$\varepsilon_{sm} := \max\left(\frac{\sigma_{s.SLS} - k_t \cdot \frac{f_{ctk.0.05}}{\rho_{\rho.eff}} \cdot (1 + \alpha_{ef} \cdot \rho_{\rho.eff})}{E_s}, 0.6 \cdot \frac{\sigma_{s.SLS}}{E_s}\right) = 0.05\%$ — SS-EN 1992-1-1:2005 7.3.4 eq (7.9)

$w_k := S_{r.max} \cdot \varepsilon_{sm} = 0.15\ mm$ — SS-EN 1992-1-1:2005 7.3.4 eq (7.8)

if $w_{max} \le w_k$	= "Crack width ok!"
‖ "Crack width NOT ok!, increase reinforcement"	
else	
‖ "Crack width ok!"	

(19)

6. Fatigue design of reinforcement

Fatigue verification of reinforcement was performed according to standards SS-EN 1992-1-1:2005 chapter 6.8.4 - 6.8.5 and SS-EN 1992-2:2005 chapter NN.3 with rekommended parameters from TRVINFRA-00227.

6.1 Mid-span main reinforcement steel stress amplitude

The maximum and minimum steel stress in the reinforcement were calculated based on the minimum and maximum dimensioning sectional force for the fatigue load case seen in Chapter 1.3. The fatigue design was carried out using the dimensioning reinforcement area, i.e maximum area needed for previous limit state calculations. The steel stresses were calculated on the same principles as in Chapter 3. Only the changed relevant equations are shown.

Maximum stress

$$A_{II.ef}(x) := x + (\alpha_{ef} - 1) \cdot A'_{s.ULS} + \alpha_{ef} \cdot A_{s.SLS}$$

(al-Emrani 2011, Bärande konstruktioner del 2) B7.3.3

$$x_{tp.eff}(x) := \frac{\frac{x^2}{2} + (\alpha_{ef} - 1) \cdot A'_{s.ULS} \cdot d' + \alpha_{ef} \cdot A_{s.SLS} \cdot d}{A_{II.ef}(x)}$$

(al-Emrani 2011, Bärande konstruktioner del 2) B7.3.3

$$I_{II.ef}(x) := \frac{x^3}{12} + x \cdot \left(\frac{x}{2} - x_{tp.eff}(x)\right)^2 + (\alpha_{ef} - 1) \cdot A'_{s.ULS} \cdot (x_{tp.eff}(x) - d')^2 + \alpha_{ef} \cdot A_{s.SLS} \cdot (d - x_{tp.eff}(x))^2$$

(al-Emrani 2011, Bärande konstruktioner del 2) B7.3.3

$$\sigma_c(x) := \frac{N_{Ed.fat.max} + F_{cs} + F'_{cs}}{A_{II.ef}(x)} + \frac{N_{Ed.fat.max} \cdot e_{ef}(x) + F_{cs} \cdot e_{s.ef}(x) + F'_{cs} \cdot e'_{s.ef}(x) + M_{Ed.Fat.max}}{I_{II.ef}(x)} \cdot z(x)$$

(al-Emrani 2011, Bärande konstruktioner del 2) (B7-73a)

(20)

$$\sigma_c(x) := \frac{N_{Ed.fat.max} + F_{cs} + F'_{cs}}{A_{II.ef}(x)} + \frac{N_{Ed.fat.max} \cdot e_{ef}(x) + F_{cs} \cdot e_{s.ef}(x) + F'_{cs} \cdot e'_{s.ef}(x) + M_{Ed.Fat.max}}{I_{II.ef}(x)} \cdot z_s$$

(al-Emrani 2011, Bärande konstruktioner del 2)
(B7-73a)

$\sigma_{s.main.max} := \frac{-F_{cs}}{A_{s.SLS}} + \alpha_{ef} \cdot \sigma_c(x) = 149.501\ \mathit{MPa}$

Maximum tension reinforcement stress
(B7-75)

Minimum stress:

$$\sigma_c(x) := \frac{N_{Ed.fat.min} + F_{cs} + F'_{cs}}{A_{II.ef}(x)} + \frac{N_{Ed.fat.min} \cdot e_{ef}(x) + F_{cs} \cdot e_{s.ef}(x) + F'_{cs} \cdot e'_{s.ef}(x) + M_{Ed.Fat.min}}{I_{II.ef}(x)} \cdot z(x)$$

(al-Emrani 2011, Bärande konstruktioner del 2)
(B7-73a)

$$\sigma_c(x) := \frac{N_{Ed.fat.min} + F_{cs} + F'_{cs}}{A_{II.ef}(x)} + \frac{N_{Ed.fat.min} \cdot e_{ef}(x) + F_{cs} \cdot e_{s.ef}(x) + F'_{cs} \cdot e'_{s.ef}(x) + M_{Ed.Fat.min}}{I_{II.ef}(x)} \cdot z_s$$

(al-Emrani 2011, Bärande konstruktioner del 2)
(B7-73a)

$\sigma_{s.main.min} := \frac{-F_{cs}}{A_{s.SLS}} + \alpha_{ef} \cdot \sigma_c(x) = 78.485\ \mathit{MPa}$

Minimum tension reinforcement stress
(B7-75)

Stress amplitude:

$\Delta\sigma_{s.main} := \sigma_{s.main.max} - \sigma_{s.main.min} = 71.016\ \mathit{MPa}$

Tension reinforcement stress amplitude

(21)

6.2 Support section shear reinforcement steel stress amplitude

The maximum and minimum steel stress in the shear reinforcement was calculated based on the minimum and maximum dimensioning sectional force for the fatigue load case seen in Chapter 1.3. The fatigue design was carried out using the dimensioning reinforcement area, i.e maximum area needed for previous limit state calculations. The steel stresses were calculated based on ultimate limit shear reinforcement design equations from SS-EN 1992-1-1:2005 6.2.3 eq (6.8) using fatigue designed sectional shear force.

$\sigma_{s.stir.max} := \frac{V_{Ed.Fat.max}}{A_{sw.ULS} \cdot z_1 \cdot \cot(\theta)} = 168.167\ MPa$ — Maximum stress in stirup SS-EN 1992-1-1:2005 6.2.3 eq (6.8)

$\sigma_{s.stir.min} := \frac{V_{Ed.Fat.min}}{A_{sw.ULS} \cdot z_1 \cdot \cot(\theta)} = 95.136\ MPa$ — Minimum stress in stirup SS-EN 1992-1-1:2005 6.2.3 eq (6.8)

$\Delta\sigma_{s.stir} := \sigma_{s.stir.max} - \sigma_{s.stir.min} = 73.031\ MPa$ — Stress amplitude in stirup

6.3 Fatigue check

$\phi_{dyn} := 1.23$ — Dynamic factor from train load used in model

$\zeta := 0.35 + 0.026 \cdot \frac{D}{\phi_{stirup}} = 0.553$ — Reduction factor for stirups SS-EN 1992-1-1:2005 Table 6.3N

$\Delta\sigma_{Rsk.main} := 162.5\ MPa$ — Critical stress amplitude for straight bars SS-EN 1992-1-1:2005 Table 6.3N

$\Delta\sigma_{Rsk.stirup} := 162.5\ MPa \cdot \zeta = 89.883\ MPa$ — Critical stress amplitude for stirups SS-EN 1992-1-1:2005 Table 6.3N

(22)

$Vol := 25.06 \cdot 10^6 \ \frac{ton}{yr}$ Trafik volume
TRVINFRA-00227 Table 7.1-7

$k_2 := 9$ SS-EN 1992-1-1:2005 Table 6.3N

$N_{years} := 120 \ yr$ Dimensioning service life of bridge

$L_{bridge} := 16 \ m$ Theoretical span width of bridge

$$\alpha_{just} := \begin{cases} 1 & \text{if } L_{bridge} \geq 10 \ m \\ 1 + \frac{10 \ m - L_{bridge}}{10 \ m} \cdot 0.33 & \text{else} \end{cases} = 1$$

Adjustment
TRVINFRA-00227 Table 7.1-11g

$\lambda_{sl.2m} := 1.05$ Continous beams, mid section, heavy traffic
SS-EN 1992-2:2005 Table NN-2

$\lambda_{sl.20m} := 0.55$ Continous beams, mid section, heavy traffic
SS-EN 1992-2:2005 Table NN-2

$$\lambda_{s.1} := \alpha_{just} \cdot \left(\lambda_{sl.2m} + \left(\lambda_{sl.20m} - \lambda_{sl.2m} \right) \cdot \left(\log\left(\frac{L_{bridge}}{m} \right) - 0.3 \right) \right) = 0.598$$

SS-EN 1992-2:2005 eq (NN.108)

$$\lambda_{s.2} := \sqrt[k_2]{\frac{Vol}{25 \cdot 10^6 \ \frac{ton}{yr}}} = 1$$

SS-EN 1992-2:2005 eq (NN.109)

$$\lambda_{s.3} := \sqrt[k_2]{\frac{N_{years}}{100 \ yr}} = 1.02$$

SS-EN 1992-2:2005 eq (NN.110)

(22)

$Vol := 25.06 \cdot 10^6 \ \frac{ton}{yr}$

Trafik volume
TRVINFRA-00227 Table 7.1-7

$k_2 := 9$

SS-EN 1992-1-1:2005 Table 6.3N

$N_{years} := 120 \ yr$

Dimensioning service life of bridge

$L_{bridge} := 16 \ m$

Theoretical span width of bridge

$$\alpha_{just} := \begin{cases} \text{if } L_{bridge} \geq 10 \ m \\ \quad 1 \\ \text{else} \\ \quad 1 + \frac{10 \ m - L_{bridge}}{10 \ m} \cdot 0.33 \end{cases} = 1$$

Adjustment
TRVINFRA-00227 Table 7.1-11g

$\lambda_{sl.2m} := 1.05$

Continous beams, mid section, heavy traffic
SS-EN 1992-2:2005 Table NN-2

$\lambda_{sl.20m} := 0.55$

Continous beams, mid section, heavy traffic
SS-EN 1992-2:2005 Table NN-2

$$\lambda_{s.1} := \alpha_{just} \cdot \left(\lambda_{sl.2m} + \left(\lambda_{sl.20m} - \lambda_{sl.2m} \right) \cdot \left(\log\left(\frac{L_{bridge}}{m} \right) - 0.3 \right) \right) = 0.598$$

SS-EN 1992-2:2005 eq (NN.108)

$$\lambda_{s.2} := \sqrt[k_2]{\frac{Vol}{25 \cdot 10^6 \ \frac{ton}{yr}}} = 1$$

SS-EN 1992-2:2005 eq (NN.109)

$$\lambda_{s.3} := \sqrt[k_2]{\frac{N_{years}}{100 \ yr}} = 1.02$$

SS-EN 1992-2:2005 eq (NN.110)

(23)

$\lambda_{s.4} := 1.0$ Largest value, konservative
SS-EN 1992-2:2005 eq (NN.111)

$\lambda_s := \lambda_{s.1} \cdot \lambda_{s.2} \cdot \lambda_{s.3} \cdot \lambda_{s.4} = 0.61$ SS-EN 1992-2:2005 eq (NN.107)

$\Delta\sigma_{S.equ.main} := \Delta\sigma_{s.main} \cdot \lambda_s \cdot \phi_{dyn} = 53.313\ \mathit{MPa}$ SS-EN 1992-2:2005 eq (NN.106)

if $\gamma_{F.fat} \cdot \Delta\sigma_{S.equ.main} \leq \frac{\Delta\sigma_{Rsk.main}}{\gamma_{s.fat}}$ = "Reinforcement check ok!"
  "Reinforcement check ok!"
else
  "Not ok! Increase reinforcement area"

SS-EN 1992-2:2005 6.8.5 eq (6.71)

$\Delta\sigma_{S.equ.stir} := \Delta\sigma_{s.stir} \cdot \lambda_s \cdot \phi_{dyn} = 54.826\ \mathit{MPa}$ SS-EN 1992-2:2005 eq (NN.106)

if $\gamma_{F.fat} \cdot \Delta\sigma_{S.equ.stir} \leq \frac{\Delta\sigma_{Rsk.stirup}}{\gamma_{s.fat}}$ = "Reinforcement check ok!"
  "Reinforcement check ok!"
else
  "Not ok! Increase reinforcement area"

SS-EN 1992-2:2005 6.8.5 eq (6.71)

(24)

7. Minimum Reinforcement

Minimum reinforcement was calculated for all structural members based on SS-EN 1992-2:2005 section 7.3.2, SS-EN 1992-1-1:2005 section 9.3 and additional minimum reinforcement requirements from TRVINFRA-00227 7.1.10.1. The maximum value from all relevant values were chosen as the dimensioning minimum reinforcement for the structural component. Minimum reinforcement for structural members with varying thickness were dimensioned for the average member thickness.

7.1 Bridge deck

Robust reinforcement for brittle failure described in SS-EN 1992-1-1:2005 9.3 were added to the other minimum reinforcement requirements. The average thickness of the bridge deck was used for dimensioning of the bridge deck

$$t_{avg.BD} := \frac{1300\ mm + h_{deck}}{2} = 1125\ mm$$ Average thickness of bridge deck

$$k_c := 0.4$$ Rekommended for bending and normal force SS-EN 1992-2:2005 7.3.2

$$k := \begin{cases} 1.0 & \text{if } t_{avg.BD} \le 300\ mm \\ 0.65 & \text{else if } t_{avg.BD} \ge 800\ mm \\ \text{linterp}\left(\begin{bmatrix} 300\ mm \\ 800\ mm \end{bmatrix}, \begin{bmatrix} 1 \\ 0.65 \end{bmatrix}, t_{avg.BD}\right) & \text{else} \end{cases} = 0.65$$ SS-EN 1992-2:2005 7.3.2

$$A_{min.BD.1} := \frac{k_c \cdot k \cdot f_{ctm} \cdot A_{c.eff}}{f_{yk}} = 3.146\ \frac{cm^2}{m}$$ SS-EN 1992-2:2005 7.3.2 eq (7.1)

$$A_{min.2} := 4.0 \cdot \frac{\frac{f_{ctm}}{MPa}}{3}\ \frac{cm^2}{m} = 3.867\ \frac{cm^2}{m}$$ TRVINFRA-00227 7.1.10.1

$$A_{min.3} := 5.6\ \frac{cm^2}{m}$$ TRVINFRA-00227 7.1.10.1

(25)

$$A_{min.BD.4} := \begin{cases} 0.05\% \cdot t_{avg.BD} & \text{if } \frac{b_{BD.FL}}{t_{avg.BD}} < 5 \\ 0.08\% \cdot t_{avg.BD} & \text{else} \end{cases} = 9 \ \frac{cm^2}{m}$$

TRVINFRA-00227 7.1.10.1

$$A_{min.5} := 4 \ \frac{cm^2}{m}$$

TRVINFRA-00227 7.1.10.1

$$A_{min.BD.6} := \max\left(0.26 \cdot \frac{f_{ctm}}{f_{yk}} \cdot t_{avg.BD}, 0.0013 \cdot d\right) = 16.97 \ \frac{cm^2}{m}$$

For brittle failure in bridge deck
SS-EN 1992-1-1:2005 9.2.1.1 eq (9.1N)

$$A_{s.BD} := \max\left(A_{min.BD.1}, A_{min.2}, A_{min.3}, A_{min.BD.4}, A_{min.5}, A_{min.BD.6}\right) = 16.965 \ \frac{cm^2}{m}$$

Required minimum reinforcement

(26)

7.2 Frame legs

No robust reinforcement was considered for the frame legs. The average thickness of the frame legs was used for dimensioning of the bridge deck

$$t_{avg.FL} := \frac{1200\ mm + 700\ mm}{2} = 950\ mm$$

Average frame leg thickness

$$k := \begin{cases} 1.0 & \text{if } t_{avg.FL} \le 300\ mm \\ 0.65 & \text{else if } t_{avg.FL} \ge 800\ mm \\ \text{linterp}\left(\begin{bmatrix} 300\ mm \\ 800\ mm \end{bmatrix}, \begin{bmatrix} 1 \\ 0.65 \end{bmatrix}, t_{avg.FL}\right) & \text{else} \end{cases} = 0.65$$

SS-EN 1992-2:2005 7.3.2

$$A_{c.eff} := A_{c.eff} = 208.616\ mm$$

Since frame legs have same $t_{avg.FL}$ as h_{deck} and same reinforcement and distances are used for the main reinforcement in the frame legs and bridge deck

$$A_{min.FL.1} := \frac{k_c \cdot k \cdot f_{ctm} \cdot A_{c.eff}}{f_{yk}} = 3.146\ \frac{cm^2}{m}$$

SS-EN 1992-2:2005 7.3.2 eq (7.1)

$$A_{min.BD.4} := \begin{cases} 0.05\% \cdot t_{avg.FL} & \text{if } \frac{b_{BD.FL}}{t_{avg.FL}} < 5 \\ 0.08\% \cdot t_{avg.FL} & \text{else} \end{cases} = 7.6\ \frac{cm^2}{m}$$

TRVINFRA-00227 7.1.10.1

$$A_{s.FL} := \max\left(A_{min.FL.1}, A_{min.2}, A_{min.3}, A_{min.BD.4}, A_{min.5}\right) = 7.6\ \frac{cm^2}{m}$$

Required minimum reinforcement

(27)

7.3 Foundation slab

No robust reinforcement was considered for the foundation slab.

$t_{foundation} := 900\ mm$

$k := \text{if } t_{foundation} \le 300\ mm \quad 1.0 \quad \text{else if } t_{foundation} \ge 800\ mm \quad 0.65 \quad \text{else} \quad \text{linterp}\left(\begin{bmatrix} 300\ mm \\ 800\ mm \end{bmatrix}, \begin{bmatrix} 1 \\ 0.65 \end{bmatrix}, t_{foundation}\right) = 0.65$

SS-EN 1992-2:2005 7.3.2

$A_{c.eff} := A_{c.eff} = 208.616\ mm$

Since foundat slab have approximatly the same $t_{foundation}$ as h_{deck} and same reinforcement and distances are used, simplification can be made

$A_{min.BS.1} := \frac{k_c \cdot k \cdot f_{ctm} \cdot A_{c.eff}}{f_{yk}} = 3.146\ \frac{cm^2}{m}$

SS-EN 1992-2:2005 7.3.2 eq (7.1)

$A_{min.BS.4} := \text{if } \frac{b_{FS}}{t_{foundation}} < 5 \quad 0.05\% \cdot t_{foundation} \quad \text{else} \quad 0.08\% \cdot t_{foundation} = 7.2\ \frac{cm^2}{m}$

TRVINFRA-00227 7.1.10.1

$A_{min.BS.6} := 5.026\ \frac{cm^2}{m}$

At least 16fiS400mm for foundation slabs
TRVINFRA-00227 7.1.10.1

$A_{s.BS} := \max\left(A_{min.BS.1}, A_{min.2}, A_{min.3}, A_{min.BS.4}, A_{min.5}, A_{min.BS.6}\right) = 7.2\ \frac{cm^2}{m}$

Required minimum reinforcement

(28)

8. Verification

8.1 Mid-span bottom longitudinal main reinforcement

Grp	Element	LC	t [m]	asu [cm2/m]	asu2 [cm2/m]	asu3 [cm2/m]	as1 [cm2/m]	as12 [cm2/m]	as13 [cm2/m]	supp [-]	shear [-]	ass [cm2/m2]
1	10001	30001	0.951				7.26	41.79			1	
		30002	0.951	1.31	5.27						1	
		30003	0.951				8.16	41.37			1	
		30004	0.951	1.49	5.22						1	
		30005	0.951				1.90	12.32			1	
		30006	0.951				5.42	37.26			1	
		30007	0.951				6.24	30.33			1	
		30008	0.951				4.57	18.67			1	
		30009	0.951				6.31	34.91			1	
		30010	0.951				3.31	17.84			1	
		30011	0.951				1.54	21.13			1	
		30012	0.951				5.43				1	
		30013	0.951				2.45	24.50			1	
		30014	0.951				5.44	26.79			1	
		30015	0.951				3.64	25.53			1	
		30016	0.951				4.42	22.83			1	
		30101	0.951				7.21	44.78			1	

$A_{s.ULS.FEM} := 44.78 \ \frac{cm^2}{m}$ Designed ULS reinforcement from Sofistik

$1 - \frac{A_{s.ULS.FEM}}{A_{s.ULS}} = 2.532\%$ Difference between analytical and numerical results

Detail Results Calculation of Crack Widths

Grp	Element	ID	dir [°]	LC	t [m]	d [m]	z [m]	x [m]	hc,ef [m]	ø [mm]	σs [MPa]	as_0 [cm2/m]	as [cm2/m]	wk [mm]
1	10001	asu	90	30902	0.951	0.903	0.571	0.071	0.120	16	33.73	2.18	2.18	0.10
		asu	90	30904	0.951	0.903	0.571	0.071	0.120	16	33.73	2.18	2.18	0.10
		asu2	0	30902	0.951	0.883	0.795	0.262	0.171	25	104.7	7.98	7.98	0.28
		asu2	0	30904	0.951	0.883	0.795	0.262	0.171	25	104.7	7.98	7.98	0.28
		as12	0	30901	0.951	0.852	0.758	0.300	0.217	25	140.8	44.78	67.09	0.15

ULS SLS

$A_{s.SLS.FEM} := 68.72 \ \frac{cm^2}{m}$ Designed SLS reinforcement from Sofistik

$1 - \frac{A_{s.SLS.FEM}}{A_{s.SLS}} = 2.317\%$ Difference between analytical and numerical results

(29)

			concrete upper face				concrete lower face				as upside		as downside	
Grp	Element	LC	σII [MPa]	σI [MPa]	dir [°]	σb [MPa]	σII [MPa]	σI [MPa]	dir [°]	σt [MPa]	σasu [MPa]	σasu2 [MPa]	σasl [MPa]	σasl2 [MPa]
1	10001	40015	-8.00	-0.75	167.	0.00	0.00	0.00	54.2	0.00	6.01	-63.06	80.72	137.53
		40016	-7.98	-0.74	12.7	0.00	0.00	0.00	126.	0.00	6.12	-62.99	79.18	137.04
		max.	-4.86	-0.74		0.00	0.00	0.00		0.00	6.12	-41.86	152.39	148.81
		min.	-8.78	-3.28		0.00	0.00	0.00		0.00	-10.83	-69.91	43.46	80.01
		range	3.92	2.54		0.00	0.00	0.00		0.00	16.95	28.05	108.93	68.80

$\Delta\sigma_{s.main.FEM} := 68.80\ \mathit{MPa}$ Designing stress range in reinforcement from Sofistik

$1 - \frac{\Delta\sigma_{s.main.FEM}}{\Delta\sigma_{s.main}} = 3.121\%$ Difference between analytical and numerical results

(30)

8.2 Support section shear check and reinforcement design

Grp	Element	LC	t [m]	zu [m]	zl [m]	zs [m]	m-s [kNm/m]	as-t [cm2/m]	ro [%]	scp [MPa]	VED [kN/m]	VED* [kN/m]	VRDc [kN/m]	VRDMAX [kN/m]	cot [-
1	10361	30107	1.231	1.096		1.096	-2021.6	40.76	0.36	0.65	929.6	785.1	539.0	4119.0	2.5

Grp	Element	LC	t [m]	asu [cm2/m]	asu2 [cm2/m]	asu3 [cm2/m]	asl [cm2/m]	asl2 [cm2/m]	asl3 [cm2/m]	supp [-]	shear [-]	ass [cm2/m2]
1	10361											
		30107	1.231	7.71	31.71						2	10.99

$V_{Rd.c.FEM} := 539 \ \frac{kN}{m}$ Shear crack capacity without reinforcement from Sofistik

$1 - \frac{V_{Rd.c}}{V_{Rd.c.FEM}} = 0.563\%$ Difference between analytical and numerical results

$A_{sw.ULS.FEM} := 10.99 \cdot \frac{cm^2}{m^2}$ Required amount of reinforcement from Sofistik

$1 - \frac{A_{sw.ULS}}{A_{sw.ULS.FEM}} = 0.352\%$ Difference between analytical and numerical results

Results of fatigue check steel, maximum concrete pressure

E=ELEM N=NODE	stress range asu [MPa]	asu2 [MPa]	on top asu3 [MPa]	stress range asl [MPa]	asl2 [MPa]	bottom asl3 [MPa]	links Ass [MPa]	concre sig-max [MPa]	steel-l sig-max [MPa]	steel-s sig-max
E 10361	108.10[1]	95.59[1]	-	7.92[1]	14.24[1]	-	72.84[1]	-7.36[1]	185.70[1]	182.16[1]

$\Delta\sigma_{s.stir.FEM} := 72.84 \ MPa = 72.84 \ MPa$ Designing stress range in stirups from Sofistik

$1 - \frac{\Delta\sigma_{s.stir.FEM}}{\Delta\sigma_{s.stir}} = 0.261\%$ Difference between analytical and numerical results

(31)

8.3 Minimum reinforcement

Reinforcementparameter two layer reinforcement

Selection Grp no.	elem no.	distance d1-u d1-l [mm]	2.lay 2.lay [mm]	bar-diameter ds-u ds-l [mm]	2.lay 2.lay [mm]	crackwidth wk-u wk-l [mm]	2.lay 2.lay [mm]	steelstress sigsu sigsl [MPa]	2.lay 2.lay [MPa]	min.reinf. asu asl [cm2/m]	2.lay 2.lay [cm2/m]
default		35.0	45.0	-	-	0.20	0.20	-	-	-	-
		35.0	45.0	-	-	0.20	0.20	-	-	-	-
1		48.0	68.5	16	25	0.30	0.30	-	-	16.97	16.97
		79.0	99.5	16	25	0.15	0.15	-	-	16.97	16.97
2		48.0	68.5	16	25	0.40	0.40	-	-	7.60	7.60
		63.0	83.5	16	25	0.15	0.15	-	-	7.60	7.60
3		48.0	68.5	16	25	0.40	0.40	-	-	7.60	7.60
		63.0	83.5	16	25	0.15	0.15	-	-	7.60	7.60
4		48.0	64.0	16	16	0.20	0.20	-	-	7.20	7.20
		58.0	74.0	16	16	0.40	0.40	-	-	7.20	7.20
5		48.0	64.0	16	16	0.20	0.20	-	-	7.20	7.20
		58.0	74.0	16	16	0.40	0.40	-	-	7.20	7.20

distance	upper / lower distance center of bar to surface
bar-diameter	upper / lower bar diameter
crackwidth	upper / lower required crack width
steelstress	upper / lower maximum steel stress in SLS check
min.reinf.	upper / lower minimum reinforcement

$A_{s.BD.FEM} := 16.97 \frac{cm^2}{m}$ Minimum reinforcement in bridge deck from Sofistik

$A_{s.FL.FEM} := 7.6 \cdot \frac{cm^2}{m}$ Minimum reinforcement in frame legs from Sofistik

$A_{s.BS.FEM} := 7.2 \frac{cm^2}{m}$ Minimum reinforcement in bottom slab from Sofistik

$1 - \frac{A_{s.BD}}{A_{s.BD.FEM}} = 0.029\%$ Difference between analytical and numerical results

$1 - \frac{A_{s.FL}}{A_{s.FL.FEM}} = 0$ Difference between analytical and numerical results

$1 - \frac{A_{s.BS}}{A_{s.BS.FEM}} = 0$ Difference between analytical and numerical results

D

Reinforcement design results and comparison with reference objects

The geometry of the two reference bridges seen in Chapter 2.5.1 was set up separately in Sofistik and designed individually using the finalized structural calculation script used for the bridges in the Set-Based work process mentioned in Chapter 3.2.2. A cut similar to the one in Figure 3.10 was placed along the longitudinal center line of the bridge and the designed required longitudinal top and bottom reinforcement as well as shear reinforcement was extracted. The required reinforcement results for both designed bridges were plotted against the required reinforcement from the two real reference bridges shown separately in Sections D.2 & D.3. As the reference bridges were designed differently from the Sofistik model by designing some structural components separately, no required reinforcement for some structural components was provided for the reference bridges and only the actual reinforcement was provided. Therefore, reinforcement results from the real reference objects that were provided as actual reinforcement, are marked with an asterisk. In addition, the ULS sectional shear forces and moments in the bridge deck for the open foundation reference bridges were extracted and compared with the ULS sectional shear force and moments from the Sofistik model replica in section D.1, to show the difference in applied loads and structural behavior.

D.1 Sectional forces comparison

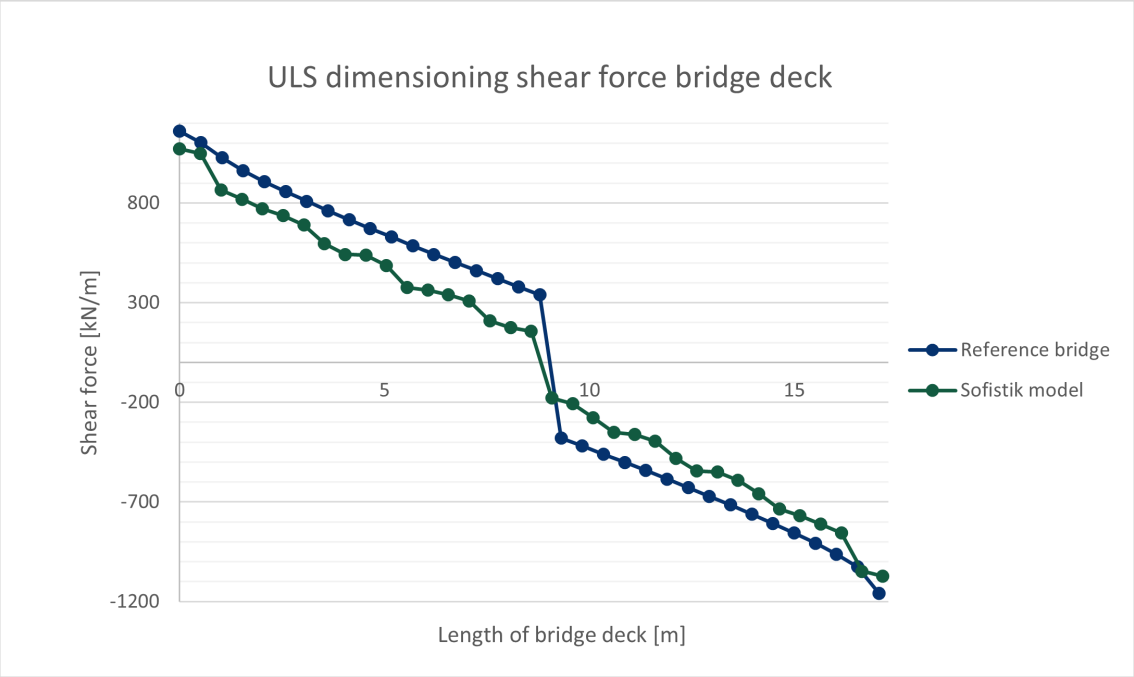

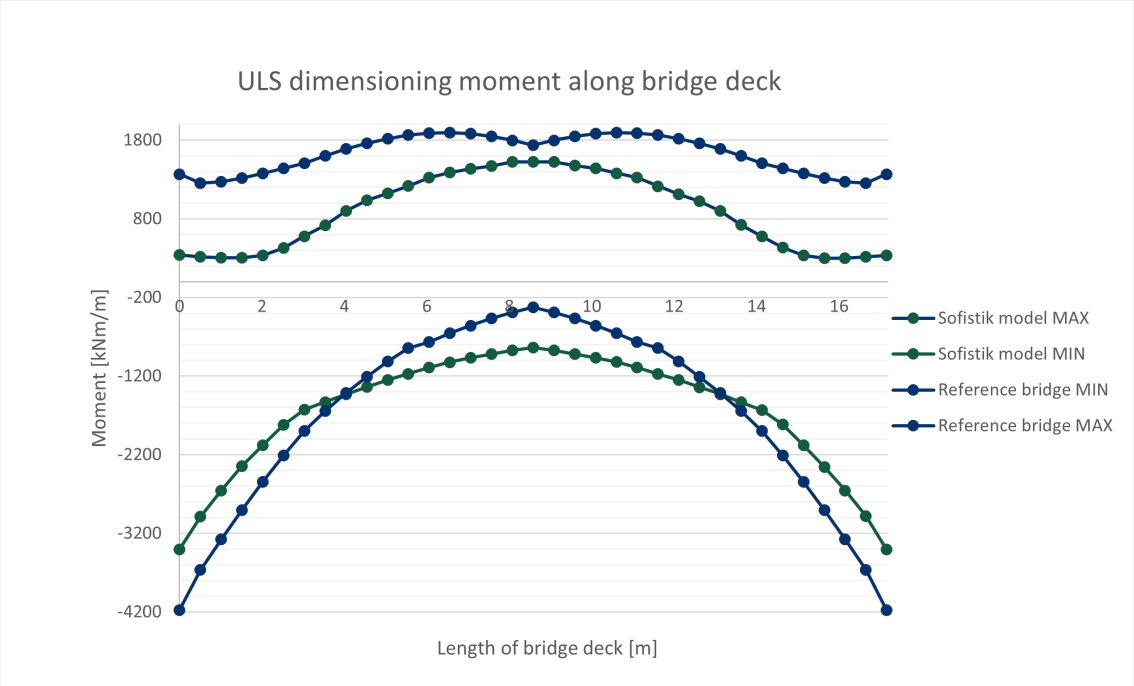

D.2 Closed foundation slab frame bridge

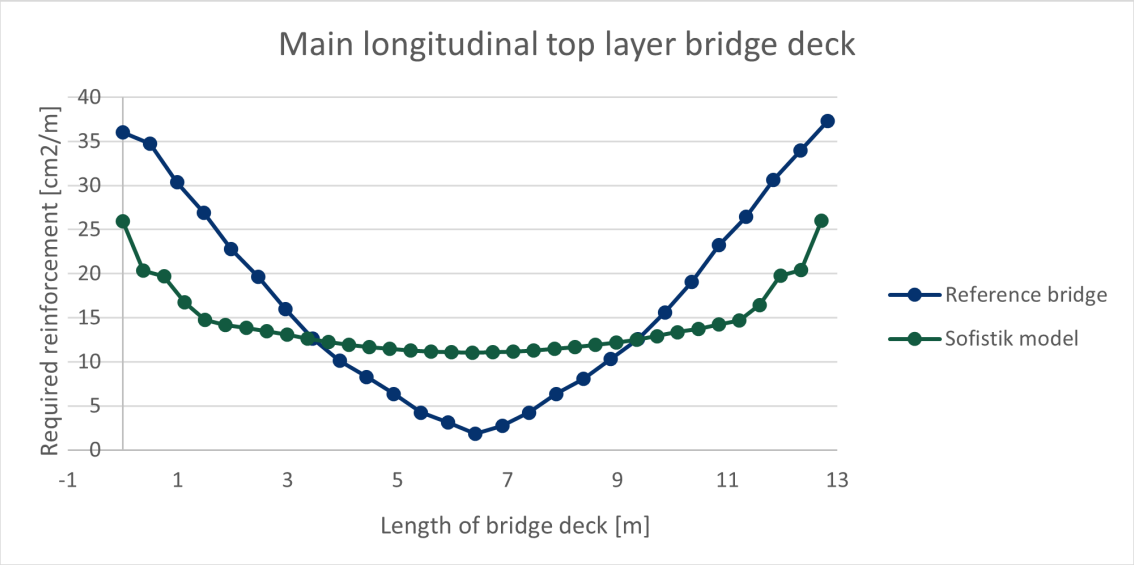

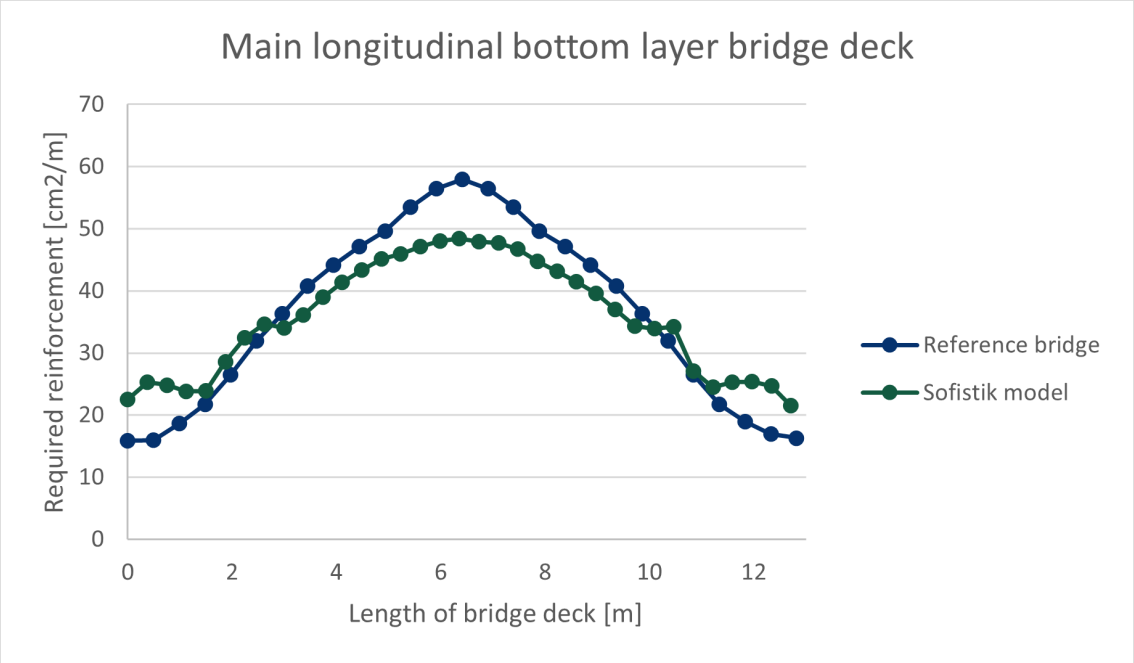

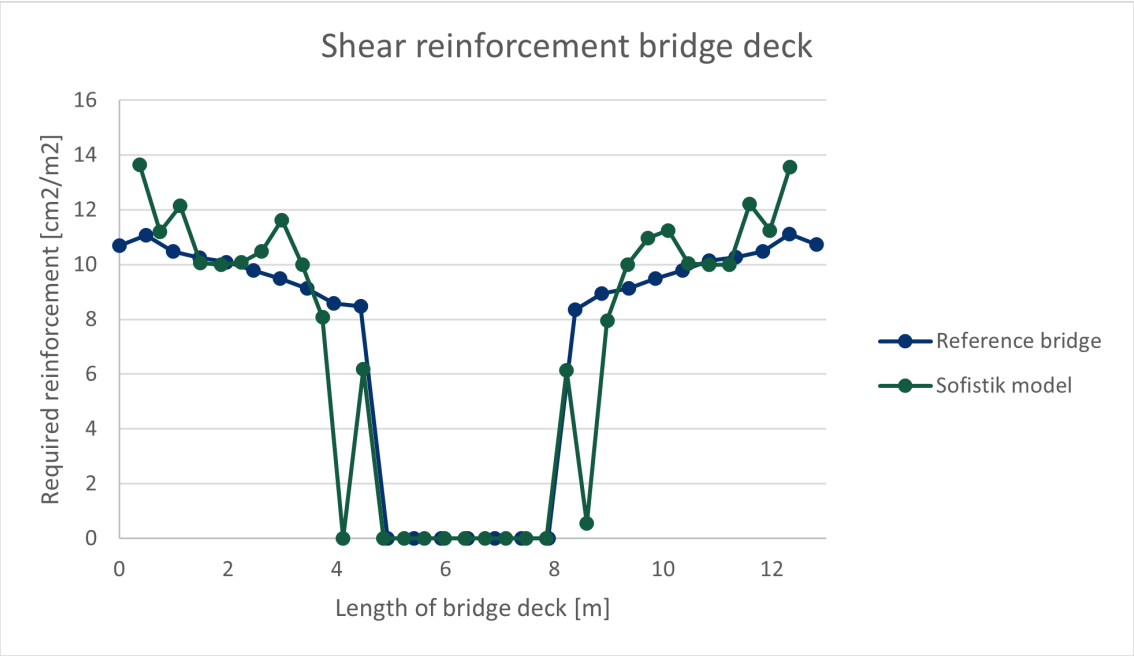
Shear reinforcement bridge deck
Required reinforcement [cm2/m2]
16
14
12
10
8
6
4
2
0
0
2
4
6
8
10
12
Length of bridge deck [m]
Reference bridge
Sofistik model

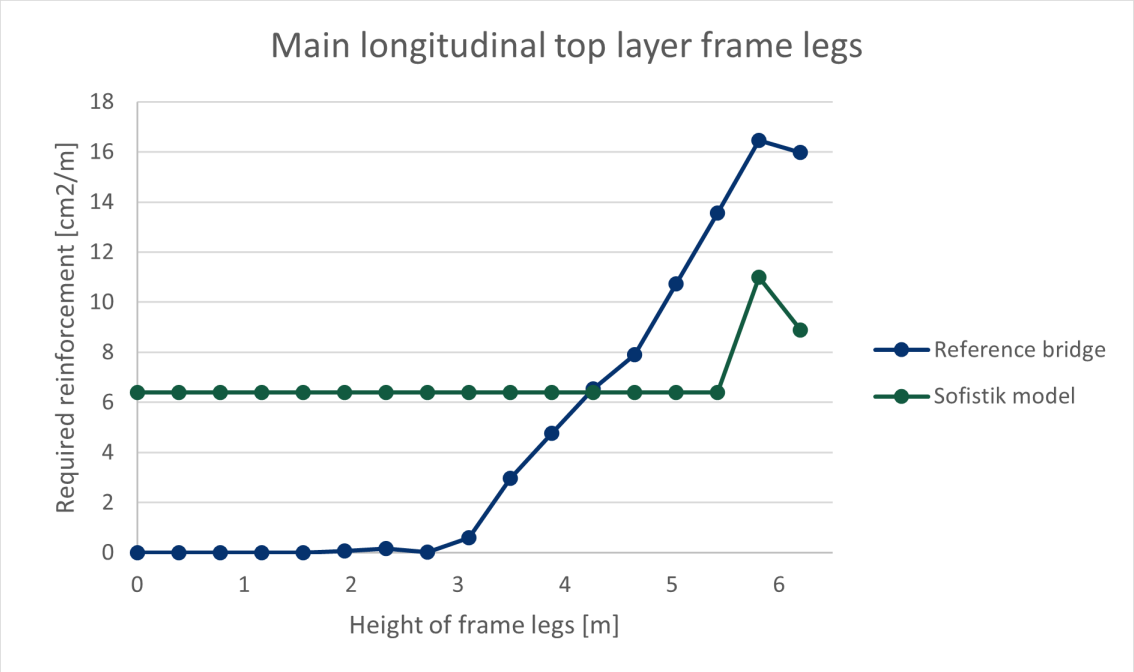
Main longitudinal top layer frame legs
Required reinforcement [cm2/m]
18
16
14
12
10
8
6
4
2
0
0
1
2
3
4
5
6
Height of frame legs [m]
Reference bridge
Sofistik model

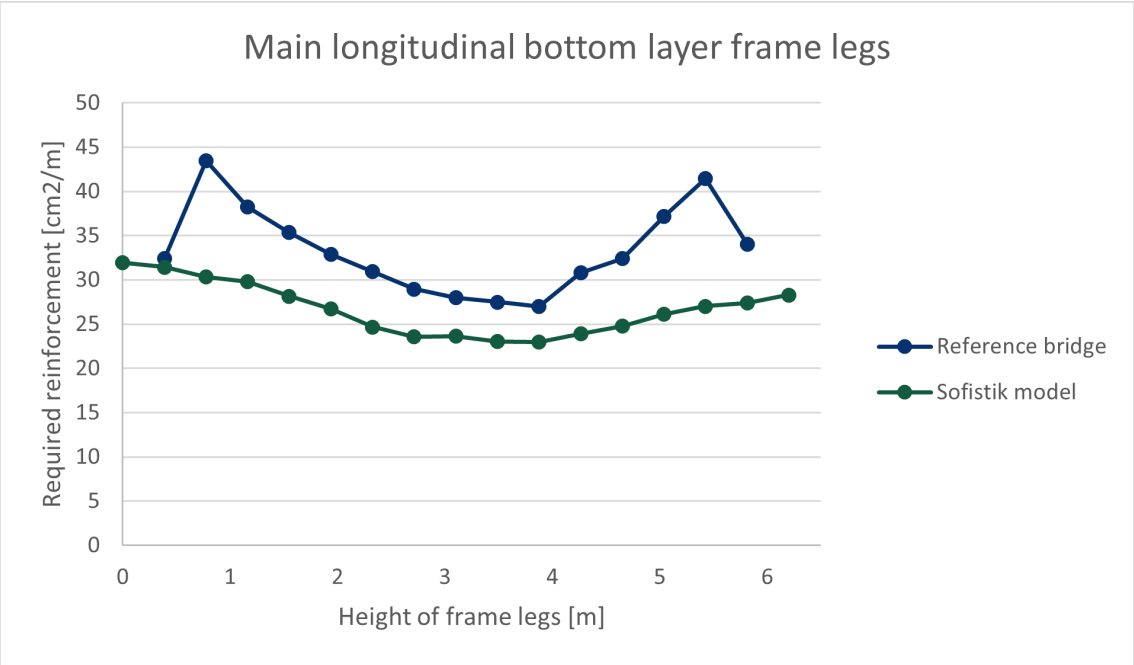
Main longitudinal bottom layer frame legs
Required reinforcement [cm2/m]
50
45
40
35
30
25
20
15
10
5
0
0
1
2
3
4
5
6
Height of frame legs [m]
Reference bridge
Sofistik model

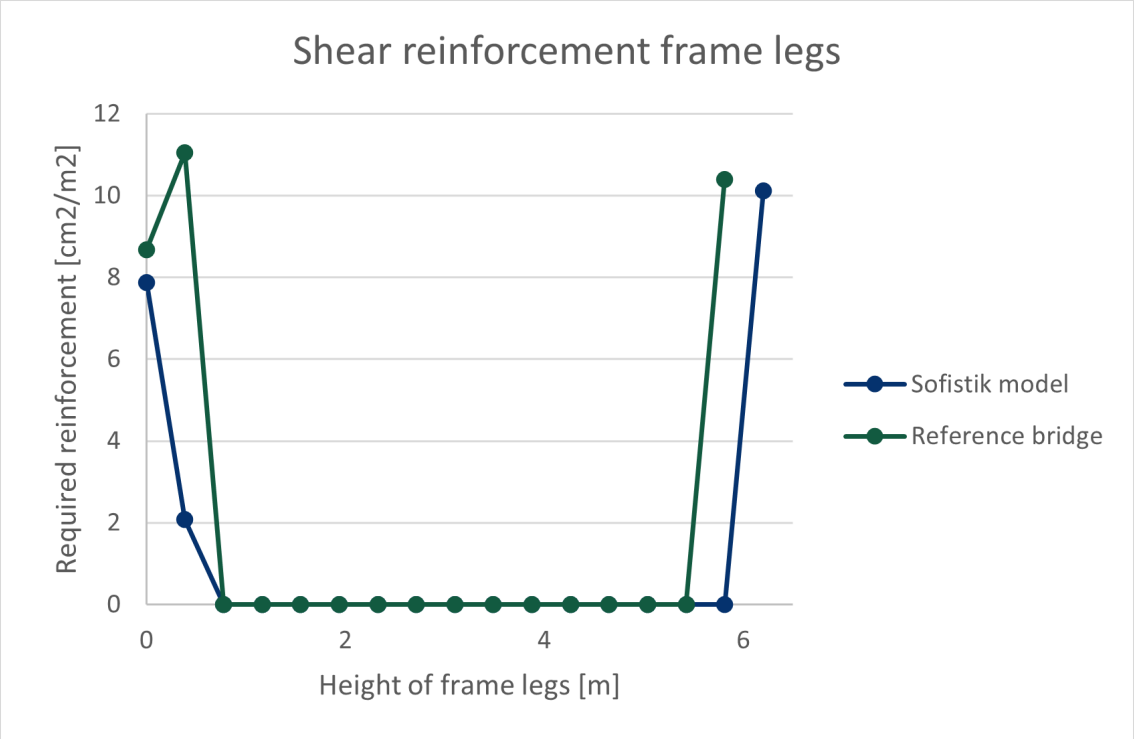
Shear reinforcement frame legs
Required reinforcement [cm2/m2]
12
10
8
6
4
2
0
0
2
4
6
Height of frame legs [m]
Sofistik model
Reference bridge

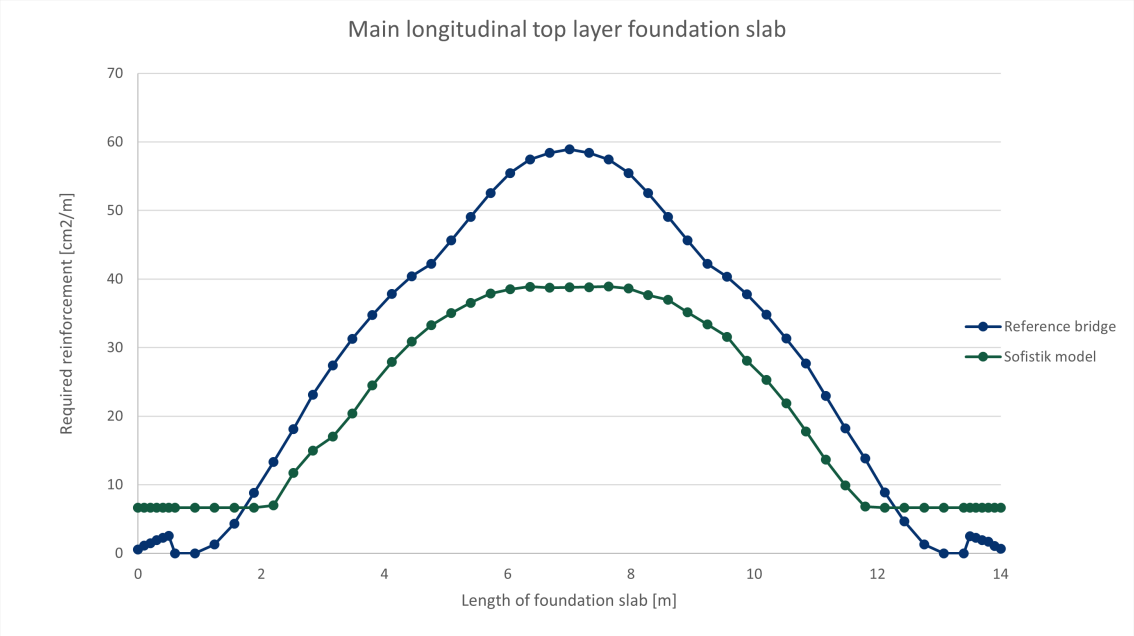
Main longitudinal top layer foundation slab
Required reinforcement [cm2/m]
70
60
50
40
30
20
10
0
0
2
4
6
8
10
12
14
Length of foundation slab [m]
Reference bridge
Sofistik model

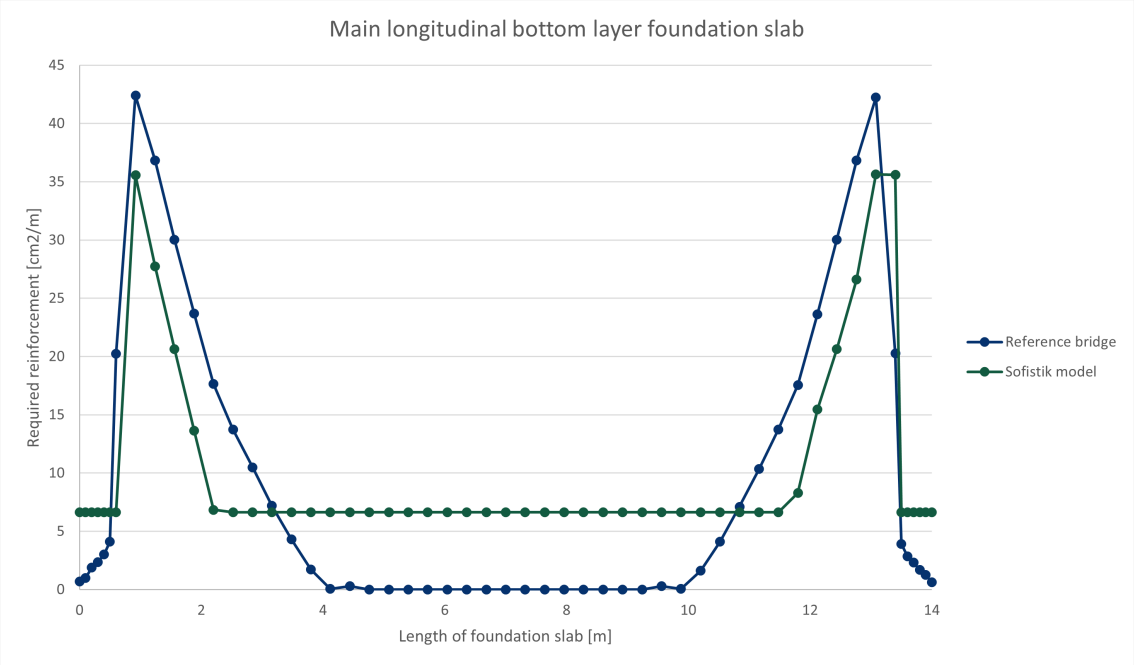
Main longitudinal bottom layer foundation slab
Required reinforcement [cm2/m]
45
40
35
30
25
20
15
10
5
0
0
2
4
6
8
10
12
14
Length of foundation slab [m]
Reference bridge
Sofistik model

D.3 Open foundation slab frame bridge

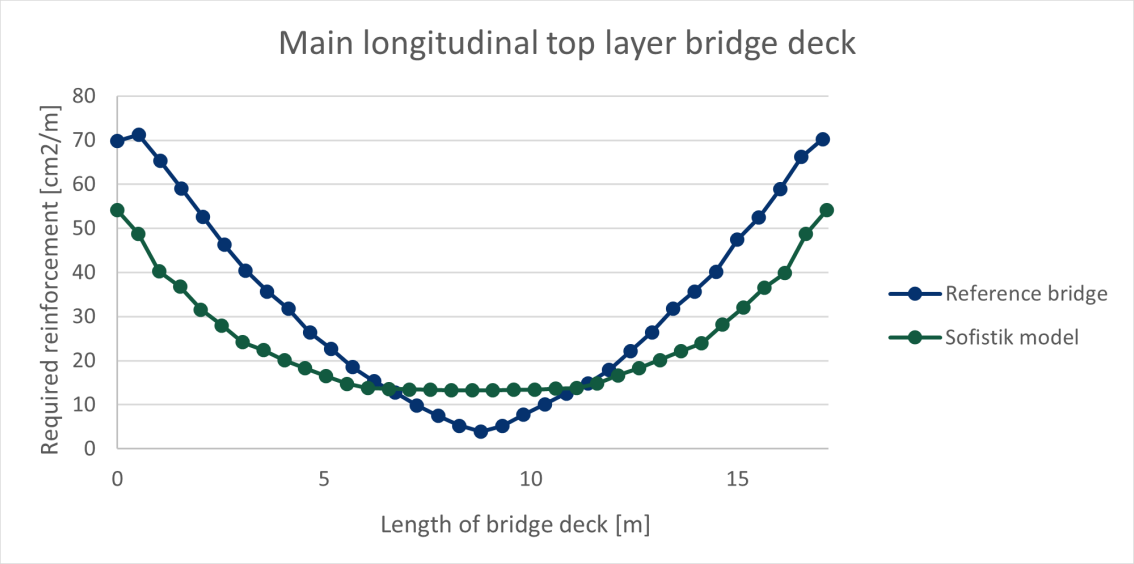

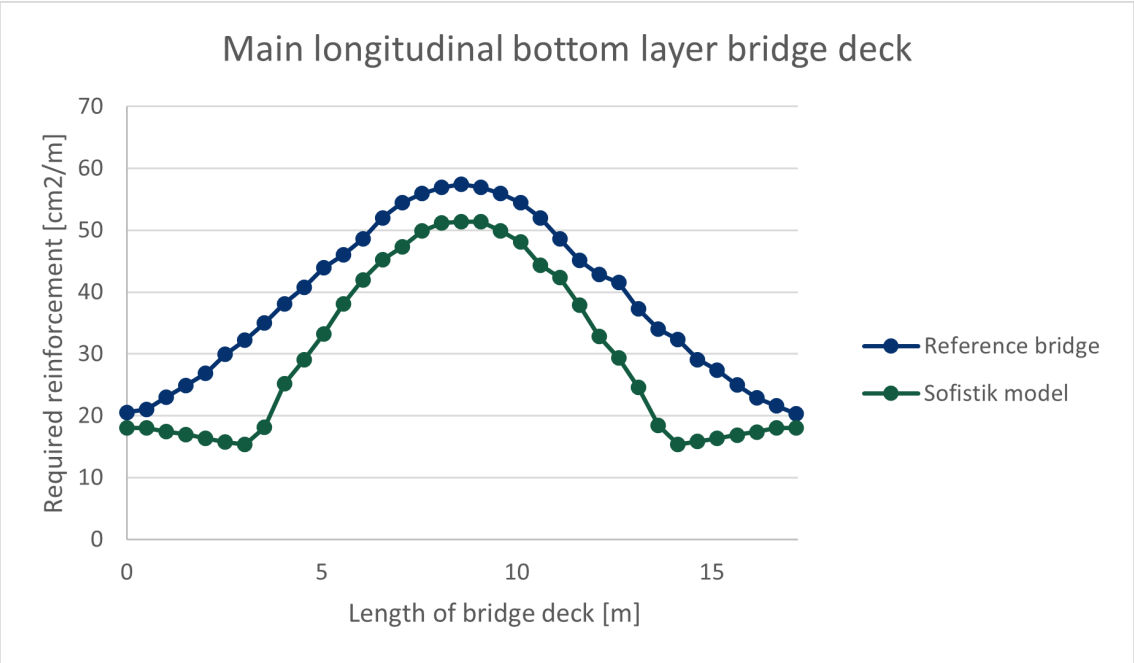
Main longitudinal bottom layer bridge deck
Required reinforcement [cm2/m]
70
60
50
40
30
20
10
0
0
5
10
15
Length of bridge deck [m]
Reference bridge
Sofistik model

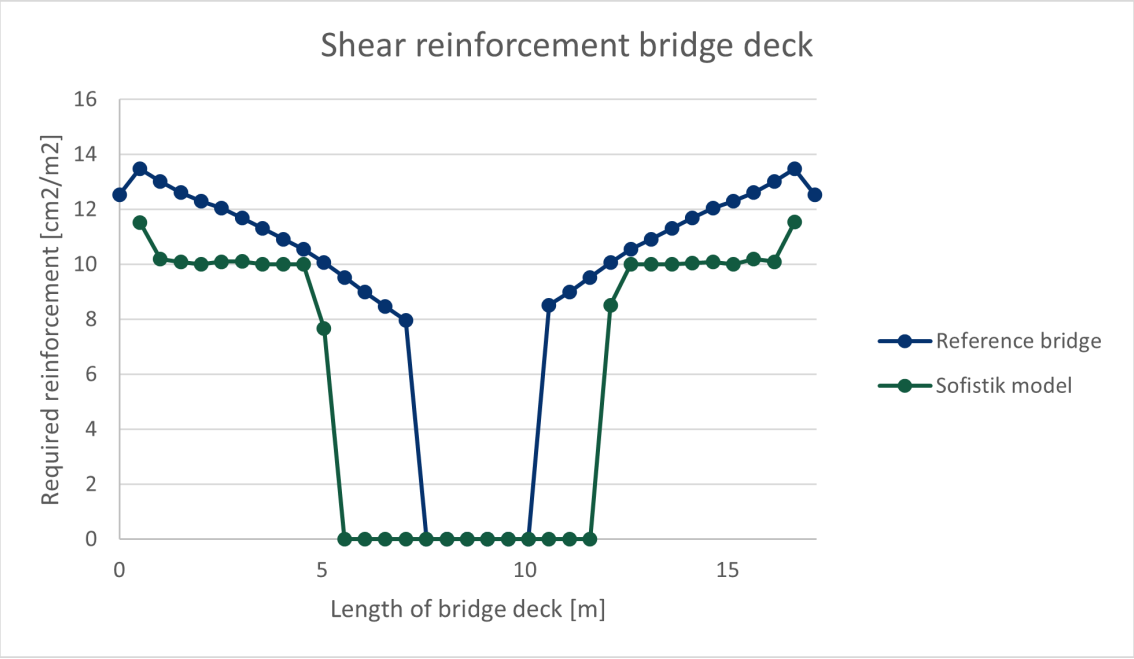
Shear reinforcement bridge deck
Required reinforcement [cm2/m2]
16
14
12
10
8
6
4
2
0
0
5
10
15
Length of bridge deck [m]
Reference bridge
Sofistik model

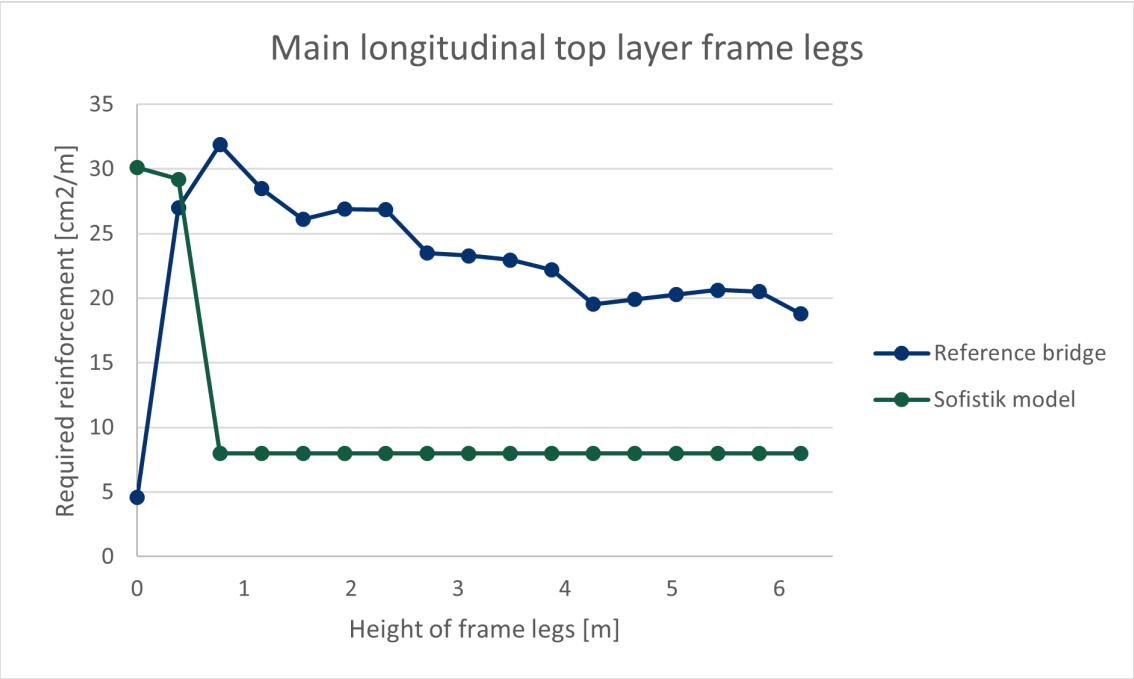
Main longitudinal top layer frame legs
Required reinforcement [cm2/m]
35
30
25
20
15
10
5
0
0
1
2
3
4
5
6
Height of frame legs [m]
Reference bridge
Sofistik model

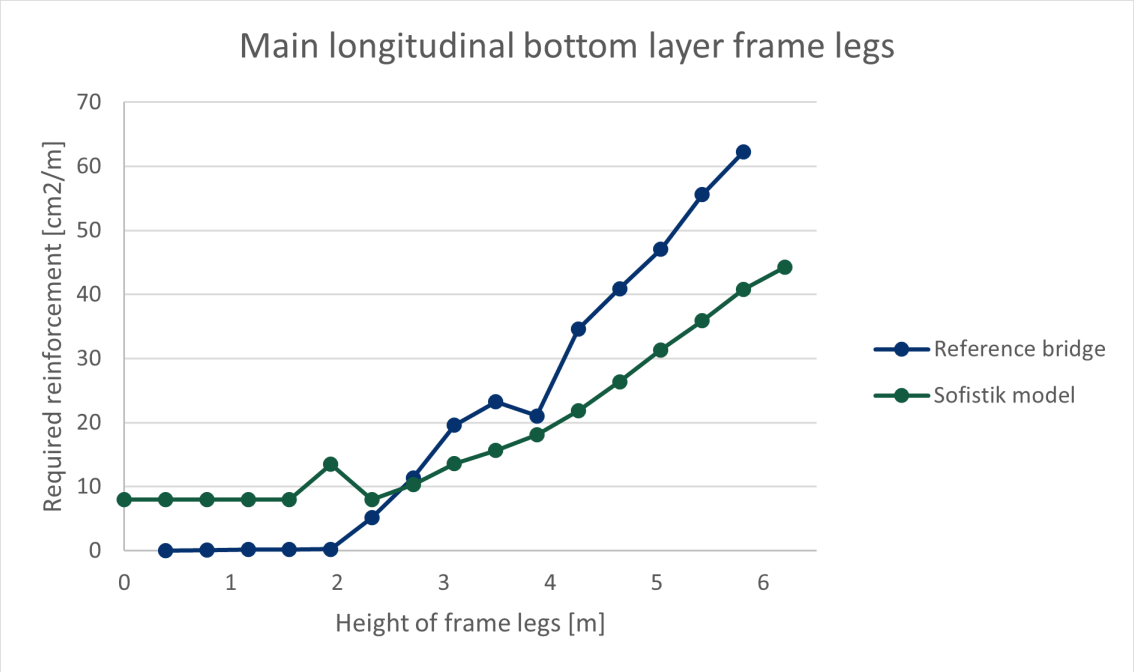
Main longitudinal bottom layer frame legs
Required reinforcement [cm2/m]
70
60
50
40
30
20
10
0
0
1
2
3
4
5
6
Height of frame legs [m]
Reference bridge
Sofistik model

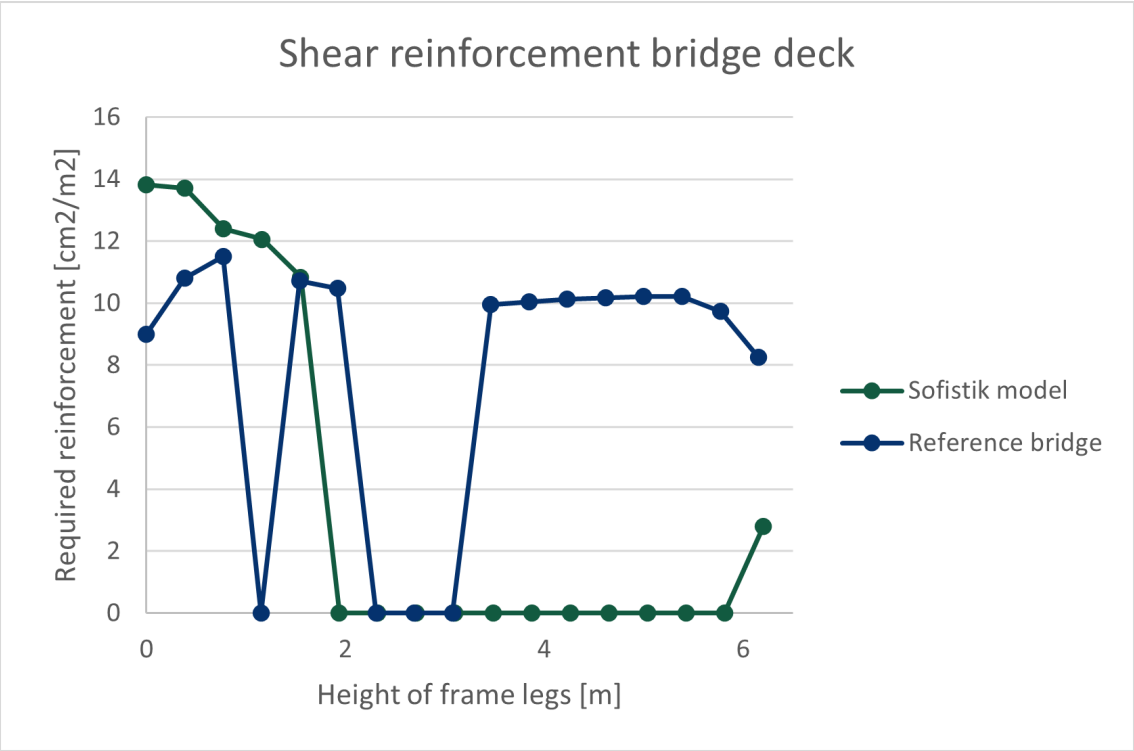
Shear reinforcement bridge deck
Required reinforcement [cm2/m2]
16
14
12
10
8
6
4
2
0
0
2
4
6
Height of frame legs [m]
Sofistik model
Reference bridge

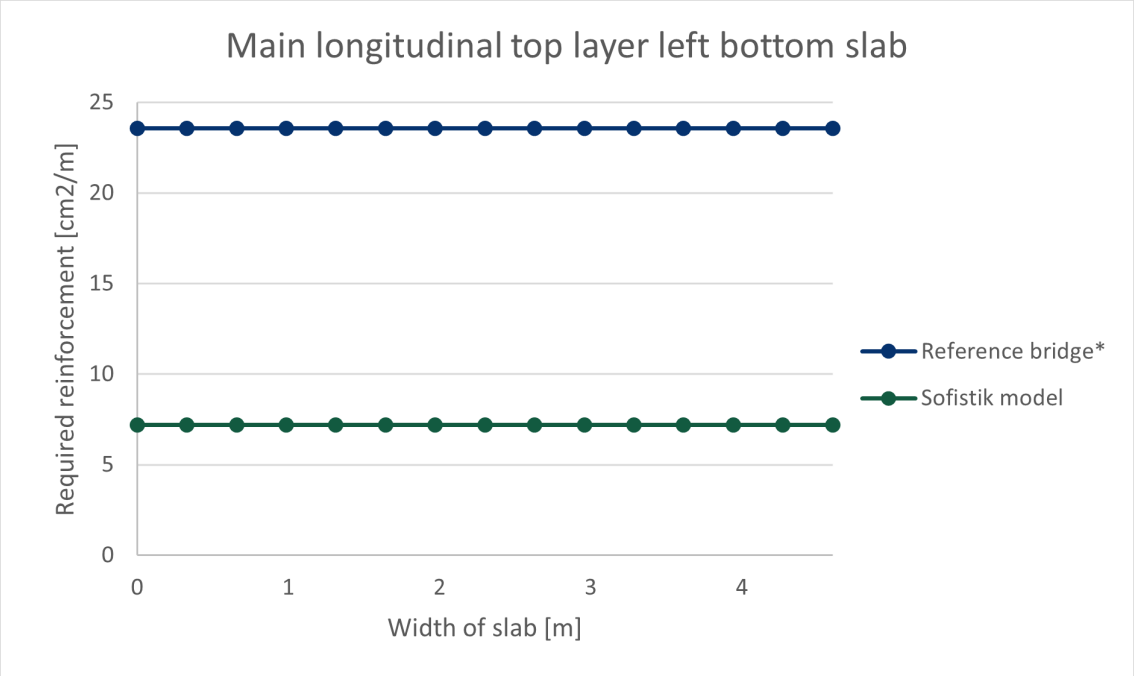
Main longitudinal top layer left bottom slab
Required reinforcement [cm2/m]
25
20
15
10
5
0
0
1
2
3
4
Width of slab [m]
Reference bridge*
Sofistik model

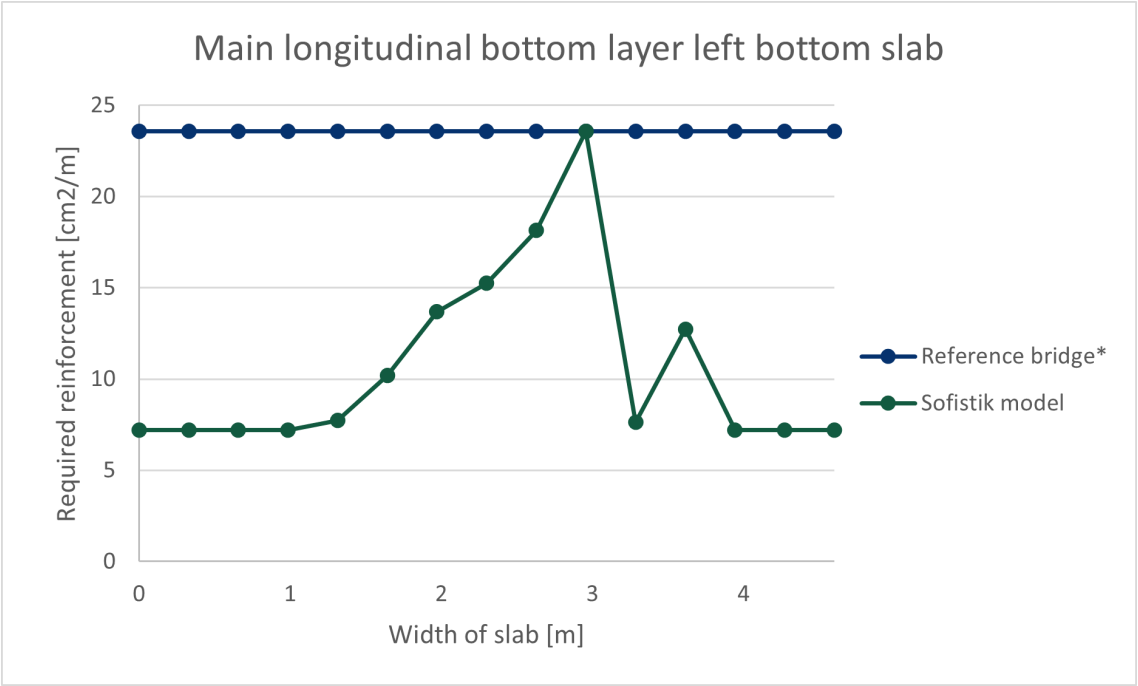
Main longitudinal bottom layer left bottom slab
Required reinforcement [cm2/m]
25
20
15
10
5
0
0
1
2
3
4
Width of slab [m]
Reference bridge*
Sofistik model

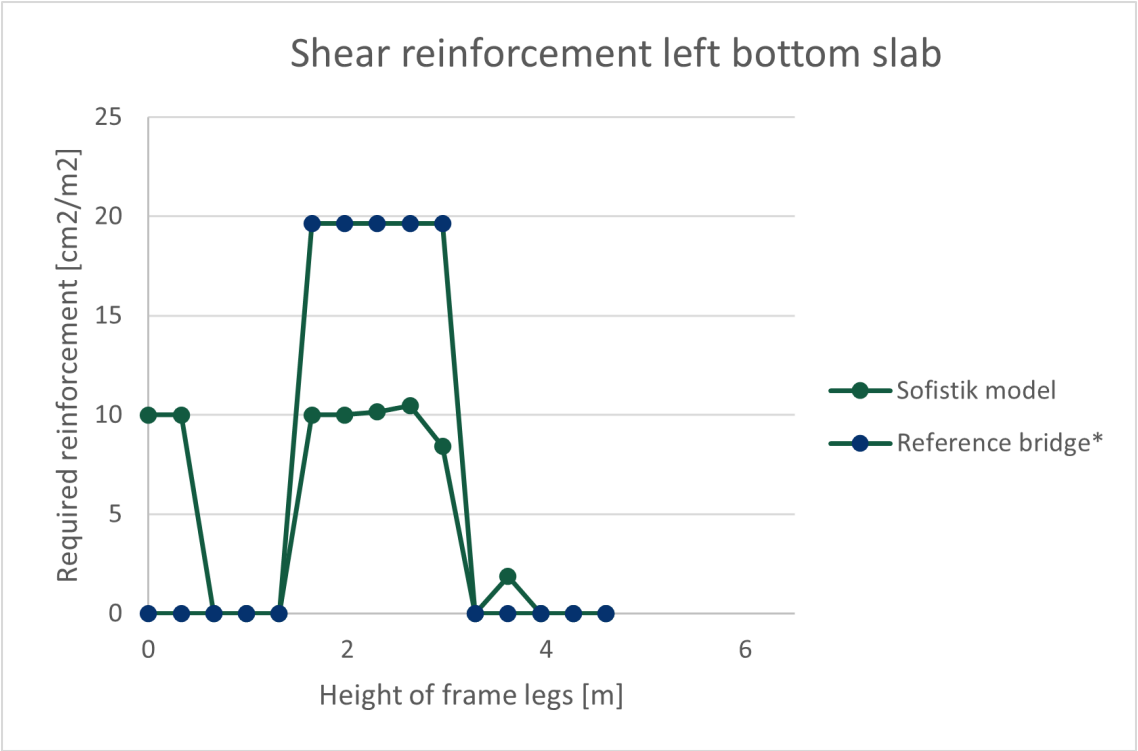
Shear reinforcement left bottom slab
Required reinforcement [cm2/m2]
25
20
15
10
5
0
0
2
4
6
Height of frame legs [m]
Sofistik model
Reference bridge*

DEPARTMENT OF ARCHITECTURE AND CIVIL ENGINEERING
CHALMERS UNIVERSITY OF TECHNOLOGY
Gothenburg, Sweden
www.chalmers.se

CHALMERS
UNIVERSITY OF TECHNOLOGY